IGNITION AND INITIATION OF COAL MINE EXPLOSIONS

Gysbert Van Rooyen Landman

A Thesis submitted to the Faculty of Engineering, University of the Witwatersrand, Johannesburg, in fulfilment of the requirements for the degree of Doctor of Philosophy.

Johannesburg, 1992

DECLARATION

I declare that this thesis is my own, unaided work. It is being submitted for the Degree of Doctor of Philosophy in the University of the Witwatersrand, Johannesburg. It has not been submitted before for any degree or examination in any other university.

G.V.R. Landman

this 20th day of August 1992

ABSTRACT

An analysis of South African coal mine explosion statistics, which serves as an introduction to this thesis, indicates an increase in the extent of the explosion hazard in recent years. The majority of explosions in South African collieries start at the coal face, where the use of electricity and blasting, together with mining bit friction are responsible for most ignitions. Consistent with experience worldwide, increased mechanization has resulted in an increased number of frictional ignitions at the coal face. In South Africa the problem is aggravated by the high mineral content of, and frequent sandstone intrusions into, the coal seams. In addition, the hard coal results in very dusty conditions.

Methane concentration levels are controlled by regulation 10.6.6 of the Minerals Act of 1991, allowing 1.4 % methane by volume in the air. Although the behaviour of methane is well understood, the potential role of excessive dust loadings around cutting drums, especially in the form of hybrid mixtures with methane, are largely unknown. While great emphasis is placed on the monitoring of respirable dust levels, total dust concentrations have not been measured or indeed been considered a potential danger by the South African coal mining industry.

This thesis investigates the sensitivity of ignition of those hybrid mixtures likely to be encountered in the working face. Methane content below the lower explosive limit of methane has been mixed with relatively low concentrations of dust, and the minimum ignition energy determined. The thermal ignition theory distinguishes between the behaviour of sources of ignition which are spacially extended and those which are spacially concentrated. In mining, ignition from a blown out shot is more voluminous than a frictional ignition and so the explosible behaviour of both volumetric and point sources have been investigated.

Apart from ignition source geometry, many factors influence sensitivity to ignition. In this study most of those factors have been kept constant, but two coal types, a very sensitive and a less sensitive coal as measured by the K_{ex} explosion index have been investigated.

Experiments were conducted in a 40 litre explosion chamber, and chemical and spark ignition sources were used. It was found that dust reduces the lower explosive limit of methane and, in fact, such mixtures can be as sensitive to ignition as a 5 % methane/air mixture. Higher fuel concentrations were required to effect ignition from a point source compared with volumetric ignition, but small percentages of methane reduced the minimum ignition energy of a dust mixture remarkably. Actual measurements of dust loadings at coal faces have indicated that a small increase in methane might well make the operational environment highly sensitive to ignition.

The thesis concludes that typical coal dust concentrations increase the chance of an explosive event in the working face. It is recommended that collieries contain dust concentration at the working face within safe limits.

This thesis is dedicated to my father

Willem Adolph Landman

ACKNOWLEDGEMENT

Appreciation is extended to the following organizations and individuals:

The National Energy Council of South Africa for sponsoring the research project and for allowing the results to be used in this thesis.

The GP Badenhorst Test Facility for the use of the 40 litre explosion vessel, and for the support of the personnel at the facility during the execution of the experiments.

The project director, Professor H.R. Phillips, for his advice and support throughout the research project.

To my wife and son, for the time they allowed me to dedicate to the accomplishment of the goals of this project.

TABLE OF CONTENTS

Content		Page
CHAPTER I	**ANALYSIS OF COAL MINE EXPLOSION STATISTICS**	
1.1	**Introduction**	1
	Colliery explosions in South Africa	2
1.2	**Acceptable Mine Explosion Risk**	4
1.3	**South African Explosion Statistics**	6
	Definition of a Coal Mine Explosion	7
	Representativeness of the Data	7
1.3.1	Risk of Fatality	7
1.3.2	Influence of Productivity Improvements on Risk of Fatality	11
1.3.3	Annual Explosion Frequency	13
1.2.4	Severity of Explosions	14
1.3.5	Location of Explosion Accidents	15
1.3.6	Sources of Ignition	17
	Frictional ignitions	17
	Other ignition sources	19
1.3.7	Influence of Preventative Technology	19

Content Page

1.3.8 Analysis of Individual Explosions 20

1.4 Interpretation of the Results 21

1.5 Conclusion 23

1.6 The Present Study 23

CHAPTER II EXPLOSION SAFETY OF THE WORKING ENVIRONMENT: STATEMENT OF THE PROBLEM 25

2.1 Introduction 25

2.2 Explosion Research Philosophies 26

2.2.1 Explosion Hazard Indices 27

Index of Explosibility 27

U.S. Bureau of Mines Hazard Index 27

The Staub Constant 29

The Explosion Constant 29

Material Properties and the Operational Environment 30

2.2.2 A Modern Approach to Explosion Hazard Research 31

2.2.3 A Research Approach for this Study 33

2.3 Quality of the Operational Environment of the Coal Working Face 33

Content Page

2.3.1	The Presence of Methane	34
	Methane generation	34
	Factors Influencing the Emission of Methane into the Operational Environment	35
	Methane Liberation Patterns	37
2.3.2	The Presence of Coal Dust in Collieries	41
	Formation of Coal Dust	42
	Quantities of Dust Formed During Mining	42
2.4	**Statement of the Problem**	43
2.5	**Objective of the Study - A Hypothesis**	45
2.6	**Structure of the Investigation**	46
CHAPTER III	**IGNITION AND INITIATION THEORY**	48
3.1	**Introduction**	48
3.2	**Ignition Theory**	50
3.2.1	Ignition Mechanism	50
	Basic Theory	50
	An Ignition Mechanism	55
3.2.2	Semenov's Steady State Theory	56
	Heat generation	57
	Heat loss	58

Content		Page
	Steady state	58
	Relation between heat loss and heat generation	58
	Reaction temperature over time	61
	The relation between concentration and temperature for critical conditions	63
3.2.3	Frank-Kamenetskii's Theory	65
3.2.4	Thermal Theory of Ignition by Hot Spots	67
3.3	**The Combustion of Methane**	68
	Exothermicity of Methane Oxidation	69
	The Reaction Rate of Methane-air Reaction	70
	Flame and Flammability Characteristics of Methane-air Combustion	71
3.4	**Coal Dust Combustion (Dispersed)**	74
	Coal Particle Ignition Mechanisms	75
	Exothermicity of Pulverised Coal Particles	77
	Reaction Rates of Coal Combustion	78
	Flammability and Flame Characteristics	78
3.5	**Combustion of Hybrid Mixtures**	81
3.6	**Summary and Positioning**	84

Content Page

4.1	**Introduction**	86
4.2	**Ignition Mechanisms of Different Types of Ignition Sources**	87
4.2.1	Ignition by Explosives	87
	Flame ignition	88
	Shock Wave Ignition	90
	Solid Particle Ignition	90
4.2.2	Ignition by Electric Sparks	91
	Spark Incendivity	92
	Spark Ignition Mechanism	93
	Protection against Electrical Spark Ignition	94
4.2.3	Frictional Ignitions from Coal Mining Bits	95
	Coal Bit Ignition Mechanism	96
	Protection Against Frictional Ignitions	98
4.3	**Ignition Source Equivalency**	100
4.4	**Assessment**	105
CHAPTER V	**INTERPRETATION OF THEORY**	107
5.1	**Introduction**	107
5.2	**Interpretation of the Theory**	107

Content Page

	Importance of Ignition Source Geometry and Volume	108
	The Ignition Path	110
	Flame Development from Volumetric Ignition Sources	112
	Flame Dissemination from a Point Source	112
5.3	**Influence of the Source of Ignition on the Ignition Blanket**	114
5.4	**Objectives of the Experimental Programme**	115
CHAPTER VI	**DESIGN OF THE LABORATORY EXPERIMENTS AND APPARATUS**	118
6.1	**Criteria for Selection**	118
6.2	**The 40 Litre Explosion Vessel**	119
6.2.1	Description of the 40 Litre Explosion Vessel	120
6.2.2	Instrumentation and Recording of Data	122
6.3	**Ignition Systems**	122
6.3.1	The Pyrochemical Ignitor	124
6.3.2	The Electric Spark Ignitor	127
	Circuit layout and components	128
	Determination of the Minimum Ignition Power	135
	Determination of the Minimum Ignition Energy	137

Content Page

	Spark Temperatures	138
6.4	**The Experimental Procedure**	139
6.5	**Repeatability of the 40 Litre Explosion Vessel**	142
6.6	**Conclusion**	145
CHAPTER VII	**IGNITION PROPERTIES OF COAL MINE ATMOSPHERES**	146
7.1	**The Experimental Programme**	146
	Material Properties of the Methane and Coal Dust Used	148
	The Experimental Results	150
	The Relationship between Spark Power and Spark Energy	151
	Particle Size Distribution	151
	General Comments on the Presentation of the Results	152
7.2	**Ignition and Initiation Properties of Methane**	153
7.3	**Ignition and Initiation Properties of Coal Dust**	158
7.4	**Ignition and Initiation Properties of Hybrid Mixtures**	163
	Maximum Pressure	163
	Maximum Rate of Pressure Rise	166

Content		Page
	Minimum Ignition Energy	169
7.5	**Ignition Blanket Determination**	172
7.5.1	Ignition Energies for Ermelo Hybrid Mixtures	172
7.5.2	Explosion Capacities (K_{ex}) for Ermelo Hybrid Mixtures	176
7.5.3	Ignition Energies for Springfield Hybrid Mixtures	176
7.5.4	Explosion Capacities (K_{ex}) for Springfield Hybrid Mixtures	180
7.6	**The Effect of the Energy Source and Coal Composition on the Explosive Behaviour of Coal Mine Atmospheres**	182
7.6.1	Lower Explosive Limits	183
	Application of Le Chatelier's Principle for Determining the Lower Explosive Limits of Hybrid Mixtures	184
7.6.2	Sensitivity to Ignition	186
7.6.3	Capacity to Initiate a Coal Dust Explosion	187
7.7	**Conclusion**	189
CHAPTER VIII	**HEAT RELEASE AND HEAT LOSS CHARACTERISTICS OF EXPLOSIVE SYSTEMS**	190
8.1	**Introduction**	190

Content		Page
	Important Observations from the Experimental Programme	191
8.2	**An Estimate of the Rate of Heat Release in the 40 Litre System**	191
8.2.1	Determination of the Apparent Heat Released During an Explosion	192
8.2.2	Procedure for Reaction Rate Estimation	193
8.2.3	Calculation of Rates of Heat Release	195
8.3	**A Discussion of Heat Loss Characteristics of Explosive Systems**	198
8.4	**Conclusion**	204
CHAPTER IX	**DUST CONCENTRATION AT THE CUTTING DRUM**	205
9.1	**Introduction**	205
9.2	**Sampling**	206
9.3	**The Sampling Procedure**	207
9.4	**Results Obtained**	212
9.5	**Conclusions**	215

Content		Page
CHAPTER X	CONCLUSIONS AND RECOMMENDATIONS	217
10.1	Explosion Safety at the Working Face	217
10.2	Conclusion	218
10.3	A Suggested Methodology for Determination of Acceptable Dust Concentration Levels	219
10.4	Closing Remarks	222
REFERENCES		223
APPENDIX I	ANNUAL COAL MINE EXPLOSION STATISTICS FOR SOUTH AFRICA FOR THE PERIOD 1897-1991	235
APPENDIX II	SOME DETAIL OF SOUTH AFRICAN COAL MINE EXPLOSIONS	237
APPENDIX III	MEASUREMENTS AND CALCULATIONS OF POWER FOR DIFFERENT RESISTOR ARRANGEMENTS FOR THE SPARK IGNITOR	248

Content		Page
APPENDIX IV	EXPERIMENTAL RESULTS OF TEST DONE TO DETERMINE THE IGNITION PROPERTIES OF COAL MINE ATMOSPHERES	251
A	METHANE TESTS	251
	Methane/air mixtures (Chemical Ignition)	
	Methane/air mixtures (Spark Ignition)	
B	ERMELO COAL DUST AND HYBRID MIXTURES	251
	Ermelo Washed (Chemical Ignition)	
	Ermelo Washed (Spark Ignition)	
	Ermelo Un-washed (Chemical Ignition)	
C	SPRINGFIELD COAL DUST AND HYBRID MIXTURES	251
	Springfield Washed (Chemical Ignition)	
	Springfield Washed (Spark Ignition)	
	Springfield Un-washed (Chemical Ignition)	
APPENDIX V	TEMPERATURE MEASUREMENTS AND HEAT RELEASE CHARACTERISTICS OF ERMELO WASHED EXPERIMENTS	251

LIST OF FIGURES

Figure		Page
1.1	Labour productivity in South African underground coal mines since 1900	12
1.2	The number of explosions per million ROM tons on an annual basis for South Africa since 1900	14
1.3	The location of explosions in South African collieries	18
2.1	The fire triangle	26
2.2	Graphical representation of the K_{ex} explosibility index	31
2.3	Airflow patterns around a longwall shearer, according to Cecala, Jankowski and Kissell[39].	38
2.4	Airflow patterns for different ventilation arrangements for mechanized bord and pillar headings. Meets[40].	40
3.1	Energy profile for the reaction A=B->C.	52
3.2	Temperature profile in the reaction vessel assumed in the Semenov theory of thermal explosions, and the temperature profile in the reaction vessel according to the Frank-Kamenetskii theory of thermal explosions after Barnard and Bradley[48].	57

Figure		Page
3.3	Heat generation, heat loss and their differences, as functions of temperature according to Gray and Lee[53].	59
3.4	Temperature-time curves for zero-order reactions for explosive, critical and stationary states. Reaction depletion is indicated in dashed lines. From Gray and Lee[53].	62
3.5	Explosion limit curve after Gray and Lee[53].	64
3.6	the straight line plot of the Arrhenius plots after Gray and Lee[53].	65
3.7	Influence of pressure and temperature on the flammability limits of methane in air - after Stull[59].	73
3.8	Delineation of ignition regimes as a function of heating rate and particle size - after Juntgen and Van Heek as reported by Essenhigh et al[62].	76
3.9	Thermal auto ignition data for an anthracite and a bituminous coal dust - Conti and Hertzberg[58].	80
3.10	Area of explosible hybrid mixtures of coal dust, methane and air with explosibility contours indicating the concentrations of optimum mixtures, based on Banhegyi and Egyedi[73].	82
4.1	Development of shock wave and gaseous products of detonation when an unstemmed charge of high	89

Figure		Page
	explosives is fired from a borehole into a flammable atmosphere, such as methane and air, after Grant and Mason[86].	
4.2	The growth of a spark kernel radius in a propane-air mixture at near minimum ignition energy conditions - Ko et al[91].	94
4.3	Heat losses from a hot frictional metal smear on rock. After Blickensderfer[104].	98
4.4	The temperature profile with time and with increased distance from the trailing edge of the tool for a smear of thickness 0.02 mm. After Blickensderfer[104].	99
4.5	The change in explosion characteristics with increased ignition energy at constant fuel concentration.	101
4.6	Comparison between explosion characteristics of the same coal dust initiated by a weak spark of energy output 1 J, and a strong chemical ignitor with an energy output of 250 J, according to Krzystolik and Sliz[83].	103
4.7	Domains of non-flammability, flammability and auto-ignitability at atmospheric pressure for a hypothetical coal dust. The widening range of flammable concentrations for ignition from electric sparks of increased energy is also shown. Compiled from Herzberg et al[84] and Conti et al[109].	105

Figure		Page
5.1	The path of events that leads to ignition, clearly showing the interaction between the source of ignition and the explosible mixture.	111
5.2	A schematic of thermal ignition from a point source. The temperature gradient established by an inert hot spot is shown together with its influence on the explosible mixture in the immediate sphere surrounding it.	113
5.3	Limits set for the investigation into the position of the ignition blanket in the space formed by methane and coal dust concentrations and by minimum ignition energy.	116
6.1	The 40 litre explosion vessel.	121
6.2	The 40 litre explosion vessel operating system	123
6.3	A disassembled and assembled detonator.	125
6.4	The pyrochemical detonator mounted on the detonator holder inside the 40 litre explosion vessel	126
6.5	Circuit layout of the continuous electric spark ignitor	129
6.6	The digital timer at which spark duration time is set.	130
6.7	A 500 Ohm resistor	131
6.8	Electrodes and the isolated electrode bulkheads.	132
6.9	The current shunt.	133

Figure		Page
6.10	The voltage divider	133
6.11	The assembled spark ignitor system. The green box is the 20 kV transformer.	134
6.12	Typical oscilloscope plots of voltage over time, measured across the current shunt and the voltage divider.	136
6.13	The relationship between ignition power obtained and the input voltage, for different current limiting resistances.	137
6.14	A typical explosion pressure time history when using a spark ignitor.	139
6.15	The "pepperpot" dust sample holder.	140
6.16	Methane addition to the explosion vessel.	142
7.1	Maximum pressure and maximum rate of pressure rise with increased ignition energy levels, for a 6 % methane/air mixture.	156
7.2	Time versus pressure for chemical and spark ignition of a 6 % methane/air mixture.	156
7.3	Methane concentration levels versus minimum ignition energy. Maximum pressure lines are indicated.	157
7.4	Methane concentration levels versus ignition energy, with K_{ex} values for spark ignition, indicated in brackets.	157

Figure		Page
7.5	Maximum pressure and maximum rate of pressure rise with increased ignition energy levels, for a 500 g/m^3 coal dust/air mixture.	160
7.6.	Time versus pressure for chemical and spark ignition of a 500 g/m^3 Ermelo coal dust/air mixture.	160
7.7	Ermelo washed coal dust concentration levels versus minimum ignition energy. Maximum pressure lines are indicated.	161
7.8	Ermelo washed coal dust concentration levels versus minimum ignition energy with K_{ex} values contoured.	161
7.9	The minimum chemical ignition energy of Ermelo unwashed coal dust for different concentration levels. Washed Ermelo is also indicated.	162
7.10	The maximum explosion pressure and rates of pressure rise with varying ignition energies for Ermelo washed and unwashed coal dust.	162
7.11	Maximum pressure of hybrid mixtures of Ermelo washed coal dust, ignited by the chemical ignitor.	164
7.12	Maximum pressure of hybrid mixtures of Ermelo washed coal dust, ignited by the spark ignitor.	164
7.13	Maximum pressure of hybrid mixtures of Springfield washed coal dust, ignited by the chemical ignitor.	165

Figure		Page
7.14	Maximum pressure of hybrid mixtures of Springfield washed coal dust, ignited by the chemical ignitor	165
7.15	Maximum rates of pressure rise for hybrid mixtures of Ermelo washed coal dust, ignited by the chemical ignitor.	167
7.16	Maximum rates of pressure rise for hybrid mixtures of Ermelo washed coal dust, ignited by the spark ignitor.	167
7.17	Maximum rates of pressure rise for hybrid mixtures of Springfield washed coal dust, ignited by the chemical ignitor.	168
7.18	Maximum rates of pressure rise for hybrid mixtures of Springfield washed coal dust, methane and air, ignited by the chemical ignitor.	168
7.19	The minimum chemical ignition energy required to effect the explosion of Ermelo washed coal dust hybrid mixtures.	170
7.20	The minimum spark power requirement to effect ignition of Ermelo washed coal dust hybrid mixtures.	170
7.21	The minimum spark ignition energy required to effect ignition of Ermelo washed coal dust hybrid mixtures.	171

Figure		Page
7.22	The minimum chemical ignition energy required to effect ignition of Springfield washed coal dust hybrid mixtures.	171
7.23	The chemical ignition energy blanket for washed Ermelo coal dust hybrid mixtures.	173
7.24	The spark ignition power blanket for washed Ermelo coal dust hybrid mixtures.	173
7.25	The spark ignition energy blanket for washed Ermelo coal dust hybrid mixtures.	174
7.26	The chemical ignition energy blanket for Ermelo un-washed coal dust hybrid mixtures.	174
7.27	The K_{ex} blanket for washed Ermelo coal dust hybrid mixtures, chemically ignited.	175
7.28	The K_{ex} blanket for washed Ermelo coal dust hybrid mixtures, ignited by electric spark.	175
7.29	The K_{ex} blanket for un-washed Ermelo coal dust hybrid mixtures, chemically ignited.	176
7.30	The minimum chemical ignition energy blanket of washed Springfield coal dust hybrid mixtures.	178
7.31	The minimum spark ignition power blanket for washed Springfield coal dust hybrid mixtures.	178
7.32	The minimum spark ignition energy for washed Springfield coal dust hybrid mixtures.	179
7.33	The minimum chemical ignition energy for un-washed Springfield coal dust hybrid mixtures.	179

Figure		Page
7.34	The K_{ex} blanket for washed Springfield coal dust hybrid mixtures, chemically ignited.	181
7.35	The K_{ex} blanket for washed Springfield coal dust hybrid mixtures, ignited by electric spark ignition.	181
7.36	The K_{ex} blanket for unwashed Springfield coal dust hybrid mixtures, chemically ignited.	182
7.37	The lower explosive limits for chemical and spark ignition for Ermelo and Springfield hybrid mixtures and areas of explosibility for Ermelo mixtures.	184
7.38	Sensitivity to chemical ignition of hybrid mixtures comparative to the ignition energy required to ignite a 5 % methane/air mixture and a 5.7 % methane/air mixture. Areas of explosibility are also indicated.	187
8.1	A typical temperature history over time for the chemical ignition of Ermelo washed coal dust at a 100 g/m^3 concentration as obtained from pyrometer readings.	194
8.2	A plot of $\ln(1/t_{max})$ versus $1/T_r$ for different concentrations of Ermelo washed coal dust.	197
8.3	Quasi heat generation curves for Ermelo washed coal dust.	199
8.4	Heat generation curves for hybrid mixtures of methane and Ermelo washed coal dust.	200

Figure		Page
8.5	Behaviour of explosive systems with reference to the relation of the rate of heat release and the rate of heat loss.	201
9.1	The base segment of the sampling pot, with a funnelled outlet which directs the air to the tube connecting the pots and the pumps.	208
9.2	The filter laid into position in the base segment of the sampling pot.	208
9.3	An O-ring fitted to hold the filter.	209
9.4	A cylindrical section threaded into the base segment, pressing the O-ring tight against the filter.	209
9.5	The assembled filter pot, with a lid fitted at the open end which protects the filter during transportation.	210
9.6	Two MSA Flow-Lite vacuum pumps connected in parallel to the sampling pot.	210
9.7	The sampling pot fitted to the extension rod with the plastic tube that joins the pumps and the pot.	211
9.8	A used sampling pot opened in the laboratory, with two used filters in the foreground.	211
9.9	Cumulative distribution of dust around mechanized coal mining drums obtained by the pot sampling method.	213

Figure		Page
9.10	Sensitivity and explosion limits for Ermelo and Springfield hybrid mixtures. The rectangles indicate likely hybrid mixtures.	215
10.1	A safety factor diagram based on Le Chatelier's principle as interpreted by Field[76] for hybrid mixtures of gas and dust.	221

LIST OF TABLES

Table		Page
I.I	Recent coal mine disasters.	1
I.II	Examples of research institutes investigating the coal mine explosion hazard.	3
I.III	Chance of an underground coal miner losing his life due to an explosion of methane or coal dust for every year between 1940 and 1989.	9
I.IV	Percentage explosions per area of the mine over the last four decades.	16
I.V	Percentage of explosions per source of ignition over the last four decades.	17
II.I	Summary of methane monitored during investigations at Indumeni Colliery in Northern Natal in 1969 by Joubert[42], six Natal collieries coded A to F by Joubert[43] and Ermelo Colliery by Stripp[35] in 1989.	41
III.I	The widening of the range of flammability limits of methane with the increase in the temperature of the methane-air mixture after Moss[60].	74
III.II	The percentage reduction in minimum spark ignition (E_{min}) energies for a bituminous coal in the presence of small quantities of methane - after Foniok[79].	83

Table		Page
VI.I	Explosion vessel reproducibility. Average, standard deviation and percentage standard deviation for 15 repetitions each under three conditions are given. Ermelo dust at concentration 400 g/m^3 and methane at 7.4 % were used.	144
VII.I	Structure of the experimental programme. Methane/air, dust/air and hybrid mixtures were tested with both a volumetric and a point source of ignition.	147
VII.II	Proximate analysis of un-washed and washed coal samples of Ermelo Seam C and Springfield Seam 2 (air dry basis).	149
VII.III	Size distributions of the coal dusts used in the experimental programme. Two distributions of the dust cloud surrounding continuous miner drums are included for comparative reasons.	152
VII.IV	Le Chatelier's principle applied for Ermelo and Springfield hybrid mixtures. Concentrations and actual quantities per 40 litre are indicated.	185
VIII.I	Calculation of $1/T_r$ and $\ln(1/t_{max})$ for concentrations of Ermelo washed coal dust.	196
VIII.II	Explosion characteristics used of Ermelo coal dust hybrid mixtures of similar minimum ignition energy.	203

Table		Page
IX.I	Concentration of the size fraction below 100 μm for dust clouds around mechanized cutting drums in South African collieries.	214

LIST OF SYMBOLS

J- Joule

K_{ex}- Explosion constant

kPa- kilo Pascal

m- metre

mJ- milli Joule

MPa- Mega Pascal

ms- milli second

mV- milli Volt

s- second

V- Volt

NOMENCLATURE

Dissemination of flame	A flame that generates enough heat to ignite the non-combusted mixture directly in contact with it. The flame is therefore self-propagational.
Ignition	The condition where the rate of chemical heat generation begins to exceed the rate of heat loss.
Initiation	When flame starts to disseminate, or the process of dispersion and ignition of coal dust.
Operational Environment	The dynamic nature, chemical composition and thermodynamic state of the air present where mining activity is being executed.
Point Ignition Source (Ideal)	An ignition source at infinite temperature but filling no space.
Post-Ignition Research	Explosion research concentrating on protective measures, aimed at extinguishing the explosion after ignition took place.
Pre-Ignition Research	Explosion research concentrating on prevention of ignition, aimed at the establishment of environmental conditions which cannot host an explosion.
Pyrochemical Ignitor	A pyrotechnics chemical ignitor
Volumetric Source of Ignition (Ideal)	An ignition source which is spacially extended and fills the volume containing the explosible mixture. The source establishes a constant temperature throughout the volume.

CHAPTER I

ANALYSIS OF SOUTH AFRICAN COAL MINE EXPLOSION STATISTICS

This chapter considers the extent of the coal mine explosion problem in South Africa. The international dimensions of the problem are also shown which illustrate that mining is always accompanied by risk and that miners are, by nature, resolute men. Risk can be managed by a better understanding of the problem, which is obtained by an analysis of the South African explosion statistics. Areas that need further investigation are identified, from which one has been selected as the topic of this study.

1.1 INTRODUCTION

Coal mine explosions, after two centuries of intense scientific attention, continue to be the cause of numerous disasters worldwide (see Table I.I). During the 18th and 19th centuries, all explosions in mines were attributed to a gas which was ultimately identified as methane. After explosions in the U.K. at Wallsend, Jarrow, Springwell, Thomsley and Haswell collieries between 1803 and 1844, it was noticed that coal dust participated in the explosions. Faraday was the first scientist to recognize the danger of coal dust explosions, but little attention was paid to his opinion by the mining industry[1].

TABLE I.I Recent coal mine disasters.

COUNTRY	COLLIERY	DATE	FATALITIES
West Germany	Scholzenbach[2]	June 1988	51
USA	William Station[3]	September 1989	10
Turkey	Merzifon[4]	February 1990	67
Yugoslavia	Dobrnja[2&5]	August 1990	180
China	Sanjiaoje[6]	April 1991	147

After the Courriers colliery explosion in 1906 in France, in which 1099 miners lost their lives, there was no doubt concerning the explosibility of coal dust, since methane was known to be absent in the Courriers mine. This prompted many countries to investigate the problem, and today the pioneering work of scientists such as Taffanel, Chernitsyn, Wheeler, Tideswell and others form the basis of the understanding of the phenomenon of coal dust and methane explosions.

Today, in every country with a developed coal mining industry, the hazards of coal mine explosions are investigated. Some of the many organizations who have been involved in the field of mine explosion research are listed in Table I.II. It can be seen that this mining safety hazard is well researched and numerous publications on the topic can be consulted.

Colliery Explosions in South Africa.

South Africa too has its history of coal mine disasters. The first coal mined in South Africa was in the Eastern Cape near Molteno, a mining town established by George Vice in 1874 and named after Sir John Molteno who was prime minister of the Cape Colony[7]. Up to that stage coal was imported from the United Kingdom to Capetown Harbour and transported by rail to the Kimberley Diamond mines. Sir John Molteno offered a financial reward to the discoverer of a local coal supply, not only to stimulate the local economy, but also to provide coal for the expansion of the Cape railway network.

The first recorded explosion from this area occurred at the Dugmore Colliery of the Indwe Company in 1902. They had driven about 9 m across a dyke when the explosion happened[8].

Subsequent to the discovery of coal in the Cape, a survey of coal fields in Natal by F.W. North was published in 1881[9]. The first ever recorded coal mine explosion in Southern Africa was in Natal in 1891. In Transvaal the first recorded explosion

TABLE I.II Examples of research institutes investigating the coal mine explosion hazard.

COUNTRY	NAME OF INSTITUTE	LOCATION
Australia	Londonderry	New South Wales
Czechoslovakia	The Scientific Research Institute	Ostrava Rakvanice
France	Centre d'Etudes at Recherches des Charbonnages de France (CERCHAR)	Paris
Germany	Deutche Montan Technologie (DMT)	Dortmund
Japan	Resource Research Institute	Kawaguchi-Saitama Fukuoka
RSA	CSIR/Kloppersbos	Pretoria
UK	Health and Safety Executive (HSE)	Harpur Hill, Buxton
USA	USA Department of the Interior. Bureau of Mines	Pittsburgh
USSR	Makeevka Institute of Scientific Research on the Safety of Work in the Minerals Industry (MAKNII)	Makeevka

occurred in 1906, and in the Orange Free State in 1913. To date, 319 explosions have taken place in South Africa, of which the 1926 Durban Navigation Colliery coal dust explosion was the worst.

Initially, all explosibility testing of South African coals was done in the UK. Small British test appliances such as the Wheeler apparatus were used by the Inspector of Mines in Natal. It was only in the early sixties that the Fuel Research Institute in Pretoria started investigations. first with the Hartmann apparatus and later with a 40 litre explosion vessel. In 1987 a 200 m long explosion gallery, the G.P. Badenhorst Explosion Gallery situated 40 km north of Pretoria, was completed.

Despite local research, legislation regarding explosion protection in South African mines is based on the findings of research done in the northern hemisphere. After some serious explosions in the eighties the then Government Mining Engineer, Mr G.P. Badenhorst, felt that local research facilities should be improved to address the problem of coal mine explosions in South African collieries.

Total protection can only be provided in mining situations by terminating operations completely. In order that society should benefit from the fruits of the mining industry, a compromise has to be reached. This compromise introduces the concept of acceptable mine explosion risk.

1.2 ACCEPTABLE MINE EXPLOSION RISK

Risk is an ingredient of all human life. Vivian[10] reports that a former Chief Inspector of Machinery once said: "If you insist on being dead safe you will have to accept being safely dead". At the same time, any exposure to risk is unjustified if the existence of the risk can be avoided within reason. That which is reasonable for the mine secretary directly involved in managing money to obtain profits might differ from the perception of adequacy for the continuous miner driver directly facing the risk.

A cost-benefit approach might bring the two perceptions closer together. Compensation paid to the continuous miner driver for his increased risk might make him more amenable, while an additional cost to ensure continued profitability might make sense to the mine secretary. However, attaching monetary value to life makes this approach difficult to pursue. The absurdness of this method is showed by

Whittaker[11]. He proposes that no sum, however large, would induce a reasonable man to willingly terminate his life at noon the following day if he had the option of living the rest of his life given the status quo.

To simplify matters, attempts to measure acceptable risk in financial terms is disregarded. Only pure risk, as defined by Bannister[12], that is risk to loss of or damage to assets, are considered. Pure risk can lead to losses only, thus profits are not a result of assuming this risk. A set of questions that might well be asked by a miner going underground will be used to obtain a measure of how acceptable the risk is.

The reasonable miner going underground at any colliery in South Africa today might ask the following questions with regard to the risk he is taking of being involved in an accidental explosion:

> What is the chance of being killed?
>
> How does this risk compare to the other risks taken by going underground? Is this risk significant?
>
> Is the explosion incidence in South Africa abnormally high?
>
> How do the recent experience compare to the past?
>
> Are protection measures being used? If so, what is the effectiveness of these measures?
>
> What is the mental attitude of mine workers towards this risk? Are they responsible or being stimulated by training, awareness programmes et cetera to be a low risk group?

Answers to these questions will provide a comprehension of acceptable risk. The risk management process is reflected in obtaining answers to these questions, that is risk identification, risk measurement and risk control.

In order to provide quantitative answers to some of these questions, South African explosion statistics have been collected and analysed. Conclusions from the analysis are used to target the risky areas for increased research or better control.

1.3 SOUTH AFRICAN EXPLOSION STATISTICS

The following information was collected from the files of the Government Mining Engineer[13]:

Annual Information

Number of explosions

Casualty figures

ROM production

Underground labour

So far information exists for some 306 explosions which have occurred in South Africa since 1890. Of these, 185 explosions have been described in more detail and this information has been classified as follows:

Specific Information

Name of colliery

Date of accident

Time of accident

Location in mine

Methane or coal dust involvement

Source of ignition

Casualty figures

Other relevant remarks

The annual information is listed in Appendix I and the specific information in Appendix II.

Definition of a Coal Mine Explosion

Landman[14] interprets the term "mine explosion" as follows. It varies from a small flash on the coal face to an explosion involving the entire mine. The common denominator is an instant where both an adequate energy source and enough fuel are present. Since these are the two risk factors to control, every explosion, despite its intensity, carries equal weight when analysing occurrences over a period of time.

Representativeness of the Data

As early as 1899, it was stated under Section XIX Regulation 145 of the regulations for the Natal Mines Act[15] dealing with "Procedure in case of an Accident" that all accidental explosions of fire-damp or coal dust, whether resulting in injury to persons or not, must be reported to the Inspector of Mines. The Minerals Act (50 of 1991)[16] today also requires that notice should be given to the Inspector of Mines of any fire or dust (Regulation 25.6). It is realistic to assume that small ignitions are not reported or not even noticed.

There comes a dividing line between that explosion which can be observed and yet concealed, and that which has to be reported. That which is reported contains factual information given the evidence at the scene of the explosion.

1.3.1. RISK OF FATALITY

Vivian[10] calculates the mean probability of any one member of the South African population dying in an occupational accident to be 5.5×10^{-5}, or one in 18 182. During the nineteen eighties, there were approximately seventeen fatalities due to underground coal mine explosions per year in South Africa. The number of underground workers in coal mines was on average 50 088. The mean probability of any one coal miner dying in an explosion was thus 3.45×10^{-4}, or one in 2899. The overall likelihood of a coal miner dying in the eighties in South Africa, all accidents included, was 2.03×10^{-3} or one in 493.

Since one should be beware of averages, annual figures over the last four decades are recorded in Table I.III. Regarding the explosion hazard, the period 1950 to 1979 was a period of relative stability with little change. Mean values from this period will be used as the norm to compare performance in recent times. The chance of a miner dying in an explosion varies substantially from year to year and is between 0 % and 0.03 %. Also, the frequency of years with no explosions are lowest in the eighties and explosions are shown to be more severe than the preceding three decades. This increased exposure of workers to the explosion danger in the eighties is furthermore reflected in the average figures per decade.

One also notices that the percentage contribution of explosion fatalities to the overall fatality rate in coal mines increased sharply in the eighties. This is due to the combined effect of a reduced fatality rate from other accidents, while the fatality rate of explosions increased.

It is important to ask the question whether a significant difference exists between the mean values of the two periods compared? What is the probability that the two samples represent identical populations? If so, the eighties was just an unlucky decade and the mean risk of death for a worker will return to the long term norm according to the central limit theorem[17]. If not, the eighties represent a new population, possibly brought about by changes in mining technology, mining methods or other reasons. The increased level of the explosion hazard might thus be due to the application of protection measures that are no longer effective.

The Student's t-test can be used to answer the question. Suppose the two samples have means $\bar{x}_1$ and $\bar{x}_2$ and are of size n_1 and n_2. Then,

TABLE I.III Chance of an underground coal miner losing his life due to an explosion of methane or coal dust for every year between 1950 and 1989. (Number of fatalities divided by total number of underground workers).

YEAR	1950-59	1960-69	1970-79	1980-89
19~0	$0.00x10^{+0}$	$0.00x10^{+0}$	$0.00x10^{+0}$	$0.00x10^{+0}$
19~1	$9.18x10^{-4}$	$1.92x10^{-4}$	$5.98x10^{-4}$	$2.79x10^{-4}$
19~2	$0.00x10^{+0}$	$3.80x10^{-4}$	$0.00x10^{+0}$	$2.30x10^{-4}$
19~3	$1.50x10^{-4}$	$2.31x10^{-5}$	$0.00x10^{+0}$	$1.44x10^{-3}$
19~4	$3.03x10^{-5}$	$0.00x10^{+0}$	$2.22x10^{-5}$	$1.19x10^{-4}$
19~5	$2.99x10^{-5}$	$0.00x10^{+0}$	$0.00x10^{+0}$	$6.43x10^{-4}$
19~6	$4.15x10^{-4}$	$0.00x10^{+0}$	$2.01x10^{-5}$	$0.00x10^{+0}$
19~7	$2.26x10^{-4}$	$6.45x10^{-5}$	$0.00x10^{+0}$	$7.16x10^{-4}$
19~8	$0.00x10^{+0}$	$8.48x10^{-5}$	$0.00x10^{+0}$	$0.00x10^{+0}$
19~9	$0.00x10^{+0}$	$0.00x10^{+0}$	$0.00x10^{+0}$	$2.21x10^{-5}$
Mean Probability (Explosion)*	$1.77x10^{-4}$	$7.45x10^{-5}$	$6.40x10^{-5}$	$3.45x10^{-4}$
Mean Probability (All)#	$2.76x10^{-3}$	$3.00x10^{-3}$	$1.84x10^{-3}$	$2.03x10^{-3}$
% of Total$	6.4	2.5	3.5	17.0

* *Mean probability over the decade of an underground coal miner dying in an explosion.*

\# *Mean probability of an underground coal miner dying in any coal mine accident.*

$ *Explosion fatalities as a percentage of all fatalities per decade.*

$$t = \frac{\bar{x}_1 - \bar{x}_2}{S\sqrt{\frac{1}{n_1} + \frac{1}{n_2}}} \qquad -1.1$$

where

$$S = \left\{ \frac{n_1 s_1^2 + n_2 s_2^2}{n_1 + n_2 - 2} \right\}^{\frac{1}{2}} \qquad -1.2$$

or the pooled sample variance, from samples with variance s_1^2 and s_2^2. The question is expressed as a null hypothesis that states that the two samples come from two populations whose means μ_1 and μ_2 are equal and that the variances are the same. Therefore,

$$H_0 = (\mu_1 = \mu_2 \,|\, \sigma_1^2 = \sigma_2^2) \qquad -1.3$$

If H_0 is true, then the samples come from identical populations and can be regarded as two samples of the same population. For the two periods

$\bar{x}_1 = 1.05x10^{-04}$ $\quad$ $\bar{x}_2 = 3.45x10^{-04}$

$s_1^2 = 4.52x10^{-08}$ $\quad$ $s_2^2 = 2.18x10^{-07}$

$n_1 = 30$ $\quad$ $n_2 = 10$

giving t=-2.155 for 38 degrees of freedom. Using a t-table, 2.5 % of the area under the t-curve for 38 degrees of freedom lies above a t-value of 2.021. This puts the calculated t-value in the critical area and it can be said that there are less than 5 in a 100 chances of these two samples having the same population mean. So H_0 is rejected at a 5 % significance level.

Recently, coal mining in South Africa has changed dramatically and characteristics thereof have followed suit. This difference is not surprising, because a lot of changes in the coal market have taken place since the energy crisis in the seventies. Sasol and Eskom, the synthetic fuel and electric supply industries respectively, expanded their coal mining operations while the export market opened up after completion

of the Witbank-Richards Bay railway line. Continuous miners and longwall shearers were introduced and increased emphasis was put on total extraction methods. All these factors resulted in changes in the mining methods. The productivity and the rate of production were increased dramatically and operations expanded into areas with more sandstone bands in the seams.

The increased risk of fatality could be due to the increase in productivity, annual explosion frequency or severity of explosions. The three aspects are tied together in the following way:

$$Risk\ of\ fatality = Productivity \times Explosion\ density \times Explosion\ severity \quad -1.4$$

where

Productivity- *Production per underground worker*
Explosion density- *Number of explosions per unit of production*
Explosion severity- *Fatalities per explosion*

The product of annual production and explosion density is the annual explosion frequency. By keeping all other factors constant, the influence of changes in productivity, explosion density or explosion severity can be obtained.

1.3.2 INFLUENCE OF PRODUCTIVITY IMPROVEMENTS ON RISK OF FATALITY

If productivity improves, each underground worker produces a larger volume of coal per shift or per annum and his exposure to the explosion hazard should increase accordingly. However, it was suspected that the increase in risk exceeded the increase in productivity but these needed to be determined. The average productivity calculated by dividing the annual average number of underground workers by the average underground annual ROM production is 1397 ton/man for the period 1950 to 1970. The same figure for the nineteen eighties increased 171 % to 3789 ton/man. See Figure 1.1.

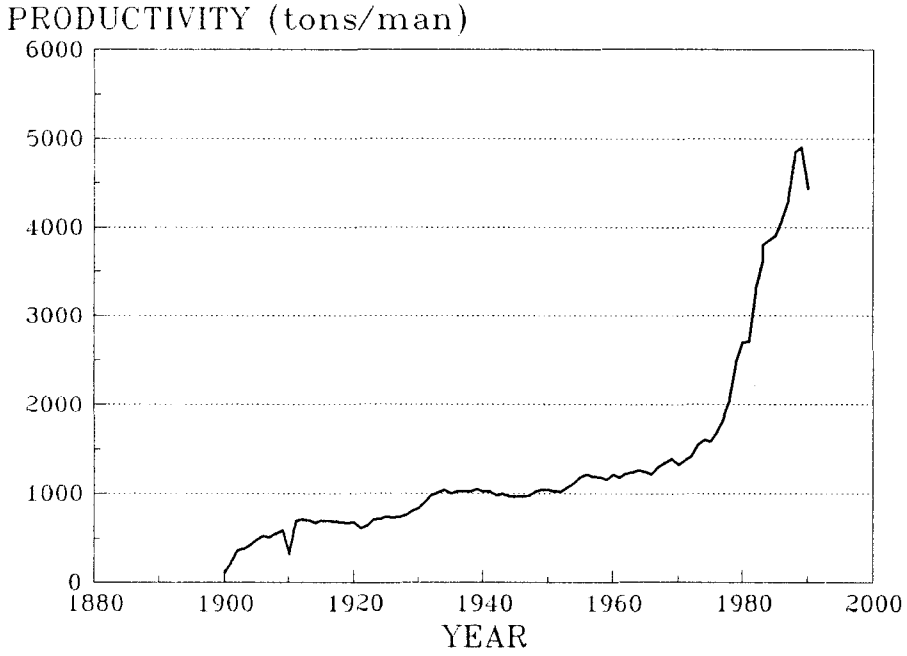

Fig.1.1. Labour productivity in South African underground coal mines since 1900 in tons/man/year.

Instead of using the product of two mean values, explosion density and severity, the mean fatality rate per tons is calculated directly by dividing the sum of fatalities by the sum of annual production for the period concerned. Since the figure is small, it is expressed as fatalities per million tons. For the first period the fatality rate due to explosions is 0.068 fatalities per million tons (and for the second period 0.0906 fatalities per million tons). The risk of fatality for the first period can be obtained by doing the following calculation:

$$\textit{Risk of fatality} = (1397\ \textit{ton/man}) \times (0.068/10^{6}\ \textit{fatalities/ton})$$
$$= \pm 1.00 \times 10^{-4}\ \textit{fatalities/man}$$

If the fatality rate is kept constant to calculate risk for the second period, a risk of fatality 2.58×10^{-4} is predicted. The actual risk of fatality for the eighties was

3.45×10^{-4}. Therefore, it appears that increased productivity was responsible for a substantial portion of the increased risk of fatality. The balance must be due to a higher frequency or severity of explosions.

1.3.3 ANNUAL EXPLOSION FREQUENCY

In the nineteen eighties there were on average 5.5 explosions per year, compared to the 2.6 explosions per year for the preceding three decades. It is fair to assume that a relationship exists between the level of coal production and the number of observed explosions. Considered against the background of the rapid increase in production, the explosion frequency of the last decade looks reasonable. The average annual production for the period 1950 to 1979 was 59 million tons, while between 1980 and 1989 an average of 190 million tons per annum was produced.

The mean number of explosions per million ROM tons for the first period under consideration was 0.0444, compared to an explosion density of 0.0324 for the latter period, an improvement of 27 %. To illustrate the consequences, an annual explosion frequency for the eighties is calculated by keeping explosion density constant. The expected annual explosion frequency for the nineteen eighties is:

$$\begin{aligned} Explosions &= (190\ million\ tons/year)*(0.0444\ explosion/million\ tons) \\ &= 8.4\ explosions/year \end{aligned}$$

Compared to the actual figure of 5.5 explosions per year, an improvement in the last ten years is obvious.

This downward trend in annual explosion frequency is a continuation of a prolonged trend that started early this century, brought about by the introduction of more effective safety measures to combat the hazard. Figure 1.2 shows the explosion density, that is the number of explosions per million ROM tons for every year since 1900. A downward trend is undoubtedly present.

Between 1980 and 1986, the USA had ± 0.04 explosions per million raw tons[14]. The UK had approximately 0.11 explosion/million raw ton produced over the same time,

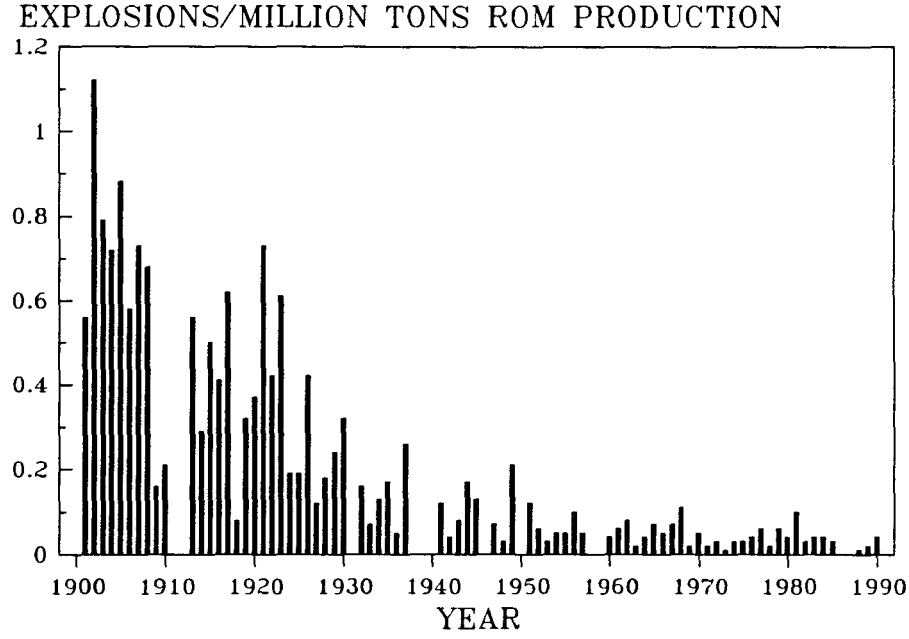

Fig.1.2. The number of explosion per million ROM tons on an annual basis for South Africa since 1900.

after a period of high incidence in 1980 and 1981 (17 and 28 explosions respectively). South Africa compares well with a figure of 0.03 per run of mine tons, but it is the severity of the explosions which is a cause of concern. For both the USA and the UK, the mean fatality rate per explosion is below one, compared to over three for South Africa. The USA figures were obtained from Sapko[18] and British figures from the annual reports of the Health and Safety Executive for Mines[19].

1.3.4 SEVERITY OF EXPLOSIONS

The average annual ROM coal production increased three fold in the last ten years compared to the preceding three decades, while the average number of fatalities due to explosions increased fourfold from 4 to 17 workers. An average of 1.57 workers died per explosion for the period 1950 to 1979, but in the last ten years that figure grew by 127 % to 3.57. This increase can either be due to more fatalities per explosion, or due to more frequent major explosions.

According to Nagy[20], prior to the passage of the Federal Coal Mine Health and Safety Act which regulates all aspects of mine safety in the USA, a "major explosion" was defined as one which caused five or more fatalities. This definition is still useful in separating more serious explosions from others when explosion statistics are investigated.

Using the same definition of major explosion, one notices that there were four major explosions in the nineteen fifties, two in the nineteen sixties, two in the nineteen seventies, but six in the nineteen eighties in South Africa. If these six major explosions are excluded, the mean fatality rate for explosions in the nineteen eighties is only 0.19 workers per explosion. This indicates that major explosions are responsible for most of the fatalities in recent times and that the increased frequency of major explosions is responsible for the abnormally high fatality rate.

To summarise, in recent times the risk of fatality has increased despite a reduction in the frequency of explosions. A sharp increase in productivity and in the severity of explosions are the reasons for this rise. Productivity improvements are responsible for a 57 % rise in risk, whilst the more severe explosions are responsible for 43 %. The actual growth in risk of fatality was 27 % less than what was expected, since the explosion frequency has dropped in recent times.

1.3.5 LOCATION OF EXPLOSION ACCIDENTS

The location of explosions is categorised into three broad classes:

1. Explosions originating in the working face or close to it
2. Explosions in accessible areas which include non-face working areas, and
3. Explosions originating in sealed-off areas or goafed areas

One explosion in the nineteen fifties and three in the nineteen eighties could not be classified. The sub-category abandoned areas also includes, apart from sealed areas, all explosions that occurred in pillar extraction sections where the explosion

was associated with the goaf. The relative division between the four classes and changes with time is shown in Table I.IV. Percentages are used to make comparison possible.

TABLE I.IV Percentage explosions per area of the mine over the last four decades. The actual number of explosions are shown in brackets.

PERIOD/ AREA	1950-59	1960-69	1970-79	1980-89
FACE	64 (7)	57 (16)	62 (13)	75 (38)
NON-FACE	27 (3)	40 (11)	10 (2)	8 (4)
ABANDONED	9 (1)	0	28 (6)	14 (7)
(UNKNOWN)	0	3 (1)	0	3 (2)
TOTAL	100 (11)	100 (28)	100 (21)	100 (51)

One notices that the face area is by far the most probable area for an explosion to happen and that the frequency of explosions in this area increased in the eighties. More explosions in recent times started in abandoned areas while the explosions in non-face areas dropped. Of the 169 fatalities due to explosions during the eighties, face explosions were responsible for 49 %, non-face explosions for 40 % and explosions in abandoned areas for 11 %. The explosions in non-face areas were therefore much more severe than explosions in other areas.

It is most important to point out that of the 47 face ignitions between 1980 and 1991, only the Bosjesspruit explosion on 30 March 1984 and the Durban Navigation explosion on 5 September 1991, both in longwalls, were in other than pillar type of mining systems. The difficulties of controlling the mining environment in a heading again exhibits itself in this observation.

1.3.6 SOURCES OF IGNITION

Sources of ignition are divided into five categories and analysed in a similar way as the location of explosions. The categories are: frictional, lightning, electricity, explosives and naked flames which include spontaneous combustion and heated surfaces. Table I.V summarises the analysis.

TABLE I.V Percentage of explosion per source of ignition over the last four decades. The actual number of explosions are shown in brackets.

SOURCE OF IGNITION	1950-59	1960-69	1970-79	1980-89
FRICTIONAL	0	4 (1)	33 (7)	61 (31)
LIGHTNING	0	7 (2)	19 (4)	6 (3)
ELECTRICITY	27 (3)	11 (3)	14 (3)	10 (5)
EXPLOSIVES	46 (5)	57 (16)	29 (6)	12 (6)
NAKED FLAME	27 (3)	15 (4)	5 (1)	2 (1)
(UNKNOWN)	0	6 (2)	0	9 (5)
TOTAL	100 (11)	100 (28)	100 (21)	100 (51)

Frictional ignitions

The first frictional ignition in South Africa was recorded in 1968. Rapid mechanization followed, resulting in an increase in the use of cutting machines with a consequent increase in frictional ignitions. The emphasis on total extraction was responsible for the growth in the use of mining methods such as pillar extraction, rib-pillar extraction and longwall mining. The number of sealed and goafed areas increased accordingly. In these areas, it is suspected roof falls ignited methane by friction when layers of quartz rich stone, such as sandstone, collided with each other.

This ignition mechanism constitutes only 10 % of frictional ignitions, while the rest come from continuous miner picks (44 %), coal cutter picks (38 %) and from roof bolters (8 %). The resulting explosions are generally relatively weak and have been responsible for 13 deaths since 1980, although 48 miners have been severely burned, usually in their faces, necks and/or exposed limbs. The importance of this source of ignition as a safety hazard at the working face is shown in Figure 1.3.

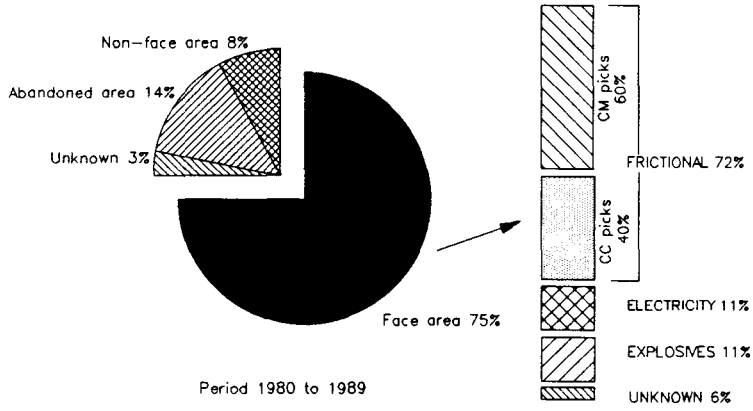

Fig.1.3. The location of explosions in South African collieries shown with the sources of ignition for the face area

Both Tideswell[21] and Ramsay[22] describe the increased importance of frictional ignitions with the introduction of mechanical power for cutting over the period 1950 to 1964 in UK coal mines. Between 1958 and 1964, for example, 66.1 % of all ignitions in headings or longwall faces were from frictional sources. Also, they found frictional ignitions less severe, but warned that large scale explosions such as the explosion at Easington Colliery (1951, 81 killed) should serve as a reminder of the seriousness of this source as a safety hazard. More recently, despite technological improvements to prevent ignitions of firedamp underground, for the year 1988/89 twelve ignitions took place in the UK[23]. All resulted from frictional sparking at the cutting tool. There were no injuries or fatalities.

Courtney[24] reports that the Mine Safety and Health Administration have indicated a general increase in the frequency of frictional ignitions in USA coal mines. Although he indicated that frictional ignitions are generally less severe, he reminds us that

the Novia Scotia explosion (1979, 14 dead) was caused by a frictional ignition from a shearer drum. It shows that internationally, ignitions due to friction of coal mining bits is a safety burden.

Other ignition sources

Lightning as a source of ignition has also become more chronic in South Africa. It is interesting to notice that this source of ignition has never been encountered in the working face area. Four ignitions in sealed areas, two in goafed areas, two in shafts and one in the mine workings were attributed to this source in recent years.

Increased mechanization requires the use of electricity in greater quantities. It is therefore surprising that electric ignitions have not become more common in recent years. The decrease in ignitions due to blasting and naked flame ignitions are encouraging.

1.3.7 INFLUENCE OF PREVENTATIVE TECHNOLOGY

Three years after the Glencoe Colliery disaster in 1908 in which 77 people lost their lives, an explosion safety committee was appointed by the then Minister of Mines, Minister F.S. Malan, and reported back to him in 1912[25]. The committee recommended improved safety measures such as lamp procedures, stone dusting, use of permitted explosives, improved ventilation and electricity.

Regarding stone dust, the committee states: "The British coal dust experiments conducted for the Mining Association of Great Britain by W.E. Garforth are well known throughout the coal mining world, and we had the additional advantage of obtaining the results of special tests of Natal coal dust made some two years ago" and "The practical use of stone dust in collieries is comparatively only just beginning, but will probably increase considerably". By 1930 it is clear from the report of the Inspector of Mines of Natal that in all fiery mines stone dusting has been carried out[13], illustrating the degree of sophistication that had been achieved.

If the mean explosion incidence figures of the first three decades of this century, during which the preventative measures were gradually introduced, are compared with the period since 1930, one observes that the average number of explosions per million tons fell from 0.42 to 0.06 explosions per million tons (standard deviations 0.28 and 0.05 respectively). Although this is a strong indication that the measures introduced do have a positive effect in curbing the hazard, refining of this practice is now necessary. For example, the exact amounts and regularity of stone dusting for most effective protection of collieries under South African conditions, are still unknown.

International proof exists that measures such as stone dust are effective. Tideswell[21] finds enough evidence from UK accident statistics to conclude that application of stone dust, more than any other factor, has been responsible for the great reduction in loss of life from explosions, since it was made compulsory in 1921.

1.3.8 ANALYSIS OF INDIVIDUAL EXPLOSIONS

In a recent study, Flint[26] analysed the official inquiries of selected incidence for each of seven main ignition sources leading to methane and coal dust explosions. The work is so extensive that it is unnecessary to pursue this avenue further. His more important conclusions are nevertheless briefly noted.

Flint views human errors resulting from carelessness, lack of training and experience, taking chances, deviations from mining practices and difficult economic conditions as the reasons for serious explosions. On the other hand ventilation, sealing of old workings, draining of methane from the goaf cavity, correct training and supervision of electricians and training of miners and mining engineers to attend to detail when using explosives are recognized as areas that need increased attention in South African collieries if safety is to be improved.

1.4 INTERPRETATION OF THE OBSERVATIONS

Regarding the drawing of conclusions from accident statistics, Wynn[27] states the following: "there are rarely any logical grounds for supposing that there is any simple linear relationship between a rational degree of belief in any conclusion and the accident figures. The proper criteria of belief must, in part, always remain a matter of opinion". In order to show clearly the relationship as drawn from this particular set of accident statistics, the observation is followed by the interpretation.

a. The technical nature of the South African coal mining industry changed dramatically in recent years.

   A general *re-evaluation* of tactics to combat the explosion hazard is required, to bring the preventative measures in line with the deteriorating geological conditions and new excavation and mining technologies.

b. The risk of fatality increased in recent years mainly due to two factors. Firstly, increased exposure as a consequence of improved productivity and secondly, the greater severity of explosions. Greater severity was brought about by the increased frequency of major explosions, rather than all explosions becoming more severe.

   The observed increase in severe explosions puts more emphasis on combating *explosion propagation.* Preventative measures should be optimised.

c. Severe explosions recently occurred in either abandoned or non-working but nevertheless accessible areas.

   The ways and means to *control the environment in abandoned and deserted areas* must receive special attention from mining engineers.

d. Evidence exists that protective measures do reduce the extent of the hazard, although measures such as the stone dusting procedure are not yet optimised for local conditions and might be inappropriate due to the recent changes in the nature of the industry.

   Suppression by agents and barriers must be tested for the South African conditions, since up to now the findings of studies performed on Laurasian coal formed the basis of our legislation and planning.

e. Three quarters of all explosions start in or close to the working face. The dominant source of ignition in the face is frictional.

   An understanding of the *explosive potential of the working environment and the role of ignition sources in the development of the explosion* should be obtained, in order to control the hazard triangle, that is, oxygen, fuel and an adequate source of ignition.

f. The human element continues to fall below the required standard of consistent and rigourous vigilance of all factors that can develop or contribute to unwanted events such as explosions.

   Training of miners and engineers to foster an awareness of the hazard and an expertise to control it is required.

This interpretations falls into three divisions. Firstly, prevention of propagation involves studies of the nature of the explosion itself. In other words, understanding and control of an explosion is looked for and can be classed as "post-ignition" research. Secondly, "pre-ignition" research, which investigates the environment before an explosion develops, is research aimed at the effective maintenance of the mining environment and conditions. Lastly, training communicates the latest knowledge to all involved in coal mining.

1.5 CONCLUSION

To return to the questions asked by a miner before going underground. His annual exposure of being involved in an explosion is approximately one in three thousand if the trend experienced in the eighties continues. This risk is significant if the recent experience of countries like the UK or USA is used as a norm. Compared to past experience in South Africa, his risk has increased. Effective protection measures are used, although he cannot be sure that these are optimised for the characteristics of the South African coals. In addition, awareness of his fellow workers regarding this hazard might not be of the standard that he would like to see.

Attempts should therefore be made to reduce the extent of the explosion hazard by obtaining a better understanding of the phenomenon through research, and to establish an ability to cope with the hazard through better and continuous training. Fundamentally, underground conditions should be controlled in such a way that explosions are not possible. For example, investigations of conditions surrounding excavation machinery at the working face should be carried out in order to establish the adequacy or inadequacy of such environments. However, if an explosion occurs, adequate measures should be available to extinguish it. Research aimed at stopping the explosion as soon as it develops should also continue, in order to refine protection measures to suit today's conditions.

1.6 THE PRESENT STUDY

The objective of this thesis is to study the "pre-ignition" conditions in the working face that might lead to an explosion. The probability of ignition of primary explosions at the working face is investigated. The risk of a primary explosion happening should be separated from the risk of a primary explosion initiating of a coal dust explosion. The explosive potential of the face environment is identified as the area of investigation. Any type of ignition, regardless of its potential extent, is considered undesirable.

In Chapter II the problem of an incomplete understanding of the explosiveness of the working environment is explained. The objective and approach of this study is further expanded upon.

CHAPTER II

EXPLOSION SAFETY OF THE WORKING ENVIRONMENT: STATEMENT OF THE PROBLEM

Pre-ignition research aims at avoiding the simultaneous presence of oxygen, fuel and a source of ignition. Early research investigations of the coal mine explosion danger, due to the presence at the coalface of combustible fuels, made use of explosive indices to categorise the coal dust and subsequently to apply safety measures. Discussed here is the inadequacy of indexing, since the explosion danger is not only determined by the material properties of the chemical substances involved, but also by the prevailing operational conditions. An approach involving both factors is explained and upon which the likely presence of hybrid mixtures of methane and coal dust is based. An incomplete understanding of the explosiveness of hybrid mixtures for South African conditions makes explosion safety control difficult, since it is unknown which combinations are likely to be dangerous. Having identified the problem, a hypothesis is stated, followed by the structure which the investigation will follow.

2.1 INTRODUCTION

Pre-ignition research is aimed at the effective maintenance of a mining environment in which no rapid flame can propagate. A combustion reaction requires fuel, oxygen and a certain quantity of energy to initiate the reaction. The combination of the three elements is known as the fire triangle, and if one of the three conditions is not met, a combustion reaction cannot take place. Bartknecht[28], when considering measures to prevent explosions, appropriately calls it the hazard triangle.

The challenge lies in breaking up this triangle. This can be achieved by replacing or removing the oxygen in the air, or by maintaining the fuel levels outside the flammability limits, or by control of all possible sources of ignition. In the mining situation, the oxygen cannot be replaced, since life must be supported in the working environment. Inertisation of the environment after ignition can be achieved by the application of stonedust, but this aspect can be considered to be post-ignition research. The pre-ignition circumstance allows only the ignition source and the fuel to be controlled.

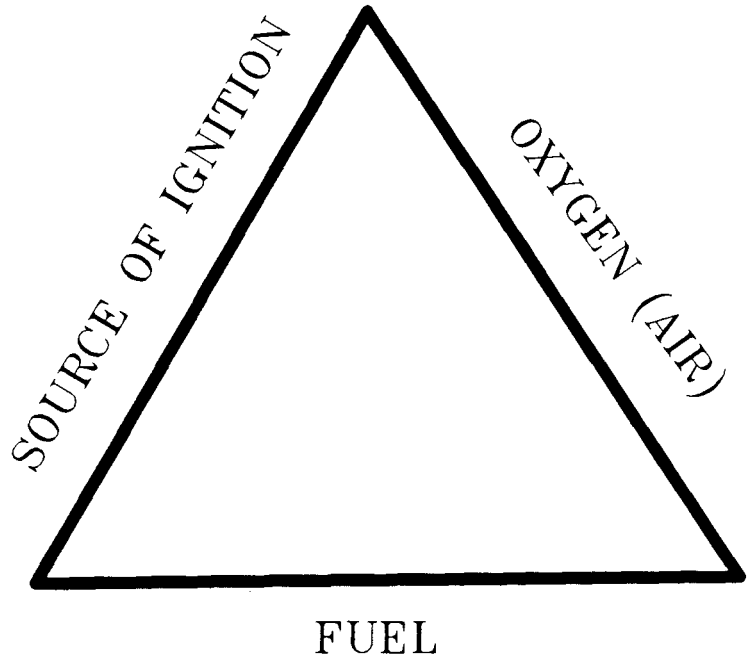

Fig.2.1. The fire or hazard triangle.

2.2 EXPLOSION RESEARCH PHILOSOPHIES

The development of an approach to pre-ignition safety is problematic, since the term "pre-ignition" embraces many disciplines. McQuaid[29] reviews notable technical milestones of the International Conferences of Coal Mine Safety Research Institutes since 1931. Amongst others, he mentions the work on permitted explosives, methane layering, ignition hazards from the use of diesel engines, flameproof electrical equipment, explosion research, methane outbursts and reliance on ventilation systems, which are all factors in achieving pre-ignition safety.

One notices a division of the techniques applied. Firstly, there are the techniques in designing machines and contrivances so that they are protected from potentially explosive environments or are safe when exposed to such environments. Secondly, there are ventilation techniques which are used to control and maintain the operational

environment within safe limits. This latter approach has put a great deal of emphasis on explosivity properties of the combustible materials. Explosive indices are a concise expression of these properties.

2.2.1 EXPLOSION HAZARD INDICES

Certain material properties related to ease of ignition, as well as the extent of explosion, have been determined and combined to give explosion recognition numbers.

Index of Explosibility

Cybulski[1] calls the percentage of incombustible solid matter which should be contained in a dust to make it incapable of propagating an explosion, the "degree of explosibility", denoted by the symbol S. An explosibility index Z, showing weight percentage of incombustible dust addition per unit of pure coal dust to prevent propagation, can be calculated as a function of S. Thus,

$$Z = \frac{S}{100 - S} \qquad -2.1$$

This index will change as particle size or operational conditions change, but is often used for comparative studies where the influence of a certain variable is investigated while others are kept constant.

U.S. Bureau of Mines Hazard Index

The U.S. Bureau of Mines in the early nineteen sixties developed a method of indexing dusts according to their explosibility. The index combines material properties in relation to ease of ignition and potential explosion violence, reflecting an emphasis on controlling both the ignition source and the fuel.

Palmer[30] explains the index as the product of explosion sensitivity and explosion severity of a dust, both ratios having been obtained by comparing various explosibility measurements of the dust with the values obtained in the same tests using a standard dust, for which a Pittsburgh coal dust was used.

$$Index = IgnitionSensitivity \times ExplosionSeverity \qquad -2.2$$

The ignition sensitivity was defined as the ratio of the products of minimum cloud ignition temperature T_{min}, minimum spark ignition energy ϵ_{min} and minimum explosive concentration C_L of the standard dust to the sample dust.

$$IgnitionSensitivity = \frac{(T_{min} \times \epsilon_{min} \times C_L)_{Pittsburgh}}{(T_{min} \times \epsilon_{min} \times C_L)_{Sample\ \ dust}} \qquad -2.3$$

The explosion severity was defined as the ratio of the products of maximum explosion pressure p_{max}, and the maximum rate of pressure rise $\left(\frac{dp}{dt}\right)_{max}$ of sample dust to the standard dust.

$$ExplosionSeverity = \frac{\left(p_{max} \times \left(\frac{dp}{dt}\right)_{max}\right)_{sample\ \ dust}}{\left(p_{max} \times \left(\frac{dp}{dt}\right)_{max}\right)_{Pittsburgh}} \qquad -2.4$$

Explosibility indices less than 0.1, between 0.1 and 1.0, between 1.0 and 10 and above 10 were classified as weak, moderate, strong or severe explosions respectively. The entities used for determining the index are determined under fixed conditions, therefore should conditions change, the indicated value will also change. The casual combination of variables led to meaningless units contained in the index. Also, the assumption was that the explosibility of one dust can be compared to that of a known dust, and in this way used in assessing the explosibility hazards of a new material. This was not totally convincing and the index has fallen out of favour in recent years.

The Staub Constant

Bartknecht[28] reports that experiments with a number of dusts have shown that:

$$\left(\frac{dp}{dt}\right)_{max} \times V^{\frac{1}{3}} = K_{st} \qquad -2.5$$

where V is the volume of a closed vessel

K_{st} is a constant

This expression is also known as the "cubic law", making it possible to compare explosion in small vessels with that in large vessels. The large number of dusts handled in industrial operations led to a classification into dust explosion hazard classes, depending on explosion violence expressed by K_{st}. Protection measures, such as explosion vents, are required according to the class of dust handled. The hazard class is therefore a statement on the explosion violence only, and does not reflect sensitivity or probability of an explosion.

The Explosion Constant

The explosion index K_{ex}, which originated in Germany, has been used for a long time in South Africa to express coal dust explosibility. K_{ex} is a development from the K_{st} index in that a material property constant is used to categorise the severity of the hazard associated with the material. Since K_{st} is used for industrial dusts, which are usually chemically and structurally homogeneous, and where the dust is already dispersed, the classification of coal mine dust according to this index is not appropriate. At the BVS in Germany, Helwig[31] observed severe pulsations from propagating coal dust flames in a 200 m long explosion gallery. He concludes that coal dust differs from industrial dust in that it possesses a much more complicated structure and is less homogeneous in particle size. This affects the propagation of a coal dust explosion.

The propagation of an explosion is dependent on the rapidity of expansion of gases during combustion in order to create strong enough movement of air ahead of the combustion zone to ensure dispersion of dust. The dust must also be sensitive enough so that the radiation from particles in the flame front can ignite the dust cloud sufficiently quickly to sustain the expansion of gases. Again, both an element of severity and sensitivity is present.

K_{ex} is calculated as follows with the nomenclature shown in Figure 2.2:

$$K_{ex} = \sqrt{\left(\frac{dp}{dt}\right)_{max} x \left(\frac{dp}{dt}\right)_{avg}} \qquad -2.6$$

where $\left(\frac{dp}{dt}\right)_{max}$ indicates expansion rate

and $\left(\frac{dp}{dt}\right)_{avg}$ represents swiftness of ignition

If the particle size, dispersion mechanism, ignition source and vessel geometry are kept constant, an index is created against which the reaction of the different materials in an unchanging environment can be judged. Through parallel testing in the 40 l explosion vessel and a 200 m surface gallery, dusts with a K_{ex} value below 7 MPa/s were observed not to propagate beyond the coal zone in a German explosion gallery. The index is a valuable scientific instrument to use when the role of the fuel in an explosion is studied. Other work involving studies of suppressants or inhibitors and hybrid mixtures of methane and dust can also be evaluated using K_{ex}.

Material Properties and the Operational Environment

Explosibility indices, when used as expressions of the potential hazard in any mining situation, are now recognized as being incomplete[32]. The hazard potential is not only determined by the explosivity properties of the dust, but also by the conduciveness of the operational environment to host an explosion. Underground operational conditions are determined by many variables, the combination of which differ in

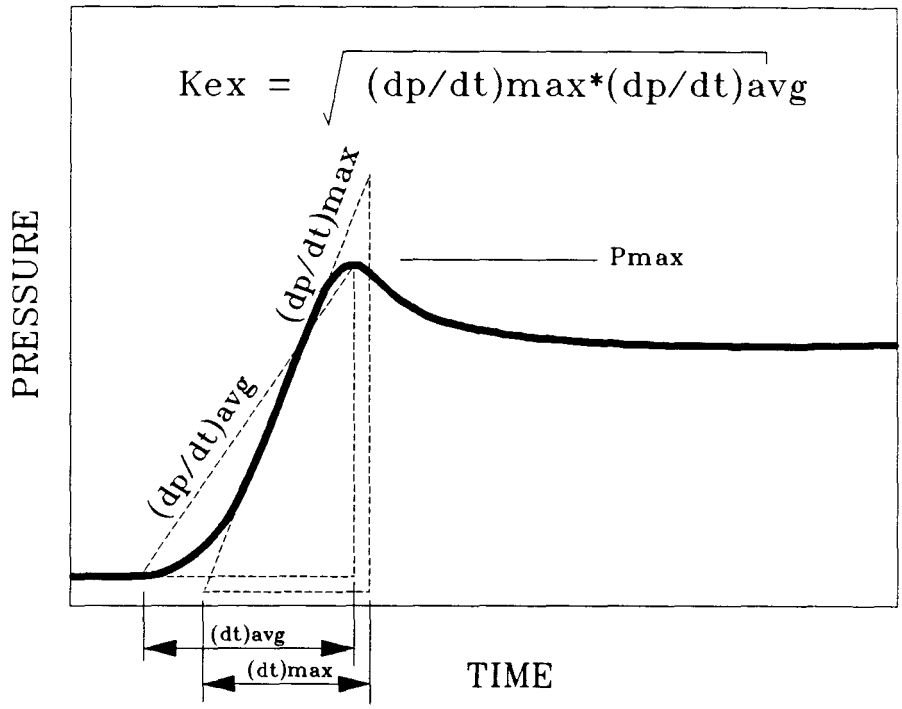

Fig.2.2. Graphical representation of the K_{ex} explosibility index.

time and location. The more complete approach to hazard potential analysis should therefore include both the intrinsic flammability properties of the dust under consideration and the relation of those properties to the operational environment.

2.2.2 A MODERN APPROACH TO EXPLOSION HAZARD RESEARCH

In 1987 Hertzberg[32] recognized the need to develop a new hazard evaluation method that is more realistic and reflects the real world. He bases his approach on the probability of the simultaneous existence of conditions that might lead to an explosion. The dust must be dispersed and mixed with air, with a concentration above the lean limit of flammability in the presence of an ignition source of sufficient power density.

From the hazard triangle it is clear that the probability of an explosion should be the product of the probabilities of oxygen, fuel and a source of ignition being present. Since it is required to maintain life underground, the probability of air being present is unity. The likelihood that fuel will be present above the lean limit of flammability equals the probability of methane being present above the lean limit of flammability, or of dust being dispersed above the lean flammability limits for the dust.

For dust, Hertzberg states that the probability of an explosion occurring *P(expl)* can be quantified in terms of the product of the probabilities of dispersion *P(d)*, the probability that the dispersion is above the lean limit of explosibility for the dust $P(f_d)$ and the probability of an ignition source being present P(i).

$$P(expl)_{dust} = P(d).P(f_d).P(i) \qquad -2.7$$

Mine explosive gases differ in the sense that, once the flammable mixture is generated, the mixing is intimate and will not easily resegregate. Dust, on the other hand, will resegregate. *P(expl)* for gas being present is therefore the same as for dust, but *P(d)* should be replaced by *P(m)* which is the probability of the gas to mix instead of forming a layer.

The mechanised excavation of gassy seams inevitably leads to the simultaneous dispersion of methane and coal dust into the environment surrounding the mining machine. It is proposed that the above expressions should be modified so that

$$P(expl)_{hybrid} = P(d).P(m).P(f_{m+d}).P(i) \qquad -2.8$$

where $P(f_{m+d})$ is the possibility that the combination of methane and dust can form an explosive mixture, even if both are below their lower flammability limits.

To illustrate the probability approach, consider the following example. If a mine contains a coal dust loading on the floor, sides and roof that will be flammable when dispersed, $P(f_d)=1$. If face ignitions occur once in every three years, then

$$P(expl)= P(d).1.1/3$$

and depend on the probability that the face ignition will disperse the dust. This superficial treatment of the probabilities involved is obviously inadequate. It serves though as a point of departure in assessing the explosion potential of working faces, combining the flammable properties of the fuel and their relation to the operation.

2.2.3 A RESEARCH APPROACH FOR THIS STUDY

The approach this study will follow is first to obtain an understanding of the normal quality and the deviations from that norm of the volume of space around mining activities. Instead of trying to predict the probability of the simultaneous presence of oxygen, fuel and ignition sources, possible combinations of the three elements of the hazard triangle will be simulated in the laboratory and its hazard potential assessed. Mining engineers can then control the operational environment in such a way that the combinations that proved hazardous are avoided.

2.3 QUALITY OF THE OPERATIONAL ENVIRONMENT OF THE COAL WORKING FACE

The rapid growth of mechanization in the South African coal mining industry in the mid-seventies resulted in modern and improved techniques of mining, substituting old for new problems. The industry is in an ongoing process of replacing labour with technology of mechanization. The greater volume of coal produced by a single person increases the exposure to mining hazards such as accidental explosions. Mechanization, with a consequential increase in production rates, intensifies ventilation problems such as pollution by methane and dust.

A pressure differential across two access points to the mine, produced by the main ventilating fans, results in a ventilation flow in the workings of the mine. The ventilation current is used as a medium to remove and dilute pollutants such as unwanted gases, dust and heat. Brattice and auxiliary fans are used to direct air into areas of air stagnancy, where no through ventilation has as yet been established. With high production rates, the ratio of volume flow of fresh ventilation to pollutants being dispersed into the air becomes excessive, and may become the limiting factor to high output. This explains the role of dust suppression devices and techniques such as pre-mining methane drainage of coal seams.

The prediction of methane and dust levels on the working face is complex and as yet incomplete. In general, studies have been conducted separately for methane and dust, due to the difference in their physical nature. For both, the amount of the pollutant per output unit is required, so that enough ventilation can be provided to maintain safe conditions.

2.3.1. THE PRESENCE OF METHANE IN COAL MINES

The presence of methane in underground excavations is a consequence of its presence in a wide variety of geological environments. The primary sources are bacterial decay in marsh and lakelands, petroleum, coal and carbonaceous shales. Large quantities are also present in the oceans, in solution, in ocean sediments or as solid gas hydrate[33]. In gold, coal and diamond mining in South Africa methane is known to be present and the Karoo Sequence is considered as the primary source.

Methane generation

Edwards and Durucan[33] have revealed that the organic content of sedimentary rocks may vary from one percent for chemically deposited sediments to almost 100 %, as is the case of coal. Less than 1 % of the total is accounted for by coal deposits which, upon breakdown, are methane source rocks. Source rocks consist mainly of

organic clays, shales, carbonate muds and coal seams. The gas transfers or migrates to other rocks with relative low porosity and permeability, explaining why methane is probably the most abundant gaseous fluid found in the earth's rocks.

Coal related methane was initially generated during coal formation in aqueous environments in the southern hemisphere in late Carboniferous or early Permian periods. Near surface it is produced by bacterial decomposition of organic matter, and after burial by thermochemical degradation during coalification. Only a small proportion of the methane formed per ton of coal during coalification is retained, the rest having been lost to the atmosphere, dissolved in groundwater or migrated to surrounding reservoir rocks. Approximately one to 10 % of gas content of the nearest coal seams is found in neighbouring rock.

Factors Influencing the Emission of Methane into the Operational Environment

A relationship between gas emission (m^3/ton) and coal output exists. The following factors contribute to the emission pattern.

Basic Gas Content

The quantity and rate of gas emitted during mining is dependent upon the initial amount of gas in the coal seam worked and the adjacent disturbed strata, according to Jolliffe[34]. Stripp[35], in a study of methane emission characteristics of South African coals, reports that methane absorption characteristics of South African coal are suitably described by the Langmuir equation, but he finds the Langmuir constants to be lower than reported for other coals [Langmuir equation; $Q=(K_1.K_2.P)/(1+K_2.P)$, Q-volume absorbed per ton, P-pressure and $K_{1\&2}$ the Langmuir constants]. Also, in-seam gas pressure was found to be considerably lower than similar measurements reported in overseas coal seams.

These observations might explain why the measured in-situ gas content of South African coal is lower than that reported for the UK and the USA. For example, a

gas content of 6.6 m^3/ton is obtained for Majuba coal in the Eastern Transvaal which is considered very gassy by South African standards, compared to 14 m^3/ton to 21 m^3/ton for coal seams in the UK - Kavonic[36]. South African coal methane content is seldom above 10 m^3/ton, and usually lies between 1 m^3/ton and 14 m^3/ton[37].

Rate of Gas Emission

Tests done by Pickering[38] on ten South Nottinghamshire coals show a high initial release occurs in the first 20 seconds after breakage. Airy, as reported by Jolliffe[34], shows that it takes 36 hours for half of the sorbed methane to desorb from a 6 to 13 mm mesh coal sample. The emission rate characteristics will differ for various coals, with an important consequence on ventilation and face safety. The higher the initial emission rate, the more hazardous the environment.

The perceived amount of methane emitted from a seam being worked will differ from the absolute gas content and is regulated by the rate of emission. The perceived amount can be assessed from the output per week and the difference between the in-situ gas content and the gas content obtained from the coal as it leaves the mine. An additional portion should be added, which is methane coming from old pillars, unworked and goafed areas.

Geological Factors

In the planning of mines, departures of the normal expected emission rate must be allowed for, since geological features such as gas outbursts, any changes in coal properties, pocketing by convergence of strata et cetera, are likely.

Barometric Variations

Gas emission into the bord and pillar workings, studied at the Ermelo colliery in the Eastern Transvaal by Stripp[35], was not significantly affected by the natural

barometric pressure. Unnatural causes such as fan stoppages did influence methane levels. He noted, nevertheless, an erratic emission pattern, probably explained by pockets of methane commonly encountered in roof cavities in pillar extraction sections. In monitoring methane drainage work at Majuba colliery in 1990, Kavonic[36] could not present any conclusive correlation between barometric pressure and methane emission. Jolliffe[34] found that in 63 % of the five drainage systems he studied, increases in methane had been associated with severe falls in barometric pressure.

Other factors

The retention time of methane in the mine can bring about a lag between a significant output change and its reaction on total gas emission. From the holiday periods monitored by Jolliffe[34], he concludes the response in emissions was evident two to three weeks following the change in output.

Daily variations due to goafing or derangements of ventilation patterns are common. It is these daily variations which are of great importance, since many incidents involving mine gases are frequently linked to these kinds of contingencies.

Methane Liberation Patterns

The actual and specific effectiveness of the ventilation design on a mechanised working face can best be judged from investigations of methane liberation patterns around machinery during mining operations.

Cecala, Jankowski and Kissill[39] determined such liberation and flow patterns around the shearer during longwall mining on two USA faces. Both were ventilated from head to tail. Figure 2.3 shows airflow patterns around the longwall shearer as well as the methane levels at the head of the shearer for both cut directions. The average head-to-tail pass was 0.72 % and for the tail-to-head pass 0.53 %. It was found that

substantial dilution was occurring downstream from the shearer. Cecala et al also noticed an almost doubling of methane levels during goafing. Methane levels were highest at 2 % when passing chock five while cutting the headgate.

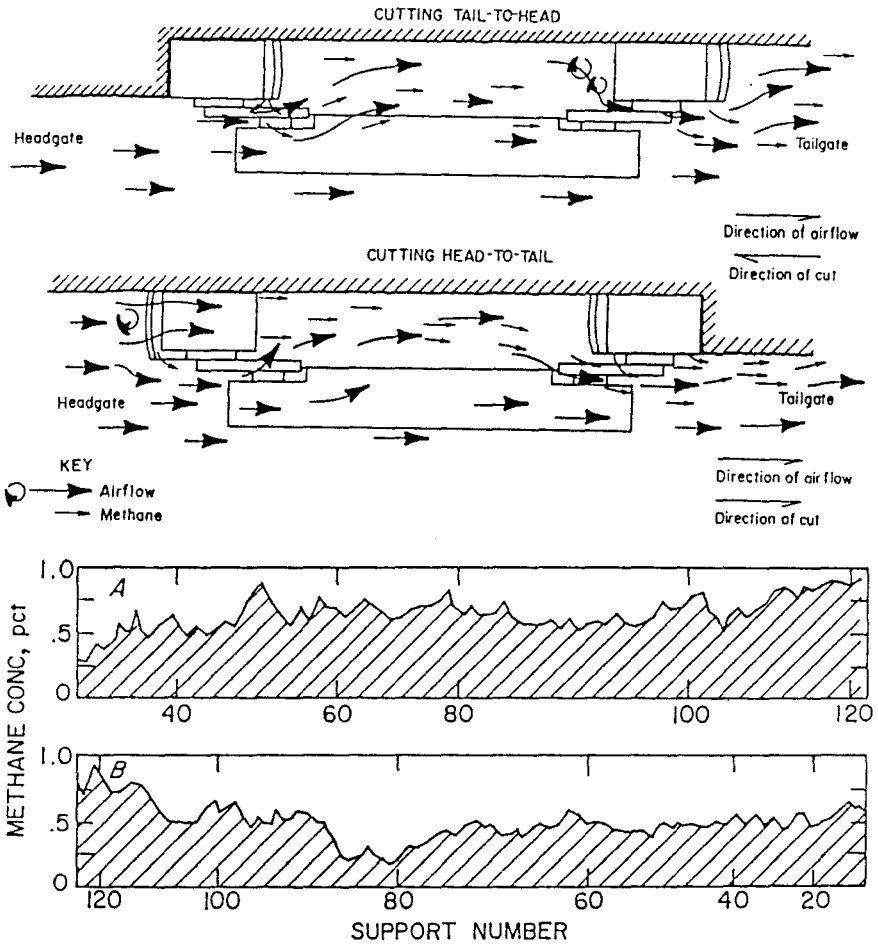

Fig.2.3. Airflow patterns around a longwall shearer (top) and the methane levels for both cut directions (bottom), according to Cecala, Jankowski and Kissell[39].

For the second face investigated, methane built-up gradually along the face from head to tailgate increasing by almost 0.5 %. Absolute methane levels also increased

as the day progressed, reaching a level of almost 1 % at about 12 noon. Methane was not liberated as quickly as in the first face by the cutting action, but was emitted almost uniformly along the face and floor.

These two situations, by no ways representative, illustrate that each face and situation is unique and that background methane levels vary substantially.

Unfortunately, continuous monitoring of methane levels around the cutting drum of a continuous miner has not been undertaken in South Africa or elsewhere. Work has been done by Meets[40] to determine the effect of airflow on methane and airborne dust in advanced bord and pillar headings. Methane and dust concentrations are not given, since the study was concerned with air movement velocities for the different ventilation arrangements in an advancing heading. Figure 2.4 shows selected illustrations from the findings. It is clear that some areas in the complex and continually changing geometry of a mechanized heading can suffer from air stagnancy and that this area is more than likely the working face.

As a continuation of this work, Meyer[41] investigated the effect of the last through road air velocity on the depth of air penetration in bord and pillar headings with no auxiliary ventilation. The airflows were simulated on a computer and in order to see if the results would apply in the underground situation field investigations were also undertaken. Again this work shows areas in the working face where air movement can be very slow.

Joubert[42] has undertaken continuous methane monitoring of each face in two bord and pillar sections at Indumeni colliery in order to study the relationship between weather patterns and methane emission. Eleven faces were monitored for sixty days between 25 April 1969 and 28 June 1969. Results of one of the faces with the highest methane levels are averaged and summarised in Table II.I. Joubert[43] also studied return airways in which average methane content has been shown to be far below

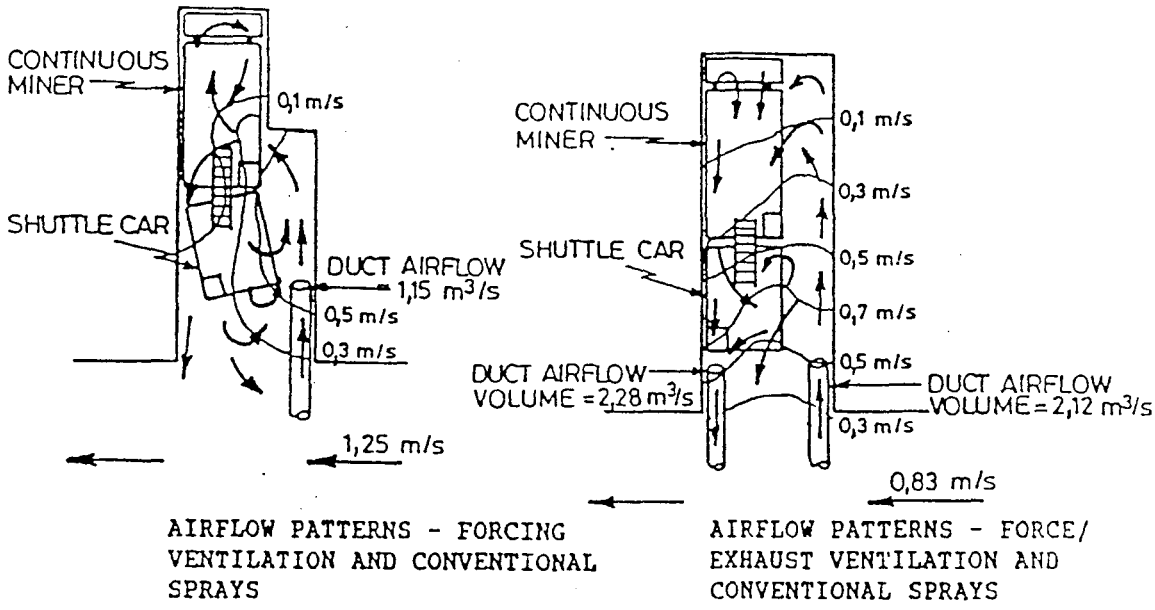

Fig.2.4. Airflow patterns for different ventilation arrangements for mechanized bord and pillar headings . Meets[40].

1 %. Stripp[35] contradicts this observation by showing average methane levels can be very high in return airways and, in a limited number of observations, methane was seldom below 1 %.

Neither of these two researchers could obtain correlation between methane emission and barometric pressure, temperature or humidity. The figures serve to illustrate that, although on average methane levels are at safe levels, they can increase far above the 1 % mark for short periods.

As accident explosion records indicate, levels above 5 %, the lower flammability limit of methane, are reached on occasion. Since the molecular size and density of methane and air are of the same order, once mixed resegregation is unlikely.

TABLE II.I. Summary of methane monitored during investigations at Indumeni Colliery in Northern Natal in 1969 by Joubert[42], six Natal collieries coded A to F by Joubert[43] and Ermelo Colliery by Stripp[35] in 1989.

COLLIERY	PERIOD	MINIMUM	MAXIMUM	MEAN
Indumeni	25/04/69 to 28/06/69	0.4 %	2.0 %	1.3 %
A to F	10 to 20 Samples/mine	0.0002 %	1.7 %	0.02 to 0.57 %
Ermelo	10/01/89 to 27/01/89	0.7 %	4.0 %	1.5 %

2.3.2 THE PRESENCE OF COAL DUST IN COLLIERIES

In order to assess the explosion hazard, the influence of coal dust particle size is important since the explosion violence decreases as particle size increases. Helwig[31] studied the influence of particle size on explosibility in great detail and found that the optimum particle size for explosion development depends on the type of coal. For example, optimum particle diameters for a semi-anthracite are 10 μm to 20 μm, a low rank bituminous coal 20 μm to 60 μm and high rank bituminous coal 10 μm to 40 μm.

Reeh[44], in contrast to Helwig[31], found no optimum particle diameter and states that a limiting particle diameter above which a coal dust explosion is no longer possible cannot be defined. If fine dust is added, coarse-grained material becomes explosive if the fines are of sufficient concentration. Cybulski[1], who as a result of experience gained over many years, states that all comminuted particles passing a 1 mm mesh sieve can be regarded as dangerous from an explosibility point of view.

Formation of Coal Dust

Coal excavation is inseparable from the formation of coal dust. Coal dust is formed during coal winning, whether mechanized coal breaking or explosives are used, and during loading, crushing and transport of coal. Roof falls, goafing and strata movements all add to dust formation. Modern excavation machines create large quantities of dust in short periods of time due to the high excavation rate. Zipf and Bieniawski[45] explain fine-fragment formation during coal/cutting tool interaction as a four step process. First, the development of a crush zone under the tool tip, then micro-crack propagation, followed by shear movement along macro-cracks and finally additional fragmentation from shear. For cutting machines, crushing and shearing are therefore the major dust forming mechanisms and are unavoidable during excavation.

Quantities of Dust Formed During Mining.

The quantities of dust formed will depend on the inherent dustiness of the coal as formed by the in-situ fracture process of coal seams, the coal properties themselves and the nature of the technological process used to excavate the coal. Generally it is believed that the softer the coal, the larger the quantity of dust produced. However, the hard coal seams of South Africa give rise to very high dust counts, and this makes it difficult to be definitive.

Cybulski[1] speaks of 0.8 % to 1.2 % of the coal seam being reduced to coal dust when cutter loaders are used, and says the figure will be less for explosives mining. Hurysz, as reported by Cybulski[1], found that 50 % of fine coal dust is produced during coal getting, 13 % during transportation, and the rest from mechanical preparation. The fraction of this dust that is dispersed into the air stream is unknown, although much work has been done on respirable dust. Kachan, Kocherga and Kolchinskii[46] did dust counts on the total size spectrum for mines in the Donbass basin in the Ukraine. Specific dust counts were found to be 4.6 g/m^3 to 12.3 g/m^3

at a distance of 0,5 m from the face, with 19.8 g/m^3 to 25.8 g/m^3 being the maximum. With watersprays the dust concentration around the cutting pick remains high at 9.2 g/m^3, but falls to 0.4 g/m^3 to 3.6 g/m^3 when 0.5 m from the face.

Kachan et al are of the opinion that without water sprays in the zone of rock removal, strongly explosive mixtures of dust and air always exist, and in most cases this can extend 1.5 m to 2.5 m from the face. Jankowski and Organiscak[47] showed the relation of operational conditions and activities to dust generation on longwall faces. Five primary dust sources were identified, which are the intake dust, coal transport, support movements, coal cutting and shearer flitting and clean-up. Depending on the mine studied, shearer cutting contributed 47 to 60 % of dust generated, and stage loader operations up to 64 %. Drum speeds and the way watersprays were applied also played an important role.

The conclusion is that dust concentrations at, below or above the lower explosibility limits of the dust are likely in the working face. The behaviour of the dust in air is different from that of methane since the mass density of the solid dust particles is a factor of a thousand greater than the air into which they are dispersed. Gravitational force tends to segregate the dust from the air and causes them to settle on surfaces in roadways.

2.4 STATEMENT OF THE PROBLEM

It has been shown that the concentration of methane and coal dust can vary substantially in the space around excavation activities. The level of these concentrations is both a function of the properties of the coal seams and surrounding strata, as well as the effectiveness of the ventilation provided and the effectiveness of suppression in the case of dust. The physical nature of the rock environment changes continually as the face advances. At the same time, activities and events within the mine can change ventilation quantities, water pressures, air velocities, et cetera.

A combination of such changes can result in a sudden increase in dust or methane levels on the working face. Although no work is allowed when methane levels are above 1.4 % by volume in South African collieries, in mechanised conventional mining continuous monitoring of methane is not practised. Although continuous monitoring methanometers are mounted to continuous miner booms, the number of frictional ignitions shows that this method is not foolproof.

It is known that methane, mixed with coal dust, does reduce the minimum explosive limits of methane. The explosive nature of these mixtures on the working face is not well known, especially for South African conditions. The increased use of electricity at the working face, as well as the use of explosives and mechanised excavation techniques, incorporates possible ignition sources into the working environment.

When studying pre-ignition environmental conditions which can be conducive to host an explosion in the working face, three questions of importance can be asked. They are:

1. Is the combustible component of the environment below the lower explosibility limits for individual fuel components or that for combined hybrid mixtures?

2. How sensitive are combustible mixtures, when present, to ignition?

3. What potential exists for a coal dust explosion to be propagated, should an explosible mixture ignite?

Although these issues are well researched with regard to both pure methane and pure dust, it is not so for hybrid mixtures of methane and coal dust. In particular, sensitivity of heterogeneous mixtures is not fully understood. The probability of such mixtures being present around the cutting drum of a continuous miner or shearer is high. Ventilation arrangements for working environments should consider

the explosibility and sensitivity of such mixtures, and if the likelihood of ignition is high, the composition of the mixture should be changed by additional measures such as increased ventilation, methane drainage or dust suppression methods.

The rate at which energy is generated by hybrid mixtures is also not clear, making it difficult to judge the possibility of such an ignition propagating itself within the face area. If propagation within the face area is possible, it is also necessary to know what the ability of the explosion is to initiate and propagate a violent coal dust explosion. From experience of frictional ignitions it seems that, in this case, propagation is unlikely, although exceptions such as the coal mine explosion at No 26 Colliery in Nova Scotia on 24 February 1979 led to 14 fatalities, caused by a shearer drum - Courtney[24].

An incomplete understanding of face environmental conditions with regard to their explosiveness, results in an equally incomplete assessment of pre-ignition safety and this may well facilitate an occurrence which leaves property and lives at unacceptable risk.

2.5 OBJECTIVE OF THE STUDY - A HYPOTHESIS

The objective of the present study is to obtain the explosible limits and sensitivity to ignition of hybrid mixtures of methane and coal dust at the working face of a typical modern mechanised face in bord and pillar mining. A comprehension of the ability of such mixtures to propagate beyond the cutting zone, or to initiate the development of an extended explosion or flame from the initial ignition zone, is also required. The combined knowledge of the likelihood of ignition and chance of initiation of explosive heterogeneous mixtures will delineate a volume within the methane-dust-energy plot, where operational environments within this volume are undesirable, and those outside are clearly preferable.

This three dimensional space, which combines methane concentration in air on the one axis, coal dust concentration on the other, and ignition energy on the third, is analogous to the thermodynamic state of a substance in a pressure-volume-temperature space. The surface to be determined should separate mixtures that can ignite and initiate from those that cannot ignite, or can ignite but not initiate, or initiate but are not likely to ignite due to high ignition energies, and this will be called the ignition blanket. The ignition blanket will change as the thermodynamic state of the substances under review also change, but for this study only the narrow band of pressures, temperatures and densities under which coal mine faces normally operate, will be considered.

Once the ignition blanket is known, the mining engineer can manipulate the variables of the ventilation design in order to ensure that the operational environment is safe.

The following hypothesis can be used to summarise the above argument; *the position of the ignition blanket in the space formed by methane concentration levels, dust concentration levels and possible ignition source intensities, must be determined in order to delineate the conditions under which coal mining can resume and proceed in absolute safety and without risk of an explosion endangering life of property.*

2.6 STRUCTURE OF THE INVESTIGATION

In chapter three, the thermal explosion theory according to Semenov and variations thereof will be considered. Ignition and combustion of methane, coal dust and hybrid mixtures of methane and coal dust are explained. Chapter four discusses the state of understanding of frictional, explosive and electric ignition of explosive mining environments. A quantitative interpretation of theory as applied to the problem of face ignitions is treated in chapter five. In chapter six the rationale behind the selection, design and operation of the equipment for experimentation is discussed. Chapter seven contains the results of the experimental programme, namely the ignition properties of mine atmospheres. Chapter eight illustrates that the obtained

data follows to some extent the explosion theory. Measurements of the actual face environmental conditions and their relation to the ignition blanket follow in chapter nine. Conclusions on pre-ignition safety of the working face are given in the final chapter.

CHAPTER III

IGNITION AND INITIATION THEORY

This chapter establishes the theoretic foundation of the investigation. The Thermal Explosion Theory, as interpreted by Semenov and Frank-Komenetskii, is reviewed. The process whereby a reactive mixture leads to an explosion, or the explosion mechanism, is explained. The explosive behaviour of the two principal fuels encountered in coal mines, namely methane and coal dust, is reviewed. Finally, the behaviour of these two substances in combination is investigated.

3.1 INTRODUCTION

The combustion of methane or coal arises from an interaction of chemical and physical processes. Combustion is initiated by the exothermic reaction of the fuel component and an oxidant. The reaction is sustained as long as the rate of energy delivery of the reaction is in excess of the summation of energy loss and initiation energy required for dissemination of the flame. According to Barnard and Bradley[48], in chemistry combustion commences with the occurrence of a self supporting exothermic reaction which provides a source of energy at a rate determined by the prevailing temperature, pressure and reactant concentrations. The transport of energy and matter are the most important physical processes involved.

When most of the heat produced by the reaction is dissipated to the environment in which the reaction takes place, such as the walls of an explosion vessel, a steady state is established and the reaction proceeds smoothly to completion. This reaction is referred to as *slow combustion*, describing phenomena such as spontaneous combustion or combustion in furnaces for energy generation. When the system is physically more isolated from the surroundings, temperature rises to a critical limit where the rate of heat loss is exceeded by the rate of heat generation. This critical temperature depends on the physical properties of both the reactants and the container or surroundings. This condition allows the reaction rate to accelerate indefinitely, leading to an *explosion.*

The state at which self-acceleration is established is called *ignition*. The temperature at which this takes place is the self-ignition temperature. When the energy is released in the form of heat, a thermal explosion has taken place. A chemical energy release in the form of active intermediate substances, leading to more exothermic reactions, is called branching-chain explosions. Baker et al[49] state that most high temperature gas phase explosions are chain branching in nature, but the majority of explosions which result in hazardous behaviour in industrial environments can be adequately treated using the thermal explosion theory.

In coal mine explosion research, coal dust explosion propagation refers to the process of ignition and dispersion of dust ahead of a flame, to sustain that flame in its path as it is channelised along the tunnels of the mine. The ability of flame to spontaneously propagate through a mixture of explosive substances must not be confused with the latter. For flame to propagate spontaneously through an already dispersed mixture, for example, may require much less energy than a flame responsible for the dispersion of its own fuel.

For spontaneous propagation of flame through a dispersed fuel-oxygen mixture, the exothermic reaction must only provide enough heat to ensure that ignition of the still unburnt dust cloud takes place. For a coal dust explosion to propagate, where dispersion must be achieved ahead of the flame, the chemical reaction must be so exothermic that the expansion effect will be rapid enough to cause dispersion of dust ahead of the flame, but then the reaction must also be so radiative that ignition is ensured ahead of the flame.

In order to prevent confusion between spontaneous flame propagation through an already explosive mixture, and propagation of a coal dust explosion along a mine tunnel, the term *flame dissemination* will be used when referring to the former situation. It is important to understand that even if a mixture allows flame dissemination, coal dust explosion propagation is not necessarily ensured.

The ignition path, established by the combination of the chemical thermodynamics and chemical kinetics of the combustion reaction, is treated here to lay the foundation for investigating the ignition process as presented in the mining situation. The explosive mixture is referred to regularly in this work, and can mean either methane, coal dust or a hybrid mixture of the two within the explosive concentration range.

3.2 IGNITION THEORY

When a volume containing an explosible mixture undergoes a change in temperature, volume or pressure, the state of that volume can become suitable for the fast combustion of the chemical substances it contains. The ignition volume can include the whole system's volume, or only a small part of the system's volume. Ignition is only concerned with the initial state of the ignition volume, and the change in this state brought about by the ignition source once it is introduced. As soon as a self-accelerating chemical process begins, the reaction itself changes the state of the immediate surroundings to a state very different from the initial conditions, allowing flame to expand and develop the explosion.

3.2.1 IGNITION MECHANISM

In order to explain the path of events that might lead to an ignition, a brief review is needed first of the chemical concepts involved during the ignition process. The chemical kinetic and thermodynamic concepts treated here have been summarised from the explanations offered by Petrucci[50]. For ease of explanation, it is assumed that all substances are in gaseous form.

Basic Theory

Chemical reaction theories

According to the Collision Theory of chemical reactions, reactions occur as a result of collisions between molecules. The number of collisions between molecules per

unit time can be derived from the kinetic-molecular theory, and is called the collision frequency. The energy that molecules must possess in order to react is called the activation energy. The rate of reaction is as follows:

$$Reaction\,Rate = p.f.Z \qquad -3.1$$

where p-probability factor

f-fraction at or above activation energy

Z-collision frequency

The Transitional State Theory focuses on an hypothesized intermediate species, called an activated complex. The complex exists only briefly, after which it either falls back to the original reactants or forms product molecules. The difference between the forward and reverse activation energies of the reaction, is the change in enthalpy or the enthalpy of formation. In Figure 3.1, a reaction profile is given which explains the concept visually ($\Delta H = E_a(forward) - E_a(reverse)$). Explosions occur when the fraction of molecules in the activated state are so large that the reaction proceeds very quickly in the forward direction.

Rate processes in combustion

When required to explain an accelerating reaction, interpretation of the above two theories leads to the same answer. The Collision Theory suggests that both the frequency of collisions and the fraction of activated molecules should be increased. Frequency of collisions can be increased by raising the concentration and temperature of the reactants, and the fraction of activated molecules can be increased by the addition of energy, which is mostly done in the form of raising the temperature. The Transitional State Theory indicates that more kinetic energy is required for collisions to form an activated complex. This, again, can be obtained by an elevation of the temperature. It is clear that both concentration and temperature will influence the rate of a reaction, and consequently control the heat production from that volume.

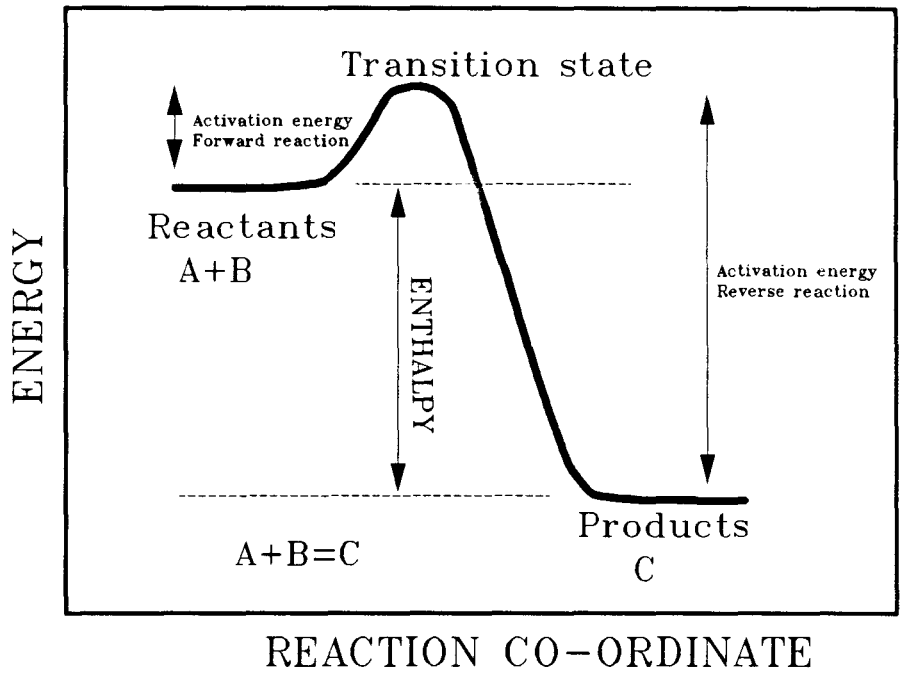

Fig.3.1. Energy profile for the reaction A+B->C

The rate law of chemical reactions expresses the reaction rate through an equation called the "rate law". For the hypothetical reaction $aA+bB=gG+hH$, where a,b,g and h stand for coefficients in the balanced equation, the reaction rate is:

$$ReactionRate = k[A]^m[B]^n \qquad -3.2$$

and $[A]$ and $[B]$ are molar concentrations. When m or n is equal to unity, the reaction is first order in A or B respectively, or when either m or n equals 2, the reaction is said to be second order in A or B. The sum of m and n determines the overall order of the reaction. According to Krazinski, Buckius and Krier[51], it is generally accepted that for heterogeneous combustion (as with coal dust clouds), the reaction rate is of first order with respect to the oxygen concentration. They add, though, that questions can be raised as to the validity of the generalization.

The effect of temperature on reaction rates is described by the Arrhenius equation:

$$\log k = \left(\frac{-E_a}{2.303R} \right) \frac{1}{T} + C \qquad -3.3$$

where k is the rate constant, R is the gas constant and C is a constant. Written as a natural logarithm, the equation becomes

$$k = Ae^{\left(\frac{-E}{RT}\right)} \qquad -3.4$$

where A is a pre-exponential constant.

Thermochemistry

The first law of thermodynamics is a law of conservation of energy. The internal energy ΔU is the difference between heat absorbed by a system q, and the work done on a system, w. When the reaction proceeds in an open environment, the heat of reaction at constant pressure is called the enthalpy of the reaction. The work done on the system will be the product of the pressure which is constant and the change in volume. For a change occurring at constant pressure, the enthalpy is as follows:

$$\Delta H = \Delta U + P\Delta V \qquad -3.5$$

Since absolute values of ΔU and ΔH do not exist, standard enthalpy of formation is used where, by convention, a value of zero is assigned to enthalpies of the elements in their most stable form at the standard temperature and pressure. The heat of reaction is the summation of enthalpies of formation of the products minus that of the reactants.

Combustion reactions do not take place at room temperature, but the change in enthalpies at other temperatures is obtained by addition of the summation of the product of heat capacity and the temperature over increments of that change, thus

by integration over the temperature difference. For constant volume processes, such as an explosion in a closed vessel, the value of the heat capacity is different from the heat capacity of the same reaction but occurring at a constant pressure.

Heat transport properties

No system is totally adiabatic, which results in the heat flows required to effect ignition being in excess of the specific quantity required. Heat is lost through conduction, diffusion and radiation. From Barnard and Bradley[48] conduction and diffusion are summarised. The conduction of heat is described by Fourier's law

$$\frac{\dot{q}}{A} = -\lambda \frac{dT}{dx} \qquad -3.6$$

where $\dot{q}$ is the heat flow per unit time through an area A, l is the thermal conductivity and dT is the temperature change over a distance dx, or the temperature gradient in the direction of heat flow.

Diffusion is described by Fick's law

$$\frac{\dot{n}}{A} = -D \frac{dn}{dx} \qquad -3.7$$

where $\dot{n}$ is the number of molecules per unit time crossing an area A, D is the diffusion constant and $\frac{dn}{dx}$ is the concentration gradient.

Radiant emittance[52], R, is described by Stefan's law

$$R = e\sigma T^4 \qquad -3.8$$

where e is the emissivity of the surface, σ is the Stefan-Boltzmann constant (5.6696×10^{-8} $Wm^{-2}K^{-4}$) and T the Kelvin temperature.

An Ignition Mechanism

It is clear that temperature plays an important role in the ignition process. The explosive mixture surrounding the ignition source is initially at ambient pressure and temperature. The source of ignition provides a flow of heat into the ignition space, resulting in a sudden temperature rise. Increasing the temperature increases the fraction of the molecules that have energies in excess of the activation energy, and the reaction accelerates in the forward direction. When the imbalance is considerable, the rate of the combustion reaction increases exponentially, and becomes so fast that an unstable state is reached where the temperature increase is almost immediate. This occurrence is called an explosion.

The source of ignition transfers energy at a certain rate in the form of heat from a surface or volume to the chemical species which is to be ignited. At the same time the chemical species which starts to react exothermically loses energy in the form of heat to the immediate environment. Heat generation starts to compete with heat loss within the system and since the increase in heat generation is exponential, a critical point is reached where generation and loss of heat are balanced, a condition first described by Van't Hoff in 1884, as reported by Gray and Lee[53]. Above this point the reaction self accelerates and an explosion takes place.

Gray and Lee[53] also indicate that from this explanation of explosion development, it is clear why very hot sources of ignition, compared to less hot sources, result in reduced induction times, as was observed by Taffanel and le Floch in 1912. The rate of energy inflow into the explosive mixture is much higher than the heat lost to the surroundings, and enough energy is provided in a short time to increase the reaction rate to such an extent that the unstable explosive state of temperature increase is reached.

The distribution of temperature in the ignition volume also plays an important role in reaction development. When ignition occurs in a volume in which the reactant is at uniformly distributed temperature, the ignition process and the eventual explosion

will develop differently from a situation where a concentrated reaction temperature exists. For the latter, a temperature gradient will exist in the reactant. These two limiting ignition situations will be investigated and, in this thesis, are defined as ignition with uniform temperature distributions or *volumetric ignition*, and ignition from hot spot, or *point source ignition*. Semenov's thermal explosion theory expresses the concepts explained qualitatively so far in a quantitive way and is also a good approximation of volumetric ignition. Changes to Semenov's theory can also accommodate point source ignition and so a discussion of Semenov's theory follows.

3.2.2 SEMENOV'S STEADY STATE THEORY

The thermal explosion theory is concerned with the contest between heat generation from an exothermic reaction and heat dissipation through processes of conduction, convection and radiation within a thermodynamic system.

Semenov developed an elementary model for thermal explosions which elegantly illustrates the principal features of the explosion phenomenon. In his model, heat distribution throughout the reactant is assumed to be constant, a situation that can arise if the explosive gas is much more conductive than the walls surrounding it. The temperature is constant over the whole volume, but differs from that of the walls of the container. The true situation is probably closer to the thermal explosion theory proposed by Frank-Kamenetskii[48], where heat dissipation from the reactant to the walls of the container results in a temperature gradient which reaches its peak at the centre of the reactant, and at wall temperature at the interface with the container. This condition can develop when the walls of the explosion vessel are much more conductive than the explosive mixture inside. The difference in the two theories presents itself clearly when the temperature profiles across the explosion vessel are compared. Figure 3.2 is a representation of the situation as given by Barnard and Bradley[48].

According to Gray and Lee[53], the Semenov theory gives a good estimate, not much altered by more sophisticated theories, of the critical temperature rise in an explosive

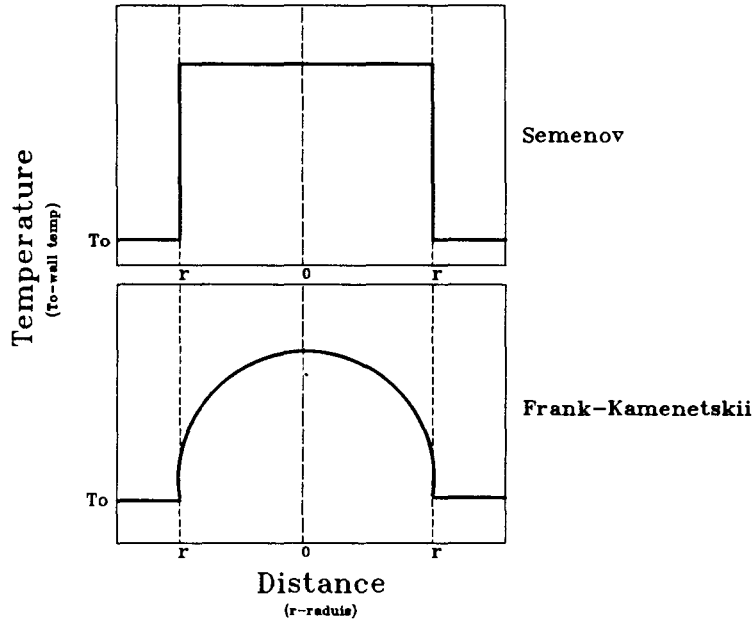

Fig.3.2. Temperature profile in the reaction vessel assumed in the Semenov theory of thermal explosions (top), and the temperature profile in the reaction vessel according to the Frank-Kamenetskii theory of thermal explosions (bottom) after Barnard and Bradley[48].

system while ignoring the effect of reaction consumption. Since the theory provides such a clear understanding of the ignition and explosion phenomena, it is treated in detail. The discussion is based on the explanation of Gray and Lee[53].

Heat generation

Due to the zero-order exothermic reaction with an Arhenius type reaction rate expression, it is assumed the reaction self heats uniformly to a temperature T_r, which is higher than the temperature of the surroundings at T_o. The rate of heat generation is given by:

$$\frac{dq_g}{dt} = QV\rho Ae^{\left(-\frac{E}{RT_r}\right)} \qquad -3.9$$

where Q is the exothermicity of the reaction in Joules per unit mass of a reactant of density p and volume V. A is the pre-exponential factor (sec^{-1} for a zero-order process), E is the activation energy in Joule per unit mass and R the universal gas constant in Joule per unit mass per degree temperature.

Heat loss

The rate of heat loss is as follows:

$$\frac{dq_l}{dt} = hS(T_r - T_o) \qquad -3.10$$

where h is the heat transfer coefficient in Joule per unit area per second and S is the surface area of the reactant in contact with the surroundings.

Steady state

A steady state is reached when heat generation and heat loss are in balance:

$$QV\rho Ae^{\left(-\frac{E}{RT}\right)} = hS(T_r - T_o) \qquad -3.11$$

A stationary state should exist for zero-order reactions where the reaction stays at T_o, but since reaction rates fall off as reactants are consumed, a steady state is never truly attainable, adding a time dimension to the process. A steady state will only exist for a limited time as the reaction rate reaches its maximum.

Relation between heat loss and heat generation

When the heat loss and heat release are plotted as functions of temperature, curves like those in Figure 3.3 are obtained. Three conditions can be distinguished. They are the stationary state condition, explosive state condition and the critical state condition. Each state will be discussed separately.

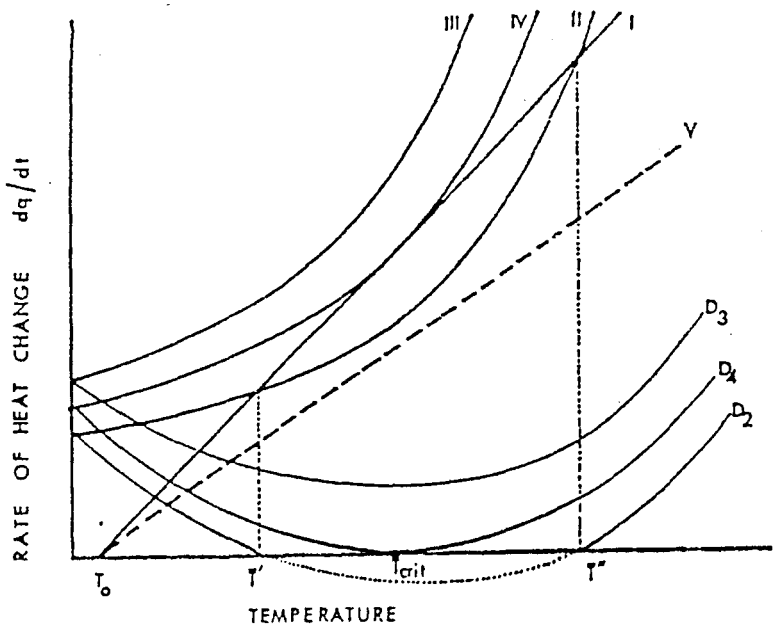

Fig.3.3. Heat generation (curves II, III and IV), heat loss (lines I and V) and the difference between them (curves D_2 to D_4), as functions of temperature according to Gray and Lee[53].

Stationary States: The heat generation curves (II, III and IV) should be S-shaped, but since heat release of the reaction alone is not enough to reach the upper part of the S-shaped curve, only the lower part is considered. The reaction self-heats when the heat generation exceeds the heat loss, but at temperature T' the situation becomes stationary. The criteria for stability is that the rate of change with temperature of the rate of heat generation becomes less than the rate of change with temperature of the rate of heat loss, i.e.

$$\frac{d\left(\frac{dq_g}{dt}\right)_{T'}}{dT} < \frac{d\left(\frac{dq_l}{dt}\right)_{T'}}{dT} \qquad -3.12$$

The reaction will therefore not be able to self-heat to temperatures above T' and cannot proceed along the dotted portion of curve D_2, since more heat is lost than generated in this region. Should a temperature T'' be reached, the situation will be unstable and will result in an explosion.

Explosive States: For this condition curve III and curve I never touch or cross each other, and heat generation always exceeds heat loss. Reactions are always in the explosive states. A change in the vessel size will drop line I to form line V, forming explosive states for reaction heat production curves II to IV.

The Critical State: When the heat generation curve is tangential to the heat loss line, a critical condition is reached. They are tangential when

$$\left(\frac{dq_g}{dt}\right)_{T_{crit}} = \left(\frac{dq_l}{dt}\right)_{T_{crit}} \qquad -3.13$$

The critical condition is

$$\frac{d\left(\frac{dq_g}{dt}\right)_{T_{crit}}}{dT} = \frac{d\left(\frac{dq_l}{dt}\right)_{T_{crit}}}{dT} \qquad -3.14$$

At the critical temperature T_{crit}, the behaviour of the reaction changes from a steady state to an unstable state. In effect, T' and T'' become coincident. If equations 3.9 and 3.10 are substituted into equations 3.13 and 3.14 and differentiated with respect to T_r (T_r and T_{crit} now equivalent), the following expression is obtained:

$$QV\rho A e^{\left(\frac{-E}{RT}\right)}\frac{E}{RT^2} = hS$$

Division of equation 3.11 by equation 3.15, results in a parabolic expression

$$\frac{R}{E}T_{crit}^2 - T_{crit} + T_o = 0 \qquad -3.16$$

Solving T_{crit},

$$T_{crit} = \frac{E}{2R}\left(1 \pm \sqrt{1 - \frac{4RT_o}{E}}\right) \qquad -3.17$$

A solution is only possible if $1 - \frac{4RT_o}{E} \geq 1$, or $\frac{4RT_o}{E} \leq 1$. A self-heating reaction may lead to ignition only if $E \geq 4RT_o$ a condition satisfied by most self heating materials.

A range of temperatures (consider the lower of the two T_{crit}) of the surroundings at which ignition will occur, can be shown. When T_o=0, the root mean square term in equation 3.17 is 1, but cannot be bigger than $\frac{E}{4R}$. Therefore,

$$0 < T_o \leq \frac{E}{4R}$$

Replacing the maximum value of T_o in equation 3.17, the maximum value of T_{crit} is $\frac{E}{2R}$. At higher temperatures no stationary state will exist, and explosions will always take place. The larger value of T_{crit}, as obtained from equation 3.17, is not applicable for conditions where the reaction rates are only controlled kinetically.

The approach to the critical state should be as follows. The rate of self-heating falls to zero as T_{crit} is reached, but if a disturbance raises the temperature above T_{crit}, the rate of self heating will rise without limit if reaction consumption is not a limiting factor.

Reaction temperature over time

It is convenient in practical situations to look at the increase in reaction temperature over time. If the absolute rate of heat flow is divided by the average heat capacity, the temperature increase can be calculated. The absolute heat inflow into the system equals the difference in the rate of heat generation and the rate of heat loss, equivalent to the subtraction of equation 3.10 from equation 3.9. The average heat capacity is $C_v pV$, where C_v is the average specific heat at constant volume.

$$\frac{dT_r}{dt} = \frac{\left(\frac{dq_g}{dt}\right) - \left(\frac{dq_l}{dt}\right)}{C_v \rho V} = \left(\frac{Q}{C_v}\right) A e^{\left(-\frac{E}{RT_r}\right)} - \left(\frac{hS}{V}\right)\frac{(T_r - T_o)}{C_v \rho} \qquad -3.18$$

The temperature-time histories, as suggested by the solution of equation 3.18 is shown diagrammatically in Figure 3.4 for the three states as discussed above. The influence of reactant depletion is indicated by the dashed lines and the physical meaning of the critical temperature is clearly illustrated.

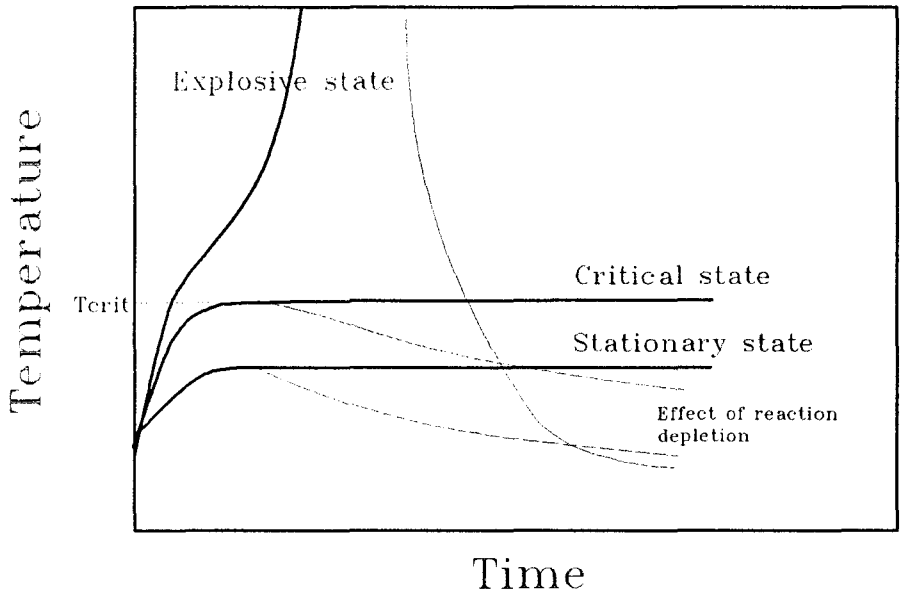

Fig.3.4. Temperature-time curves for zero-order reactions for explosive, critical and stationary states. Reaction depletion is indicated in dashed lines. From Gray and Lee[53].

To summarise, the reaction rate is equivalent to the rate of heat generation, but since heat is lost to the surroundings the absolute amount of heat is the difference of the two heat flow rates. This heat differential increases the temperature until a critical temperature is reached. At the critical temperature, a steady state of heat generation and loss is maintained. Above the critical temperature, a non-steady state is reached and an explosion develops.

The relation between concentration and temperature for critical conditions

Barnard and Bradley[48] state that explosion limits are usually described in terms of a concentration-temperature relationship. The concentration matching the critical conditions can be obtained by substituting the expression for T_{crit} (equation 3.17) in equation 3.11, the equation for steady state conditions, leading to the following expression after manipulation:

$$f(c)_c = \frac{hSRT_o^2}{EAVQe} e^{\left(\frac{E}{RT_o}\right)} \qquad -3.19$$

or

$$\ln\left[\frac{f(c)_c}{T_o^2}\right] = \left(\frac{E}{RT_o}\right) + \ln\left(\frac{hSR}{EAVQe}\right) \qquad -3.20$$

where $f(c)_c$ represents p, or the density as a function of the concentration c. For a gas of partial pressure p_c at the critical point, $c=p_c/RT$. For simple gas reactions where $f(c)_c=c^m$,

$$\ln\left[\frac{p_c^m}{T_o^{2+m}}\right] = \left(\frac{E}{RT_o}\right) + constant \qquad -3.21$$

Explosion limit data can be shown on an explosion limit diagram such as Figure 3.5, where critical reactant concentrations are plotted against temperature. Equation 3.19 suggests that plots of $\ln\left(\frac{c_{crit}^m}{T_o^{m+2}}\right)$ against $\frac{1}{T_o}$ should be a straight line, as shown in Figure 3.6. Many thermal explosions are found to obey this relationship, particularly for gaseous systems.

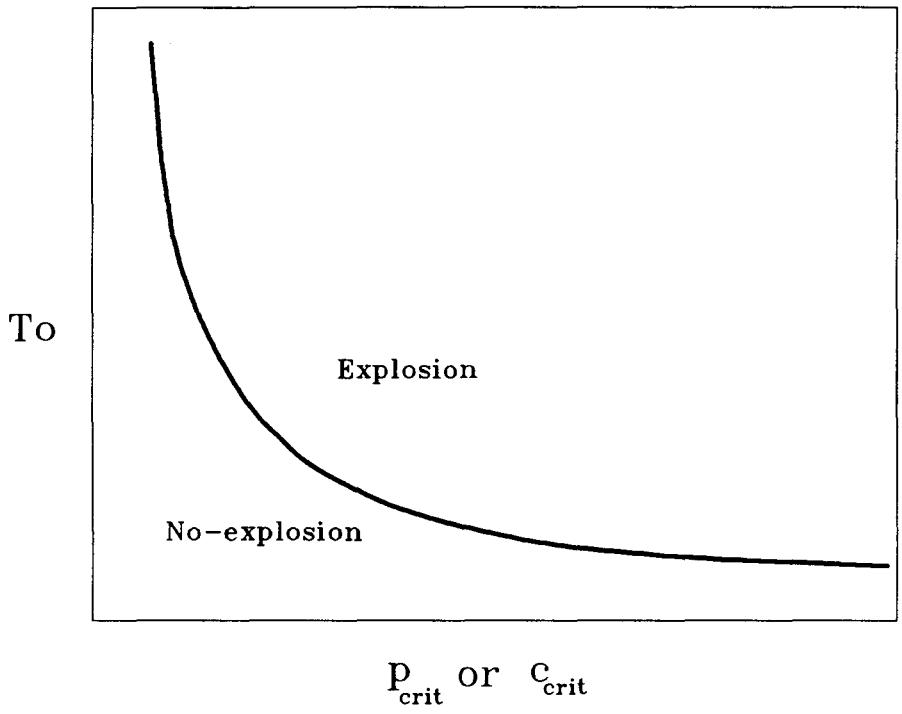

Fig.3.5. Explosion limit curve after Gray and Lee[53].

The deviation at lower temperatures and higher pressures can either be due to the self-accelerating process not being totally thermally driven, but rather chain-thermal, or to the more important role convective heat transfer plays in this region.

The Semenov theory is powerful in understanding the thermal explosion theory, although the assumption that temperature is uniform throughout the reactant is applicable only in gaseous systems under lively convection, or in systems where the energy transfer from the source of ignition is spacially uniform in energy transfer. For situations where the gaseous system is not stirred, an ignition zone exists that is surrounded by unstirred gases of similar conductivity. This situation is better described by the Frank-Kamenetskii's interpretation of the thermal explosion theory, which is discussed below.

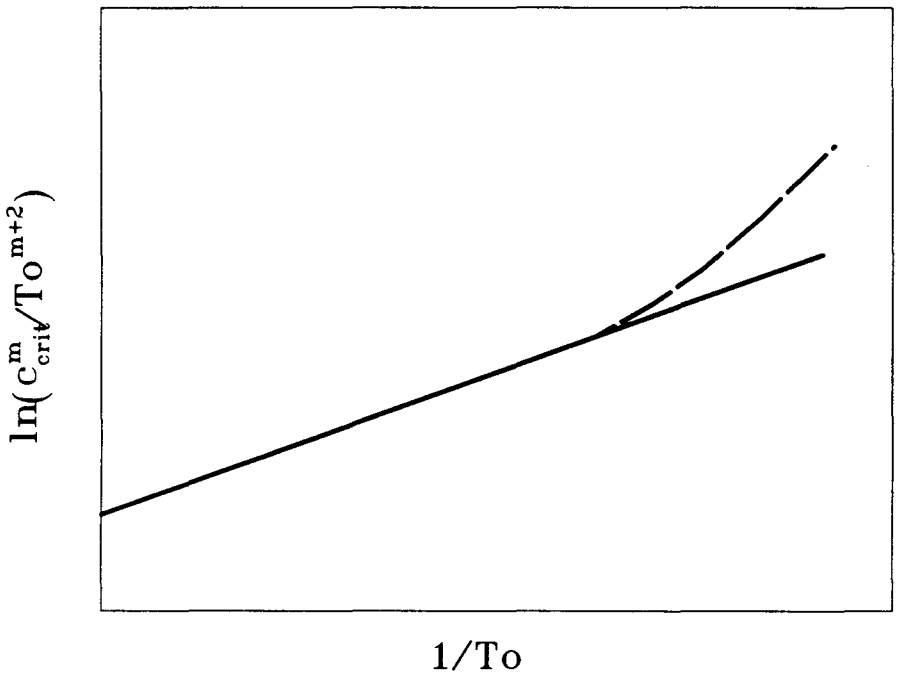

Fig.3.6. The straight line plot (and deviation at low temperature and high pressure) of the Arrhenius plots after Gray and Lee[53].

3.2.3 FRANK-KAMENETSKII'S THEORY

Situations can arise where conductive heat transfer within the reactant implies that a temperature gradient will exist within the reactant if, for example, the source of ignition is from a conductor heated by electric current. Semenov's idea of a uniform temperature is not applicable for such situations, since heat conduction within the reactant will take place. The Frank-Kamenetskii theory provides a solution to the problem and is given, as summarised by Barnard and Bradley[48].

Equivalent to the Semenov theory, a heat generation term is equated to a heat loss term at the critical point. The more complete equation includes a term for energy contained in the system if heat generation and heat loss do not balance. When heat conductivity λ is assumed constant for all temperatures, heat contained in the system will equal the sum of the heat generation and heat conduction.

$$Qf(c)Ae^{\left(-\frac{E}{RT}\right)}+\lambda\nabla^2T=C_vf(c)\left(\frac{dT}{dt}\right) \qquad -3.22$$

where ∇^2 is the Laplacian operator, *f(c)* the density as a function of concentration and C_v the specific heat of the gas. For critical conditions the change of the temperature differential over time becomes zero, and equation 3.22 becomes

$$Qf(c)Ae^{\left(-\frac{E}{RT}\right)}+\lambda\nabla^2T=0 \qquad -3.23$$

The steady state equation is solved by defining boundary conditions as follows: $T=T_o$ at $x=r_o$, r_o being the radius of the enclosure and x any point at or away from the centre of combustion, and $dT/dx=0$ at $x=0$. In order to solve equation 3.23, Frank-Kamenetskii defined a dimensionless temperature θ where $\theta=\frac{E(T-T_o)}{RT_o^2}$ and a dimensionless radius *z* where $z=x/r_o$. Equation 3.23 becomes

$$\nabla_z^2\theta=-\delta e^{\left(\frac{\theta}{(1+\epsilon\theta)}\right)} \qquad -3.24$$

with boundary conditions $t=0$ at $z=1$, and $(dt/dz)=0$ at $z=0$.

Solutions to this equation exist only when the dimensionless parameter, δ, is less than a critical value δ_{crit} and a stable temperature profile $T=f(r)$, *r* the radius of the vessel. δ is a dimensionless heat release rate, balanced to the temperature of the surroundings, and is given by

$$\delta=\frac{QEr^2f(c)Ae^{\left(-\frac{E}{RT_o}\right)}}{\lambda RT_o^2} \qquad -3.25$$

The theory provides an expression for the maximum pre-explosion temperature rise ΔT, which is given by

$$T_c-T_o=constant\times\frac{RT_o^2}{E} \qquad -3.26$$

where T_c is the temperature at the centre of the volume and the *constant* equals 1.20, 1.37 or 1.60, depending on the geometry of the system being an infinite slab, infinite cylinder or a sphere respectively. The values of δ_{crit} for the different geometrical shapes are 0.88 for the infinite slab, 2.00 for the infinite cylinder and 3.32 for a sphere.

The Semenov theory can be given a similar format by rearranging equation 3.19 to obtain

$$\frac{1}{e} = \frac{QEVf(c)Ae^{\left(\frac{-E}{RT_o}\right)}}{hSRT_o^2} \qquad -3.27$$

with the critical value of 1/e=0.368.

3.2.4 THERMAL THEORY OF IGNITION BY HOT SPOTS

A further development from the Frank-Kamenetskii theory leads to the ignition theory of hot spots. Only the broad outlines of this theory are given. The theory aims at predicting the size and temperature of the smallest hot spot that will ignite a self-sustaining reaction which will spread and involve the whole mass. The same steady state reaction as above holds true, namely:

$$C_v \rho V(dT/dt) = \lambda \nabla^2 T + QV\rho Ae^{\left(-\frac{E}{RT}\right)} \qquad -3.28$$

Initial conditions are $T=T_i$ for $r < r_o$ and $T=T_o$ for $r > r_o$ where r_o is the radius of the hot spot, T_i is the temperature in the hot spot and T_o is the ambient temperature. The same dimensionless heat release rate δ given by equation 3.25 is applicable. Rideal and Robertson attempted in 1948 to make a theoretical calculation of the critical size of the hot spot at different temperatures, as reported by Gray and Lee[53]. The heat generation term is simply the product of the volume of the hot spot times the exothermicity of the reaction:

$$q_{gen} = \left(\frac{4}{3}\pi r_o^3\right)\rho t Q A e^{\left(-\frac{E}{RT}\right)} \qquad -3.29$$

and heat loss:

$$q_{loss} = \int_{r_o}^{\infty} 4\pi r^2 \theta C_v \rho \, dr \qquad -3.30$$

Thomas[54] related T_i to the heat of combustion generated within a spherical hot spot to the heat generated within the hot spot volume, as follows:

$$T_i = T_o + \left(\frac{q r_o^2}{2\lambda}\right) \qquad -3.31$$

where $q_{gen} = QAe^{\left(\frac{-E}{RT}\right)}$. The dimensionless heat release rate is given by:

$$\delta_{crit} = 2\left(\frac{E}{RT_i^2}\right)(T_i - T_o) \qquad -3.32$$

and the critical radius as:

$$r_{crit} = 1.414\sqrt{\left(\frac{\lambda}{QA}\right)e^{\left(\frac{E}{RT_i}\right)}(T_i - T_o)} \qquad -3.33$$

The model is only applicable for a spherical hot spot.

3.3 THE COMBUSTION OF METHANE

From the Thermal Explosion Theory it is clear that the minimum ignition temperature of a certain fuel is not determined as a fuel property alone, but also by the thermodynamic system characteristics in which it ignites. What is constant though, is the heat content of that fuel, and that the product of exothermicity of the reaction, Q, with the rate of the reaction, r, provides an expression for the heat generation tempo within a system. It can be written as follows:

$$\dot{q}_{gen} = Qr \qquad -3.34$$

where $\dot{q}_{gen}$ is the rate of heat production. Usually, the reaction rate is given as an exponential function of temperature, according to the Arrhenius equation. The heating potential of methane, the dominant gas contained in firedamp, is now considered.

Exothermicity of Methane Oxidation

Combustion involves the liberation of energy by oxidation of constituents in the fuel that reacts, and can therefore be represented by a chemical reaction. Quantities of the substances involved are balanced by means of the conservation of mass.

Methane can react with oxygen in two ways, either producing carbon monoxide through incomplete combustion ($CH_4 + \frac{3}{2}O_2 \rightarrow CO + 2H_2O$), or carbon dioxide through complete combustion as given by

$$CH_4 + 2O_2 \rightarrow CO_2 + 2H_2O \qquad -3.35$$

Since the first situation culminates in incomplete combustion, only complete combustion will be considered. If a reaction as described by equation 3.35 takes place at a pressure of 0.1 MPa and 25 °C, exothermicity can be calculated as follows:

$$Q = (\Delta H_{CO_2} + 2\Delta H_{H_2O(g)}) - \Delta H_{CH_4}$$

$$= [-393\ 522 + 2(-241\ 827)] - [-74\ 873]\ kJ/kmol$$

$$= -802\ 303\ kJ/kmol$$

where the subscript g refers to water in gaseous form. The change of enthalpy between 25 °C and 0.1 MPa and any given state must be known. For ideal gas behaviour, enthalpy is a function of temperature alone, and can be obtained by using the specific heat C_v or C_p.

In mines the methane reacts with air, which is composed of 21 % oxygen and 79 % nitrogen by volume, if the argon content is ignored (atmospheric nitrogen has a molecular weight of 28.16, compared to clean nitrogen of 28.01 - Van Wylen and Sonntag[55]). Thus, for each mole of oxygen, 79/21=3.76 moles of nitrogen are involved. The above reaction equations changes to:

$$CH_4 + 2O_2 + 2(3.76)N_2 \rightarrow CO_2 + 2H_2O + 7.52N_2 \qquad -3.36$$

This stoichiometrically balanced reaction occurs if 9.5 % of methane is mixed with air. Depending on the concentration of the reactant, a proportion of the reactant might remain after the completion of the reactant, or the reactant might be consumed completely without necessitating the complete consumption of oxygen. At the point where complete combustion occurs without oxygen in the products, the amount of air provided is called the theoretical air. For complete combustion 100 % theoretical air is required. Oxygen quantities in excess of the stoichiometric balanced quantity are expressed as percentages above 100 %. For example, when 220 % theoretical air is present, the mixture contains only 5 % methane, and reaction 3.35 will change to

$$CH_4 + 2(2.2)O_2 + 2(2.2)(3.76)N_2 \rightarrow CO_2 + 2H_2O + 2.4O_2 + 16.5N_2 \qquad -3.37$$

The Reaction Rate of Methane-air Reaction

Initiation of a methane-air reaction presumably starts by some surface process yielding radicals such as HO_2 (CH_4+O_2->CH_3+HO_2). The radicals might attack methane or undergo radical-radical reactions. The reaction proceeds by a chain of sub-reactions, which might differ for different temperature and pressures. Rate expressions for the individual steps are commonly expressed in the Arrhenius form. Activation energies E_a and the pre-exponential term A typically lie between 20 kJ/mol and 400 kJ/mol for the former, and between $1x10^7$ $m^3/(mol.s)$ and $2x10^{11}$ $m^3/(mol.s)$ for the latter.

Since only a global or overall reaction rate is required to predict the heat generation tempo of the generation reaction, the detailed chemistry of the high temperature oxidation of methane is not discussed.

Flame and Flammability Characteristics of Methane-air Combustion

Burning velocity: The burning velocity is defined as the velocity with which a plane flame front moves normally to its surface through the unburnt mixture. Barnard and Bradley[48] report a value of 0.45 m/s for a methane-air mixture, but state that a small dependence on pressure and temperature exists in that the burning velocity increased with reduced pressures and increased temperatures. The fuel concentration has a more dominant effect, with a maximum value for fuel rich mixtures. One should remember that under certain conditions, such as in a mine tunnel, the flame is non-stationary flame as it is 'pushed' forward by the expanding gaseous product behind the flame front, and a second concept, namely *flame speed*, can be introduced. Flame speed will be the flame speed relative to the tunnel and not relative to the unburnt gas. With rapid expansion the burning velocity (at high temperature and pressure in the flame zone) increases dramatically, and the explosion develops into a detonation.

Flame temperature: Barnard and Bradley[48] give the flame temperature of methane at atmospheric temperature to be 2222 K. The exothermicity and rate of energy release determine the flame temperature, and is therefore influenced by pressure and temperature.

Ignition temperature: Naylor and Wheeler[56] realised that the ignition temperature of any particular mixture will depend largely upon the conditions under which it is heated. For example, for a 15 cc vessel, they found the minimum ignition temperature to be just above 1000 K, and for a 275 cc vessel to be about 900 K. The observation is explained easily through the application of the Thermal Explosion Theory, where increased heat loss can be expected for a higher volume to surface ratio to exist, such as for small vessels. The fuel concentration also influences the

minimum ignition temperature, generally a minimum of between 7 % and 9 %, depending on the source of ignition. Increased oxygen content will reduce the ignition temperature.

Hertzberg[32] defined the *auto ignition temperature* as the temperature of the entire system in order to host spontaneous ignition and generation of an explosion. Bond[57] defines the *auto ignition temperature* as the mimimum temperature at which that substance will initiate and sustain a combustion process. He adds that it is not an exact temperature, due to inter alia the method of determination. The temperature referred to by Bond appears therefore to be different from the auto ignition temperature as interpreted by Hertzberg, since the latter is a fixed temperature because the ignition source is isothermal, spacially extended and steady state in time. Nevertheless, Bond tabled the auto ignition temperature of methane to be between 810 K and 868 K, while Conti and Hertzberg[58] report a value of 874 K.

The minimum ignition energy is related to the minimum ignition temperature in the sense that the energy transfer to the system, or part of it, effects a temperature increase which results in ignition. The amount of energy required to raise the temperature sufficiently relies on the type of ignition source. Ignition energy is therefore not considered to be a true material property, and will not be separated from the auto ignition temperature here. In Chapter 4 different types of ignition sources and typical minimum ignition energies are discussed.

Lag on ignition: Naylor and Wheeler[56] measured ignition lag times which increased with increased methane concentration, and decreased as temperature was lifted. For example, they found a 7 % methane-air mixture with ignition source temperature at 1048 K to react after 1.15 seconds, but only after 1.68 seconds could a similar source ignite a 12 % mixture. The same value at 1448 K was 0.01 seconds.

Flammability limits: Flames can only occur within a range of compositions of reactant and oxidizer bounded by the limits of flammability. For methane at 25 °C

and 0.101 MPa pressure, the explosive limits lie between 5 % to 5.3 % and 14 % to 15 % methane per volume of the mixture. Pressure and temperature both shift the limits, as shown in Figure 3.7.

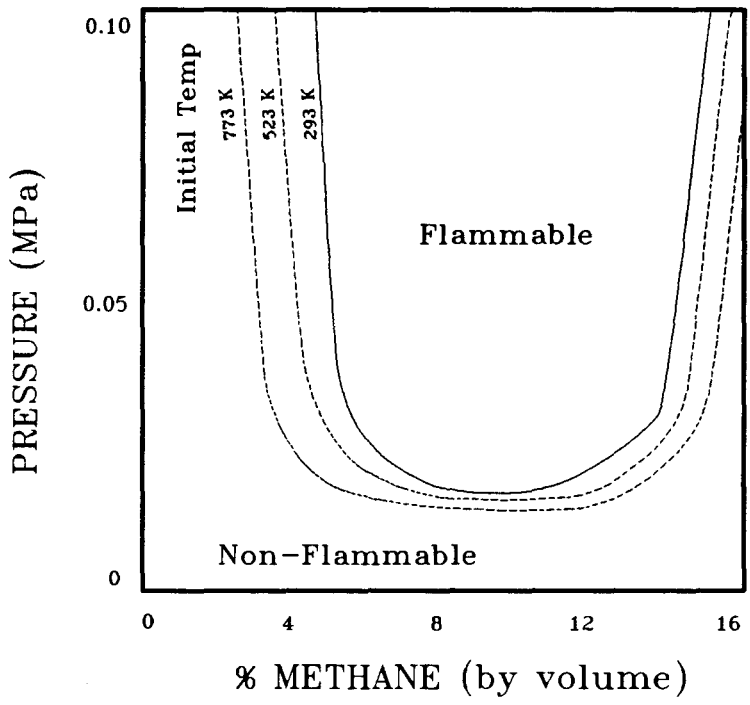

Fig.3.7. Influence of pressure and temperature on the flammability limits of methane in air - after Stull[59]. Flammability limits are only approximately shown.

The oxygen content also determines the flammability limits of explosible substances, which can be obtained from the well known Coward's diagram. For a pure methane-oxygen mixture, flammability limits stretch from that given at standard temperature and pressure to approximately between 4 % to 60 % by volume.

Moss[60] reproduced figures from an investigation into the influence of ignition source temperatures on the flammability limits of methane by Burgess and Wheeler earlier this century. It has been observed that the flammability range widens for increased temperature of the CH_4 mixture. The values reported by Moss are given in Table III.I.

TABLE III.I The widening of the range of flammability limits of methane with the increase in the temperature of the methane-air mixture after Moss[60].

Initial Temperature °C	Lower Explosible Limit	Upper Explosible Limit
20	6.00	13.40
100	5.45	13.50
200	5.05	13.85
400	4.00	14.70
600	3.35	16.40
800	-	29.00

More recently, Wieman[61] confirmed the above trend of temperature dependence, but obtained a much more dramatic shift of explosibility limits with increased temperature. The lower explosibility limit reduced only by 1 % from 5 % to 4 % for all starting temperatures tested, but the upper limits moved from 16 % at an initial temperature of 50 °C to 18.5 % at an initial temperature of 250 °C. The maximum pressure reduced from 0.65 MPa for a 50 °C initial temperature to 0.36 MPa for a 250 °C initial temperature, while the maximum rate of pressure rise was unaffected. Additionally, he observed that with decreasing oxygen concentration, not only the explosion limits are narrowed, but the values for the explosion pressure and the maximum rate of pressure rise are also reduced.

3.4 COAL DUST COMBUSTION (DISPERSED)

The combustion of coal is a complicated process, requiring a multi-disciplinary approach involving fluid mechanics, thermo dynamics and chemistry. A particular type of coal behaves differently when exposed to varying conditions, but is further complicated by the fact that different coals react differently when exposed to the same conditions. The complexities involved make quantitative description of the combustion process exceedingly difficult. Quantitative descriptions are based on the

Thermal Explosion Theory, but the heat transfer and actual burning process seem to be radically different from burning of gaseous systems. Although gaseous combustion forms part of coal particle combustion, a chain of events precedes volatile burning. These events follow two distinct routes, depending on heating rate and particle size.

Coal Particle Ignition Mechanisms

Homogeneous ignition ignites by prior pyrolysis and subsequent ignition of the volatiles and this is also called the *Faraday mechanism* after his explanation in the 19th century of coal particle combustion. This occurs when large particles burn and, due to their size, heat slowly. The idea of *Heterogeneous ignition* came later, first speculated by Wheeler in a 1912 report of a committee on U.K. coal mine explosions (see Essenhigh, Misra and Shaw[62]), but substantiated over the last thirty years by progressive sampling from various combustion reactors such as the plug-flow reactor used by Howard and Essenhigh[63], and the jet stirred reactor used by, inter alia, Goldberg and Essenhigh[64]. For small particles heating quickly, direct oxygen attack of the particle surface is observed, and the particle diameter becomes smaller without necessarily pyrolysing the unburnt solid.

Essenhigh, Misra and Shaw[62] describe heterogeneous ignition as either a one step or three stage process. The primary ignition occurs by direct attack of the reactant gas on the solid, namely the whole coal and not the char, which is single step true heterogeneous ignition. The reaction removes material that otherwise would have been expelled as volatiles. Sometimes this reaction is quenched as pyrolysis becomes appreciable and ignites, combusts and re-ignites the char residue, moving from single step to tri-stage ignition. A third ignition mechanism, which combines the previous two, is therefore possible.

Figure 3.8 is a delineation of the ignition regimes as a function of heating rate and particle size, after Juntgen and van Heek and reported by Essenhigh, Misra and Shaw[62]. From the diagram it is clear that a third ignition regime exists for high heating rates, which is a combination of homogeneous and heterogeneous combustion.

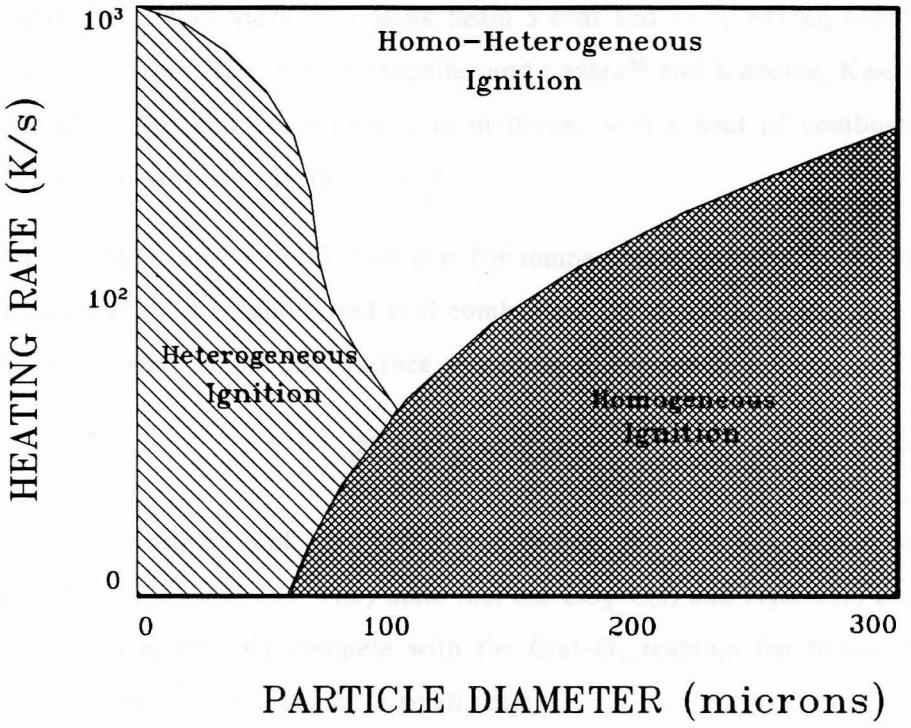

Fig.3.8. Delineation of ignition regimes as a function of heating rate and particle size - after Juntgen H. and van Heek K.H. as reported by Essenhigh, Misra and Shaw[62]. The limits indicated are not absolute.

What is consistent with gaseous ignition is that the rate of heat generation $\dot{q}$ from a rapid combusting dust cloud is obtained by calculating the product of exothermicity Q with a rate expression r, or $\dot{q}_{gen} = Qr$.

Exothermicity of Pulverized Coal Particles

In fuel technology, the term 'heat of combustion' is replaced by 'calorific content', expressed in units MJ/kg and obtained from the combustion of coal in a bomb calorimeter. Values vary widely, for example 33.35 MJ/kg for low volatile bituminous Pocahontas coal, 28,50 MJ/kg for Bank Seam 5 coal and 18.00 MJ/kg Goedehoop Seam 4 coal (as from Hertzberg, Cashdollar and Lazara[65] and Knoetze, Kessler and Mthombeni[66]). This can be compared to methane, with a heat of combustion of 55.16 MJ/kg, if expressed in these units.

Krazinski, Buckius and Krier[51] state that for temperatures between 1000-2000 K, typically encountered in pulverised fuel combustion, evidence indicates that CO is the primary product at the coal surface according to the reaction

$$2C + O_2 \rightarrow 2CO \qquad -3.38$$

giving a heat of formation of -110 600 J/mol. Besides this reaction, carbon can also react with CO_2, H_2O and OH. They state that the CO_2-C(s) and H_2O-C(s) reactions are too slow to effectively compete with the C(s)-O_2 reaction for heterogeneous reactions, but might still occur on a small scale.

Rates of devolatization are also known to be influenced by the heat of reaction. A variety of compounds, instead of the simple oxidation reactions obtained from the ultimate analysis, is released each with different heat of reactions. Particle size, coal structure and coal petrology all affect heat generation, which leads to the conclusion that no equation exists that can universally provide a heat of generation for coal dust.

Reaction Rates of Coal Combustion

The reaction rate is measured by the rate of loss of the unreacted mass multiplied by a rate constant k, and can be expressed as $-dm(t)/dt=k\ m(t)$. For coal, the decomposition is not complete and a residue of char is left. The final mass after a long or infinite time delay must be subtracted from the initial mass.

It is practice to describe the rate constant k by the Arrhenius exponential function shown in equation 3.4 and repeated here:

$$k = Ae^{\left(\frac{-E_a}{RT}\right)}$$

According to Krazinski, Buckius and Krier[51], disagreement regarding the value for the overall activation energy of the heterogeneous reaction rate exists. Values ranging from 67 kJ/mol to 260 kJ/mol are quoted. Although a reaction order of unity with respect to oxygen is agreed upon, Hertzberg, Zlochower and Edwards[67] declare that the rate is not only a function of temperature, but also of heating rate dT/dt.

Flammability and Flame Characteristics

Since coal is a complex substance, no definite values for flammability or flame characteristics can be given, as is the case for methane. Typical values, measured by other researchers and quoted in the literature, are given indiscriminately.

Burning Velocity: The burning velocities of coal dust have been studied by Hartman, Jacobson and Williams[68]. They photographed the flame produced by a burner, and found that smaller particles and increased dust concentrations increase flame speed. Dust concentrations were not increased to the point where the burning velocity starts to decrease with increased dust concentration. For an 11 micron coal dust/air mixture, burning velocity was nearly 0.10 m/s. Values obtained in a small furnace by Brooks and Essenhigh[69] and called 'limit flame speed' which might not be the burning velocity, are 0.17 m/s for a Pennsylvania anthracite and 0.50 m/s for a Pittsburgh bituminous coal.

Regarding flame speed, Palmer[30] comments that when dust concentration is increased above the lower explosibility limit, but keeping other conditions the same, the flame speed usually increases to a maximum and subsequently decreases as the upper limit is approached. The peak area is wide, making the determination of a most favourable concentration difficult. It is well known from experiments, such as those at Experimental Mine Barbara as described by Cybulski[1], that detonation in explosion galleries is possible. Flame speeds can therefore accelerate under the right conditions to reach speeds in the order of thousands of metres per second.

Flame Temperature: Flame temperature will be influenced by the dust composition, particle size, dust concentration, the system's heat transfer properties and the source of ignition. Flame temperature varies between 1000 K and 3000 K while peak particle temperature measured in a 7.8 litre chamber by Hertzberg, Cashdollar and Lazzara[65] for a 7 μm Pittsburgh coal dust has been given as approximately 2200 K at a concentration of 250 g/m^3.

Ignition Temperature: Conti and Herzberg[58] did measurements of auto ignition temperatures of different coal dusts in a 1.2 litre isothermal furnace. Auto ignition temperatures tend to increase indefinitely as the dust concentration is decreased to reach the lower explosive limits. A constant auto ignition temperature is maintained over a very wide range of concentrations, and curves back upwards at extraordinarily high dust loadings. The thermal auto ignition temperatures reported for Pittsburgh bituminous coal (36 % volatiles) is 833 K, and for an anthracite (8 % volatiles) is 1033 K. The auto ignition temperature of high volatile coal is generally lower than that of lower volatility coals. Figure 3.9 illustrates.

Conti and Hertzberg[58] also investigated the influence of particle size. A characteristic diameter below which the minimum auto ignition temperatures become size invariant, has been identified. The higher volatile dusts have larger characteristic diameters. For low volatile coal, the characteristic particle diameter is much smaller at 20 to 30 micron, while for higher volatility coals, it is above 20 to 30 micron.

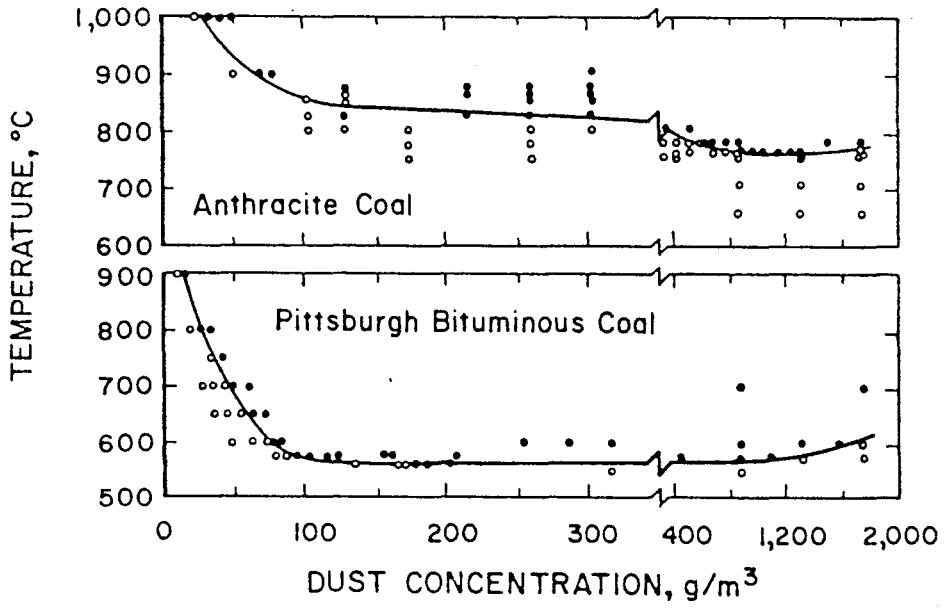

Fig.3.9. Thermal auto ignition data for an anthracite and a bituminous coal dust - Conti and Hertzberg[58].

For South African coal dusts, Knoetze[70] obtained a linear correlation with a correlation factor of 0.66 between volatile matter and the K_{ex} explosibility index. The correlation between K_{ex} and the calorific content of the volatiles, is 90.9 %. In experiments to investigate a combustion model that assumes CH_4 to be devolatilized from coal and the gas phase reaction to be dominant, Bradley, Dixon-Lewis and El-Din Habik[71] burned graphite dust and methane mixtures near the lean limit. They concluded that all the volatiles can be represented by CH_4, which mixes with the surrounding air.

This observation, suggesting a strong relationship between explosibility and volatile content of coal, suggests homogeneous combustion, but the observations of Howard and Essenhigh[63] that particles still contain volatiles after partial combustion suggest heterogeneous combustion. In this thesis the conflicting observations are interpreted as actually in agreement, where heterogeneous combustion is seen as a surface burning of a melted particle, consuming the volatilizable substances more easily than

the carbon. Below a characteristic particle diameter, surface area allows all volatilizable material to be consumed instantly, but for larger particles, products from the initial combustion shield the particle from further attack by oxygen.

Ignition Lag: Observations from experimentation in this thesis indicated that the same trend as for methane holds for coal dust, that is the higher the ignition temperature the shorter the lag time. However, the lag times were generally longer than those of methane.

Flammability Limits: Palmer[30] tabled the lower and upper explosibility limits for coal from various investigations. Despite variation in volatile content, the values for the lower limits are in the range 40 g/m^3 to 90 g/m^3. For upper explosion limits, values of 680 g/m^3 to 2100 g/m^3 are given. Volatile content does influence the explosion limits, and so does particle size. Limits narrow out with reduced volatile content, and broaden as particles become smaller.

3.5 COMBUSTION OF HYBRID MIXTURES

The flammability of mixtures of different gases with air can be determined by the Le Chatelier additive principle. Studies such as that of Nagy and Portman[72] and Banhegyi and Egyedi[73] have indicated that Le Chatelier's Law is applicable for calculating the lower explosive limit for coal dust and methane hybrid mixtures, but that these two substances may produce synergistic behaviour, lowering the required concentrations as indicated by Singer[74] and Napier and Roopchand[75]. Field[76] expressed the lower explosive limits mathematically as follows:

$$\frac{d}{N_d} + \frac{s}{N_s} = 1 \qquad -3.39$$

where d is the concentration of gas-free dust which produces a minimum explosible concentration with a gas at a concentration s. N_d and N_s are the minimum explosible

concentrations, or lower explosion limits of the dust and gas respectively. The area of explosibility of hybrid mixtures of coal dust and methane with air is well indicated by Banhegyi and Egyedi[73] in their explosive area plots, and is shown in Figure 3.10.

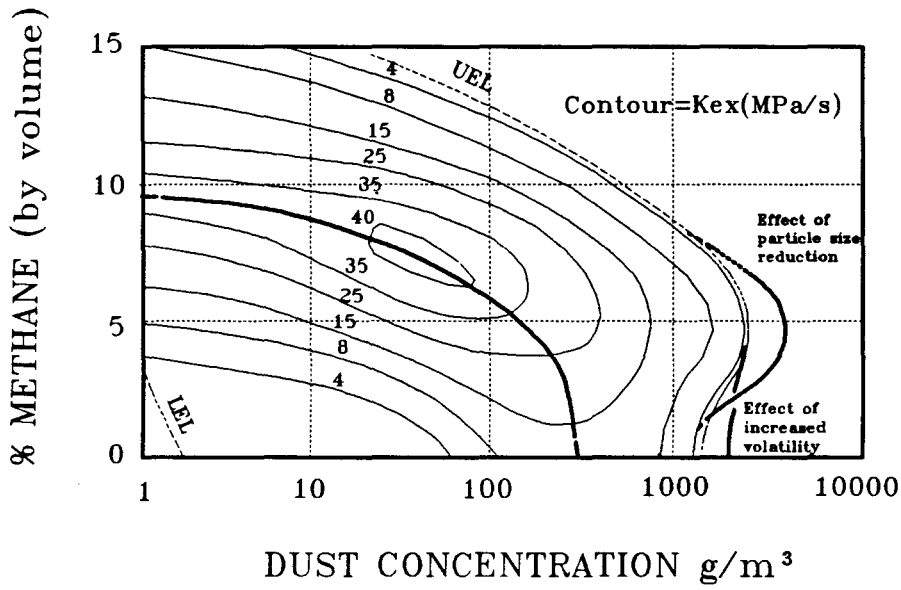

Fig.3.10. Area of explosible hybrid mixtures of coal dust, methane and air with explosibility contours indicating the concentrations of optimum mixtures, based on Banhegyi and Egyedi[73].

Ishihama, Enomoto and Takagi[77] found that mixtures containing more than the upper explosive limit of coal dust can be made explosible by the addition of methane. On the other hand, when the upper explosion limit of methane is exceeded, dust addition will not make it explosible. They also found that the explosive limits broaden for hybrid mixtures when the particle size is reduced, but without methane the upper explosive limit decreases when particle size is reduced.

Ishihama et al also found that in the explosible range of methane, volatile content has little effect, but below the lower explosive limit of methane, it determines to a great extent whether propagation will occur. The point of highest dust concentration which is still explosible, or the "tip of the explosible area peninsula", stays constant

for any volatility, but the line connecting that point and the upper concentration point moves out with increased volatility. Reeh[78] reports an increase in explosibility above coal alone mixtures for hybrid mixtures, and a stronger amplification of explosibility the more carbonised the coals are. For example, a low rank semi-bituminous coal explosibility (K_{ex}) increased 26 % with the addition of 1 % methane. For the same percentage addition to an anthracite, a 72 % increase in explosibility has been observed.

Studies undertaken by Reeh[78] in a Godbert-Greenwald type vertical tube oven, confirm methane concentrations do not lower the ignition point markedly. He concludes that the ignitability of hybrid mixtures is not increased by hot surfaces. Foniok[79] studied the decrease in the minimum ignition energy required to ignite a coal alone mixture when introducing small percentages of methane. Table III.II shows the rapid decrease in ignition energy of an electrostatic spark, when a bituminous coal with 31 % volatiles is mixed with methane.

TABLE III.II The percentage reduction in mimimum spark ignition (E_{min}) energies for a bituminous coal in the presence of small quantities of methane - after Foniok[79].

% CH4	0.0	0.5	1.0	1.5	2.0	3.0
E_{min}	100	45	24	14	10	5
% SD	0	25	10	7	6	5

At methane concentrations below 5 %, the maximum explosion pressure is relatively independent of CH_4, the only effect being to increase the rate of pressure rise according to Hey[80]. Above 8 % to 10 %, maximum explosion pressure falls rapidly, as can be deduced from Figure 3.9. Hybrid mixtures yielding the greatest pressures and rate of pressure rise are generally achieved slightly below stoichiometric methane concentrations with low dust loadings.

Experiments carried out in an explosion gallery by Lunn, Quince and Brookes[81] revealed increased pressure in the gallery with the addition of small quantities of methane. A linear increase in heat output and rate of heat output for methane addition between 0 % and 4 % in the gallery has been obtained. The amount of coal consumed falls linearly with increased methane content, with almost no dust participation at 5 % methane.

In conclusion, it is clear that the behaviour of each component of hybrid mixtures has been well researched, but when mixed surprising behaviour not yet fully explained occurs. Most important for the aims of this research is the increased tendency of dust clouds to ignite (sensitivity) when methane is present in low concentrations. In other words, it is important to realise that a reduction in the lower explosive limits of methane occurs when small concentrations of coal dust are present. In addition, Reeh[78] states the following: "The tests with graduated ignition energies show that one can conceive of ignition sources which do not ignite coal dust/air mixtures but which cause ignition when the combustion air contains methane".

3.6 SUMMARY AND POSITIONING

This chapter explains the mechanism of the thermal explosion phenomenon, which is best portrayed by the Thermal Explosion Theory. A contest occurs within the volume containing the explosible reactant between heat generation, which attempts to establish an exponential rate of heat addition to the system, and the rate of heat loss from the system. From the theory it is clear that explosions of identical explosible mixtures will behave differently if the nature of the ignition source is changed from volumetric to point source.

Methane and coal dust were investigated in their capacity as explosible fuels. The physical quantities as measured by various researchers have been reviewed, in order to establish an understanding of ignition and combustion of the individual

components, and the difference in ignition and combustion of gaseous and dust fuels. The burning of the two types of fuel in combination has also been treated, revealing an incomplete understanding of the explosive behaviour of hybrid mixtures.

Throughout this chapter, the importance of the method and intensity of ignition is suggested. The relationship between ignition energy and ignition temperature leads to the idea of equivalence of the two concepts. In the next chapter, the emphasis shifts from the fuel to the way in which temperature and heat flow is delivered from different sources of ignition.

CHAPTER IV

IGNITION SOURCE MECHANISMS

The three major sources of face ignitions, namely explosives, electricity and friction are discussed. The ignition mechanisms are explained and the protection measures expanded upon. Recent studies which represent an approach emphasizing the equivalence of different types of ignition sources are reviewed. The need in this study for a more uniform explanation of ignition is justified, and the chapter concludes with a suggestion of how such an understanding can be achieved.

4.1 INTRODUCTION

In 1877 a commission was appointed in France to inquire into the question of ignitions of firedamp by explosives. A report tabled in 1880 concluded that there was no explosive known which would not ignite methane - Marshall[82]. Reduction of flame temperature by addition of cooling salts led to "safety" or "permissible" explosives, which had a much lower propensity to ignite methane when used in collieries.

Mechanisation and increased productivity have resulted in the introduction of electricity and mechanical excavation techniques. The development of flameproof or intrinsically safe electrical equipment and work aimed at the understanding of the ignition of methane by cutting tools started in earnest in the late nineteen forties[29]. Today, research on all these aspects continues, but frictional ignitions have not been reduced to the same extent as ignitions from explosives and electricity.

The three sources of ignition differ so much in nature and the way in which ignition is effected, that they were traditionally studied separately. In the nineteen eighties however, researchers such as Krzystolik and Sliz[83] and Hertzberg, Conti and Cashdollar[84] started to consider different sources of ignition comparatively, leading to the idea of equivalency of all types of ignition sources.

This chapter starts with a brief review of the current understanding of ignition from explosives, electricity and friction and this is then followed by a comparison of the more detailed approaches to ignition sources.

4.2 IGNITION MECHANISMS OF DIFFERENT TYPES OF IGNITION SOURCES

The interest of scientists in colliery safety played a major role in establishing safer coal mining conditions - Urbanski[85]. After the 1812 Branding Main colliery explosion near Gateshead-on-Tyne in which 92 miners lost their lives, the "Sunderland Society" was formed aimed at the prevention of accidents in coal mines. The society persuaded Sir Humphry Davy to investigate the problem of methane in collieries, which led to the invention of the flame safety lamp. Another example is the study of Mallard and Le Chatelier, which identified the temperature dependence of the lag on ignition of methane. Explosive engineers realised that if the duration of flame is kept short, methane ignition might not occur irrespective of the flame temperature. The long lasting flame of gunpowder and its high explosion temperature of approximately 2400 °C excluded blackpowder from use in coal mines. In testing galleries, it was found that methane was not very sensitive to ignition when using high explosives with short flame durations. A short discussion follows.

4.2.1 IGNITION BY EXPLOSIVES

According to Ramsay, Wass and Hartwell[22], the mechanisms by which explosives can cause ignition of methane/air mixtures are as follows:

1. Ignition directly by flame or inert but hot gas
2. Ignition by compression and
3. Ignition by solid particles of the reacting explosive either at the cartridge or thrown out by the explosion. They may in some cases be preceding ahead of the shockwave front. Inert particles at high temperature, or brought to high temperature by impact, might have the same effect.

In the U.K., a Home Office Testing Gallery Committee was appointed in 1896 with the aim of establishing the best test for determining the safety of explosives in coal mines. A gallery was established at Woolwich (which moved to Buxton in 1922), and testing of explosives for inclusion in the "Permitted List" began in 1897. Permitted explosives are explosives adjusted by either primary composition or by additives, in order to prevent *a)* flame of long duration as a result of slow burning, and *b)* violent shock-wave formation caused by a high rate of detonation. The safest explosives are those with intermediate properties, which explode relatively slowly but still fast enough to be below the lag on the ignition of methane.

Flame Ignition

Various studies to determine the dimension, intensity and duration of flame produced by explosives are reported by Urbanski[85]. The more important conclusions from these studies are given. Explosives with an adequate oxygen balance deliver only a primary flame, while products such as CO, H_2, CH_4 and NO are formed as a result of incomplete reaction for an oxygen poor explosive composition. The combustible products result in a secondary flame which is highly incendive. Ammonium nitrate ensures much greater safety than dynamites, chlorides or perchlorate explosives. Salts such as chloride of alkali metals, e.g. potassium and sodium, are particularly efficient in cooling the flame. These measures can reduce the duration of flame flash from approximately 8 ms for a nitroglycerine based explosive to less than 0.5 ms for an ammonium nitrate explosive. Further operational aspects such as provision of an additional free faces (face cutting and delay electric detonators), stemming of holes, hole diameter and charge diameter and wrappings, play a role.

The actual mechanism of ignition is well described by Grant and Mason[86]. They studied tetryl charges when exploded in an unstemmed borehole. Observations of photographs from a high speed camera aimed at the rim of a blast hole, led to the following understanding of the ignition process. As the explosive ignites, a detonation wave develops, progressing towards the open end of the blast hole. The detonation wave is curved, as shown in Figure 4.1. As the wave breaks through the end of the

charge, the centre leads the wave at the rim, and a jet of unexpanded hot gases (3500 °C) penetrates the methane-air mixture. The subsequent ejection of already expanded and therefore cooler gases from the earlier phase of the detonation surrounds the hot jet and, if this occurs in time, no ignition will occur.

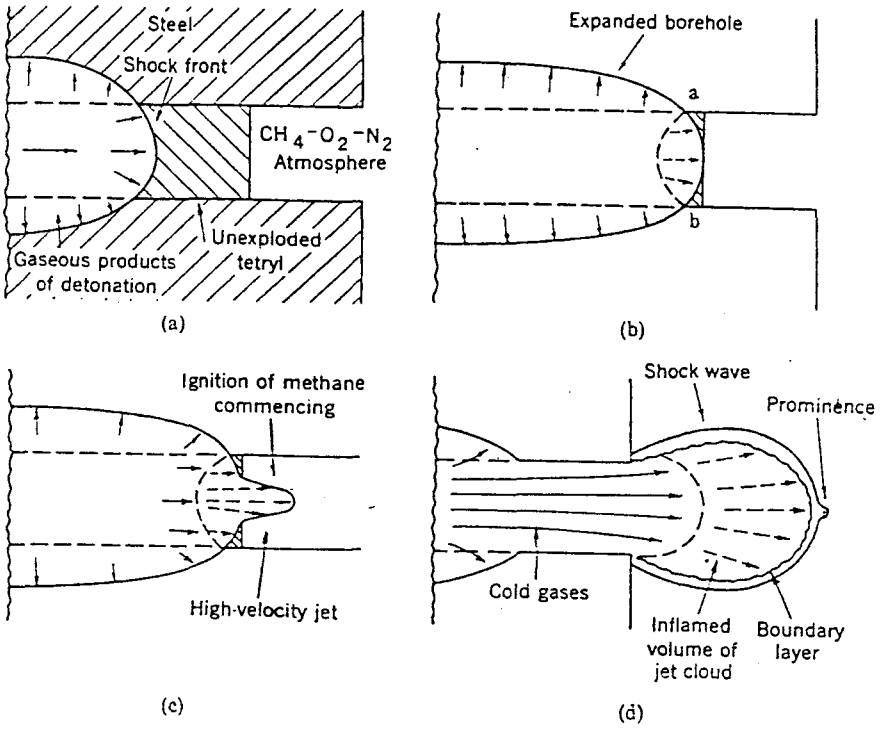

Fig.4.1. Development of shock wave and gaseous products of detonation when an unstemmed charge of high explosives is fired from a borehole into a flammable atmosphere, such as methane and air, after Grant and Mason[86].

Deflagration of explosives, instead of detonation, provides a flame produced from a relatively slow burning process, resulting in a highly incendive ejection of flame into the explosible atmosphere. Deflagration takes place if desensitization by means of inadequate ignition occurs, either by transmission problems between cartridges, or if conditions render the explosive less sensitive.

Shock Wave Ignition

Some explosives, when used in large quantities, ignite methane therefore a charge limit is often set. This ensures that all the energy of the charge is transformed into work, preventing a shock wave from adiabatically compressing a methane-air mixture, forcing the mixture to ignite. As the shock wave travels through the hot gaseous products, ignition might occur, but ignition might also start in spots not yet reached by the flame of detonation, since the shock wave velocity is higher. Fordham[87] also mentions that the indirect action of the shock wave, after it has been reflected from a solid surface, can also act as source of ignition.

It was found that a mixture of 6.5 % methane with air may ignite when subjected to rapid compression to 5.5 MPa by mechanical means according to Urbanski[85]. Although the adiabatic equations of state for the vapour of a compressible substance are applicable here for the gaseous ignition by compression $T_2/T_1 = (V_1/V_2)^{\gamma-1}$, a more complex mechanism for shock wave ignition of dust is given by Sichel et al[88]. As the shock wave passes over the dust particle, supersonic flow around the particle is induced, and convective heating causes a rapid temperature increase of the particle surface. The drag forces accelerate the particle, reducing the relative velocity of particle in relation to the hot gaseous environment. The rate at which the particle and the gaseous oxidizer react increases until the critical temperature is reached and a runaway reaction starts.

Solid Particle Ignition

A possibility exists that still undecomposed explosive can be ejected with the detonation products and that this may undergo further explosive decomposition as temperature and pressure change along the path of travel. The wrapping materials and cartridge closure clips can also act as sources of ignition, and therefore harmless material is selected for these purposes.

4.2.2 IGNITION BY ELECTRIC SPARKS

The are two methods by which electricity can cause ignition. Firstly, a conductor carrying an excessive current might become heated due to the resistance it presents, causing methane ignition by heat transfer to the surrounding gas. This mechanism is similar to ignition from heated surfaces, assuming that the metal involved, e.g. copper, will not act catalytically. Secondly, conductors can be close together, but not touching, and a spark might pass if the potential difference across that point is sufficient.

A gas in its normal state is one of the best insulators of electricity known. For a small potential difference across two electrodes, an extremely small but proportional current will pass. As the potential difference increases, a saturation voltage is reached quickly, beyond which the current stays constant and independent of voltage. If the electric field is increased substantially above saturation point, another critical potential is reached where current again starts to increase until a spark, accompanied by a large current, passes between the electrodes. The process of gaseous conduction is explained by Crowther[89]. He assumes the set up of a charged system of gaseous ions conveying current across the gas by moving in opposite directions (depending on their charge), through the gas, under the action of the electrostatic field. Energy for ionization might come from the kinetic energy of colliding particles, as they are moving in opposite directions. Released ionization energy produces heat and consequently radiation.

Visually, the appearance of the spark can change as conditions such as spark gap, electrode characteristics and electric input is changed according to Ramsay, Wass and Hartwell[22]. This observation is confirmed in this thesis, and a low current spark is observed to be a reddish colour while a high current spark is bright white. Ramsay et al also point out that the arc temperature is 2500 °C or higher.

Spark Incendivity

The minimum ignition energy of a dust is defined as the quantity of energy just not capable of igniting the most easily ignitable mixture in a series of concentrations. The energy W dissipated by a spark passing through air is given by

$$W = \int V I dt \qquad -4.1$$

where V is the potential difference across the spark and I the current flowing. The power P dissipated in the arc is given by

$$P = I^2 R \qquad -4.2$$

where I is again the current flowing and R the electrical resistance of the spark.

The incendivity of a spark depends on the capacitance, inductance, voltage, current, the way in which the circuit is broken, spark gap, spark duration and the shape and material of the conductors between which the spark occurs - Cross and Farrer[90] and Ko, Anderson and Arpaci[91]. When an inductive circuit is broken, $(LI^2)/2$ energy is released, L being the self-inductance. A secondary winding on all coils in the circuit, a non-inductive resistance and a capacitor can absorb the energy in order to make the circuit safe. Energy level for ignition of gases such as methane is of the order 0.1 mJ for large inductances (1H) and 0.25 mJ for smaller inductances (0.3 mH). Sparks may also be produced from energy stored in capacitance, which is given by $0.5CV^2$ where C is the capacitance. For example, to limit spark energy below 0.2 mJ, a 24 V circuits capacitance must therefore be limited to at most 0.7 μF.

The minimum ignition energy decreases with increased spark gap until a critical value is reached, beyond which it stays constant over a considerable range, and then increases linearly with further increases. The minimum ignition energy also varies with spark duration, with an optimum duration that is determined by the mixture

and geometry of the situation. The absolute minimum ignition energy is obtained at the lowest energy at which the critical spark gap still ignites a gas for the optimum duration of the spark. The minimum ignition point is not sharply defined, but rather a transitional belt of energies. Probability of ignition, and thus incendivity, decreases from 100 % to 0 % as energy is reduced across the minimum ignition band.

Spark Ignition Mechanism

Ko, Anderson and Arpaci[91] studied empirically the ignition process as an inductive spark develops, by analysis of images obtained from a high speed camera. The flame kernel growth over time as the spark develops, reveals a critical radius that the flame kernel must reach for the successful establishment of a propagative flame. The existence of a marginal state is described, separating growth and collapse of the kernel. For a non-ignition event, the kernel growth rate decreases until it stops completely and starts to grow negatively. When ignition takes place, the rate of kernel growth decreases from the time of appearance until the critical radius is established, and continues from there with accelerated kernel growth until the adiabatic flame speed is reached. Figure 4.2 illustrates this graphically.

Ko, Arpaci and Anderson[92] modelled the ignition of propane as observed from the empirical investigation. Qualitatively explained here, their model separates flame establishment from kernel development. Flame formation is always taking place with spark formation, because a high temperature kernel is produced by the electrical breakdown of the gas. The thermal transmission of heat to the adjacent gas sphere determines kernel development, with successful progression if the energy input produces a kernel radius in excess of the critical radius. The two processes are observed separately, with flame establishment producing a shock wave that decays into an acoustic wave in a few milliseconds, followed by the relatively slower diffusive boundary layer of the growing hot kernel. If the reaction rate produces within the kernel more heat than is lost to the immediate gas layer encapsulating it, propagation of an adiabatic flame is established.

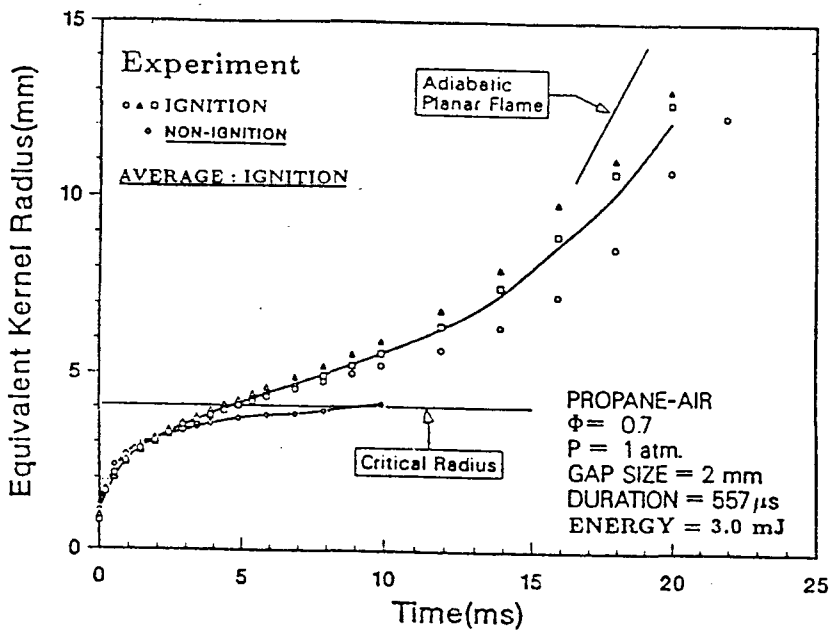

Fig.4.2. The growth of a spark kernel radius in a propane-air mixture at near minimum ignition energy conditions - Ko, Anderson and Arpaci[91].

The model adequately explains the observed behaviour of reduced minimum ignition energy with increased spark gap. Very conductive electrodes will act as a heat sump, increasing the energy required for ignition. Larger geometrical sized electrodes will have a similar influence.

Protection against Electrical Spark Ignition

Generally, precaution against the accidental ignition of an explosible atmosphere is taken by making circuits intrinsically safe as explained above, or by enclosing the potential spark generation elements in a casing. Flameproof enclosures must be strong enough to withstand an internal explosion of firedamp, and the gaps in the joints between various parts of the casing must be so designed that no flame from an internal explosion will be able to ignite an explosible mixture outside the casing. Power cables, whether permanent, semi-permanent or trailing cables are, however,

a source of great danger when damaged in the course of operation. Adequate maintenance of the operational environment stays, therefore, the primary action for the elimination of explosions.

4.2.3 FRICTIONAL IGNITIONS FROM COAL MINING BITS

The ignition of firedamp by the impact of tools on rock only became regarded as a problem in the nineteen twenties, with the first review of the hazard by Burgess and Wheeler, as mentioned in a recent review of Powell[93]. A wealth of work investigating the phenomenon has since been published, and periodically the work has been summarised by authors such as Powell[93], Wynn[94] and Courtney[95].

Ignition by impact and friction can broadly be divided into frictional ignitions in which energy stems purely from mechanical motion, such as mining bits cutting rock, and frictional ignitions in which the effect of mechanical motion is amplified by the chemical generation of heat. The temperatures reached in frictional ignitions of the first group are much less than those of the second group, the former unlikely to exceed 1200 °C and the latter of the order 2500 °C or more - Ramsay, Wass and Hartwell[22]. The lag on ignition of firedamp, as shown by Naylor and Wheeler[56], is reduced substantially with higher temperature of ignition sources. For lower temperature sources therefore, relatively large areas must be in contact with the explosible methane-air mixture for a relatively long period, otherwise the lag of ignition exceeds the period of contact, and no ignition occurs. In contrast, the chemically active frictional sources reach such high temperatures that they can afford a short exposure time and still effect ignition.

Light and strong metals such as magnesium and aluminium tend to react exothermically with oxygen. Furthermore, if rubbed on rusted steel, incandescent sparks are noticed. Their incendivity can be reduced by combination with other metals into alloys, but usually the benefit of lightness is then lost. Methane can also be ignited by rubbing steel on steel, but considerable loads and exposure times are required.

The incendivity of sparks from friction of metal on metal, metals on rock or rock on rock have been studied inter alia by Titman and Wynn[96], Rae[97], Blickensderfer et al[98], Lobejko[99] and Bartnecht[100]. Sparks are observed as hot particles which are torn off the material by the mechanical process and are ejected glowing visibly. The studies show that both reactive and inactive metal and rock particles can ignite methane, although it can be concluded that in practice it is not the mechanically produced sparks, but rather the hot surfaces of the rubbing part that should be the most frequent source of ignition.

Coward and Ramsay[101] reviewed the ignition of firedamp by means other than electricity and explosives. They mention work done by Silver in 1937, who increased the diameter of quartz and platinum spheres from 1 mm to 5 mm and projected them at a velocity of 4 m/s from a furnace at high temperature into a mixture of explosible gas with air. He observed much higher ignition temperatures than the expected temperatures for ignition of gaseous mixtures, and found that increased sphere diameter resulted in a considerable reduction in the minimum ignition temperature. This is analogous to the critical radius of an electric spark and the ratio of energy generating volume to energy receiving volume determines whether an ignition will take place or not. Methane was found to be very difficult to ignite, and only an 8 % methane-air mixture could be ignited with a 6.5 mm diameter sphere heated to 1200 °C. The incendive spark shower behind a coal cutting bit is made up of particles at probably similar temperature but with much smaller diameters, making ignition from such sparks seem highly unlikely.

Coal Bit Ignition Mechanism

Blickensderfer, Deardorff and Kelley[102] showed that the cause of ignition during cutting using a coal mine pick, is the hot spot left behind the trailing edge of the pick on the rock. The hot spot can be formed by a thin layer of metal wiped onto the rock, or rock adhering to the metal and then smeared. The maximum hot spot temperature was found to be 1420 °C, falling to 800 °C within 40 ms. Rae[103] investigated the role of quartz in the ignition of methane by the friction of rocks,

and concluded that quartz is the only common mineral with a high enough melting point to cause ignition of methane. Increased loadings and speed also raise the probability of ignition. The ignition process starts with the pick tip being heated by friction, and the softening temperature of either the metal or rock, depending on which is the lowest, being reached. The softer material is then smeared by the forward motion of the pick, and a thin filament is left on the rock. If the softening temperature is within the range that can ignite methane, ignition is possible. Only rock and metal remaining strong up to these temperatures (about 1250 °C) can cause ignition by continuous rubbing.

Blickensderfer[104] explains that the kinetic energy of the wheel or drum holding the pick is converted into several other forms of energy during impact. He calculates from a quantitative model that only 1 % of input energy goes into rock removal, while the rest is mostly converted into heat. The creation of new surface area, the ejection of rock particles, the creation of elastic waves in the tool and rock and the plastic deformation of the material are the major elements of energy consumption. In the latter case, energy is required both to achieve and maintain the molten state of the material, while heat is being conducted into the rock and tool during the time of contact.

As the tool moves on, this molten material on the rock surface is exposed to the explosible mixture of methane and air, as is shown in Figure 4.3 for an element of length dx of a smear of thickness b and width w. The parameters that now determine ignition are the temperature, lifetime and area of the hot smear. The temperature at which a medium carbon steel solidifies and liquefies are 1450 °C and 1500 °C, and the melting point of both SiO_2 and Tungsten Carbide is about 1710 °C. Blickensderfer calculated the heat loss by radiation to be less than 2 % of that lost by conduction, and that the convective loss is even less. His conductive heat loss profile over time is shown in Figure 4.4, together with the temperature profile with distance from the tool's edge. The width of the streak is equal to the width of the

tool, *w*, and the length is determined by the speed. Smear dimensions were found to be 10 mm x 25 mm for a cutting speed of 1.5 m/s, and 10 mm x 80 mm for a cutting speed of 4.6 m/s.

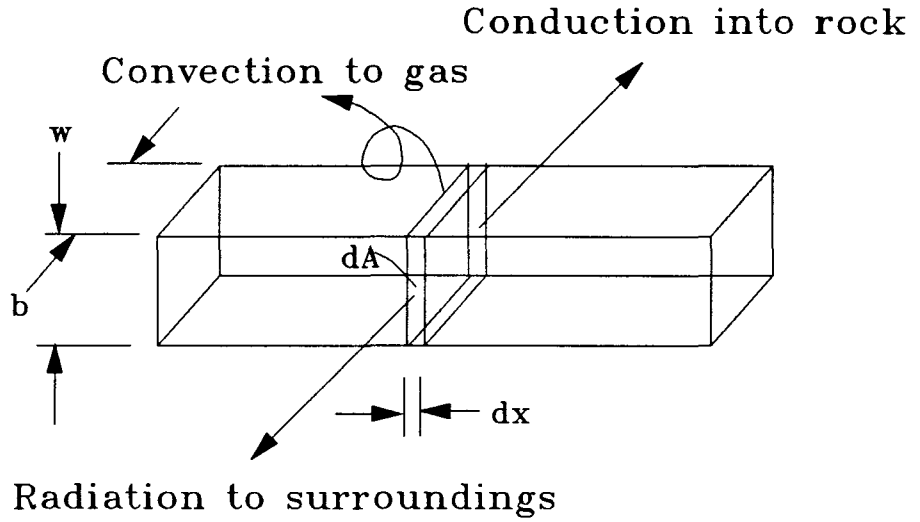

Fig.4.3. Heat losses from a hot frictional metal smear on rock, of thickness *b* which is greatly exaggerated. The streak width is w, and an element dx is considered, giving an area $dA=wdx$. After Blickensderfer[104].

From the explanation, it is clear that for inactive materials the solidus and liquidus temperatures are limiting the maximum temperature of the hot spot, resulting in longer lag times and slower pressure build-up during ignition and initiation of the explosion. Such explosions are therefore expected to be less violent.

Protection against Frictional Ignitions

The probability of ignition can be reduced by better designed cutting tools, by provision of water sprays directed at the area directly behind the tool and by reduction of the loading and power of the cutting process. In 1967 a laboratory rock cutting machine came into use at the Safety in Mines Research Establishment in the U.K. to study the influence of pick speeds and water sprays on the probability of

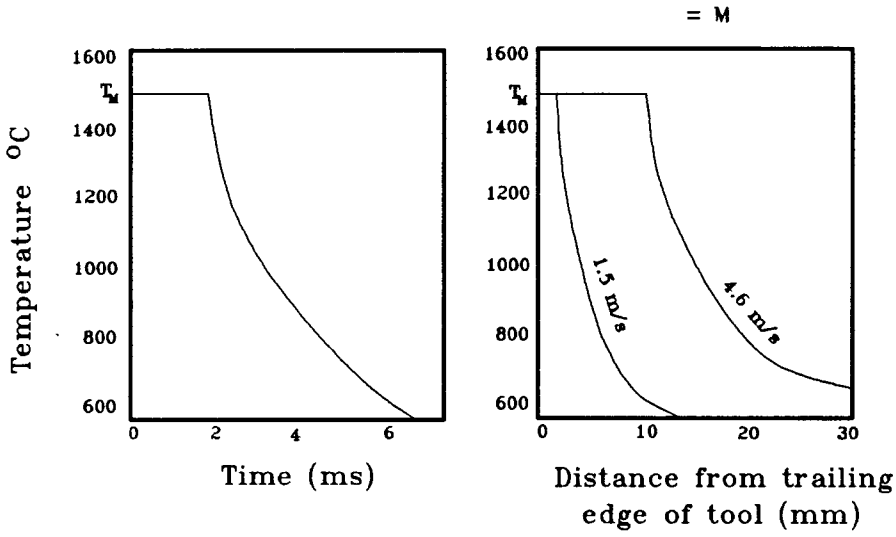

Fig.4.4. The temperature profile with time (left) and with increased distance from the trailing edge of the tool (right) for a smear thickness of *0.02* mm. After Blickensderfer[104].

ignition[93]. A similar machine, simulating the cutting conditions of a continuous miner drum, has been used by the Bureau of Mines in the U.S.A. in order to improve cutting bit designs - Larson et al[105].

The conclusions reached by these two research programmes are sometimes contradictory. For example, Larson et al[105] found rotating conical bits very effective if rotation is ensured, while Powell[106] states that the worst results at Buxton were obtained with point attack picks and that the best results were obtained by forward attack picks. Powell suggests a round-nosed forward attack pick with polycrystalline diamond on the rake face to be best suited to limit ignitions by friction. Cutting speed must be kept low, although lower speed can increase probability of ignition if the cutting tool is hot, according to Larson. Powell and Billinge[107] show a dramatic drop in the time required for a 50 % probability of ignition (t_{50}) if cutting speed drops below 1.25 m/s when using new picks, and 0.7 m/s when using worn picks.

Powell and Billinge[107] also show that the parameters affecting the efficacy of a spray in preventing ignitions are the spray density (or quantity of water per unit area), the droplet size and, to a lesser extent, droplet velocity. An empirical relationship between these variables is given as:

$$t_{50} = 5.31 + 3.3 \times 10^{5} q v^{0.35} / d^{3} \qquad -4.3$$

where t_{50} is the time to a 50 % probability of ignition in seconds, q the spray rate in $l/(m^2 s)$, v the droplet velocity in metre per second and d the droplet diameter in micron metre. The spray increasing t_{50} most, must be selected.

In another paper, Powell and Billinge[107] show that rocks susceptible to ignitions generally contain more than 30 % quartz by volume, with quartz particles being greater than 10 μm in size. Siltstones, sandstone and iron pyrites are dangerous, while ignition is unlikely when cutting mudstone, shales, clays or ironstones.

Wet head cutting drums, continuous inerting, methane drainage and water infusion into the seam are examples of other measures that can be taken to reduce the probability of ignition. Recent history proves, however, that the problem is far from solved, and that another look at the environment around such cutting drums might prove worthwhile.

4.3 IGNITION SOURCE EQUIVALENCY

As is predicted by the ignition theory as discussed in Chapter III, the behaviour of an explosion is influenced by the strength of the source of ignition. As energy increases, so does temperature. In an explosion vessel, the amount of potential energy contained in the explosible fuel is equal to the fuel's enthalpy. When an explosion is initiated, the energy of the source determines the reaction rate. When energy is increased, the reaction rate also increases. The maximum pressure obtained when the fuel loading is kept unchanged will therefore stay constant and only the rate of pressure rise will differ - Bartknecht[28]. Close to the minimum ignition energy, any

small increase in energy greatly increases the rate of pressure rise, but with higher energies the influence weakens until a plateau is reached where energy increase only marginally affects the rate of pressure rise. Figure 4.5 explains.

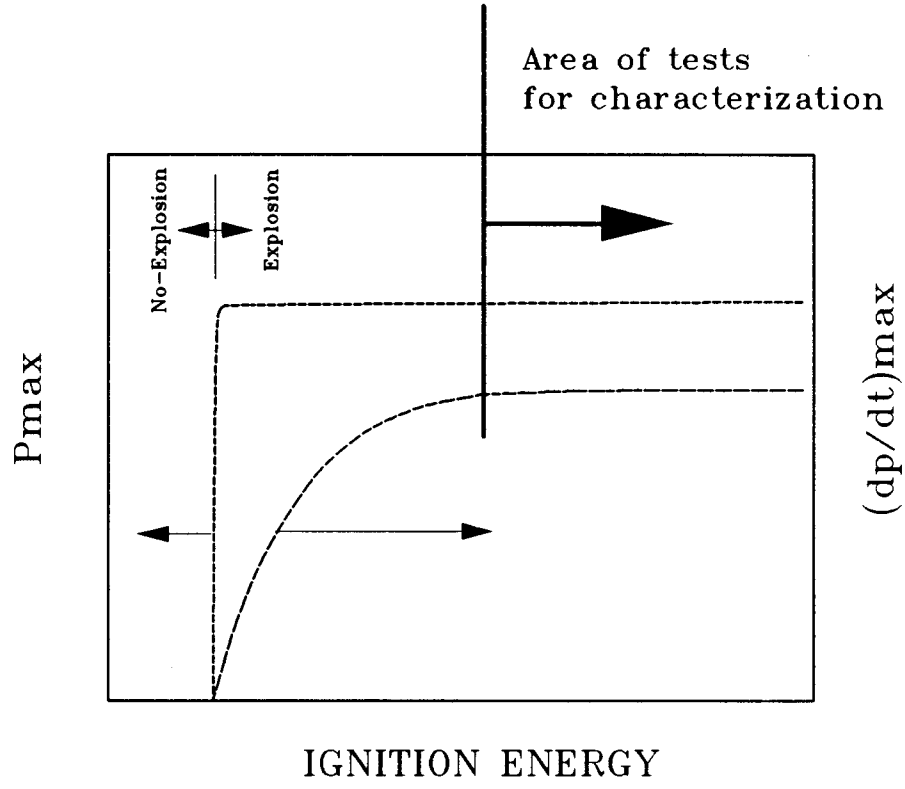

Fig.4.5. The change in explosion characteristics (maximum pressure P_{max} and maximum rate of pressure rise $(dp/dt)_{max}$) with increased ignition energy at constant fuel concentration. The area of more constant maximum pressure rise where explosibility characterization is done, is indicated.

When an attempt is made to characterise the explosibility of an explosible material, the energy source should be powerful enough to ensure that testing is done in the zone where the rate of pressure rise only changes marginally with increased ignition

energy, which will ensure both reproducibility and an expression of the maximum explosion potential of the substance under consideration. Weak explosion behaviour has therefore not been studied until recently.

The independent development of testing facilities worldwide led to a lack of standardization of testing facilities and procedures, making comparison of results difficult. In recent years a start has been made to standardize testing procedures[83]. In order to standardize the source of ignition, the influence of strength and type of ignition on explosion behaviour needed to be understood. Experiments investigating the dependence of explosion behaviour with different sources of ignition have been carried out at most major research institutes, of which the work of Cybulski[1] serves as the best example. A more uniform understanding and explanation of the phenomenon was nevertheless lacking. Krzystolik and Sliz[83] realised in the early nineteen eighties that such a global understanding of the ignition process might enable comparison of results from different testing facilities.

They continued to compare experimental results from laboratory scale explosion vessels and large scale galleries in which type and strength of the initiators were varied. The effect of the explosion was measured in terms of the explosion index Z, which shows percentage incombustible addition per unit pure coal to prevent propagation (see Chapter II). The method allowed application in both vessels and galleries.

A significant coincidence of test results was obtained when an electric arc and a chemical detonator of similar energy were used in identical conditions, resulting in the same values for rate of pressure rise and explosibility value Z. Despite the different nature of the ignition sources, they acted identically. It was also found that although absolute values of rate of pressure rise and the explosible concentration range were not equal for two totally different ignition sources, namely a 1 J electric spark ignitor and a 250 J chemical detonator, the pattern of change in values with

change in concentrations could be matched, as is illustrated in Figure 4.6. Clearly, proof has been obtained that all sources of ignition are related, and that each source is only a different combination of the ignition variables involved.

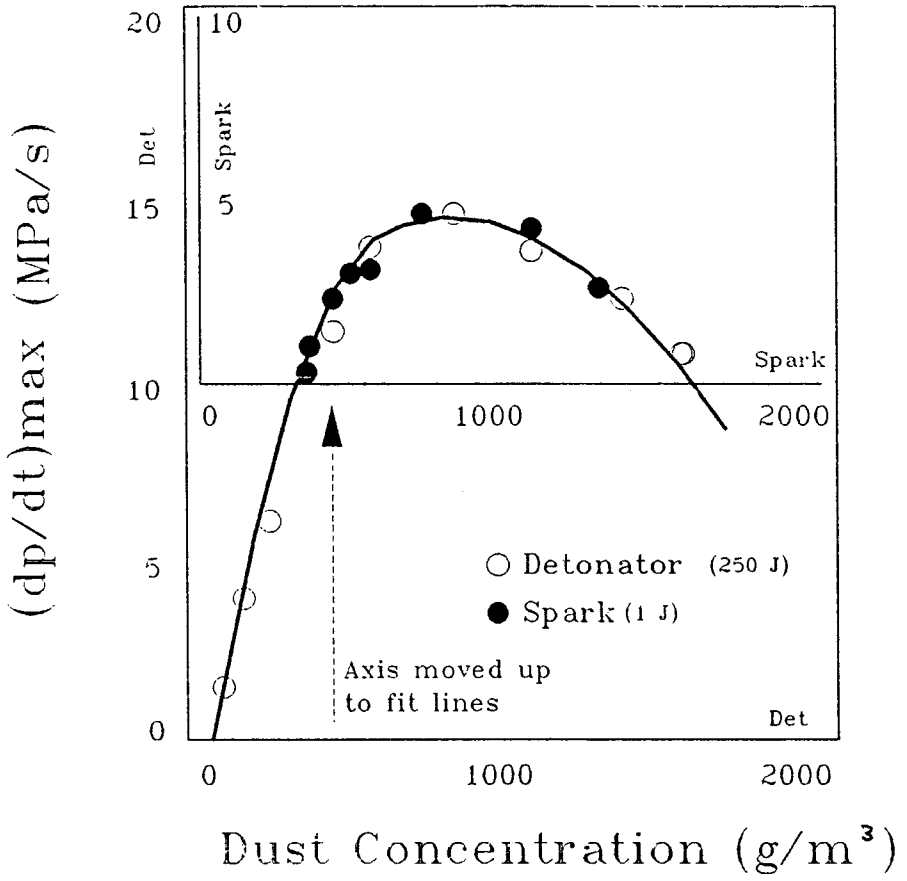

Fig.4.6. Comparison between explosion characteristics of the same coal dust initiated by a weak spark of energy output 1 J, and a strong chemical ignitor with an energy output of 250J, according to Krzystolik and Sliz[83].

At the same time, the U.S. Bureau of Mines started to evaluate the explosion hazard in terms of the product of probabilities of the existence of a flammable volume and the presence of a source of ignition - Conti et al[109]. In considering the second aspect, a domain of varying probability of ignition, bordered by areas of 0 % and 100 % probability of ignition, has been identified. Hertzberg, Conti and Cashdollar[84] explain

the thermodynamic state of a uniform mixture of fuel is multi dimensional, with temperature, pressure and initial compositional variables such as fuel concentration the independent variables. The flammability range is described as a surface separating a domain in which flame propagation is possible from one where it is not possible. In other words, the domain of 100 % probability of ignition of a flammable volume is separated from a domain of 0 % probability of ignition and can be seen in Figure 4.7.

If an isothermal plane of average atmospheric temperature is taken from the thermodynamic state-space, it is clear that a non-flammable mixture at atmospheric temperature can become flammable at an elevated pressure. Similarly, on an isobaric plane at atmospheric temperature, a non-flammable mixture at atmospheric temperature may become flammable at elevated temperatures. As temperature increases further, a point may be reached where spontaneous ignition will occur, a point defined as the *auto ignition temperature*. The plane of constant atmospheric pressure (0.101 MPa) for a hypothetical coal dust is shown in Figure 4.7. Curve *(f)* is the lower flammability limit, and curve *(i,t)* the auto-ignition limit. The flammable, but not auto-ignitable, domain is perceived by Hertzberg, Conti and Cashdollar[80] as the domain in which typical sources of ignition found in mines operates. Typical ignition/non-ignition lines for electric sparks of different energies are also indicated in Figure 4.7.

An area is therefore delineated within which ignition is possible, provided a combustion wave (the source of ignition) is present. The explanation provides, to a much greater extent, the uniformity required to truly understand the ignition process. The clear pattern that electrical spark ignition follows within this domain illustrates the dominant influence of the thermal processes during ignition. The analysis, however, is still not comprehensive enough since, although one domain for all sources of ignition is indicated, the dissimilar behaviour of different types and strengths of ignition sources within that domain continues to be apparently unrelated.

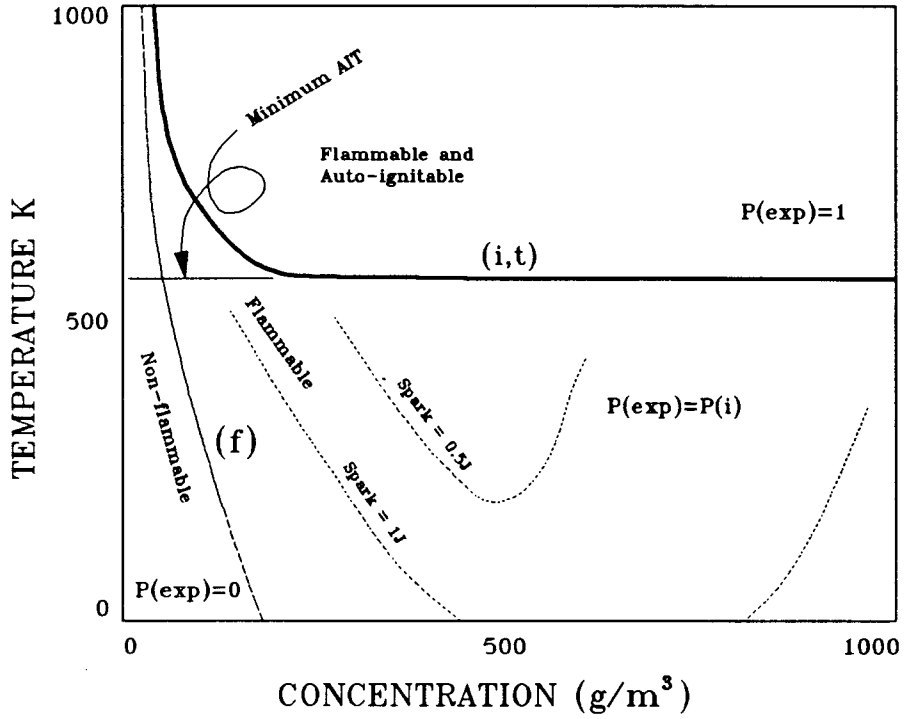

Fig.4.7. Domains of non-flammability, flammability and auto-ignitability at atmospheric pressure for a hypothetical coal dust. The widening range of flammable concentrations for ignition from electric sparks of increased energy is also shown. Compiled from Hertzberg, Conti and Cashdollar[84] and Conti et al[109].

4.4 ASSESSMENT

It is clear from the above discussion of ignition sources that, although individual types have been investigated extensively, the way in which ignition parameters combine to effect explosions is not yet fully understood. The correlations in behavioural trends, even if absolute values of the parameters involved are not comparable, prove that all ignition processes generally relate to one another.

The aim of this study is to delineate a volume within the space formed by combinations of methane, coal dust and different energy levels from ignition sources, which indicates unacceptable high probability of ignition. Since the same fuel mixture can

contain an unacceptable high risk to explode when exposed to one type of ignition source, and an acceptable low risk to explode when exposed to another, a generic understanding of the ignition process is required, in order to show progressively the change in probability of ignition within the domain of all probabilities of ignition.

The Thermal Explosion Theory, as discussed in Chapter 3, looks at the thermal, physical and chemical processes within the reactant mixture that lead to ignition of a runaway reaction. Studies of ignition sources tend to concentrate on the thermal, physical and chemical processes that might lead to ignition, but connected to the source itself. The study of Krzystolik and Sliz[83] shows that, despite the type of interaction between the energy source and reactant, the consequential development of the reaction in the reactant mixture indicates some uniformity. The Bureau of Mines[32,84&109] studies explain the uniformity of change in ignition properties of ignition sources as the state of the initial conditions vary.

What is required is a simultaneous review of the sources of ignition and their effect on the surrounding reactant mixture. This requires interpretation of ignition source parameters such as energy, temperature, duration, volume and geometry with the ignition reaction process, as explained by the Thermal Explosion Theory. In Chapter 5, the relationship between the ignition reaction and ignition sources is discussed, as understood for the purposes of this study.

CHAPTER V

INTERPRETATION OF THEORY

The development of an explosion according to the Thermal Explosion Theory as discussed in Chapter III, and the understanding of ignition sources as summarized in Chapter IV, are simultaneously interpreted here. A more generic understanding of the process of ignition is obtained and used to explain the influence of different modes of ignition on the ignition blanket. The boundaries of the experimental programme to determine the ignition blanket are defined, however, the descriptions of the processes are purely qualitative and it is recognized that data presented later in this thesis will be central to obtaining a qualitative understanding of the mechanisms involved. Finally, the objectives of the experimental programme are listed.

5.1 INTRODUCTION

The Thermal Explosion Theory explains the thermal processes controlling the reaction rate within an explosible substance, leading to an explosion. Studies of ignition sources mostly concentrate on the energies and temperatures required to start ignition. Presented here is an interpretation of the theory in a way which combines the properties of ignition sources with the process initiated by such sources within the explosible substance. The influence of different sources of ignition on the position of the ignition blanket in the energy, methane and coal dust volume can then be explained.

5.2 INTERPRETATION OF THE THEORY

The Thermal Explosion Theory describes the rate of combustion as an exponential function of temperature. The rate of heat generation, $\dot{Q}_{gen}$, is therefore also an exponential function of temperature. When a critical temperature, T_{crit}, is reached, the rate of heat loss is exceeded by the rate of heat generation, and an explosion takes place.

Usually, the reactant mixture is at an ambient temperature at which no reaction takes place. When an external heat source is introduced, the temperature is elevated. Heat inflow from the source of ignition, $\dot{Q}_{inflow}$, increases the number of molecules within the explosible mixture that are in the activated state, and after a short delay a combustion reaction starts to proceed.

The suddenness of this transformation is dependent on the rate of absolute heat transfer, or $\dot{Q}_a$. The rate of absolute heat transfer, $\dot{Q}_a$, is the difference between the rate of heat inflow, $\dot{Q}_{inflow}$ and the rate of heat loss $\dot{Q}_{loss}$. To ensure an explosion, the source of ignition must be exposed long enough to the explosible mixture. If the duration of exposure is time t, the amount of energy transferred is $\dot{Q}_a t$. Relatively low ignition source temperatures will require longer ignition exposure times to allow for enough energy to be transferred to effect an explosion. At very high temperatures, $\dot{Q}_a$ is so rapid, that virtually no lag on ignition is observed.

The reaction rate, initially non-existent, now proceeds at the rate commensurate to the new temperature brought about by the ignition source. At minimum ignition energy conditions, the ignition source temperature must at least be marginally above the critical temperature. This initial temperature determines the rate of reaction and, consequentially, the rate of heat generation, $\dot{Q}_{gen}$. Only a $\dot{Q}_{gen}$ established above T_{crit} will initiate an explosion. Ignition sources with short duration times require source temperatures far above T_{crit}, to ensure that the temperature established within the explosible mixture in time t, is at least above T_{crit}.

Importance of Ignition Source Geometry and Volume

The geometry of the source, or the way in which the ignition source is introduced, determines the heat loss properties of the system. When a source of ignition suddenly injects hot gaseous reaction products into the volume containing the explosible mixture, the energy transfer occurs throughout a substantial proportion of the volume. After the lag period, heat generation starts throughout the volume and heat loss is determined by the surface area and material of the walls of the container. This

situation is defined as *volumetric ignition*. Since no temperature gradient within the reactant exists, Semenov's interpretation of the Thermal Explosion Theory is expected to describe this situation adequately.

When ignition starts from a small localized point within the reactant mixture, the surrounding reactant mixture forms the walls of the reacting volume. Heat loss is now determined by the heat flow properties of the reactant mixture itself, and by the surface area of the hot spot exposed to the reactant mixture. Heat dissipation, due to the thermal gradient within the reactant mixture itself, allows the flame to propagate. This situation is defined as *point source ignition*. The Frank-Kamenetski and "hot spot" theories might be representative of this situation.

An unequivocal volumetric or point source does not exist. For example, weaker volumetric ignitors which only fill a small part of the total reactant volume, contain properties of point source ignition, or very strong point source ignitors incorporate volumetric ignition properties. An absolute volumetric source of ignition will be infinitely extended in space and duration, while an absolute point source will not contain any volume. The auto ignition temperature, as defined by Hertzberg[32] and discussed in Chapter III and Chapter IV, is the ultimate volumetric condition that can be created practically. A very hot electric arc is the best point source that can be created practically.

All sources of ignition lie between the two extremes of volumetric and point source ignition. For example, a frictional hot smear behind a coal cutting bit incorporates a surface area and therefore holds volumetric properties, but in relation to the dimensions of the reactant mixture surrounding it, acts much more like a point source. On the other hand, ignition from hot gases of a blown out shot when using explosives will be much more volumetric in nature. Other good examples of volumetric sources of ignition are the methane explosions that initiate coal dust explosions, or the flame front of coal dust explosions that self-ignites and propagates such explosions.

The Ignition Path

Figure 5.1 shows schematically the path of events that lead to ignition. First, an energy source heats up a volume containing a reactant mixture. Energy in the form of heat flows from the high temperature area of the ignition source into the surrounding explosible mixture. Apart from the geometry of the ignition source (volumetric or point source), the temperature of the ignition source and the duration of exposure determines the amount of energy transferred to the explosible mixture. This energy increases temperature in the explosible mixture and raises the fraction of molecules in the activated state. After the lag on ignition elapses, heat starts to evolve from the combustion reaction. Heat generation exceeds heat loss from the system, and an explosion takes place. Heat loss is different depending on whether volumetric or point ignition initiated the process.

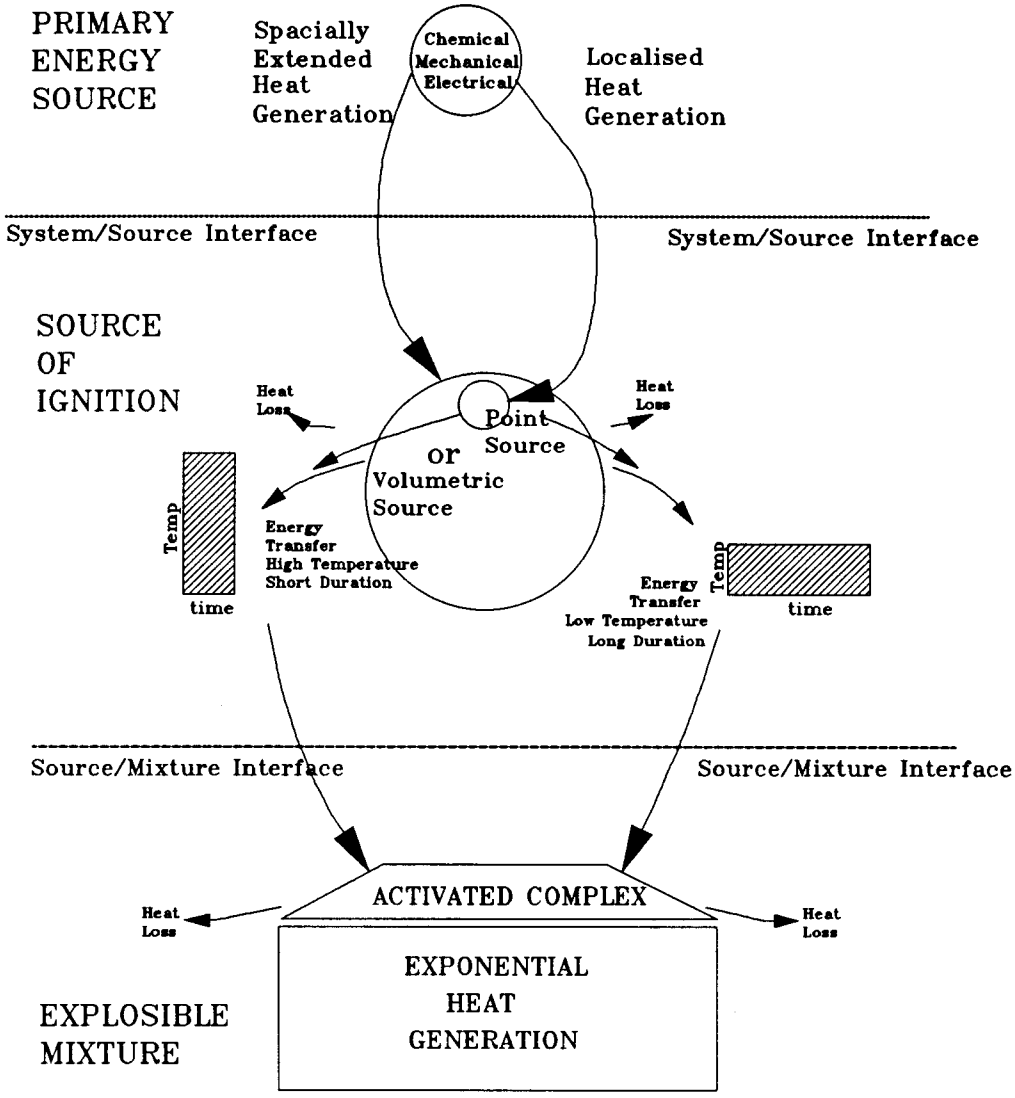

Fig.5.1. The path of events that leads to ignition, clearly showing the interaction between the source of ignition and the explosible mixture.

Although in this interpretation the events around ignition source heat inflow and heat generation from the reaction when it starts are separated, some degree of overlapping does occur. In Figure 4.2 on page 94 the hot spot development from an electric arc is shown over time, both with and without an explosible mixture surrounding it. From the same figure, one notices that without an explosible mixture, it takes 10 ms for the hot spot to develop completely. When an explosible mixture is present, the hot spot after 10 ms is already much greater compared to the hot spot size in a clean air environment.

Ignition from volumetric sources acts adiabatically, while the large volume surrounding the point source acts as a heat sump. Since the heat loss from point source ignition by far exceeds that of volumetric ignition, the lower explosive limit will be higher and the upper explosive limit lower for point sources than for volumetric sources. The rate of pressure build-up should be smaller for point source ignition, since so much more heat is lost to ensure flame propagation.

Flame Development from Volumetric Ignition Source

Volumetric sources of ignition distribute energy throughout the volume, and start ignition almost simultaneously everywhere within that volume. Flame development is therefore, to a large extent, adiabatic. All the energy released is used for explosion development, resulting in wider concentration ranges and generally higher pressure rise rates than is observed from point sources.

Flame Dissemination from a Point Source

Figure 5.2 shows a hot spot being created by an electric arc. If the reaction of the explosible mixture within the hot spot is ignored, one can assume that a declining heat gradient will be formed outside the hot spot in a time dt_1. A hollow sphere of explosible mixture surrounding the hot spot, of thickness dx_1, starts to react and generates additional heat after the lag of ignition elapsed.

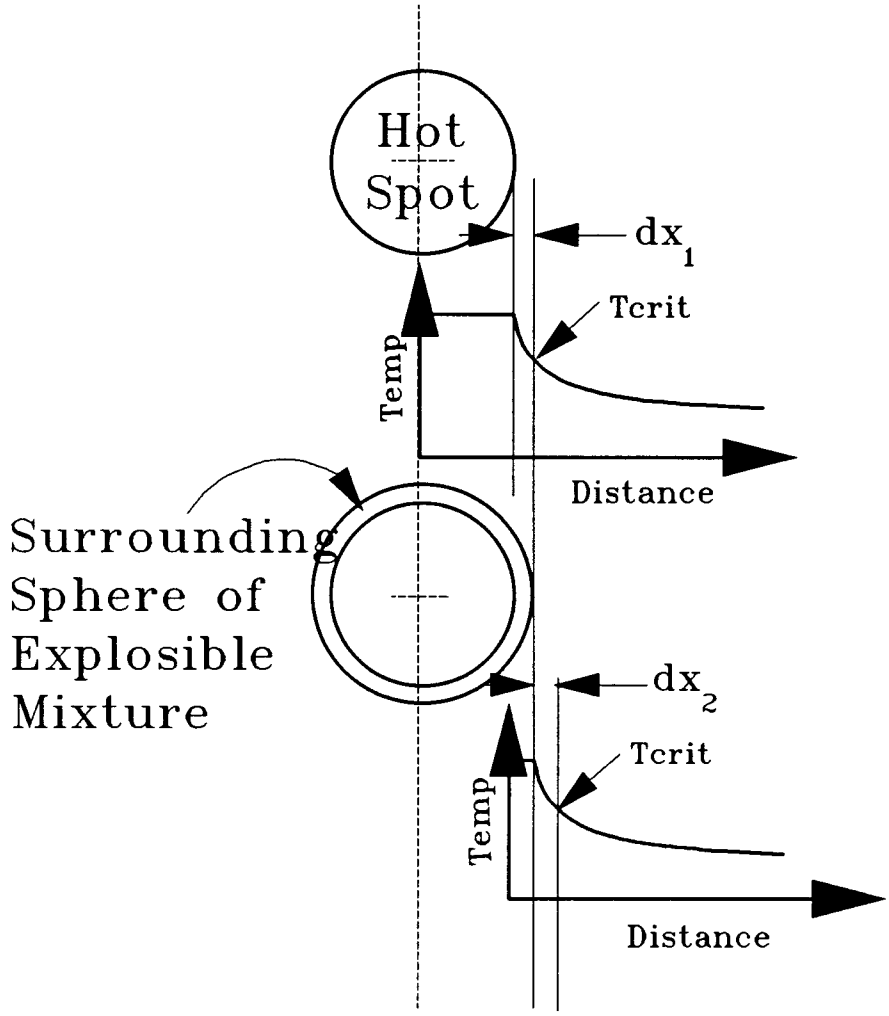

Fig.5.2. A schematic of thermal ignition from a point source. The temperature gradient established by an inert hot spot is shown together with its influence on the explosible mixture in the immediate sphere surrounding it.

This heat will re-establish a temperature gradient in time dt_2, and the new sphere of thickness dx_2 will start to react. When the distance dx is allowed to became zero, the process becomes continuous and the flame propagates through the mixture.

The time dt in which temperature can be elevated limits the rate of reaction and consequentially the flame speed. Higher initial temperatures will increase the velocity of propagation of flame through the mixture. This process also limits the rate of pressure rise within the system.

5.3 INFLUENCE OF THE SOURCE OF IGNITION ON THE IGNITION BLANKET

The main objective of this study is to determine the exact position of minimum ignition energy requirements with different combinations of methane and coal dust. The theoretical discussion clearly shows that both the source of ignition and the environment in which the explosion takes place, influence the variables that determine the position of the blanket, namely explosible fuel concentration ranges and minimum energy levels. The infinite number of different shapes and geometries that ignition sources can have, makes individual investigation of each combination impractical. At the same time many alternative heat loss curves are possible, because each setting in the mine where explosions are possible, differs.

In order to reduce the subjective nature of the determination of the ignition blanket for South African coal mine conditions, the experimental boundaries must be well considered and defined. If the ignition blankets of both a true point source and a true volumetric source can be determined, the volume between the two blankets will contain all combinations of possible ignition sources.

As long as the fuel composition and concentration stay the same, the relationship between temperature and the rate of heat generation will also stay constant. The change in system variables, for example a change from a steel walled explosion vessel to a coal mine heading, will only alter the relationship between temperature and the rate of heat loss $\dot{Q}_{loss}$, but not between temperature and rate of heat generation $\dot{Q}_{gen}$. When both these relationships are known, the influence of a change of

environment within which the reaction takes place, can be predicted by adjusting the variables of the heat loss functions accordingly. Scaling is nevertheless difficult to achieve, and therefore determination of K_{ex} values within a standardized explosion vessel is essential. The results of comparative studies between explosion vessels and large scale galleries undertaken in Germany by researchers such as Helwig[31] and Reeh[44], will then have to be used as a guide to the interpretation of the results.

Coal is a complex substance, which greatly differs in properties depending on its maceral composition or rank. The ignition blanket will therefore be influenced by the coal used. Again, the situation can be simplified by testing both a relatively weak explosible coal (low K_{ex} value) and a relatively strong explosible coal (high K_{ex} value), assuming that an understanding of boundary conditions will clarify behaviour in between.

Finally, Baker et al[49] state that the majority of explosions in industrial environments can be adequately treated using the thermal explosion theory. For this reason, only the thermal effects at a fixed starting pressure will be considered in this study. A starting pressure of 0.01 MPa, a value found to be slightly higher than the atmospheric pressures in most underground collieries in South Africa (pressures are around 0.0083 MPa), will be used throughout this study.

Figure 5.3 is a visual representation of the boundaries set for the determination of the ignition blanket.

5.4 OBJECTIVES OF THE EXPERIMENTAL PROGRAMME

The study aims at acquiring a quantitative and qualitative assessment of the explosion potential in a modern mechanised working face. The following information regarding the fuel involved and the environment in which the explosion takes place, is required:

1. The sensitivity to ignition of methane, coal dust and hybrid mixtures of the two.

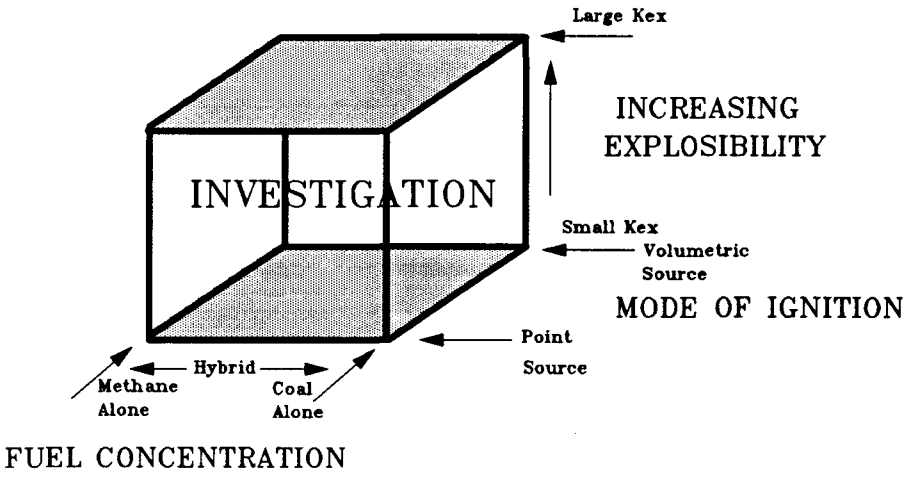

Fig.5.3. Limits set for the investigation into the position of the ignition blanket in the space formed by methane and coal dust concentrations and by minimum ignition energy.

2. The ability to self-propagate flame and the capacity for propagation of a coal dust explosion for the different fuel combinations.

3. The ignition blanket for volumetric ignition sources.

4. The ignition blanket for point ignition sources.

6. An understanding of the heat generation properties of methane, coal dust and hybrid mixtures of the two and of the heat loss properties of the system containing the explosion.

The objective of the experimental programme is to obtain the required information within the limitations as already set out. Selection and development of equipment and the design of experiments and experimental procedures are discussed in

Chapter VI, while the determination of the ignition blankets and an interpretation of the heat flow characteristics of the system follow in Chapter VII and Chapter VIII respectively.

CHAPTER VI

DESIGN OF THE LABORATORY EXPERIMENTS AND APPARATUS

The criteria for selection of a closed explosion vessel are discussed. The selection and design of equipment are then explained in detail. Physical descriptions of the 40 litre explosion vessel and the ignition systems are included, with photographic illustrations. The experimental procedure is described and the accuracy of the instrumentation investigated. It is concluded that the instrumentation is accurate and that the results are comparable with those of other research workers.

6.1 CRITERIA FOR SELECTION

The experimental programme was designed to establish the explosible behaviour of different air/methane/coal dust mixtures when ignited by volumetric or point ignition sources. A basic requirement was that a volume within which methane, coal dust and mixtures of the two can be introduced, and ignited by either a volumetric or a point source of ignition. The energy levels of the ignition sources should be adjustable, and the criteria for successful ignition must be clearly defined. The number of tests required to establish a grid of points across the plain of possible mixtures was considered to be so high that large scale testing is not feasible.

In order to undertake the classification of dust explosibility, various laboratory test apparatus have been devised. They can broadly be divided into "open" and "closed" explosion vessels. Open vessels allow the developing explosion to escape from confinement, with a pressure release into the surrounding atmosphere. Various vertical and horizontal tube open vessels are in use, for example the Hartman vertical tube apparatus developed at the U.S. Bureau of Mines. A more complete description of this apparatus is inter alia given by Palmer[30]. In open vessels, the criterion of ignition is either flame propagation to the end of the tube or the rupture of a diaphragm at a predetermined pressure. The 1.2 litre furnace for example, also

developed at the U.S. Bureau of Mines[58] and used for the determination of auto ignition temperatures, makes use of a fibreglass diaphragm which ruptures at an overpressure of between 10 kPa and 30 kPa.

Open vessels therefore can distinguish only between an ignition and a non-ignition event, but post-ignition behaviour cannot be collected. Since explosion risk evaluation, as defined here, requires the post-ignition data such as K_{ex} values, an open vessel cannot be considered. A closed fixed volume spherical vessel, which records pressure over time, is more suited to the requirements of this work.

The maximum pressure generated multiplied by the volume of the vessel provides a measure of the total energy released by the explosion (N/m^2 x m^3 = Joule). The average product of maximum and mean rate of pressure rise, or K_{ex} (see equation 2.6, page 30), is an indication of the propagation potential of the dust. If the ability to measure temperatures and the ability to introduce both a volumetric and a point source of ignition at various energy levels can be added to the vessel, both ignition sensitivity and propagational behaviour of mono and hybrid fuel/air mixtures can be evaluated.

A 40 litre explosion vessel of German design was modified and re-equipped for the purposes of this investigation. The vessel is normally used for explosibility classification of South African dust, and is calibrated to be comparable with the 40 litre vessel currently in use by the Deutche Montan Technologie in Dortmund, Germany.

6.2 THE 40 LITRE EXPLOSION VESSEL

In South Africa, the Hartman Explosion apparatus of the U.S. Bureau of Mines had been used from 1966 to 1970 for coal dust explosion classification. According to Joubert[110], few South African coals could be ignited with the maximum spark energy of 25 J (and 25 Watt power). At the time, Helwig[111] completed a study which compared the explosion characteristics of coal dust when exploded in a 40 litre explosion vessel and in a 200 m long large scale gallery. In the 40 litre explosion

vessel, a powerful chemical ignitor of 4 kJ ensured that most coal dust could be ignited, making it possible to determine K_{ex} values for virtually all coal dusts. The German 40 litre vessel was copied in South Africa, but the results produced were not repeatable, and so the instrument was not considered satisfactory. Efforts to improve the reproducibility of the instrument led to the acquisition of a German manufactured 40 litre chamber which was commissioned in 1980[110]. Reproducibility was greatly improved when using the new instrument.

6.2.1 DESCRIPTION OF THE 40 LITRE EXPLOSION VESSEL

The body of the explosion vessel is cylindrical in shape which, together with the concave end plates give it a near spherical shape, since the length to diameter ratio of 330 mm/380 mm is less than one. The internal volume is approximately 40 litres. The front end plate is hinged, and when closed is sealed by two peripheral steel channelled arms hinged and clamped at it ends. Figure 6.1 shows the explosion vessel.

The back end plate has at its centre a pressure relief duct leading to a ball valve which is pneumatically controlled. After an explosion, before the vessel is reopened, the valve is opened and the excess pressure escapes through a pipe leading to a water scrubber outside the building. The soot is captured by the scrubber, allowing clean gases to escape to the atmosphere. The vessel can withstand a pressure of 1.5 MPa - Kessler[112].

To the right of the vessel, a vertical cylinder is connected to the vessel by a horizontal pipe, leading into the vessel at three o'clock. The vertical cylinder holds a small pneumatic reservoir at the top and a pneumatically controlled valve at the bottom. The reservoir is pressurised to 1 MPa, and on release the dust sample contained in the vertical piped connection piece is flushed into the vessel. Flush time can be adjusted between 30 ms and 110 ms, but was adjusted to 60 ms throughout this research to allow for complete sample injection.

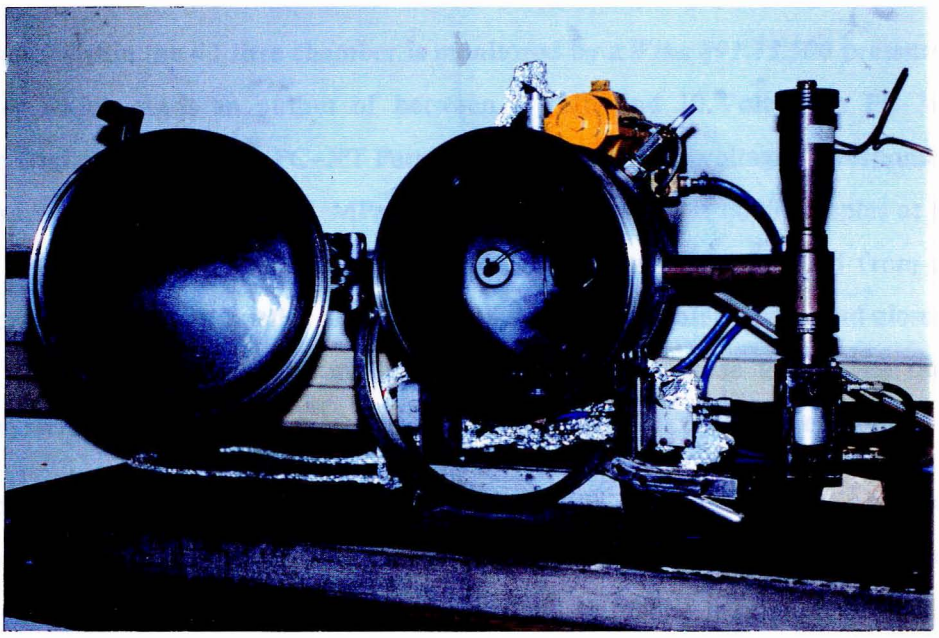

Fig 6.1. The 40 litre explosion vessel. The pressure relief valve is the yellow part at 12 o'clock. The pressure transducer is directly in front of it, while the dust dispersion mechanism is to the right of the vessel.

Access ports, sealed when not in use, exist at 3, 6, 9 and 12 o'clock on the back plate and at 10, 12 and 2 o'clock on the cylindrical part. The 3 and 9 o'clock ports on the back plate were used for the spark ignitor electrode bushes access points. The ports on the cylindrical part were used for the pyrometer window at 10 o'clock, the pressure transmitter at 12 o'clock and for methane addition at 2 o'clock. Methane addition was executed by means of a variable volume contained in a 1 litre capacity syringe.

6.2.2 INSTRUMENTATION AND RECORDING OF DATA

The pressure within the 40 litre chamber is monitored by a *Wika 891.13.500* pressure transmitter which sends an output of between 2 Volts and 10 Volts to a PC-30 Analog to Digital card inside a PC-XT Personnel Computer. The voltage corresponds to a pressure range of 0 MPa to 1 MPa. The system's capacity is 6000 samples at a sampling rate of 6 kHz with a 12 Bit resolution. The system is controlled from a switch box connected to a Kistler amplifier, which when activated opens and closes the dust dispersion valve and 40 ms later sends an electric pulse to activate the ignition system and start the data acquisitioning. Figure 6.2 explains the system.

Data is processed using a computer programme written in Turbo Pascal 5. A five point moving average is used to smooth the data and a polynomial fitment is done through 49 unsmoothed points around the smoothed line. The maximum pressure P_{max}, maximum rate of pressure rise $(dp/dt)_{max}$, time to maximum pressure t_{max} and the K_{ex} explosion index are determined and filed in a data directory. A graph showing pressure over time can then be obtained from the program.

In order to monitor the temperature in the chamber, a Thermo/Hunter BF/12/G2 pyrometer with a calibrated output of 1 Volt to 5 Volts, corresponding to a temperature range between 1000 °C and 2000 °C, was connected to an oscilloscope. A printer made the production of hard copies of the temperature history of the explosion event possible.

6.3 IGNITION SYSTEMS

The ideal volumetric ignitor should raise the temperature homogeneously throughout the explosion vessel and maintain it for a long period relative to the duration of the explosion event. In practice, the ideal situation could not be reconstructed. Instead, the pyrochemical ignitor used as the standard source of ignition for K_{ex} determination was modified. The pyrochemical ignitor consists of a stoichiometric mixture of barium nitrate and aluminium dust which fills the whole volume when exploding, and has duration times between 10 ms and 20 ms.

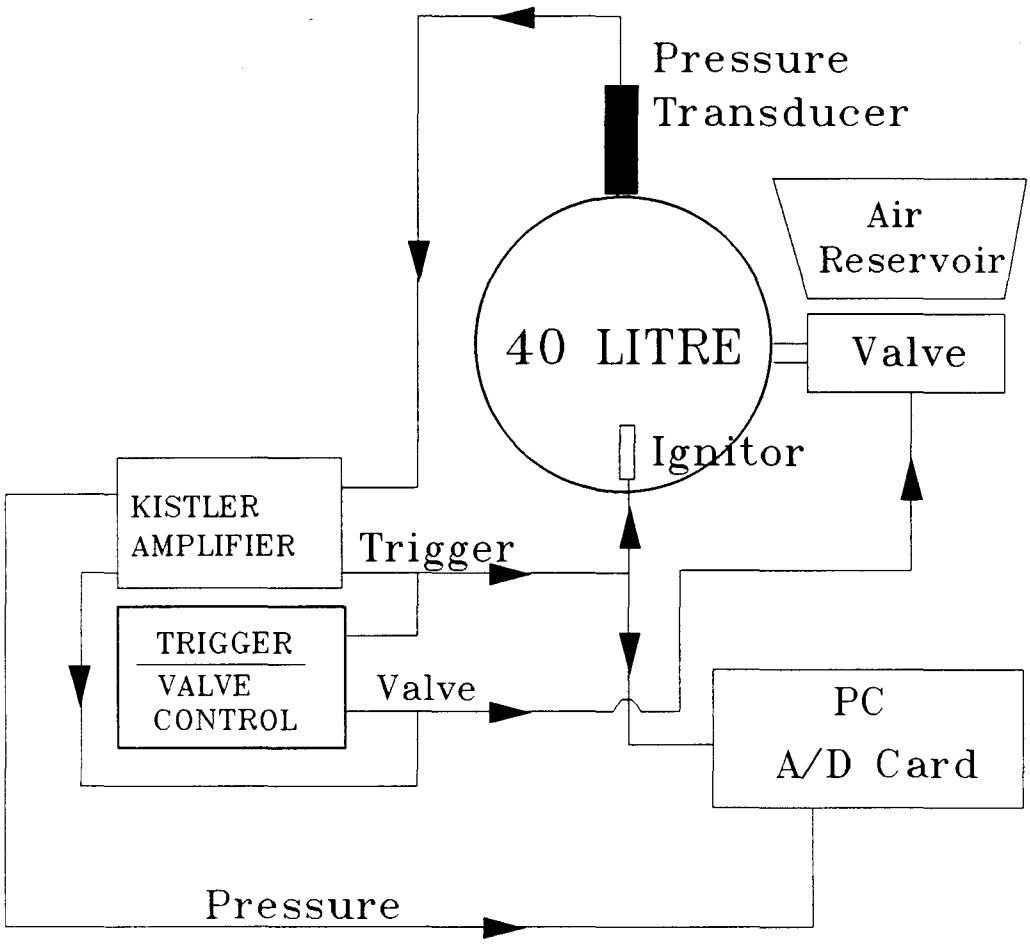

Fig.6.2. The 40 litre explosion vessel operating system.

The ideal point source, on the other hand, should be an infinitely small spot of very high temperature. The most suitable source of ignition to represent this situation is an electric spark ignitor, with small spark gap distances relative to the dimensions of the explosion vessel. A continuous spark ignitor was designed and installed in the 40 litre explosion vessel.

Descriptions of the pyrochemical and electric spark ignitors follow.

6.3.1 THE PYROCHEMICAL IGNITOR

The combustion of the barium nitrate and aluminium proceeds as follows:

$$3Ba(NO_3)_2 + 10Al = 3BaO + 3N_2 + 5Al_2O_3 \qquad -6.1$$

A stoichiometric mixture is obtained by mixing 74.41 % of $Ba(NO_3)_2$ with 25.59 % *Al* by mass. The energy released per gram of mixture is then 6694 J and the rate of energy release is influenced by the particle size and compactness of the reactants, which are therefore standardised. Both the barium nitrate and the fine aluminium powder are obtained from Riedel-de Haën AG, Hanover, with product numbers 11420 and 11010[112]. The crystalline nitrate is pulverized by grinding for one minute in a "siebtechnik" mill. An electric fusehead, used for initial ignition of the mixture, adds another 472 J of energy to the system.

Figure 6.3 shows a disassembled detonator. An ebonite fuse holder with a rubber centre supports the electric fusehead and slides into a 12 mm diameter female yellow copper holder threaded on the inside. A male stainless steel tube threaded on the outside is then screwed into the yellow copper holder securing the ebonite fusehead holder, with the electric wires of the fusehead protruding from the bottom. The powder is loaded into the detonator with the help of a small funnel and compressed to a pressure of 1 kg/cm^2 in a manual press with digital pressure reading. The open end of the detonator is closed with a small piece of masking tape.

The detonator is mounted in the 40 litre vessel on a detonator arm, with the electric wires connected to two electrodes, as shown in Figure 6.4. The mounted detonator with the fusehead wires connected can be seen. The electric pulse sent to the ignition system from the PC is connected through the control system to the electrodes inside the vessel.

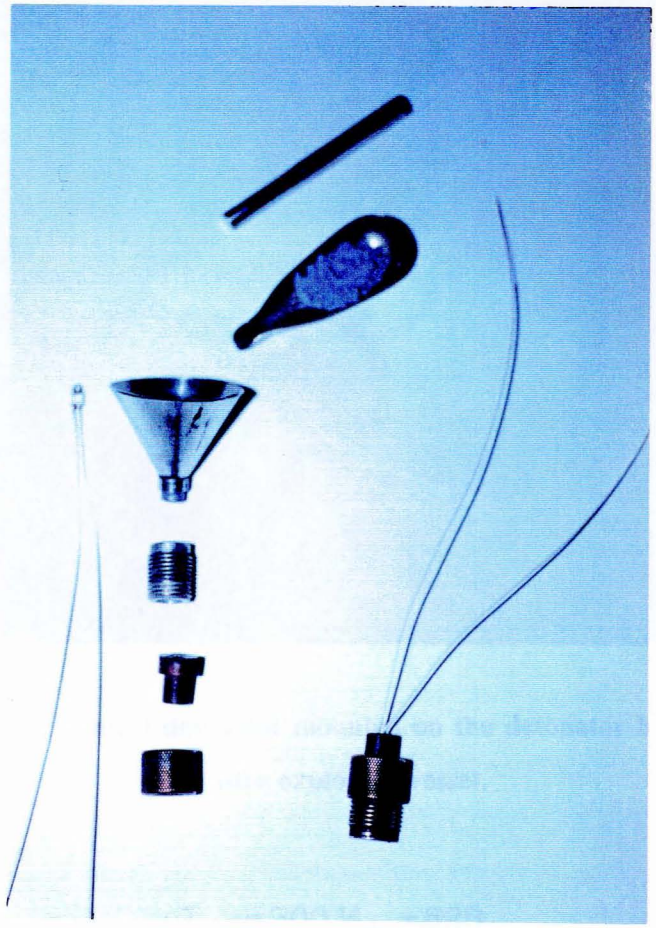

Fig.6.3. A disassembled (left) and assembled detonator. Far left is an electrical fusehead. In the middle from top to bottom; a loading rod, barium nitrate aluminium powder, loading funnel, male stainless steel tube, ebonite fuse holder and the female copper holder.

Lower ignition energies are obtained by reducing the quantity of detonator powder in the detonator. The lowest practical loading of 0.01 g of powder corresponds to 13.5 J per litre of the explosible mixture. The average temperature reached inside the explosion vessel is a function of the quantity of the barium nitrate aluminium mixture and a linear relationship has been observed:

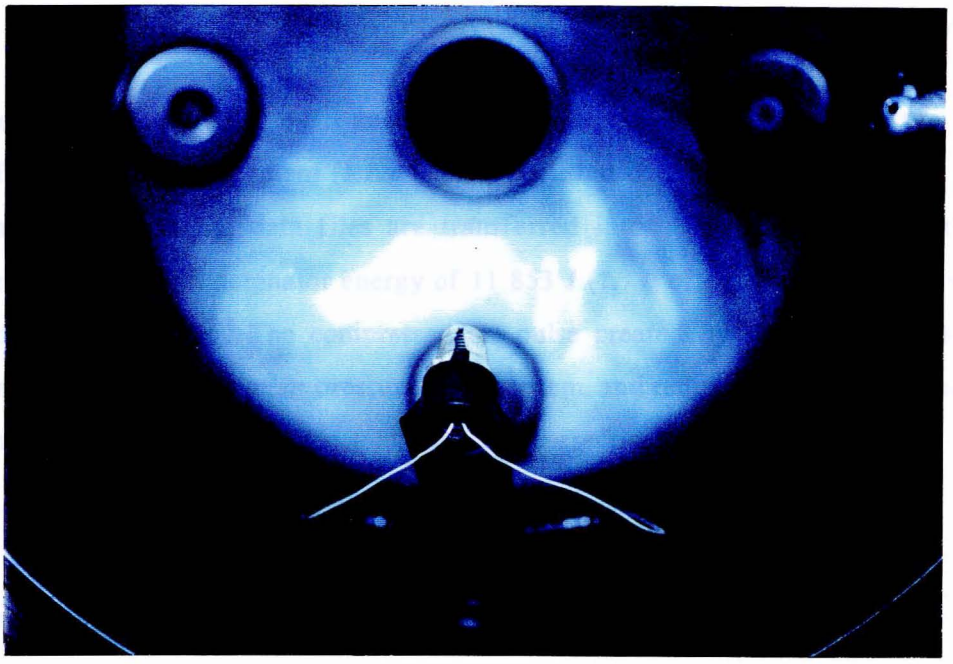

Fig.6.4. The pyrochemical detonator mounted on the detonator holder inside the 40 litre explosion vessel.

$$T_{det} = 300 M_{det} + 828 \qquad -6.2$$

with T_{det} the average temperature in the 40 litre vessel during ignition in degrees Celsius, and M_{det} the quantity of detonator powder in grams. However, a great scatter has been observed and the correlation factor between the two variables is 0.51 for 100 observations. The actual values lie between 800 °C and 1400 °C for 0.01 g and 1.7 g of detonator powder respectively. Values as high as 1750 °C for 1.7 g have on occasion been observed.

The maximum pressure P_{max} obtained in the explosion vessel during a test requires adjustment by subtracting the pressure created by the detonator. A linear relationship between the detonator energy R_{ener} and the detonator pressure P_{det} has been obtained. With a correlation factor of 0.79, the relationship is as follows:

$$P_{det} = 0.0264364 R_{ener} \qquad -6.3$$

where P_{det} is measured in *mbar* and R_{ener} in J. The system's program uses the *bar* unit for pressure measurement (1 *bar* = 0.1 MPa), but data are later adjusted to the SI unit MPa when the data files are transferred into a spreadsheet for further processing. P_{det} for a detonator energy of 11 853 J (1.7 g of detonator powder) was found to be 313 *mbar*. The compressed air pulse created by the dust dispersion system adds another 179 *mbar* pressure to the system, and requires P_{max} to be reduced by an additional 179 *mbar*. The total pressure corrections are:

$$P_{tc} = 0.0264364 R_{ener} + 179 \qquad -6.4$$

The system proved to be reliable and accurate.

6.3.2 THE ELECTRIC SPARK IGNITOR

According to Hertzberg, Conti and Cashdollar[113], ignition energies required for gaseous ignition from a capacitive discharge spark are small (0.01 mJ to 5 mJ). For such low energies the external circuit energy losses are small, and ignition energy can be accurately expressed in terms of the stored electrical energy. For dusts, ignition levels are very much higher and gross inaccuracies can occur.

A further complication to the measurement of spark energy is the need to determine accurately the stored energy and energy release rate of a capacitive discharge spark. Both voltage and current continuously change with time and spark duration cannot be controlled. South African coal dusts were found to be difficult to ignite from such sparks[110]. It is not clear whether the short duration of the capacitor discharge or a lack of spark energy was responsible for the insensitivity to spark ignition. A large and expensive capacitor bank would have been required to increase the energy level of the spark.

To be able to control the spark duration and to obtain higher energy levels, it was decided to use the normal domestic 220 Volt, 50 Hertz alternating current electric source. A transformer was used to step up the voltage to 20 kV. The spark is not truly continuous, but breaks down twice for every full current cycle of 20 ms. With only 0.8 ms between break down and re-establishment of the spark for every half cycle of 10 ms, the pulsating spark is approximately continuous and the energy levels of the sparks are identical, resulting in a constant average energy.

Circuit layout and components

The circuit layout of the system is explained in Figure 6.5. On the low voltage side of the circuit, a variable alternating current voltage adjuster, or variac, is used to adjust the input voltage between 100 Volts and 210 Volts and a circuit breaker is included for safety purposes. A solid state relay serves as an automatic circuit breaker, closing for the period an electric pulse is received from the digital timer. Adjustment of the spark duration time can be done on the digital timer, shown in Figure 6.6. The triggering pulse from the 40 litre control system activates the timer, which in turn instructs the solid state relay to close. The solid state relay is connected to the 20 kV transformer.

On the high voltage side the transformer is connected to a current limiting resistor. Due to the high voltage, a variable resistor could not be used. Instead, the current limiting resistor is made up of one to four smaller 50 $k\Omega$ resistances, which can be connected in series or parallel. For the very low spark energy range, two 500 $k\Omega$ resistors are used. A single resistor, two in series or two in parallel allow three energy ranges. For a specific resistance, energy adjustments are achieved on the low voltage side by adjustment of the variac.

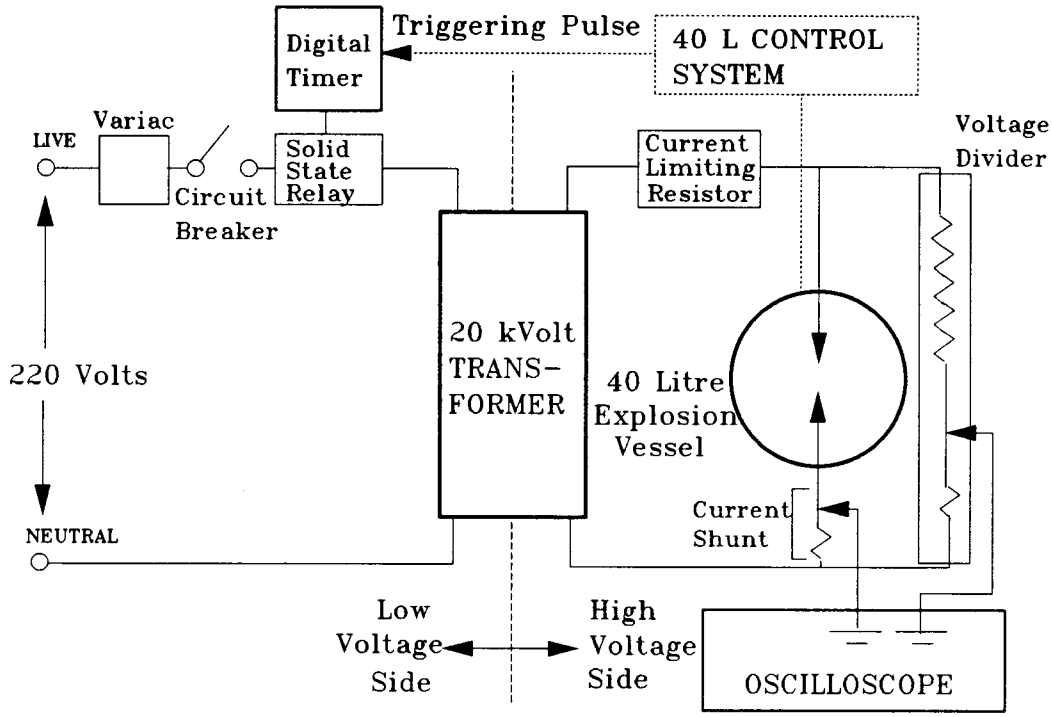

Fig.6.5. Circuit layout of the continuous electric spark ignitor.

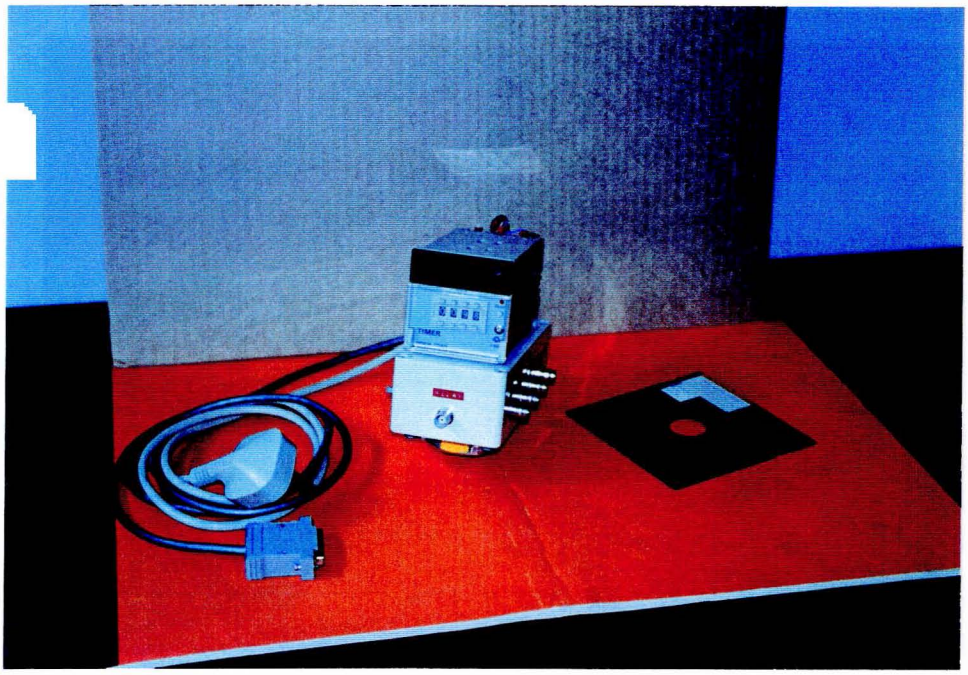

Fig.6.6. The digital timer at which spark duration time is set.

Each resistor unit is made up of smaller resistors connected in series. A plastic tube, sealed at the ends by two copper plugs, is filled with a high density silicon oil to help heat dissipation. The copper plugs also serve as the circuit connection points. A 500 $k\Omega$ resistor is shown in Figure 6.7.

From the current limiting resistor bank cables leads to isolated electrode bushes entering the 40 litre explosion vessel. Figure 6.8 shows the bushes which thread into either the 9 o'clock or 3 o'clock access ports of the explosion vessels. Silicon plastic isolates the circuit from the explosion vessel. Each electrode fits into the hollow end of the electrode clamp and is held in place by tightening a screw. The electrodes themselves are made of 2 mm thick stainless steel rods, sharpened at the ends. A standard spark gap of 4 mm was used throughout the experimental work.

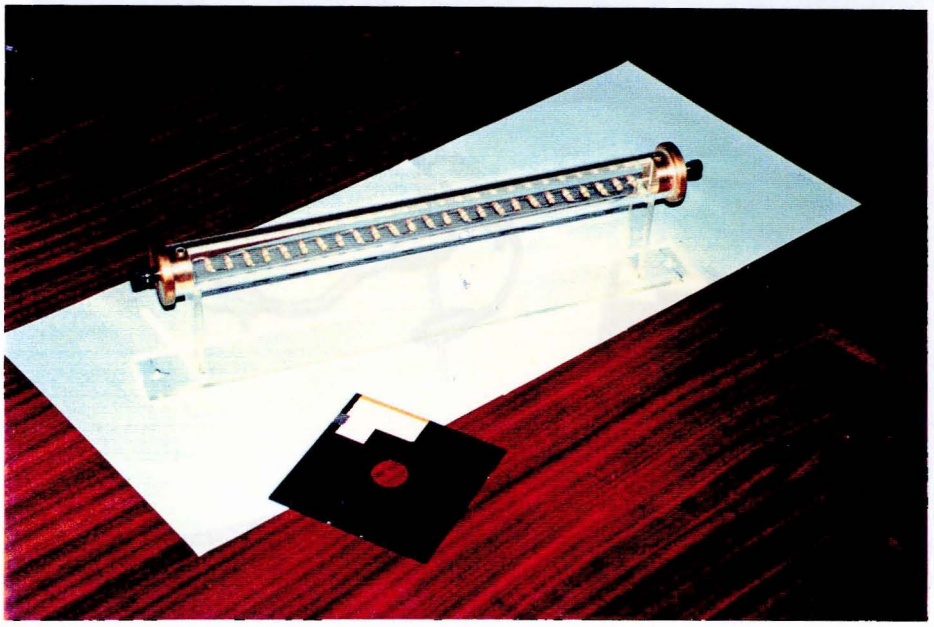

Fig.6.7. A 500 $k\Omega$ resistor.

The current generated by the spark is measured by means of a current shunt connected in series to the spark. The voltage across the resistance is recorded on an oscilloscope and when this voltage is divided by the shunt resistance, the current going through the spark is obtained. Since the curve is sinusoidal, the root mean square value must be used. In a parallel connection across the spark, a voltage divider was installed. A division ratio of 1000 was selected and this voltage was also recorded on the oscilloscope, which provides the actual voltage across the spark. The current shunt is shown in Figure 6.9 and the voltage divider in Figure 6.10. To restrict access, the high voltage elements of the circuit were protected by a metal container. The container fits to the back of the 20 kV transformer, and is shown in Figure 6.11.

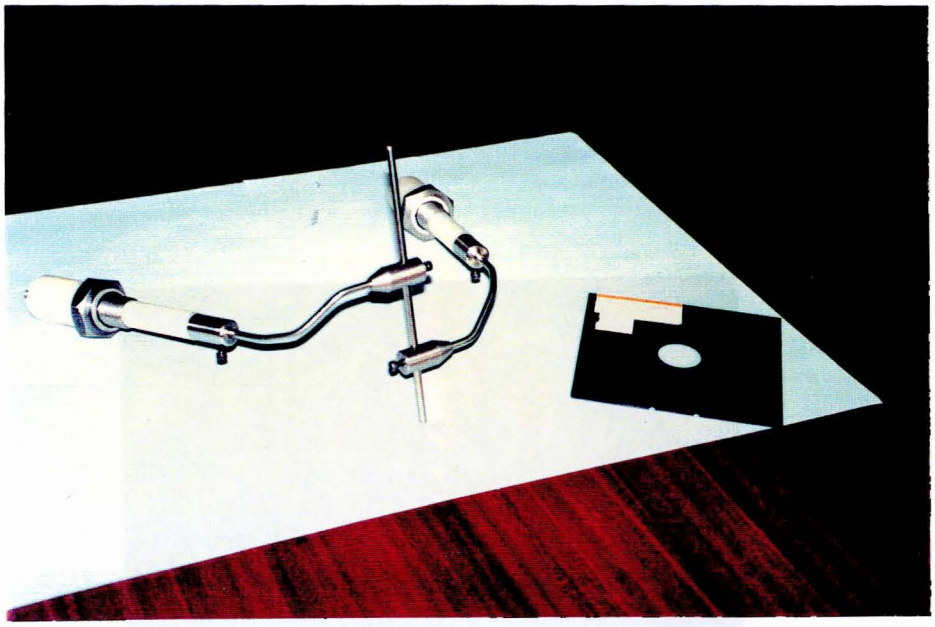

Fig.6.8. Insulated bushes for electrode attachment.

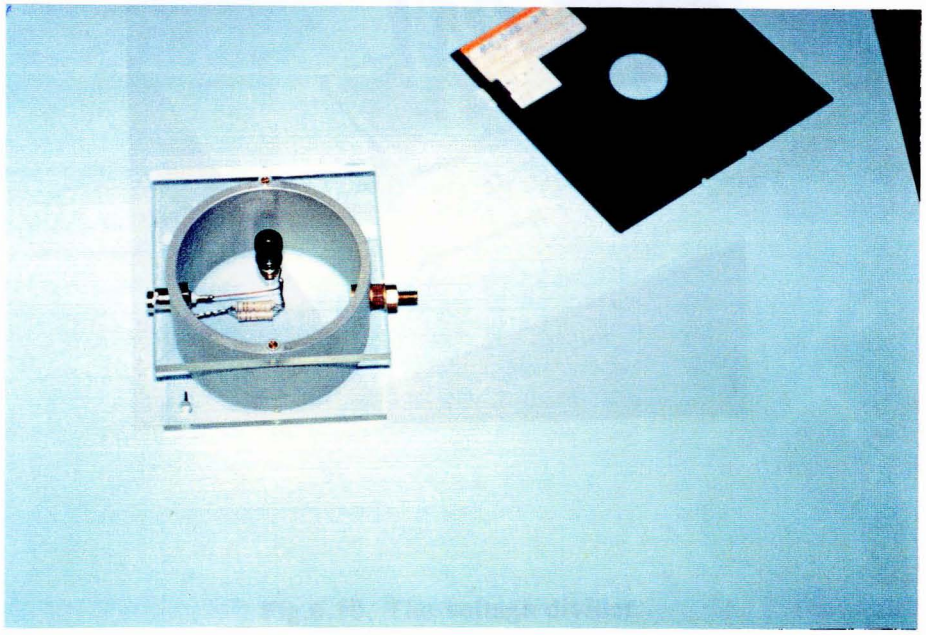

Fig.6.9. The current shunt.

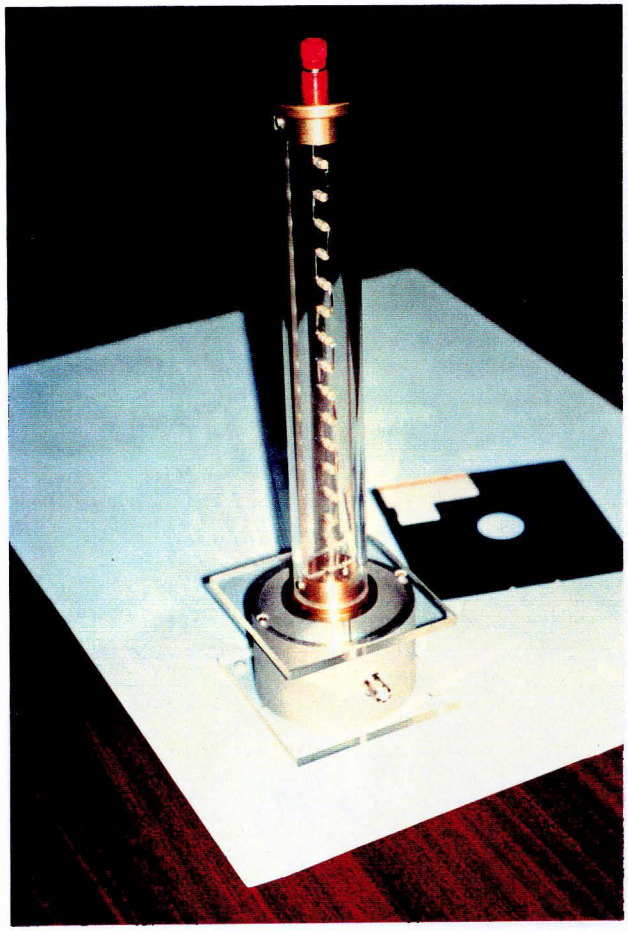

Fig.6.10. The voltage divider.

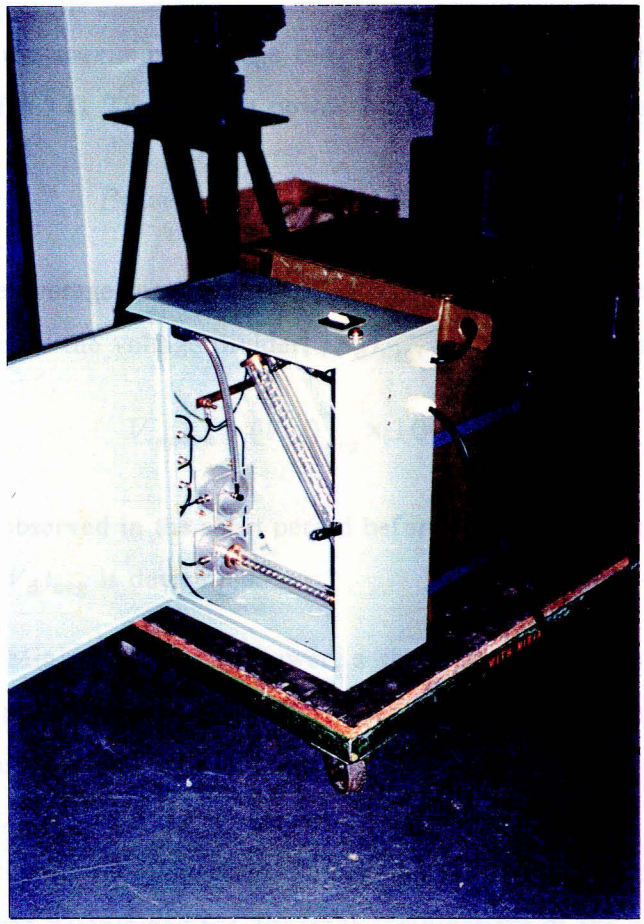

Fig.6.11. The assembled spark ignitor system. The green box is the 20 kV transformer.

Determination of the Minimum Ignition Power

Figure 6.12 shows the voltages received from the current shunt and the voltage divider. The maximum electric current, I_{max}, is determined as follows:

$$I_{max} = (V_i)_{max} / R_{shunt} \qquad -6.5$$

where $(V_i)_{max}$ is the maximum voltage over the current shunt and R_{shunt} is the shunt resistance of 8.3 Ω The average power is calculated as follows:

$$Power = (I_{max} / \sqrt{2}) \times V_{spark} \qquad -6.6$$

where V_{spark} is the average spark voltage. The latter is obtained by multiplying the average voltage across the voltage divider, $(V_d)_{avg}$, with the division ratio:

$$V_{spark} = (V_d)_{avg} \times 1000 \qquad -6.7$$

The voltage spike observed in the short period before the spark breaks down should be ignored when $(V_d)_{avg}$ is determined.

To determine the Minimum Ignition Power, a small current limiting resistance is selected and the input voltage set at 210 V. When an explosion is observed, the input voltage is reduce until it runs out of range at 100 V. The current limiting resistor is then increased to the next power level, allowing a stepped decrease in power until the minimum ignition power is obtained. Figure 6.13 shows how any power between 1 J/s and 100 J/s can be obtained for different combinations of the current limiting resistors and variac settings. The calculations required to obtain Figure 6.13 are presented in Appendix III.

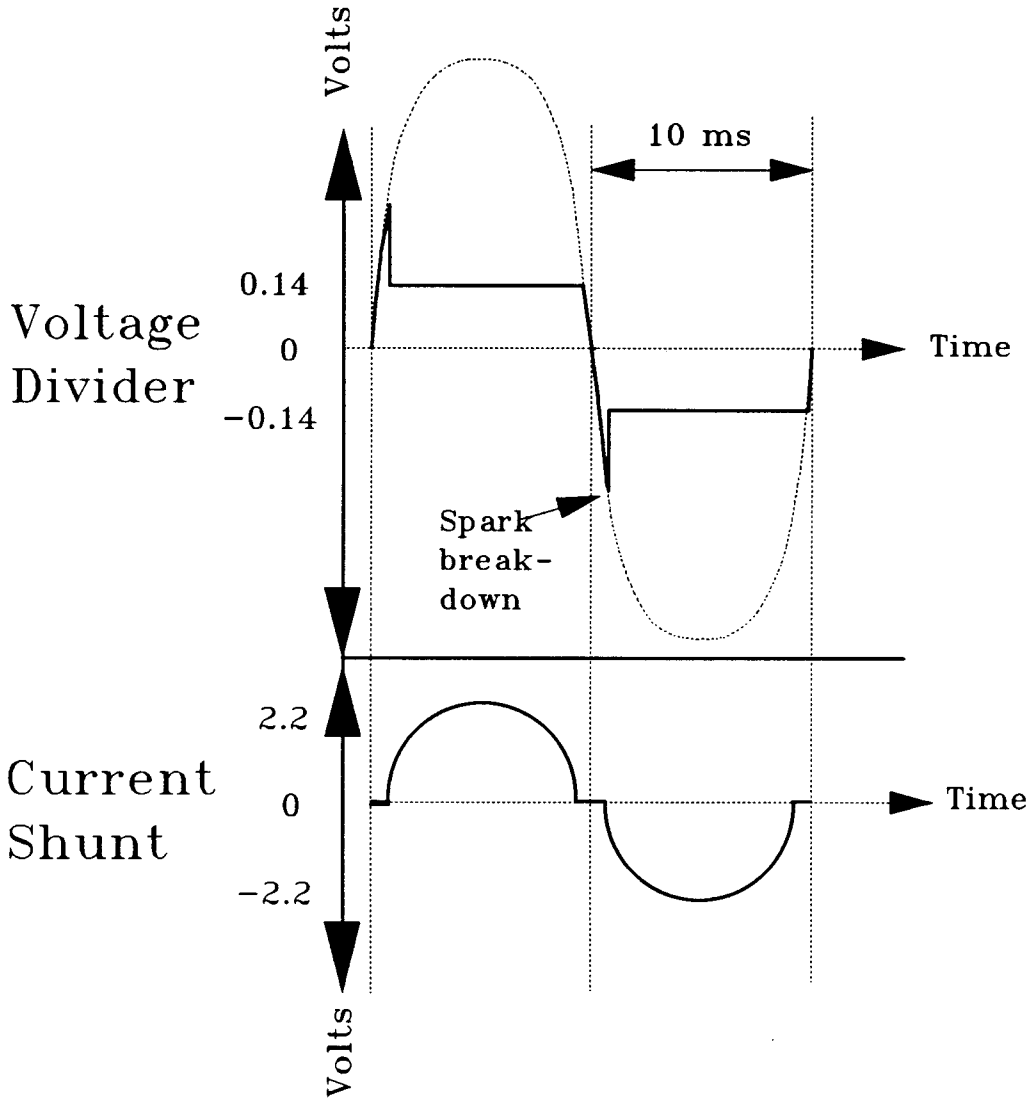

Fig.6.12. Typical oscilloscope plots of voltage over time, measured across the current shunt and the voltage divider.

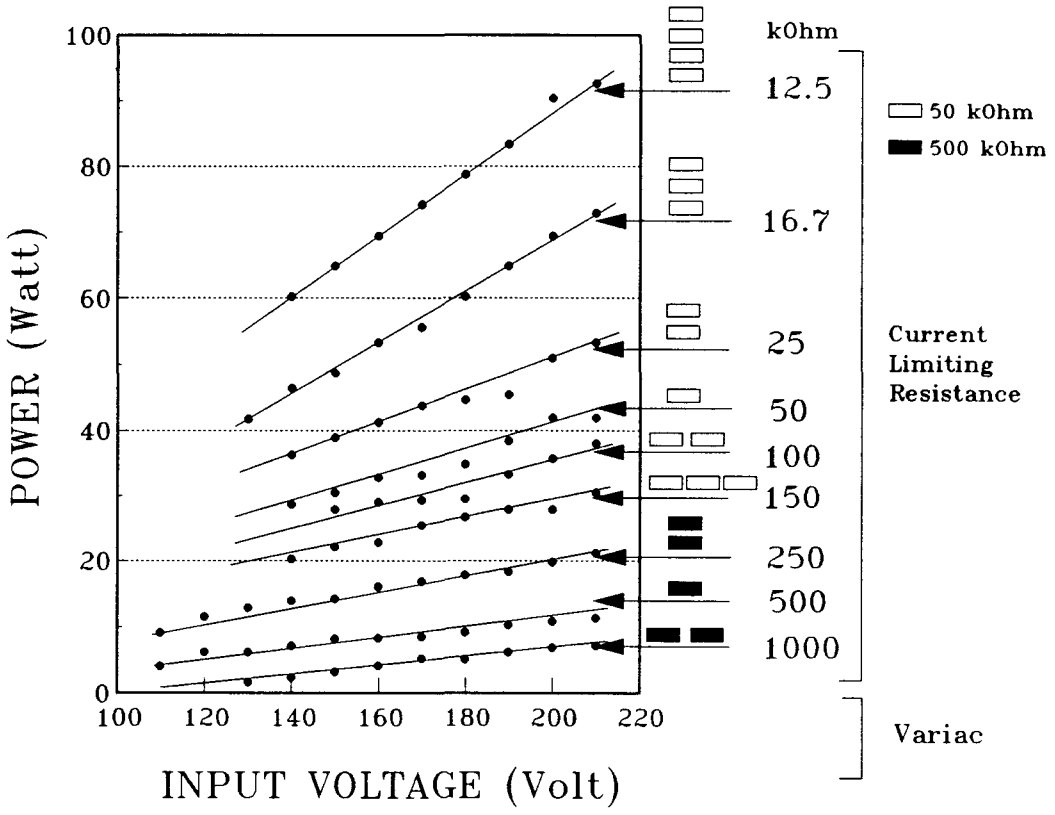

Fig.6.13. The relationship between ignition power obtained and the input voltage, for different current limiting resistances. The solid dots show measured points. Filled and open rectangles indicate the number of resistances connected in series or parallel.

Determination of the Minimum Ignition Energy

The Minimum Ignition Energy, E_{min}, can be calculated by multiplying the Minimum Ignition Power (equation 6.6) with the spark duration time, t_{spr}. It was found impractical to attempt to obtain the minimum spark duration time using timer adjustment. Instead, the spark was maintained for the full duration of the test

(1000 ms), and spark duration time was taken as the time between switch-on time and the instant when an over-pressure starts to develop. A typical pressure versus time plot obtained from the data processing programme when using the spark ignitor is given in Figure 6.14. Minimum Ignition Energy is therefore calculated as follows:

$$E_{min} = Power \times t_{spr} \qquad -6.8$$

The method includes the lag on ignition as part of the spark duration time, and can therefore be inaccurate. Attempts were made to determine the lag time by reducing the spark duration time with the timer. The lag time proved to be too short to determine with the resolution allowed by the timer. The extremely short lag time is probably due to very high spark temperatures. The gradual growth of the spark into the flame front might also eliminate the lag on ignition, as observed by Ko et al[91] and discussed in Chapter IV.

Spark Temperatures

Attempts to obtain the spark temperature by infrared thermometry were unsuccessful. The instrumentation used could read only light emission frequencies of nitrogen up to 2500 °C. Since the range was insufficient, it could be concluded that the temperature lay above 2500 °C. Cobine[114] quotes a 2 Ampere, 50 Hertz arc to begin at 3700 °C and to peak at 5000 °C, as the current increases from zero to full current. For small currents, only a glow is observed. Cobine states that temperatures for glow sparks should never be more than a few hundred degrees. With increased current, a point is reached where the glow changes into an arc of high temperature, a point observed to be about 0.05 Ampere for this apparatus.

The maximum current for this apparatus is 1 Ampere. According to Cobine[114], an arc temperature of 4350 °C is reached when the spark current reaches 1 Ampere and this has been assumed for this apparatus. Arc temperatures therefore lie between 3700 °C and 4350 °C.

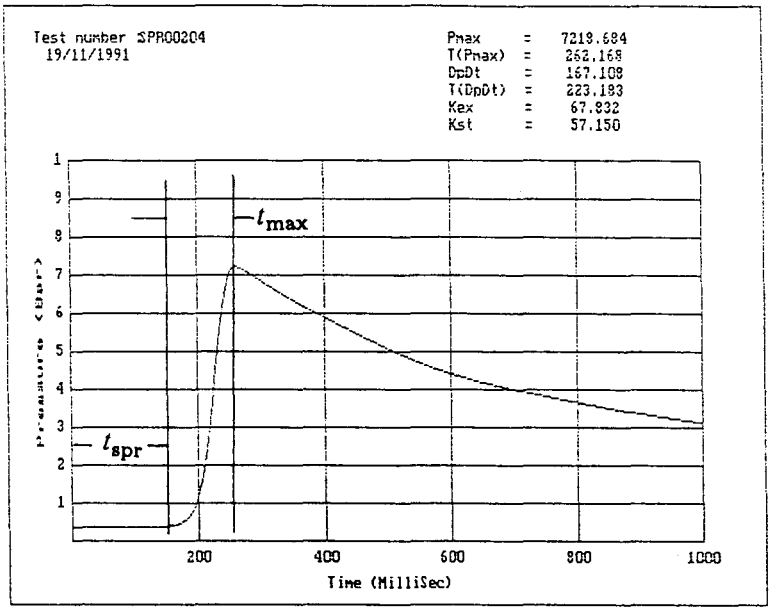

Fig.6.14. A typical explosion pressure time history when using a spark ignitor. The spark duration time t_{spr} and the time to maximum pressure t_{max} are shown.

When the spark ignitor was installed in the explosion vessel, radiation re-booted the PC. Capacitors and inductors were added to suppress the radiation. The pyrometer registering the combustion flame temperature could, however, not be protected and consequently no flame temperatures were measured.

6.4 THE EXPERIMENTAL PROCEDURE

Coal dust is explosible up to concentrations of 1000 g/m^3 or more. However, it was decided to focus the investigation on the lower dust loadings which are more likely to be found on the working face. The following concentrations were selected: 12.5 g/m^3 (*0.5 g/40 l*), 25 g/m^3 (*1 g/40 l*), 37.5 g/m^3 (*1.5 g/40 l*), 50 g/m^3

(*2 g/40 l*), 75 g/m³ (*3 g/40 l*), 100 g/m³ (*4 g/40 l*), 125 g/m³ (*5 g/40 l*), 150 g/m³ (*6 g/40 l*), 200 g/m³ (*8 g/40 l*), 250 g/m³ (*10 g/40 l*) and 300 g/m³ (*12 g/40 l*). Higher concentrations up to 1000 g/m³ were selected arbitrarily for testing.

The following methodology was followed during the experimental programme. Coal samples were collected from the mine and then broken down to 5 mm size. Each sample was then divided in two, the one half being washed at a density of 1,45 and the other half being left un-washed. Both samples are then milled to a mean particle size of about 20 μm in the coal milling plant at Kloppersbos. A more detailed discussion on particle size follows in Chapter VII.

The sample was weighed accurately on a laboratory scale to the second decimal. Figure 6.15 shows a sample added to a dust "pepperpot", with the dispersion holes sealed with masking tape. The sample was then compacted into the holder by a vibrator for one minute, and then fitted into the explosion vessel. After fitting, the masking tape was removed.

Fig.6.15. The "pepperpot" dust sample holder.

For chemical ignition, the detonator was made up and put into position in the detonator holder and the electric wires were connected to the trigger electrodes. The explosion vessel was then closed. For spark ignition, the spark gap was set before the vessel was closed.

For hybrid mixtures, methane was added. Multiples of 0.4 litre (1 % of 40 l) of methane were injected by means of a 1 litre syringe, specially manufactured for the purpose. Multiples of 0.4 l of methane were added, corresponding to 0.99 %, 1.96 %, 2.91 %, 3.85 %, 4.76 %, 5.66 % and 7.40 % methane by volume. The pressure increase was proportional to the amount of methane added. For example, 3 % methane produced an over pressure equal to 3 % of the ambient pressure (83 kPa). The effect was assumed negligible, and no adjustments were made to the results to correct it.

Figure 6.16 shows the addition of methane to the explosion vessel. The syringe is first connected to a methane pressure bottle and filled to the required capacity. The open end is then sealed with the finger and connected to the vessel's inlet valve. The methane is then injected. A tri-port outlet of the inlet valve, combined with a fast stroke from the syringe, ensured mixing of the methane with air. The turbulent air pulse from the dust disperser also aided mixing. Reproducibility was found to be satisfactory. Evacuation through the inlet valve of an un-ignited methane/air mixture, while measuring the methane content with a methanometer, confirmed the accuracy of the method. Better methods such as flushing from a mixing tank are considered superior, but funds for the design and installation of such a system were not available.

Following methane addition, sample particulars such as fuel concentration, energy level and test ID were recorded in the computer. When the spark ignitor was used, the voltage and resistor settings were made and the system was then triggered.

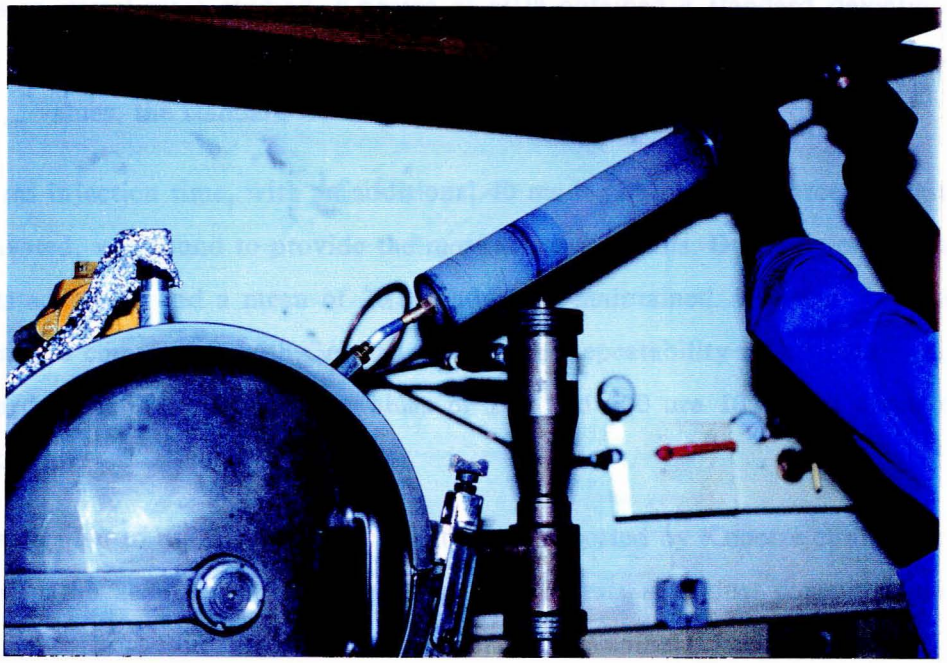

Fig.6.16. Methane addition to the explosion vessel.

Before opening the vessel, the pressure relief valve was opened and compressed air was used to flush the inside. The vessel was then opened and cleaned by brush. The cycle was repeated and an average of 20 tests per day was maintained throughout the period of experimental work.

6.5 REPEATABILITY OF THE 40 LITRE EXPLOSION VESSEL

The reproducibility of results from the 40 litre explosion vessel was tested in 1981 by Joubert[115]. For 153 explosibility tests on 45 coal samples at a dust concentration of 400 g/m^3, a 20 % standard deviation for the K_{ex} values was obtained. The standard test method for a 1 m^3 vessel required by ISO 6184[116], states that for maximum pressure measurements, an accuracy of 4 % should be obtained. In a recent series of experiments, the controllable factors that influence the repeatability of the 40 litre

explosion vessel were studied. Knoetze et al[116] obtained a standard deviation of 1.3 % for the maximum pressure. For both the maximum rate of pressure rise and for K_{ex} values, the standard deviation was 7.9 %.

A 60 ms injection time, with an additional 40 ms lag before the source of ignition is activated, was found to provide the most accurate results. Dust particle size also affects accuracy, and a mean of 20μm should be maintained. Knoetze also points out that, in comparison with German figures, the repeatability is satisfactory since standard deviations for the K_{st} values of 200 and 300 are 10 % and about 6 % respectively.

It was decided to use the same vessel settings as reported by Knoetze et al. In order to verify the accuracy of Knoetze's figures, 15 tests at a dust concentration of 400 g/m^3 with chemical ignition were undertaken. Another 15 tests were done, but with electric spark instead of chemical ignition. Finally, a further 15 tests using the spark ignitor with a 7.4 % methane/air mixture were also undertaken. The average, standard deviations and percentage standard deviations are listed in Table VI.I. Spark ignition power was set at 92 Watts, but for chemical ignition 1.3 g of the initiation powder was used. The accuracy of all tests are within acceptable limits, although the spark ignition of methane showed a reduction in accuracy.

TABLE VI.I Explosion vessel reproducibility. Average, standard deviation and percentage standard deviation for 15 repetitions each under three conditions are given. Ermelo dust at concentration 400 g/m^3 and methane at 7.4 % were used.

CONDITION	P_{max} MPa	T_{max} ms	$(dp/dt)_{max}$ MPa/s	K_{ex} MPa/s
Chemical/dust				
Average	7.187	46	51.8	28.3
Std	0.121	2	2.5	1.1
% Std	1.7	4.6	4.8	4.0
Spark/dust				
Average	7.206	110	31.4	14.2
Std	0.096	3	2.4	0.7
% Std	1.3	2.9	7.6	5.1
Spark/methane				
Average	6.427	76	48.1	19.9
Std	0.218	6	4.9	1.2
% Std	3.4	8.0	10.3	5.9

6.6 CONCLUSION

Experimental equipment which provides accurate, repeatable and internationally comparable results has been selected, designed and commissioned. The results of the experimental programme, as discussed in Chapter 7, can therefore be relied upon with confidence.

CHAPTER VII

IGNITION PROPERTIES OF COAL MINE ATMOSPHERES

The objectives and structure of the experimental programme are explained. Methane/air mixtures, coal dust/air mixtures and hybrid mixtures have been tested for minimum ignition levels. Fuel air mixtures have been subjected to both chemical ignition and spark ignition, which represent volumetric and point source ignition respectively. Explosion properties such as maximum pressure, rate of pressure rise and minimum ignition energy have been recorded and analysed. Ignition blankets for the coal under investigation have been determined. The observed trends are now interpreted in a comparative way in order to illustrate the effect of the coal dust properties and sources of ignition on the explosive behaviour of the mine atmosphere. Conclusions are listed in the final paragraph.

7.1 THE EXPERIMENTAL PROGRAMME

The objective of the experimental programme was to determine, through laboratory experimentation, the position of the ignition blanket. The ignition blanket is the minimum ignition surface in the volume formed by concentrations of methane and coal dust with air and the minimum ignition energies. The ignition blankets for mixtures of similar composition, but initiated by a volumetric ignition source and then by a point source, have both been determined. Apart from the sensitivity to ignition, the significance of the explosion severity has also been registered.

Although the explosion properties of methane/air mixtures and coal dust/air mixtures are well known, such mixtures were nevertheless included in the experimental programme. The behaviour of explosions of methane/air and coal dust/air mixtures was determined by examining the change in explosion characteristics with changes in the mode and strength of the source of ignition. Secondly, hybrid mixtures of methane and coal dust with air were formed, and the ignition blanket established.

As shown in Chapter II, methane concentration levels above 5 % and dust concentrations levels above 300 g/m^3 are unlikely to be encountered in modern collieries. Concentration levels below 5 % methane and 300 g/m^3 will therefore be concentrated upon. For Ermelo coal, 70 different combinations of concentrations of methane and coal dust were tested, while for Springfield coal, 40 combinations were tested. Each combination was tested between two and ten times, each time reducing the ignition energy until the minimum ignition energy was determined. In total, 2000 tests were executed. The structure of the experimental programme is summarised in Table VII.I.

TABLE VII.I Structure of the experimental programme. Methane/air, dust/air and hybrid mixtures were tested with both a volumetric and a point source of ignition. The number of different combinations of fuel mixtures tested is indicated.

MIXTURE/IGNITION	VOLUMETRIC	POINT
Gaseous:		
Methane/air	10	10
Coal Dust:		
Ermelo Washed/air	10	20
Ermelo Un-washed/air	11	-
Springfield Washed/air	8	8
Springfield Un-washed/air	8	-
Hybrid Mixtures:		
Ermelo Washed/CH_4/air	70	70
Ermelo Un-washed/CH_4/air	55	-
Springfield Washed/CH_4/air	40	40
Springfield Un-washed/CH_4/air	40	-

Material Properties of the Methane and Coal Dust Used

Methane of 99.5 % purity was used. Two coals, one with a relatively high K_{ex} value and a high volatile content, and one with a relatively low K_{ex} value and a low volatile content, were selected for testing. The more explosible coal was obtained from Section II, Seam C Bottom, of the Ermelo Mine Services Colliery (K_{ex} = 18.4 MPa/s). The mine was opened in 1977, and is situated 225 km east of Johannesburg, close to the town Ermelo. Coal is provided exclusively to the export market, and the annual ROM production is about 3 million tons. In order to obtain the required qualities for export, the coal is washed at a yield of 67 % to deliver a sales volume of approximately 2 million tons. As can be seen from Appendix II, ten explosions have occurred at the mine since 1980.

The relatively inactive coal came from Springfield Colliery, Seam 2 (K_{ex} = 9.3 MPa/s). The mine is situated 97 km south of Johannesburg, about 20 km north east of the town Balfour. Although coal mining in this area started in 1923, Springfield Colliery started production in 1950. Coal is supplied to Eskom's Grootvlei Power Station, which requires 3,3 million tons of coal per annum. Six explosions have occurred at the mine since 1980. Operations terminated in 1990.

Since the properties of the pure coal were required, the product as received from the mine was washed at a density of 1.65 g/cm^3, in order to reduce the ash content. A direct un-washed seam sample was also milled and tested. The true situation will contain dust with a quality somewhere between the washed and un-washed samples. Table VII.II provides the results of the proximate and ultimate analysis of each coal under investigation.

TABLE VII.II Proximate analysis of un-washed and washed coal samples of Ermelo Seam C and Springfield Seam 2 (air-dry basis).

MATERIAL	ERMELO UN-WASHED	ERMELO WASHED	SPRINGFIELD UN-WASHED	SPRINGFIELD WASHED
Proximates:				
H_2O %	2.2	3.1	4.3	4.5
Ash %	22.1	11.1	28.2	12.2
V.M. %	30.2	32.4	19.6	21.8
F.C. %	45.5	53.4	47.9	61.5
C.V. MJ/kg	24.4	28.8	20.5	27.0
C.V. of Vol.	9.5	11.3	4.9	6.8
Ultimates:				
C %	61.6	70.1	45.4	67.9
H %	4.0	4.5	2.5	3.67
N %	1.7	1.8	1.1	1.8
S %	1.4	0.9	0.7	0.4
O_2 %	7.1	8.6	14.0	9.4
%C in Vol	-	51.7	-	29.4
%H in Vol	-	13.7	-	16.8
Other:				
K_{ex} (MPa/s)	12.3	18.4	4.7	9.3

The following information was recorded for each explosion:

Test number

Dust concentration - g/m^3

Methane concentration - % by volume

Ignition power (P_{min}) - Watt

Ignition energy (E_{min}) - Joule

Maximum pressure (P_{max}) - MPa

Time to maximum pressure (T_{max}) - ms

Maximum rate of pressure rise $(dp/dt)_{max}$ - MPa/s

Explosion index K_{ex} - MPa/s

Temperature of combustion (T_r) - K

For the chemical ignitor (volumetric), the energy input was recorded in Joule per litre. Temperature of combustion could only be recorded for Ermelo Washed hybrid mixtures, since the pyrometer only became available towards the end of the experimental programme. The excessive radiation from the spark ignitor affected the pyrometer negatively, and no temperature estimates of combustion reactions ignited from the electric spark ignitor could be obtained.

The Experimental Results

The unadjusted data as obtained from the 40 litre computer program was tabulated and changed into SI units. The adjusted values for the variables as indicated above for all explosion tests on methane, washed and unwashed Ermelo and Springfield coal and hybrid mixtures are listed in Appendix IV. Although a pressure versus time graph was produced for each explosion, they could not all be presented in this thesis due to the volume they would occupy. Interpretation of the variables can nevertheless be used to reconstruct the pressure change over time accurately.

The Relationship between Spark Power and Spark Energy

For the electric spark ignitor, the relationship between the spark power and the spark energy is complex. In the experiments described in this work, increased spark power resulted in a slight reduction of ignition energy for some explosible mixtures, while for others a slight increase in ignition energy was observed. It was decided, however, to define minimum ignition energy as the energy consumed at the minimum power at which ignition still occurs. The minimum ignition level for fuel of different concentrations was found to be a narrow ignition belt, instead of a sharply defined minimum ignition line as was the case for volumetric ignition. This behaviour is consistent with the observations of Ko, Anderson and Arpaci[91], as discussed in Chapter IV (see page 93). For spark ignition, the power at which the probability of ignition becomes zero, will be defined as the minimum ignition energy.

Particle Size Distribution

Gravimetric samples of the dust clouds surrounding continuous miner drums were obtained from various collieries - see Chapter IX. The samples varied substantially, with mean particle sizes of between 20 μm and 50 μm being recorded. In order to represent the more dangerous situation, a mean grain size of 20 μm was decided upon for the test programme. The coal milling plant at the Kloppersbos explosion facility was adjusted to provide a product with a mean particle size of 20 μm, and a size distribution similar to that found on the working face. In addition, it has been observed that a mean grain size of 20 μm is used at most explosion facilities worldwide, and it was adopted for this work in order to make the results internationally comparable. Table VII.III shows the size distributions of the products tested.

TABLE VII.III Size distributions of the coal dusts used in the experimental programme. Two distributions of the dust cloud surrounding continuous miner drums are included for comparative reasons.

DUST/SIZE	MEAN μm	%<10 μm	%<20 μm	%<30 μm	%<40 μm	%<50 μm
Experiments:						
Ermelo Washed	22	24	45	62	75	82
Ermelo Unwashed	18	35	54	65	75	85
Springfield Washed	21	30	48	61	70	77
Springfield Unwashed	20	34	50	61	70	76
Field Samples:						
Coarse	56	9	16	23	33	40
Fine	17	32	53	65	73	77

General Comments on the Presentation of the Results

Results are presented in graphical form. Axis scales were standardized as far as possible and were selected to incorporate the whole range of values obtained. This arrangement makes comparisons between graphs simple.

In some graphs the minimum ignition energies of both the chemical and spark ignitors are shown. Since it is the power level that is changed, and energy is not a controllable variable, the spark ignition power is considered a more accurate reflection of the ease of ignition of an explosible mixture. For most instances, both spark ignition power and spark ignition energy are given. Spark power is measured in Watts, spark energy in Joules and the chemical ignitor's ignition energy, is given in Joules per litre.

The explosion pressure measured is the pressure above atmospheric pressure. An event was classified as an explosion according to the over-pressure developed in the explosion vessel. Generation of an over-pressure equal or above 0.01 MPa was classified as an explosive event.

Banhegyi and Egyedi[73] have indicated that there is a continuous set of most explosible mixtures, starting on the percentage methane line at 9.5 % and ending on the dust concentration axis at the stoichiometrical balance dust-air mixture. For hybrid mixtures, the most explosible line always lies in fuel rich mixtures. Since only the leaner mixtures were tested here, this line was not determined. It was however decided to add a line suggesting the position of the most explosible mixtures. The line can be used to position the graph in relation to the sketch shown on page 82 (Figure 3.10). The most explosible mixtures for methane occur at the stoichiometrically balanced point of 9.5 % methane, and for coal dust depend on the properties of the coal under investigation. For washed Ermelo coal dust mixed with air, stoichiometric balance is achieved at 625 g/m^3 of coal dust, for un-washed Ermelo coal at 670 g/m^3, for washed Springfield coal at 928 g/m^3 and for un-washed Springfield coal at 1033 g/m^3.

7.2 IGNITION AND INITIATION PROPERTIES OF METHANE

In coal mining it is well known that a methane/air mixture ignites between 5 % and 15 % of methane by volume. Methane is also considered as being very sensitive to ignition, with a minimum spark ignition energy of 0.25 mJ often quoted. The Thermal Explosion Theory explains adequately the dependence of minimum ignition energy on the heat loss properties of the environment in which the explosion takes place. Since all the experiments were executed in the same explosion vessel, the sensitivity to ignition and the explosion capacity of coal dust or hybrid mixtures can conveniently be compared to the sensitivity and explosion capacity of methane when tested in the same system.

The methane experiments were intended to illustrate the change in pressure and rate of pressure rise with increased ignition energies. The influence on these two properties when changing from a volumetric to a point ignition source was also illustrated. Finally, sensitivity to ignition was investigated.

Figure 7.1 shows the behaviour of maximum pressure P_{max} and maximum rate of pressure rise $(dp/dt)_{max}$ with increased ignition energies for a 6 % methane/air mixture. The minimum ignition energy for this mixture is 50 J/l for the chemical ignitor, and 3 J for the spark ignitor. P_{max} is constant at about 0.44 MPa for any ignition energy above the minimum ignition level, for both types of ignition sources. The rate of pressure rise, however, is twice as rapid for the chemical than for the spark ignition. A much greater dependence on ignition energy is noticed, but a plateau is also reached beyond which there is only a slight increase in rate of pressure rise with increased ignition energy.

The pressure time histories of two explosions, the one ignited by the chemical ignitor and the other by a spark ignitor, are shown in Figure 7.2. A 6 % methane/air mixture is used. Both explosions reach a P_{max} of 0.46 MPa, but this is reached after 83 ms for the chemical ignitor compared to 550 ms for the spark ignitor. The K_{ex} for the former is thus 7.8 MPa/s and for the latter only 2.1 MPa/s.

Due to the jump in pressure from slightly above atmospheric to 0.20 MPa or above, depending on the fuel concentration, pressure is a convenient indicator of an explosive event. However, both the average rate of pressure rise and the maximum rate of pressure rise indicate the explosion severity. It is clear that volumetric ignition results in a much more energetic and dangerous explosion than that of spark ignition.

As fuel concentration increases, a greater fraction of the available oxygen reacts in combustion and higher pressures are registered. For the stoichiometric balanced mixtures, peak pressures are recorded. Above the stoichiometric point, pressures start to fall due to the deficiency of oxygen.

The average and maximum rates of pressure rise follow a similar trend. The time to maximum pressure is at a minimum for the stoichiometrically balanced mixtures, but increases for mixtures above and below this level. Lowest ignition energies are also registered for stoichiometrical balanced mixtures, increasing for both lean and rich fuel mixtures. The K_{ex} value which is calculated by taking the mean of the average and maximum rates of pressure rise, is a convenient indicator of the above variables.

Figure 7.3 relates fuel concentration to minimum ignition energy for both chemical and spark ignition. The chemical ignition energy can be read on the left vertical axis (J/l), while spark ignition energies can be obtained from the right vertical axis. Both the power in Watts and corresponding energy of the spark are given. Pressure contours for the chemically ignited explosive area are indicated, but it was found that the same pressures were developed for spark ignition. The contours therefore hold for both ignition sources. Figure 7.4 also shows fuel concentration in relation to minimum energy, but instead of maximum pressure developed, the explosion index values (K_{ex}) are contoured in the explosive area. Here, values were different for chemical and spark ignition, but the same trend of change as energies are increased is noticed. One also notices that ignition from a point source occurs in a narrower concentration band compared to volumetric ignition. It can therefore be concluded that the maximum pressures reached are the same for both ignition sources, but much lower K_{ex} values are registered from point sources.

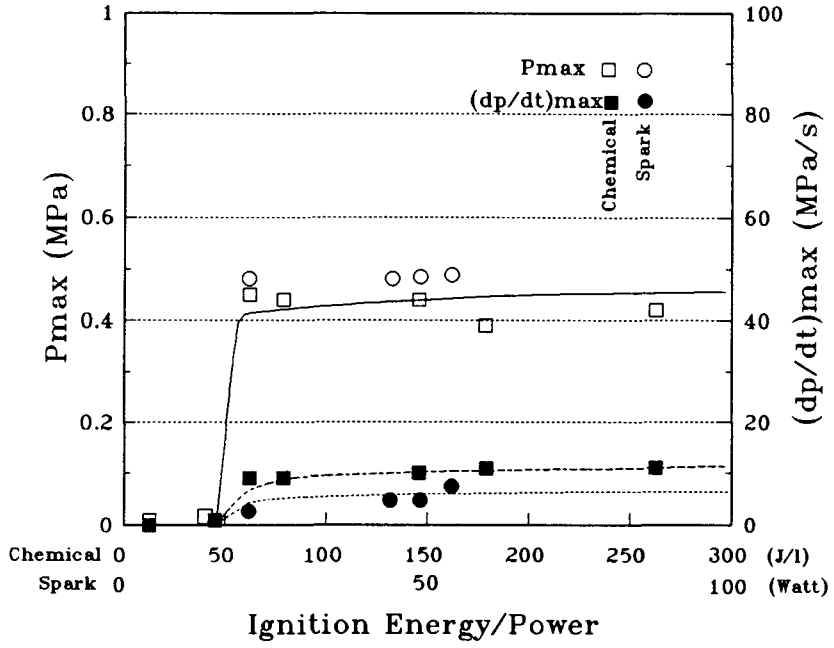

Fig.7.1. Maximum pressure and maximum rate of pressure rise with increased ignition energy levels, for a 6 % methane/air mixture.

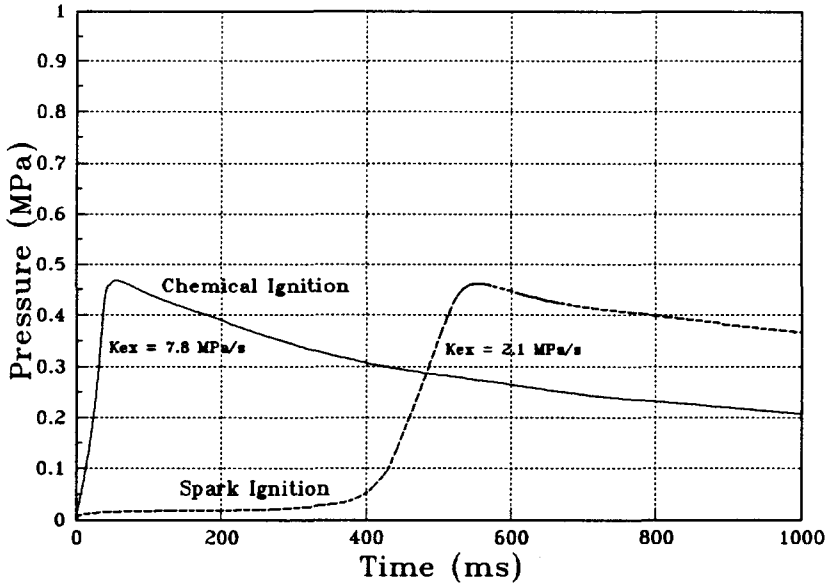

Fig.7.2. Time versus pressure for chemical and spark ignition of a 6 % methane/air mixture.

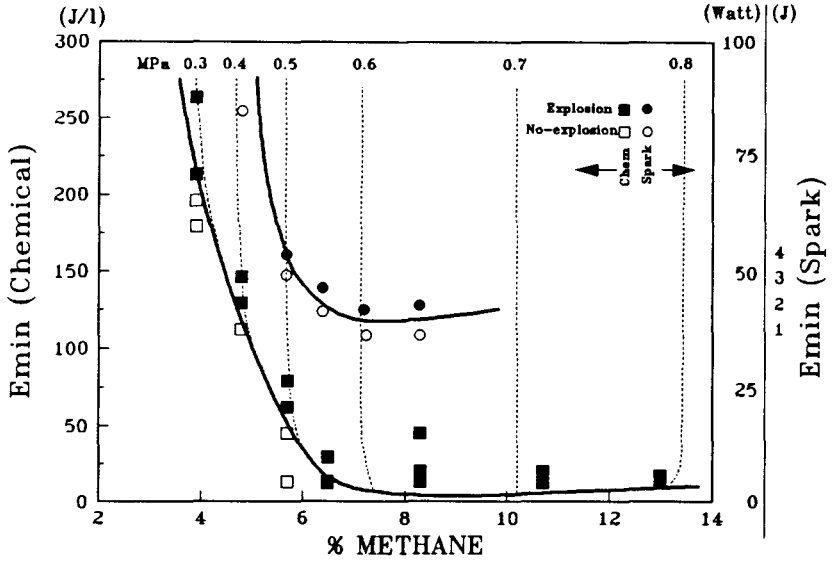

Fig.7.3. Methane concentration levels versus minimum ignition energy. Maximum pressure lines are indicated.

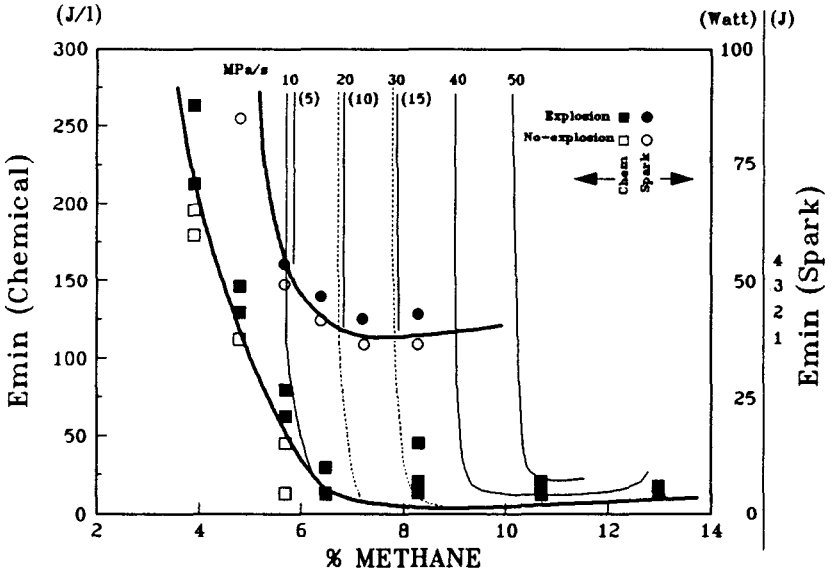

Fig.7.4. Methane concentration levels versus ignition energy, with K_{ex} values indicated. Notice the drop in K_{ex} values for spark ignition, indicated in brackets.

7.3 IGNITION AND INITIATION PROPERTIES OF COAL DUST

The general behaviour of dust when it explodes is similar to the behaviour of gaseous mixtures. For example, maximum pressures for a gaseous mixture ignited by any source of ignition stayed constant. The maximum pressures developed when a dust/air mixture is ignited by either a volumetric or a point source are also observed to be constant. As with methane, the rates at which the maximum pressures were obtained are observed to be dependent on both the type and energy level of ignition sources. The rate of pressure rise for volumetric ignition is much higher than that of point source ignition while for both types of ignition source, the rate of pressure rise increases with increased energy levels of the ignition source.

Figure 7.5 shows maximum pressure and maximum rate of pressure rise for different energy levels of both the chemical and the spark ignitor. Ermelo washed coal at a concentration of 500 g/m^3 is shown. A comparison with Figure 7.1, which shows the same information for methane at 6 %, confirms the similarity of explosion behaviour for the two, very different, substances. For dust mixtures, much higher spark ignition energy is required to effect ignition than is necessary for gaseous mixtures. This indicates that flame dissemination requires far less effort in a gaseous mixture than in heterogeneous mixtures.

The pressure time histories of two explosions for the same Ermelo dust/air mixture, the one ignited by the chemical ignitor and the other by a spark ignitor, are shown in Figure 7.6. Both reach a P_{max} of 0.70 MPa, but this is reached in 76 ms for the chemical ignitor compared to 447 ms for the spark ignitor. The K_{ex} for the former is thus 16.1 MPa/s and for the latter only 3.1 MPa/s.

Figure 7.7 relates fuel concentration to minimum ignition energy for both chemical and spark ignition. The chemical ignition energy is shown on the left vertical axis with units *J/l*, while spark ignition energy is shown on the right vertical axis. Both the power (*Watts*) at which the spark was created, and the corresponding energy (*J*) of the spark are indicated. Pressure contours are shown in the explosive zone. These

contours hold for both ignition sources, and when Figure 7.7 is studied, one notices that the pressures registered for spark ignition of Ermelo dust always resulted in pressures above 0.7 MPa, but never higher than 0.8 MPa. No contour for 0.8 MPa is therefore present.

Figure 7.8 also shows fuel concentration in relation to minimum energy, but with K_{ex} values contoured in the explosive areas. As with gaseous ignition, ignition from a point source occurs in a narrower concentration band when compared to volumetric ignition. The maximum pressures reached are the same for both ignition sources, but much lower K_{ex} values are registered from point sources compared to volumetric sources.

The minimum ignition energy for any concentration of dust is clearly defined for the chemical ignitor, while a belt of values exists for spark ignition. For methane, no such zone of spark ignition energies was observed, and the values were clearly defined (see Figures 7.3 and 7.4). The spark energy required to ignite dust is also much higher than for methane, but volumetric ignition energy is of the same order for both substances.

The minimum ignition energies for volumetric ignition of Ermelo un-washed coal dust are shown in Figure 7.9. Compared to the washed coal, ignition energies are higher, and the difference is most marked in the lower concentration ranges. Figure 7.10 compares the maximum pressures and maximum rates of pressure rise of washed and un-washed Ermelo coal dust at a concentration of 500 g/m^3. The higher ash content of un-washed coal dramatically reduces the maximum rate of pressure rise, although maximum pressure is similar for both. This is understandable since the volatile contents do not differ greatly. Volatile content for washed Ermelo is 32.4 %, compared to the 30.2 % for unwashed Ermelo.

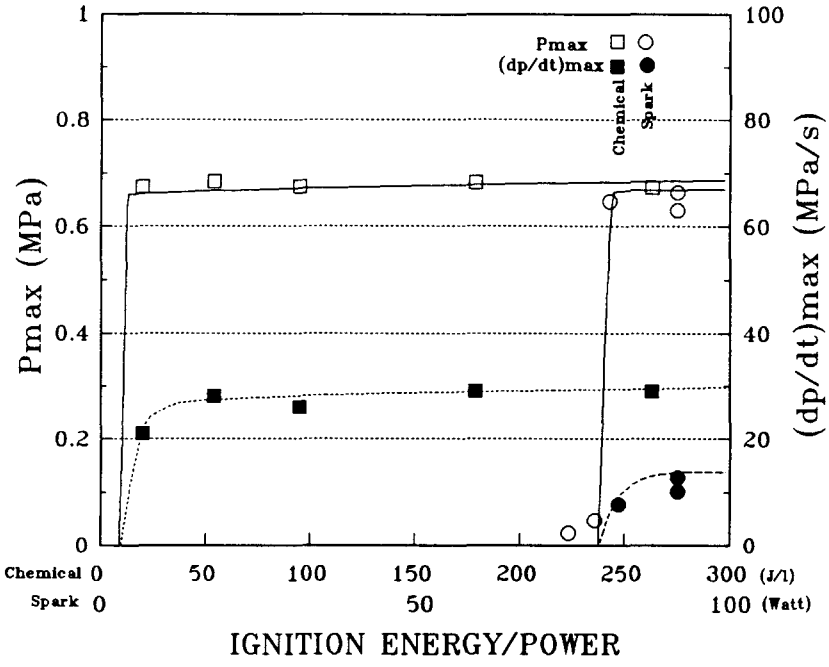

Fig.7.5. Maximum pressure and maximum rate of pressure rise with increased ignition energy levels, for a 500 g/m^3 coal dust/air mixture.

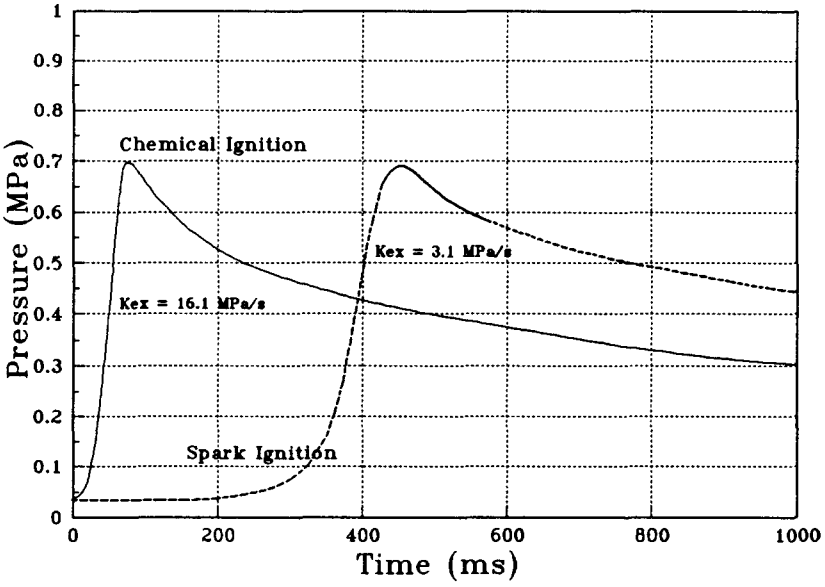

Fig.7.6. Time versus pressure for chemical and spark ignition of a 500 g/m^3 Ermelo washed coal dust/air mixture.

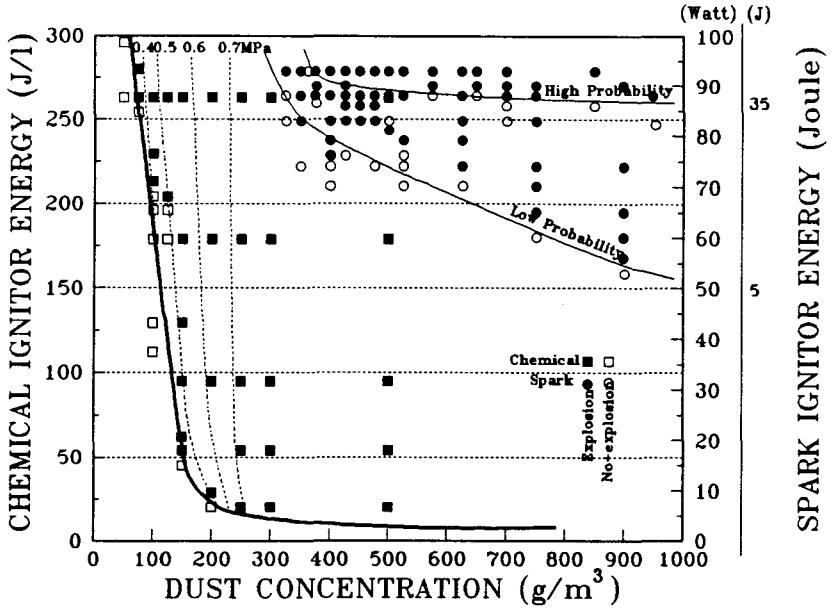

Fig.7.7. Ermelo washed coal dust concentration levels versus minimum ignition energy. Maximum pressure lines are indicated.

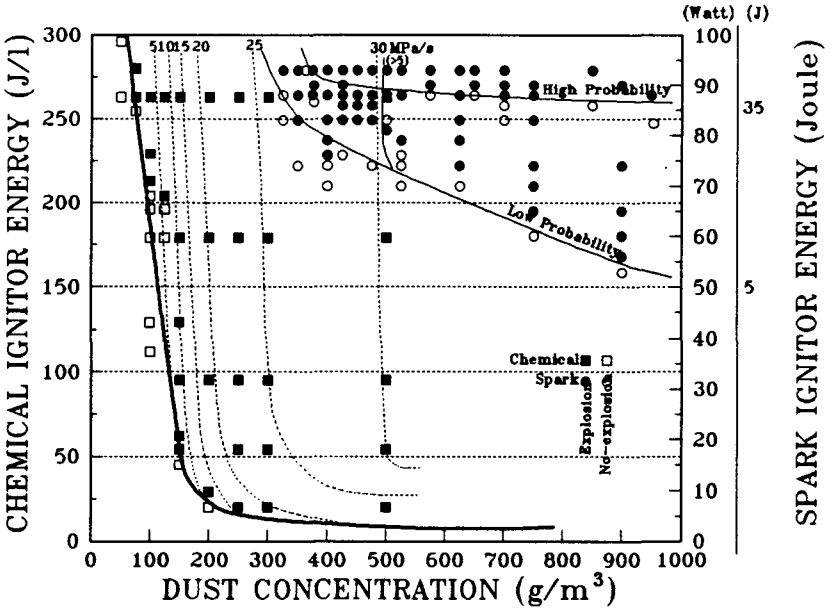

Fig.7.8. Ermelo washed coal dust concentration levels versus minimum ignition energy with K_{ex} values contoured. The lower K_{ex} values obtained with spark ignition are shown in brackets.

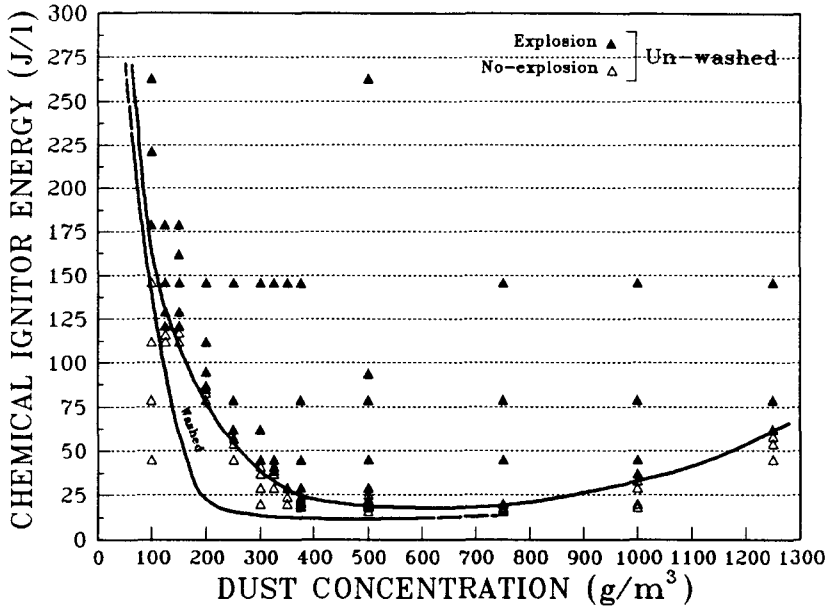

Fig.7.9. The minimum chemical ignition energy of Ermelo unwashed coal dust for different concentration levels. Washed Ermelo is also indicated.

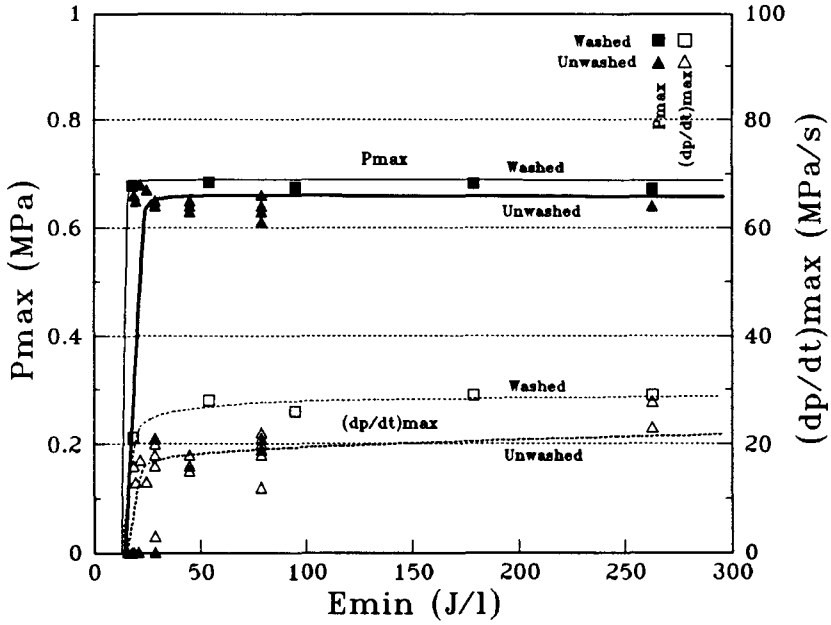

Fig.7.10. The maximum explosion pressures and rates of pressure rise with varying ignition energies for Ermelo washed and unwashed coal dust.

The explosion behaviour when ignited from a volumetric or point source of ignition for methane/air and coal dust/air mixtures has been investigated and analysed. The logical next step involved the combination of methane, coal dust and air into a hybrid mixture which could be tested using the same procedures.

7.4. IGNITION AND INITIATION PROPERTIES OF HYBRID MIXTURES

Consistent with the investigation of methane and coal dust mixtures, hybrid mixtures were formed and ignited by both the chemical and the spark ignitor. The properties investigated were again maximum pressure, maximum rate of pressure rise and minimum ignition energy. Results from tests on Ermelo washed and Springfield washed coal dusts are plotted to illustrate the influence of coal properties on the explosive behaviour of hybrid mixtures.

Maximum Pressure

Figure 7.11 shows the maximum pressures developed for different concentrations of Ermelo washed coal dust, mixed with varying percentages of methane and ignited by the chemical ignitor. Observed is the higher pressures obtained in lower dust concentrations when methane is increased. Maximum pressures when spark ignition is used, are shown in Figure 7.12. The concentration range within which spark ignition is possible is much narrower than that for chemical ignition. Only hybrid mixtures with the potential to create pressures above 0.60 MPa are ignitable from a point source. A dramatic drop in the minimum concentration of dust with only a small amount of methane present is also noticed.

For Springfield washed coal dust, the same trend of increased pressure in lesser concentrations of coal dust with increased concentrations of methane was observed. Figure 7.13 and Figure 7.14 show the maximum pressure developed for Springfield hybrid mixtures ignited by the chemical and spark ignitors respectively.

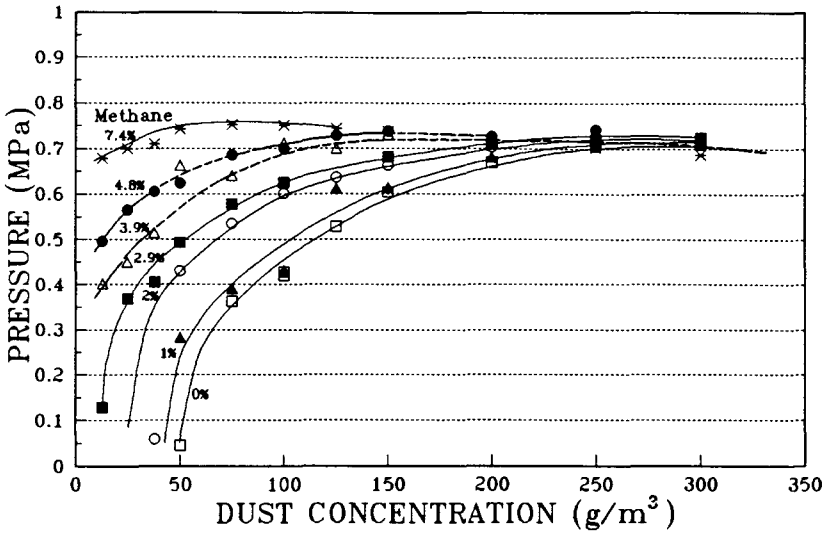

Fig.7.11. Maximum pressure of hybrid mixtures of Ermelo washed coal dust, ignited by the chemical ignitor.

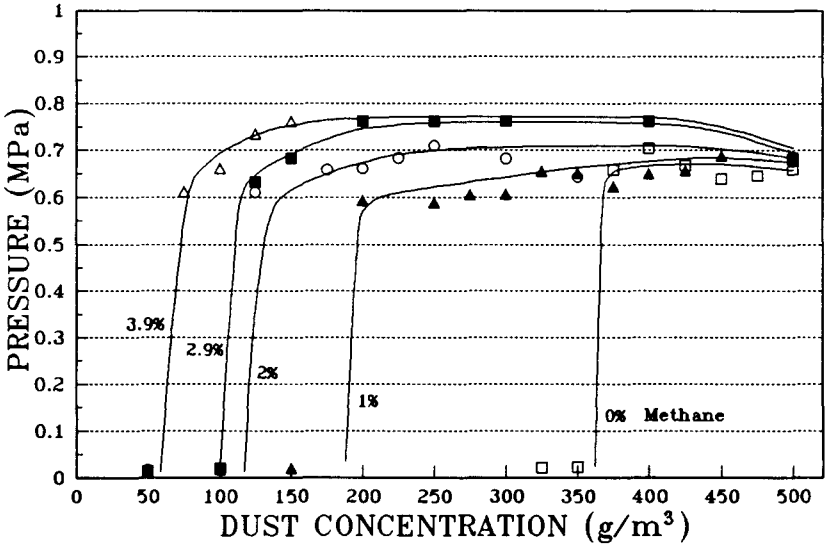

Fig.7.12. Maximum pressure of hybrid mixtures of Ermelo washed coal dust, ignited by the spark ignitor.

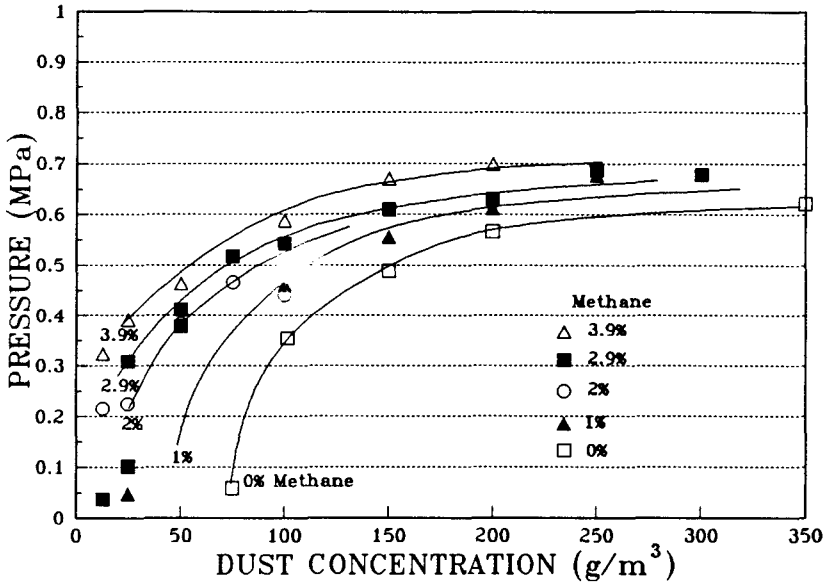

Fig.7.13. Maximum pressure of hybrid mixtures of Springfield washed coal dust, ignited by the chemical ignitor.

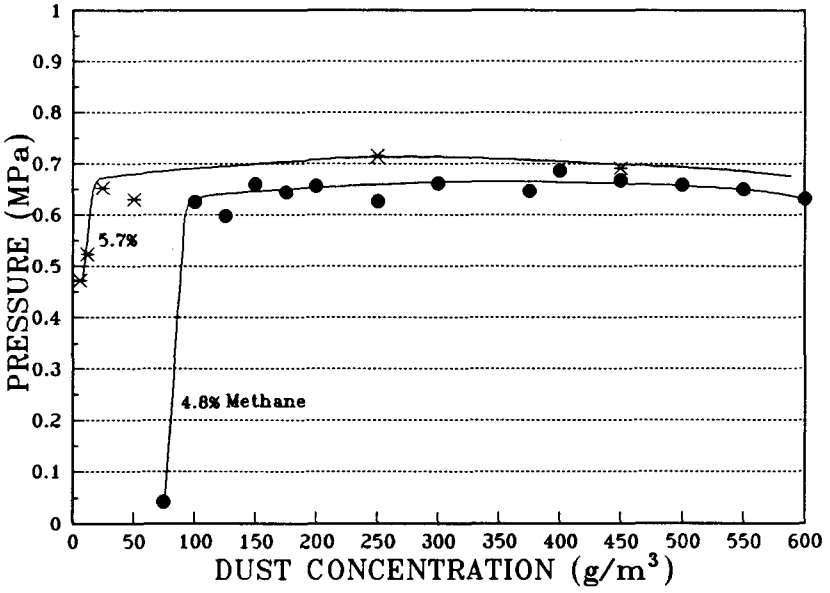

Fig.7.14. Maximum pressure of hybrid mixtures of Springfield washed coal dust, ignited by the spark ignitor.

When compared to Figure 7.11 and Figure 7.12 which show the equivalent data but for Ermelo dust, much higher concentrations of Springfield dust are required to assure an explosion. Figure 7.14 also shows that pure Springfield coal dust is not ignitable from a point source. It only ignites when methane levels exceed 4.8 %.

Maximum Rate of Pressure Rise

The maximum rate of pressure rise increased with increased dust concentration over the concentration range tested for both Ermelo and Springfield washed coal dusts. Figures 7.15 and 7.16 show Ermelo dust/methane/air mixtures ignited by the chemical and spark ignitors respectively. It can be seen that only mixtures which present rates of pressure rise above 20 MPa/s when ignited by the chemical ignitor are ignitable by the spark ignitor. Also, a dramatic drop in the minimum dust concentration is required to effect ignition with low percentages of methane present in the mixture. This is noticed for both ignition sources.

Figure 7.17 shows that no hybrid mixtures of Springfield dust and methane concentrations of up to 3.9 % develop pressure rise rates above 20 MPa/s and that no such mixture was ignitable by the spark ignitor. Only mixtures containing 4.8 % or more methane could be ignited from the spark ignitor, developing rates of pressure rise much lower than those of Ermelo dust mixed with similar amounts of methane. The results are shown in Figure 7.18.

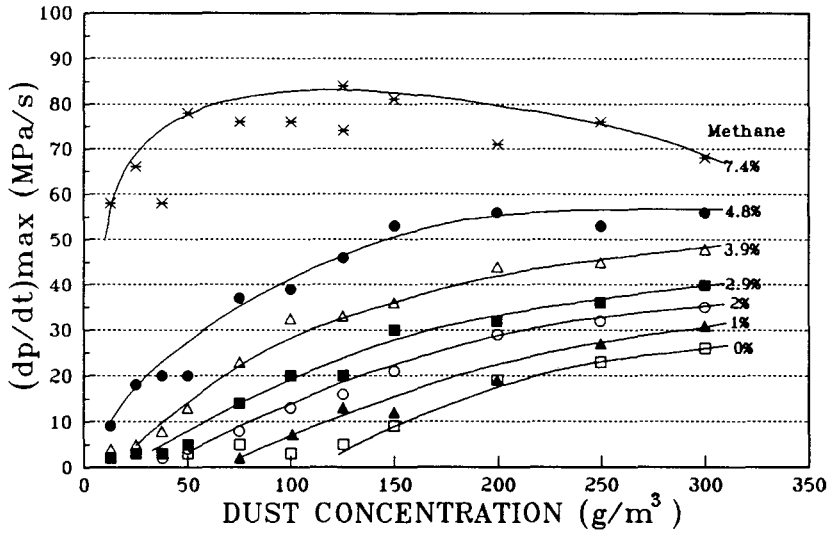

Fig.7.15. Maximum rates of pressure rise for hybrid mixtures of Ermelo washed coal dust, ignited by the chemical ignitor.

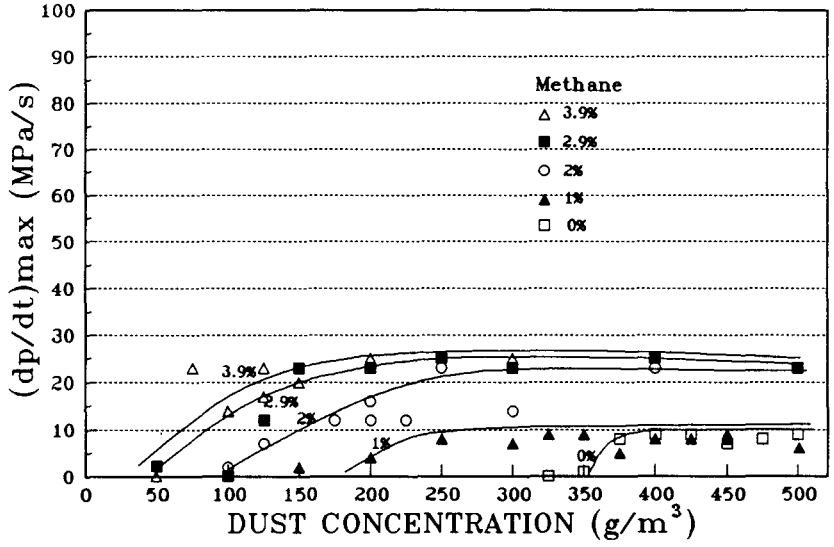

Fig.7.16. Maximum rates of pressure rise for hybrid mixtures of Ermelo washed coal dust, ignited by the spark ignitor.

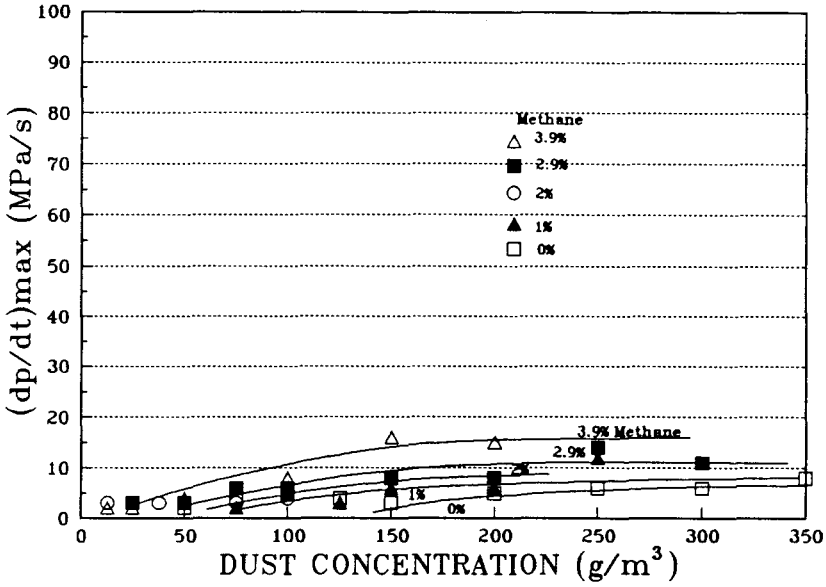

Fig.7.17. Maximum rates of pressure rise for hybrid mixtures of Springfield washed coal dust, ignited by the chemical ignitor.

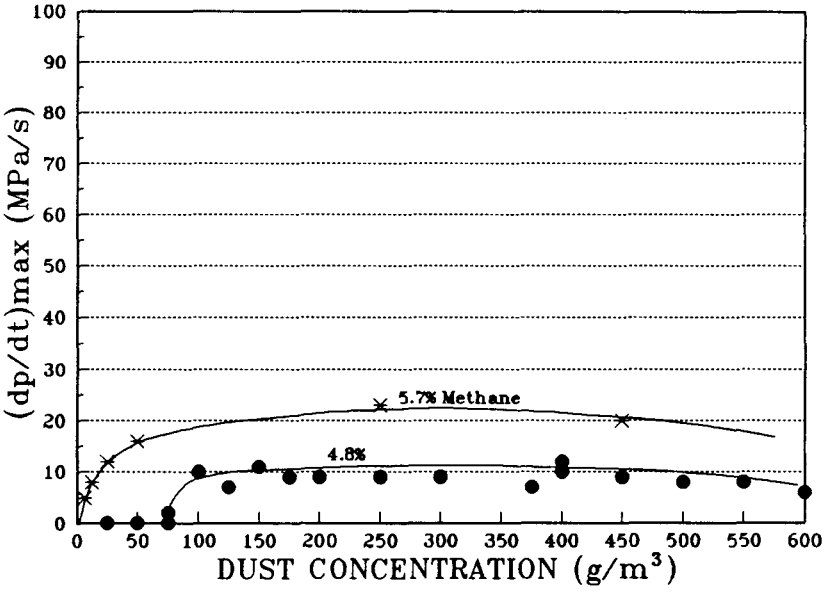

Fig.7.18. Maximum rates of pressure rise for hybrid mixtures of Springfield washed coal dust, methane and air, ignited by the spark ignitor.

Minimum Ignition Energy

The minimum ignition energy falls as the coal dust concentration increases for the concentration range tested while the addition of methane reduces the lower explosible limit of coal dust. Figure 7.19 shows the reduction in minimum ignition energy for chemical ignition. A dramatic drop in the minimum ignition energy of coal dust is noticed when low percentages of methane are added to the mixture. For higher methane contents, the reduction is less drastic. When the chemical ignitors are replaced with spark ignitors, the drop in minimum ignition energy is even more vivid and there is an extraordinary drop in the spark power required to effect ignition if low percentages of methane are added to coal dust. Figure 7.20 and Figure 7.21 show the minimum spark power and minimum spark ignition energy requirements respectively for ignition of hybrid mixtures of Ermelo dust.

The minimum chemical ignition energy for hybrid mixtures with Springfield washed coal dust is shown in Figure 7.22. The same trends as for Ermelo dust are observed, but at higher dust concentrations. Spark ignition energies for Springfield mixtures have not been plotted, since ignition was observed only at high concentrations of methane.

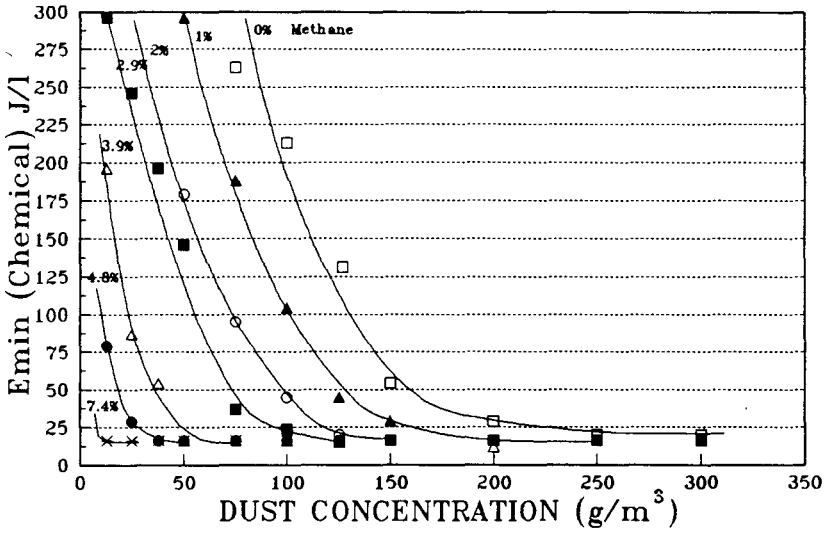

Fig.7.19. The minimum chemical ignition energy required to effect the explosion of Ermelo washed coal dust hybrid mixtures.

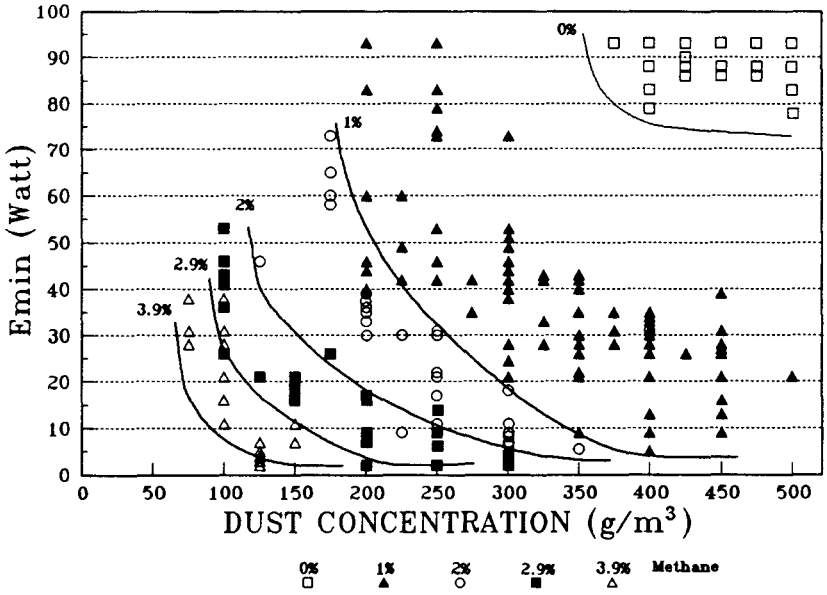

Fig.7.20. The minimum spark power requirement to effect ignition of Ermelo washed coal dust hybrid mixtures.

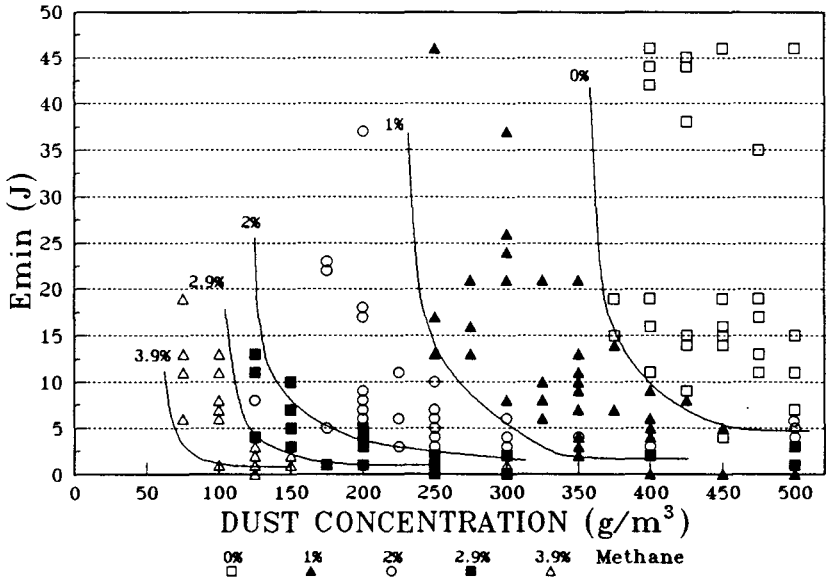

Fig.7.21. The minimum spark ignition energy required to effect ignition of Ermelo washed coal dust hybrid mixtures.

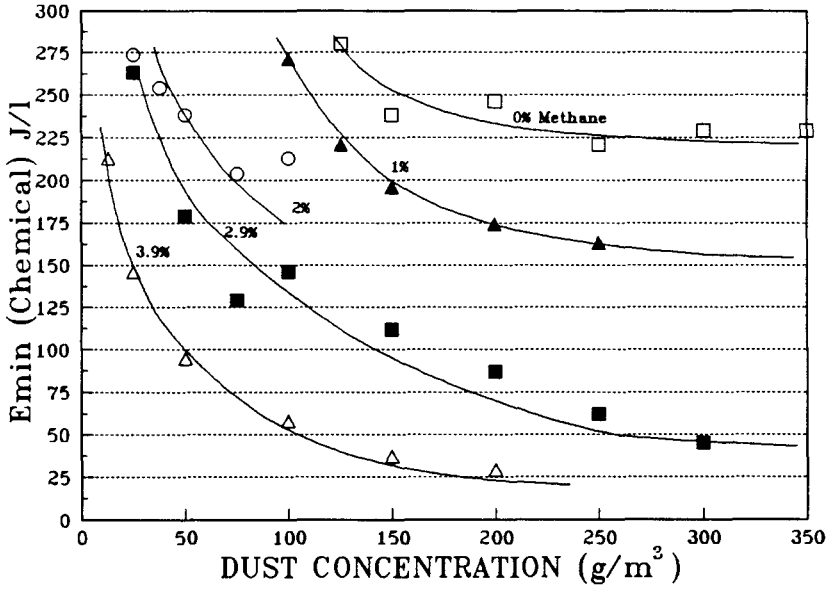

Fig.7.22. The minimum chemical ignition energy required to effect ignition of Springfield washed coal dust hybrid mixtures.

7.5 IGNITION BLANKET DETERMINATION

The ignition blanket is a minimum ignition energy surface in the volume formed by concentrations in air of coal dust and methane, and the minimum ignition energy to ignite them. The three dimensional nature of the concept makes the presentation of the blanket difficult and so it has been decided to represent the blanket by means of energy contours in a surface formed by dust concentrations and methane percentages with air. The contours were manually fitted and are therefore prone to a degree of inaccuracy. For this reason, the contours are given in thin lines, while the values and position of points are enlarged to be more dominant. This will allow interpretation of the graphs without relying on the contours given.

In addition to minimum ignition energy, the K_{ex} values are also given in the form of a blanket for the different test conditions. The change in explosion capacity for different fuel concentrations can clearly be seen in these graphs.

7.5.1 IGNITION ENERGIES FOR ERMELO HYBRID MIXTURES

Figure 7.23 shows the minimum chemical ignition blanket for Ermelo washed hybrid mixtures. The 16 J/l contour, which is the minimum ignition energy required to ignite a 6 % methane/air mixture, shows how sensitive methane/dust mixtures are to the addition of concentrations of methane below the lower explosive limit of methane.

Figure 7.24 and Figure 7.25 show the spark ignition power and energy respectively for the same explosible mixtures. The explosible area is smaller than with chemical ignition and a surprising sensitivity to ignition is evident. For example, the same amount of energy required to ignite a 5 % methane/air mixture will ignite a mixture containing 3 % methane and 125 g/m^3 of coal dust. For completeness, the minimum chemical ignition blanket for Ermelo un-washed coal dust hybrid mixtures is shown in Figure 7.26.

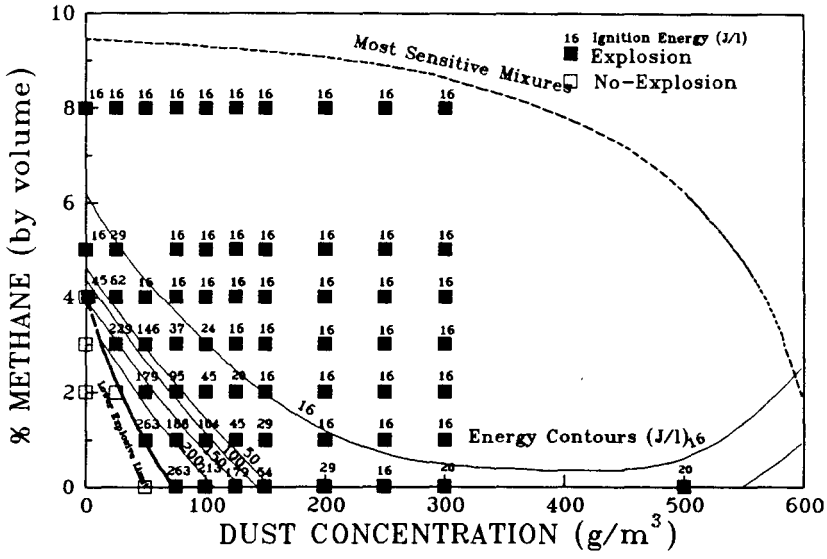

Fig.7.23. The chemical ignition energy blanket for washed Ermelo coal dust hybrid mixtures.

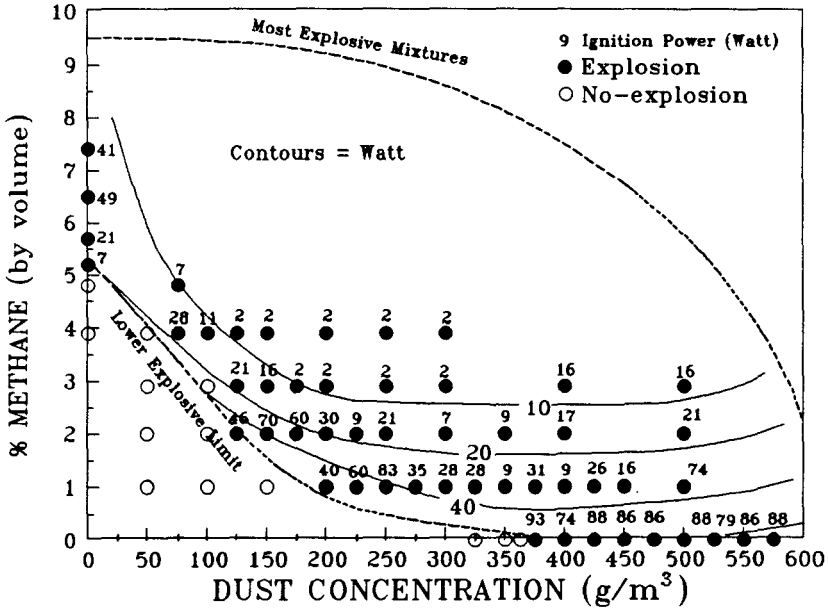

Fig.7.24. The spark ignition power blanket for washed Ermelo coal dust hybrid mixtures.

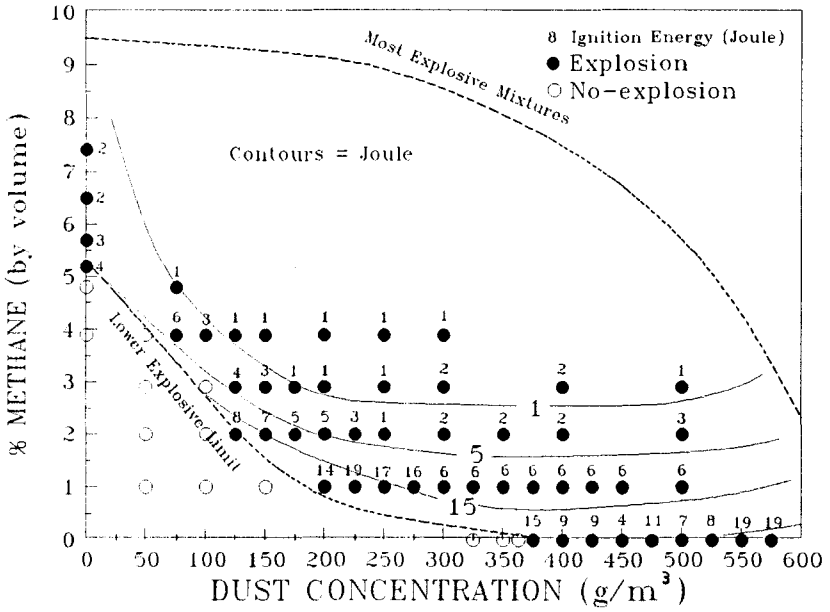

Fig.7.25. The spark ignition energy blanket for washed Ermelo coal dust hybrid mixtures.

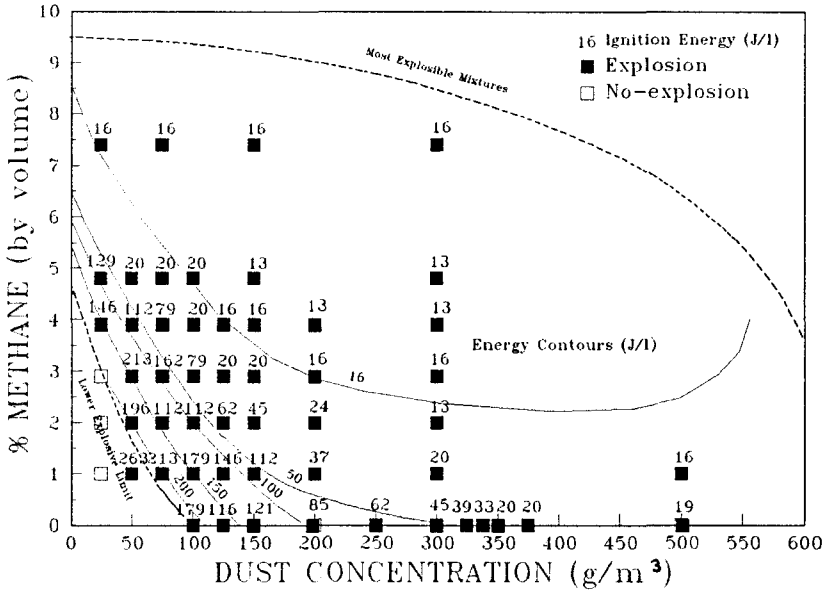

Fig.7.26. The chemical ignition energy blanket for Ermelo un-washed coal dust hybrid mixtures.

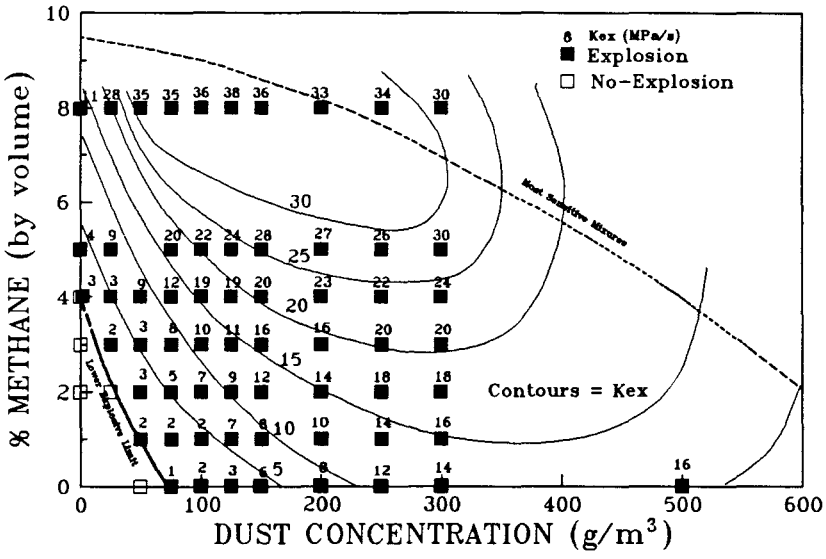

Fig.7.27. The K_{ex} blanket for washed Ermelo coal dust hybrid mixtures, chemically ignited.

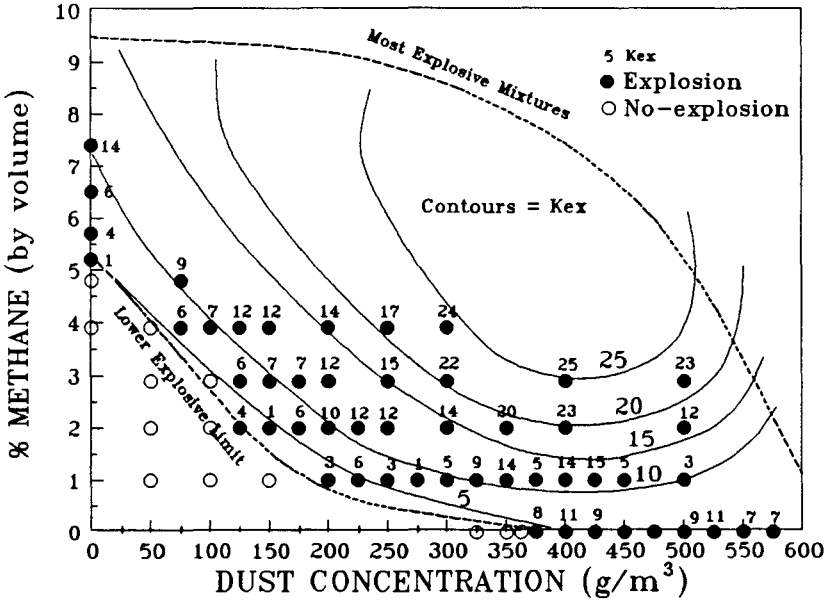

Fig.7.28. The K_{ex} blanket for washed Ermelo coal dust hybrid mixtures, ignited by electric spark.

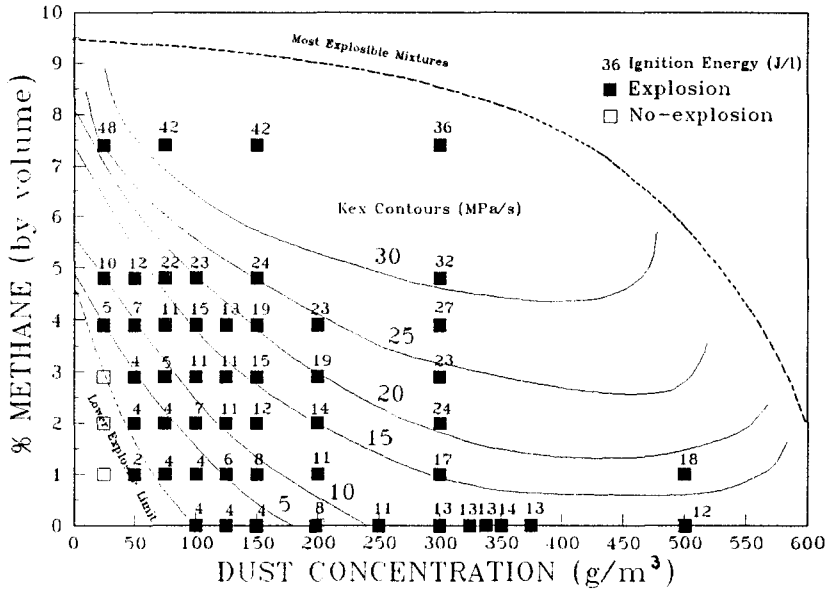

Fig.7.29. The K_{ex} blanket for un-washed Ermelo coal dust hybrid mixtures, chemically ignited.

7.5.2 EXPLOSION CAPACITIES (K_{ex}) FOR ERMELO HYBRID MIXTURES

K_{ex} contours for chemical ignition are given in Figure 7.27 and the spark ignition K_{ex} values are shown in Figure 7.28. A marked reduction in K_{ex} values is noticed for spark ignition compared to chemical ignition. Point ignition sources should therefore present a lower potential for propagation of a coal dust explosion than is the case for volumetric ignition. The K_{ex} values of Ermelo un-washed coal are shown in Figure 7.29. Although a reduced explosive danger exists for lower concentrations of un-washed coal dust compared to washed coal, an increased danger is apparent for high methane concentrations.

7.5.3 IGNITION ENERGIES FOR SPRINGFIELD HYBRID MIXTURES

Figure 7.30 shows the minimum chemical ignition energies for Springfield washed coal dust hybrid mixtures. The ignition energies are substantially higher than those required for ignition of Ermelo washed hybrid mixtures shown in Figure 7.23.

Figure 7.31 shows the minimum spark power blanket, and Figure 7.32 the minimum spark ignition energy blanket for Springfield washed hybrid mixtures. Compared to Figures 7.24 and 7.25 showing the spark power and ignition energy for Ermelo washed hybrid mixtures, the explosible area is much reduced. Only with very high methane contents can ignition be effected. It appears that the explosive participation of the Springfield coal dust is limited when point source ignition is used. The coal dust acts much like a suppression agent.

Figure 7.33 shows the minimum chemical ignition blanket for un-washed Springfield coal dust hybrid mixtures. The reduction in size of the explosible area is surprisingly little, but ignition energies are higher than for washed Springfield mixtures. The smaller grain size of the un-washed Springfield dust might contribute to this behaviour.

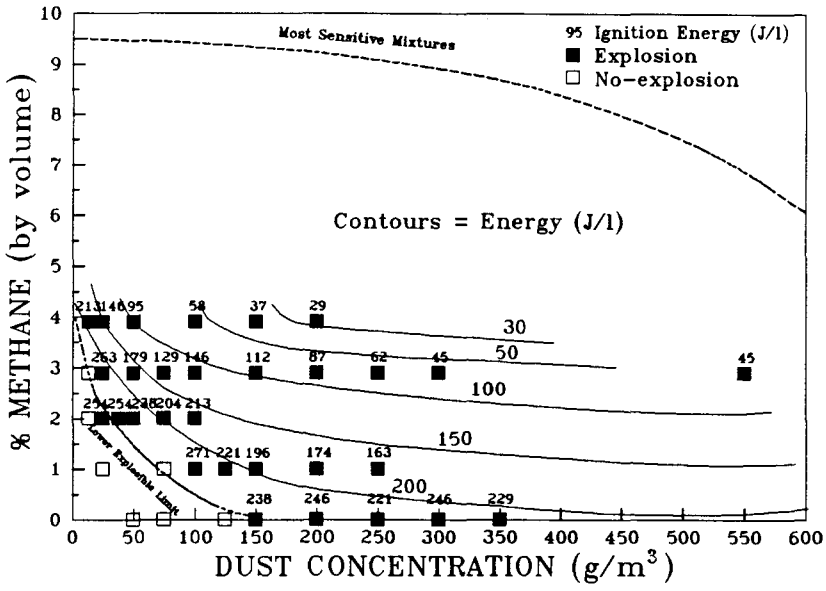

Fig.7.30. The minimum chemical ignition energy blanket of washed Springfield coal dust hybrid mixtures.

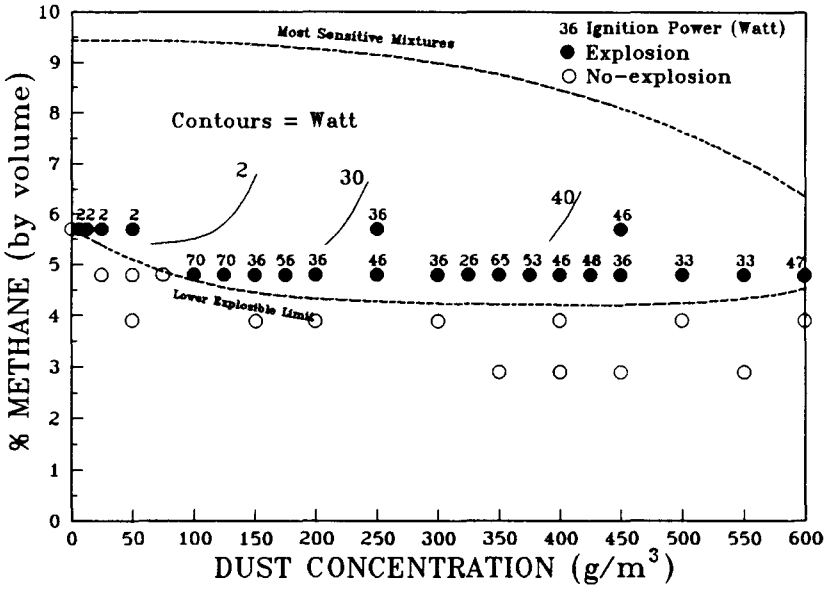

Fig.7.31. The minimum spark ignition power blanket for washed Springfield coal dust hybrid mixtures.

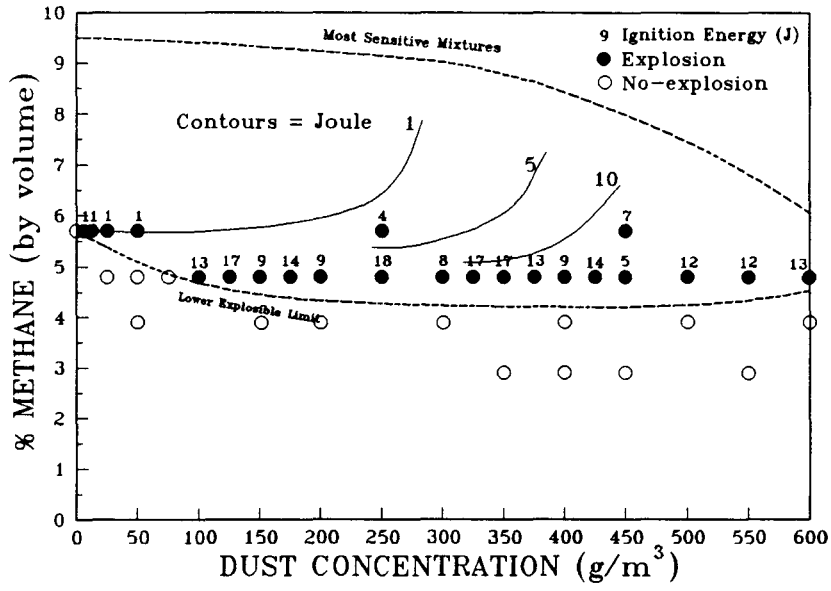

Fig.7.32. The minimum spark ignition energy for washed Springfield coal dust hybrid mixtures.

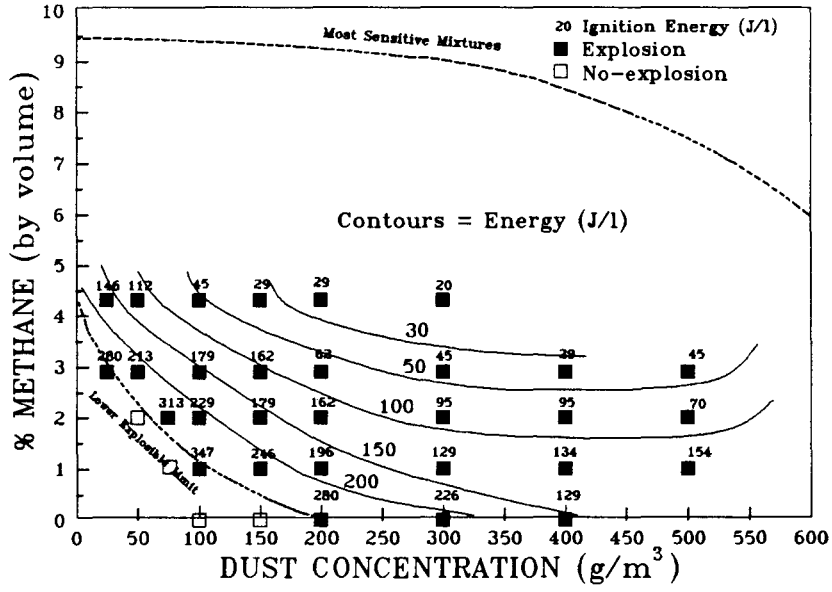

Fig.7.33. The minimum chemical ignition energy for un-washed Springfield coal dust hybrid mixtures.

7.5.4 EXPLOSION CAPACITIES (K_{ex}) FOR SPRINGFIELD HYBRID MIXTURES

The explosion potential or capacity, as indicated by K_{ex} values, is shown in Figure 7.34 for washed Springfield coal initiated by chemical ignition. For dust alone, the K_{ex} explosion index is under 7 MPa/s, but increases with higher dust and methane concentrations to above 8 MPa/s. This is much lower than the maximum of 30 MPa/s for washed Ermelo hybrid mixtures, as is shown in Figure 7.27. K_{ex} values for spark ignition are shown in Figure 7.35. The K_{ex} values are much lower than those shown in Figure 7.28, which are the values for washed Ermelo hybrid mixtures with spark ignition. The K_{ex} values for un-washed Springfield coal chemically ignited is given in Figure 7.36. Although low K_{ex} values are observed close to the lower explosible limit, much higher K_{ex} values for methane concentrations above 3 % are reported, compared to the values of washed Springfield dust as shown in Figure 7.34. This behaviour is analogous with the behaviour of Ermelo hybrid mixtures. The lower volatile contribution from the high ash coal might result in stoichiometrically more balanced mixtures at high concentrations of dust, resulting in higher K_{ex} values.

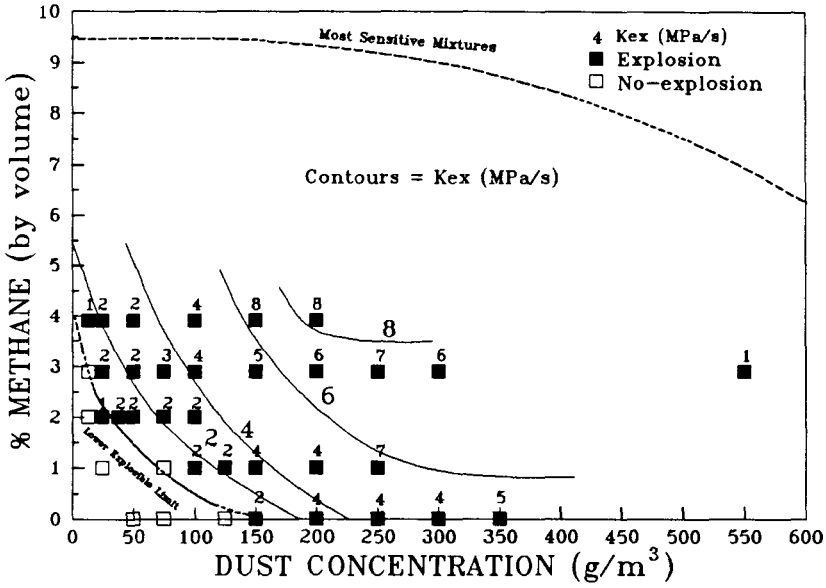

Fig.7.34. The K_{ex} blanket for washed Springfield coal dust hybrid mixtures, chemically ignited.

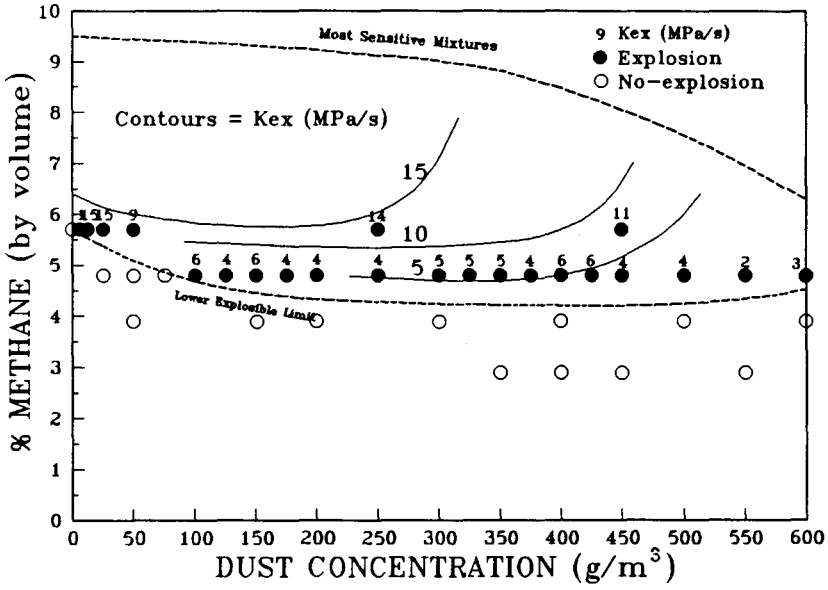

Fig.7.35. The K_{ex} blanket for washed Springfield coal dust hybrid mixtures, ignited by electric spark ignition.

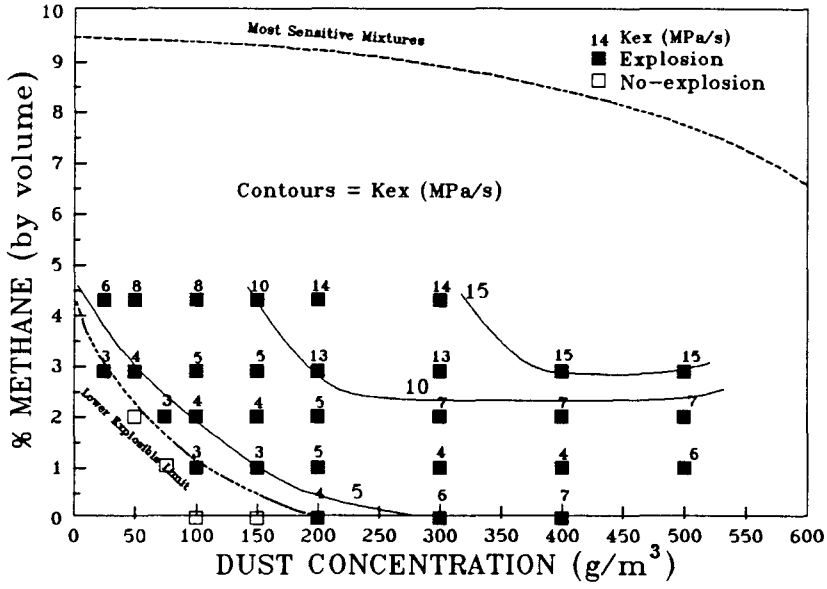

Fig.7.36. The K_{ex} blanket for un-washed Springfield coal dust hybrid mixtures, chemically ignited.

7.6 THE EFFECT OF THE ENERGY SOURCE AND COAL COMPOSITION ON THE EXPLOSIVE BEHAVIOUR OF COAL MINE ATMOSPHERES

As was discussed in Chapter IV, three aspects should be considered when evaluating the pre-ignition environmental conditions which can be conducive to hosting an explosion. They are:

1. The lower explosible limits of the air/fuel mixtures present
2. The sensitivity to ignition of the mixtures, and
3. The potential for propagation of a coal dust explosion

All three aspects are influenced by the amount of methane present, the composition of the coal dust and the way in which it is ignited. The selected coal samples represent two extreme cases. Ermelo coal dust is an active high volatile coal, but Springfield coal dust is relatively inactive and contains far less volatiles. The relative explosible behaviour of the two coals therefore describe the boundary conditions within which

most South African coals lie. The chemical and point source ignition sources likewise represent the two boundary conditions, that of true volumetric ignition and point source ignition respectively.

Each of the three aspects can now be examined individually in order to clarify how they are influenced by ignition source and coal composition.

7.6.1 LOWER EXPLOSIVE LIMITS

Figure 7.37 shows the lower explosible limits of concentrations of methane and coal dust with air. The lower explosive limit of methane drops as coal dust is added. For example, for methane alone, the lower explosible limit is 3.9 % methane by volume if chemically ignited. With 75 g/m^3 of Ermelo dust present in the air, the mixture explodes with only 1.4 % of methane present. When the Ermelo dust line ignited by spark is studied, it is clear that higher concentrations of methane and coal dust are required for spark ignition than for chemical ignition.

Although the less active Springfield coal's lower explosive limit for chemical ignition lies close to that of the more active Ermelo limit, the lower limit for spark ignition is far removed from the equivalent Ermelo limit. A much wider zone between chemical and spark ignition is observed for Springfield dust. Not enough volatiles can be obtained from the Springfield coal dust to ensure an adequate rate of heat addition which self propagates the explosion in the mixture.

When Figure 7.37 is again considered, three areas for each coal dust can be distinguished. The Ermelo coal is taken as an example. Mixtures in the area below the lower explosive limit of the chemical ignitor cannot ignite. Above this line, but below the lower explosible limit when ignited by spark, the mixtures are ignitable by volumetric ignition, but will not spontaneously disseminate flame. In this area frictional ignitions are unlikely to occur. Above the lower spark ignition limit, the mixtures are both volumetrically and point ignitable, and will be self propagational.

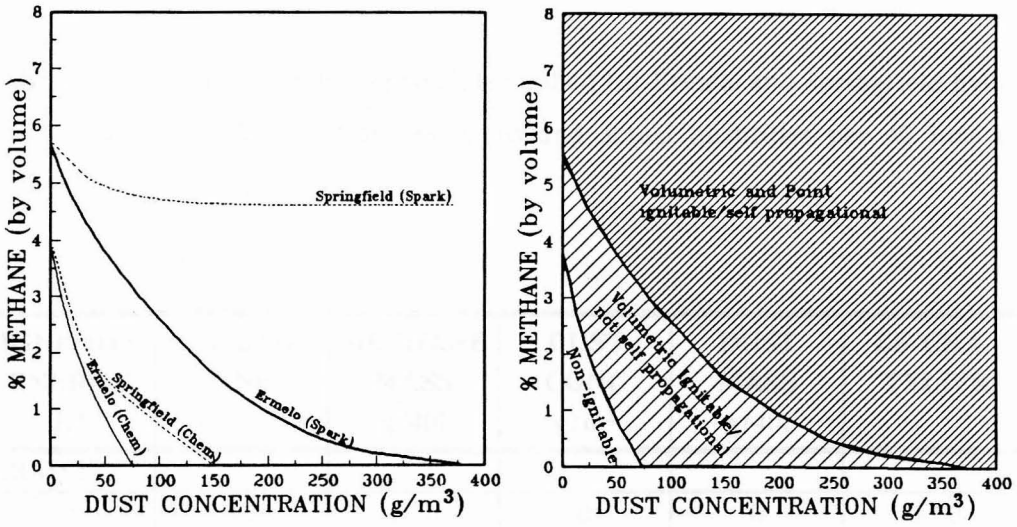

Fig.7.37. The lower explosive limits for chemical and spark ignition for Ermelo and Springfield hybrid mixtures (left). Areas of explosibility for Ermelo hybrid mixtures (right).

Application of Le Chatelier's Principle for Determining the Lower Explosive Limits of Hybrid Mixtures

As is stated in Chapter III, Le Chatelier's law can be used for calculating the lower explosive limit for hybrid mixtures. The validity of this rule for the observed data is investigated. Singer[74] observed a positive synergistic behaviour between methane and coal dust in a hybrid mixture. The possibility of synergism is examined by application of Equation 3.39 (page 81):

$$\frac{d}{N_d} + \frac{s}{N_s} = 1$$

Chemical ignition of Ermelo and Springfield coal dust at 16 J/l, 50 J/l and 200 J/l ignition energies can be selected for investigation. The results are summarised in Table VII.IV.

TABLE VII.IV Le Chatelier's principle applied for Ermelo and Springfield hybrid mixtures. Concentrations and actual quantities per 40 litre are indicated.

IGNITION ENERGY J/l	% METHANE	METHANE MASS g/40l	DUST CONC g/m³	DUST MASS g/40l	LE CHATELIER
ERMELO:					
16	6.2	1.70	0	0	1.00
16	5.1	1.38	25	1	0.89
16	4.4	1.19	50	2	0.83
16	3.6	0.96	75	3	0.77
16	3.0	0.80	100	4	0.73
16	2.3	0.61	125	5	0.68
16	2.0	0.53	150	6	0.70
16	1.2	0.31	200	8	0.69
16	0.7	0.18	250	10	0.74
16	0.4	0.10	300	12	0.81
16	0.0	0.00	400	16	1.00
50	4.5	1.21	0	0	1.00
50	3.9	1.05	25	1	1.03
50	3.0	0.80	50	2	1.00
50	2.2	0.58	75	3	0.99
50	1.4	0.37	100	4	0.98
50	0.8	0.21	125	5	1.01
50	0.0	0.00	150	6	1.00
200	3.9	1.05	0	0	1.00
200	3.0	0.80	25	1	1.02
200	1.9	0.50	50	2	0.99
200	1.0	0.26	75	3	1.01
200	0.0	0.00	100	4	1.00
SPRINGFIELD:					
200	3.9	1.05	0	0	1.00
200	2.7	0.72	50	2	0.82
200	1.5	0.39	100	4	0.63
200	1.0	0.26	150	6	0.63
200	0.7	0.18	200	8	0.68
200	0.5	0.13	250	10	0.75
200	0.4	0.10	300	12	0.85
200	0.3	0.08	350	14	0.95
200	0.0	0.00	400	16	1.00

Evidence of synergistic behaviour between the substances is clear. As ignition energy is increased, the synergistic effect seems to disappear. Synergism appears to be more apparent for the Springfield dust than for Ermelo dust, if constant ignition energy (200 J/l) is compared. The fuel concentration required for hybrid mixtures is therefore proportionally less than expected, especially for weak ignition sources and for lower volatile contents.

7.6.2 SENSITIVITY TO IGNITION

Springfield hybrid mixtures are observed to be much less sensitive to ignition than Ermelo hybrid mixtures. From the ignition blankets shown under section 7.5, it can be seen that as the lower explosive limits are approached, the minimum ignition energy increases exponentially. Also apparent is that the lower ignition limit can be stretched with higher ignition energies. For example, although the lower explosible limit of methane is often stated to be 5 %, a strong volumetric source of ignition, as was used in this experimental programme, reduces the limit to 3.9 %. At low fuel concentrations a large energy increase results in only an insignificant lowering of the lower explosible limit. Therefore, an absolute lower limit can be distinguished. With the powerful ignition energies used in this study, the lower explosive limit and areas of explosibility shown here can be regarded as absolute limits.

Although the lower explosive limits for hybrid mixtures can be defined, no definite upper boundary for ignition energies can be established. Concentrations that are explosible, but unlikely to occur due to high ignition energies, are therefore difficult to determine. To provide a degree of relativity, the minimum ignition energy of a 5 % methane/air mixture is selected as a boundary. Mixtures with ignition energies under that are regarded as highly sensitive, and above the boundary value as not so sensitive to ignition.

In Figure 7.38, an equivalent methane ignition energy line is drawn for hybrid mixtures of methane and coal dust. For the area which is volumetrically ignitable, but not self propagational, an equivalent 5 % methane ignition energy line is shown

(MIE-Methane Ignition Energy). For point ignition, however, methane is only ignitable above a methane concentration of 5.7 %. To illustrate the relative sensitivity of mixtures in this area, an equivalent 5.7 % methane ignition energy line is shown. All mixtures above the 5 % line should nevertheless be avoided.

Increased safety due to a reduced sensitivity of the less active Springfield coal is evident if compared to Ermelo hybrid mixtures. Ermelo coal is shown to be very sensitive at relatively low methane and dust concentrations, and is consequently regarded as extremely dangerous. Again, most South African coals can be expected to lie between the boundaries these two coals represent.

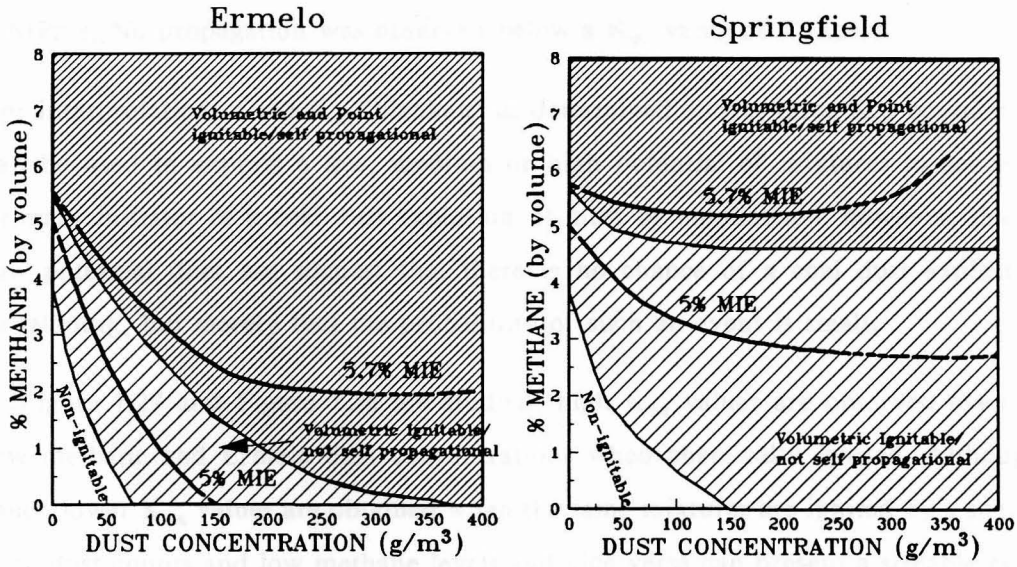

Fig.7.38. Sensitivity to chemical ignition of hybrid mixtures comparative to the ignition energy required to ignite a 5 % methane/air mixture and a 5.7 % methane/air mixture (MIE). Ermelo hybrid mixtures are shown at left, and Springfield hybrid mixtures at right. Areas of explosibility are also indicated.

7.6.3 CAPACITY TO INITIATE A COAL DUST EXPLOSION

When an accidental explosion occurs in the working face, the explosion endangers the safety of the mine workers in the immediate proximity. Apart from this hazard, the explosion can act as a primary initiator of a major coal dust explosion. Such

explosions involve much larger areas and are a most dangerous phenomenon. To evaluate the potential maximum hazard that a face ignition contains, some measurement of the capacity of such explosions to initiate a coal dust explosion is required.

A study which was started by Helwig[31] in the sixties, and extended in early eighties by Reeh[44], provides a way of evaluating the potential of explosions to serve as initiators of coal dust explosions. The K_{ex} values determined in a 40 litre explosion vessel were compared to a parallel test of the same dust in a large scale explosion tunnel. It was observed that propagation of dusts with K_{ex} values above 9 MPa/s always took place, and sometimes took place for K_{ex} values between 7 MPa/s and 9 MPa/s. No propagation was observed below a K_{ex} value of 7 Mpa/s.

For interpretation of the K_{ex} "blankets" as determined above, these K_{ex} boundaries can be used to express a low, medium or high potential of mixtures to act as a primary initiator of a coal dust explosion. It must be emphasized, however, that a low potential does not suggest that there is no chance of a coal dust explosion developing, but merely that the probability of such an event is small.

If Figure 7.27 and Figure 7.28 are studied, high K_{ex} values are observed even at low methane and Ermelo dust concentrations when chemically ignited. Although much lower K_{ex} values are obtained when the same mixtures are ignited by a spark, high dust counts and low methane levels and vice versa can present a sizeable risk. For example, for both a 1 % methane level and a 325 g/m^3 Ermelo dust concentration which is ignited by spark, a K_{ex} value of 9 MPa/s is registered.

Figure 7.34 and Figure 7.35 show that Springfield dust presents a danger at high methane levels, but at low methane and dust concentrations explosions can be expected to be localised. For spark ignition, it appears that no propagation of any dust concentration at a methane level below 4 % is possible.

One can conclude that South African coal dust, when forming hybrid mixtures with methane and air, can possess a varying degree of ability to act as an initiator of a coal dust explosion. This can vary from a relatively low to a high probability.

7.7 CONCLUSION

In this chapter, methane/air, coal dust/air and hybrid mixtures were tested for minimum ignition energy and other explosive properties. The lower explosive limits, the sensitivity to ignition and the potential to initiate a coal dust explosion have been determined. The influence of the type of ignition source and the coal dust properties on the explosion characteristics has been illustrated.

The major objective of the study, namely the determination of the ignition blanket in order to specify the conditions under which coal mining can proceed safely, has been obtained. What is left to determine is how the position of the ignition blanket will be altered with a change in the surrounding environment. This objective can only be obtained if the heat generation and heat loss properties of the explosible substances and the explosion environment are understood. Chapter VIII investigates this aspect.

In Chapter IX, actual face dust concentrations are determined and compared to the findings of this chapter. Final conclusions regarding the explosion risk at a modern South African coal face can then be made.

CHAPTER VIII

HEAT RELEASE AND HEAT LOSS CHARACTERISTICS OF EXPLOSIVE SYSTEMS

The objectives of this section are twofold. Firstly, it aims to illustrate that ignition limits are not absolute, but determined by the relation of heat inflow and heat loss from the system. Secondly, it illustrates that the behaviour of explosive mixtures is a chemical reaction and therefore a constant, but that the surrounding environment controls the likelihood of the reaction taking place. The analysis is regarded as speculative and serves only to illustrate that there is evidence from the experimental data which justifies the line of thought followed in this work. In conclusion, the heat loss properties of the working face are briefly discussed.

8.1 INTRODUCTION

The steady state ignition theory of Semenov (described in Chapter III under section 3.2.2, page 58, equation 3.11) equates the rate of heat generation and the rate of heat loss during an explosive reaction at the point of minimum ignition. Further development of this expression, which describes the self acceleration of the reaction until heat generation is exceeded by heat loss, is complex and considered to be beyond the objectives of this study. During the experimental programme, however, it has been observed that the strength of the ignition source, the average reaction temperature and the average duration of the explosive reaction are related. This information is used here to illustrate that an exponential relationship does exist between the average reaction rate and reaction temperature and can be fitted to an Arrhenius type rate controlling reaction.

Ermelo washed coal at concentrations of 100 g/m^3, 150 g/m^3, 200 g/m^3 and 250 g/m^3 is used to illustrate the principle. Mixtures of 1 % and 2 % methane with 100 g/m^3 dust are included to show the effect of low concentrations of methane on the heat generation and reaction rate of an explosion. A hypothetical discussion of heat loss from the explosive system concludes this chapter.

Important Observations from the Experimental Programme

In Chapter VII it was observed that the minimum ignition energy decreases and pressure increases with an increased fuel concentration. However, for a constant fuel concentration, maximum pressure developed stayed constant regardless of the type or intensity of the ignition source (see Figure 7.1, page 156). Just above the point of minimum ignition, a small increase in ignition energy resulted in a significant increase in the rate of pressure rise. As ignition energy was increased even further, the rate of pressure rise increased but less noticeably until an energy was reached above which the rate of pressure rise was nearly constant.

The maximum pressure is indicative of the amount of heat released during the reaction and can serve as an indication of the exothermicity of the reaction. The time in which this pressure is reached is also the time in which all reactants are consumed, and therefore the average reaction time. For an Arrhenius type rate equation, the reaction temperature and the reaction time of the process are required to determine the activation energy and a pre-exponential factor. This method will now be applied, but activation energy as determined here will be called an activation constant in order to point out that it is not the true activation energy as required for the determination of the instantaneous reaction rate.

8.2 AN ESTIMATE OF THE RATE OF HEAT RELEASE IN THE 40 LITRE EXPLOSION VESSEL

The term "heat release" is used instead of "heat generation". The former will refer to the total amount of heat released during the process, while the latter refers to the instantaneous generation of heat that helps the reaction to self-accelerate. The following expression for the rate of heat release (dq_g/dt) will be used to model the observed empirical results:

$$dq_g/dt = (QV\rho)(Ae^{(-E/RT_r)}) \qquad -8.1$$

where Q is the exothermicity of the reaction in Joules per unit mass at density ρ and volume V. A is a pre-exponential constant with units sec^{-1}, E is an activation constant in Joule per mole and R the universal gas constant in Joule per mole per degree Kelvin. T_r is the reaction temperature in degrees Kelvin. In short, the equation is the product of the amount of heat generated and the reaction rate (brackets separate the two parts).

For the chemical ignitor, the ignition energy is spread throughout the explosion vessel. The reaction that is initiated starts throughout the whole volume and heat is only lost to the walls of the vessel. The amount of heat loss through the walls compared to the heat generated is assumed small, and will be neglected here.

8.2.1 DETERMINATION OF THE APPARENT HEAT RELEASED DURING AN EXPLOSION

The total heat of reaction can be calculated by summation of the standard enthalpies of formation of the products minus that of the reactants (see section on *Thermochemistry* on page 53). At temperatures above 25 °C, a summation of the product of heat capacity over the incremental temperature range must be added to the standard enthalpies of formation. This is difficult to undertake for the observed data for the following reasons. The exact starting temperature of the reaction, after the source of ignition has been removed, is not known. Also, the exact chemical reactions taking place when coal explodes are not known. Instead, the maximum pressure was used as an estimate of the amount of heat released and the time to reach the maximum pressure was used to estimate the rate of reaction.

When maximum pressure (N/m^2) is multiplied by the volume of the vessel (m^3), an energy release is calculated which is given in Joule (Nm). For a methane/air reaction ($CH_4 + 2O_2 = CO_2 + 2H_2O(gas)$) no increase in the mole gaseous substances are involved and the pressure rise is totally as a result of the temperature increase. For combustion of coal, Krazinski, Buckius and Krier[51] found the reaction $2C(g) + O_2 = 2CO$ to be a fair estimate of the actual explosion reaction taking place.

Here, as well, no addition of gas takes place that can contribute to the increase in pressure if it is assumed that the carbon component represents the volatized fraction. The pressure increase is therefore mostly due to the addition of heat from the exothermic reaction.

8.2.2 PROCEDURE FOR REACTION RATE ESTIMATION

The rate expression in equation 8.1 is of Arrhenius type and given by $k = Ae^{(-E/RTr)}$, where k is the rate constant. The expression can then be written as follows:

$$\ln k = \frac{-E}{R}\left(\frac{1}{T_r}\right) + \ln A \qquad -8.2$$

Equation 8.2 is a straight line of the form $y=mx+c$, where $y=\ln k$ and $x=1/T_r$. The time to maximum pressure, t_{max}, is also the time in which all reactants are consumed and can therefore be equalled to the reaction time. The rate constant, k, is the inverse of the reaction time (sec^{-1}), and can be obtained by taking the inverse of t_{max}.

The reaction temperature, T_r, was obtained from pyrometer readings, shown in Appendix V. A typical temperature time plot is shown in Figure 8.1. The ignition source is shown as a short 2 to 4 ms temperature spike, followed by an induction period between zero and 10 ms, depending on the concentration of the fuel. The combustion process is then shown as the longer period at more or less a constant temperature.

Explosions involving methane alone resulted in inaccurate temperature measurements due to the high combustion temperatures above the upper accuracy limit of the pyrometer. Coal dust combustion and hybrid mixtures involving relatively small quantities of methane resulted in combustion temperatures between 900 °C and 2100 °C. The reading errors that could have been obtained at the top and bottom ends of this temperature range are assumed to be insignificant.

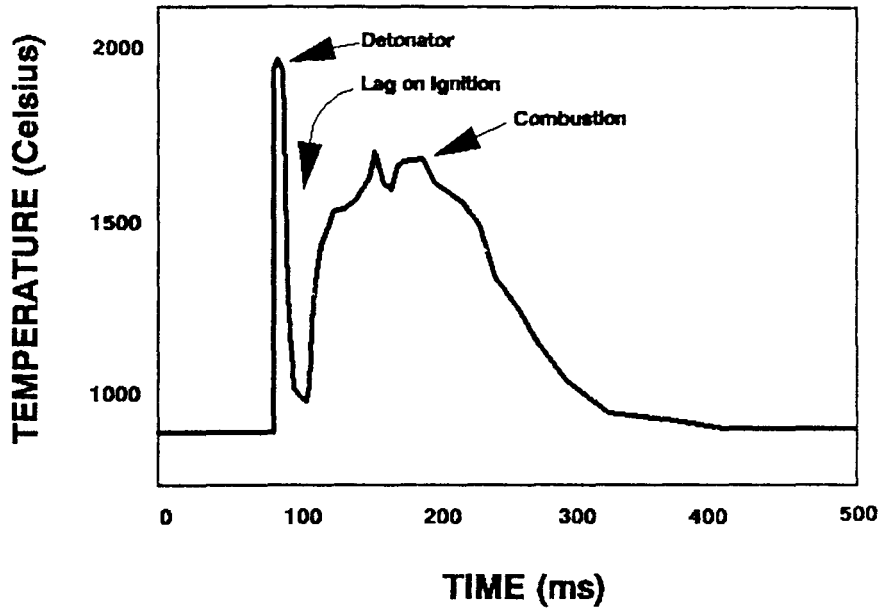

Fig.8.1. A typical temperature history over time for the chemical ignition of Ermelo washed coal dust at a 100 g/m^3 concentration as obtained from pyrometer readings.

When ignition energy was increased and the fuel concentration kept constant, an increase in the combustion temperature T_r was observed. At such higher temperatures, the time to maximum pressure was reduced.

The constants E and A in equation 8.2 are unknown. With k and T_r known, however, the constants can be determined by plotting values of $1/T_r$ against values of ln$k$ on an XY-scatter diagram. A linear line can be fitted, of which the slope of the line equals $-E/R$ and the Y-axis intercept equals ln A.

E is an estimated activation constant and can be determined as follows:

$$E = -R \times (slope \quad of \quad the \quad line) \qquad -8.3$$

where R is measured in J mol^{-1} K^{-1} and E is obtained in J $mole^{-1}$.

A pre-exponential factor A, can be obtained as follows:

$$A = e^{Y-intersection} \qquad -8.4$$

where the units of A are sec^{-1}.

8.2.3 CALCULATION OF RATES OF HEAT RELEASE

All temperature measurements obtained using the pyrometer and from explosions of Ermelo washed coal dust and hybrid mixtures with methane are tabled in Appendix V. The calculation of $1/T_r$ and $\ln(1/t_{max})$ for selected coal concentrations is shown in Table VIII.I. Values for $1/T_r$ and $\ln(1/t_{max})$ are shown is Appendix V.

The average pressures developed from explosions of Ermelo washed coal dust of concentrations 100 g/m^3, 150 g/m^3, 200 g/m^3 and 250 g/m^3 are 400 kPa, 600 kPa, 660 kPa and 700 kPa respectively. Multiplied by the volume of the 40 litre explosion vessel i.e. 0.04 m^3, the approximate amount of heat released for 100 g/m^3 of dust is 16 kJ, for 150 g/m^3 dust 24 kJ, for 200 g/m^3 dust 26.4 kJ and for 250 g/m^3 28 kJ.

Figure 8.2 is a plot of $\ln(1/t_{max})$ against $1/T_r$ for the same concentrations of Ermelo coal dust. The 150 g/m^3 line lies far above the 100 g/m^3 line, and the 200 g/m^3 line above the 150 g/m^3 line, but with a reduced gap between the lines. The 200 g/m^3 and 250 g/m^3 lines appear to lie on top of each other.

The slope of the lines in Figure 8.2 is approximately -4310.5. Therefore, $-E/R$=-4310.5, and with R=8.314KJ mol^{-1} K^{-1}, E=35.837 kJ mol^{-1}. The Y-axis intercept of the lines for concentrations 100 g/m^3, 150 g/m^3, 200 g/m^3 and 250 g/m^3, are 4.4531, 4,9261, 5.3496 and 5.3994 respectively. This gives A values of 85.89 s^{-1} for 100 g/m^3, 137.84 s^{-1} for 150 g/m^3, 210.52 s^{-1} for 200 g/m^3 and 221.27 s^{-1} for 250 g/m^3. The heat release curves shown in Figure 8.3 have been generated by substituting the determined E and A values into the following equation:

$$Heating\ \ Rate\ \ =\ \ (Heat\ \ Released)\times(Ae^{(-E/RT_r)})\quad -8.5$$

TABLE VIII.I Calculation of $1/T_r$ and $\ln(1/t_{max})$ for concentrations of Ermelo washed coal dust. The 100/1% and 100/2% indicate hybrid mixtures of 100 g/m^3 dust and 1 % and 2 % methane.

DUST CONC g/m^3	DET ENERGY J/l	P_{max} kPa	t_{max} ms	T_r K	$1/T_r$ 1/K	$\ln(1/t_{max})$ s^{-1}
100	213	380	450	1273	0.000786	0.7995
100	229	420	312	1310	0.000763	1.1639
100	263	430	236	1398	0.000715	1.4433
150	54	490	345	1023	0.000978	1.0647
150	62	470	446	1098	0.000911	0.8076
150	95	580	225	1173	0.000853	1.4919
150	129	590	179	1398	0.000715	1.7203
150	179	550	150	1423	0.000703	1.8971
150	263	600	135	1523	0.000657	2.0017
250	20	630	262	1223	0.000818	1.3408
250	54	710	134	1273	0.000786	2.0133
250	95	710	105	1398	0.000715	2.2503
250	179	700	88	1523	0.000657	2.4316
250	263	690	77	1573	0.000636	2.5607
100/1%	104	270	740	1023	0.000978	0.3005
100/1%	112	200	865	1123	0.000890	0.1455
100/1%	179	350	465	1248	0.000801	0.7664
100/1%	263	430	247	1273	0.000786	1.3991
100/2%	45	540	306	1273	0.000786	1.1834
100/2%	62	540	248	1323	0.000756	1.3933
100/2%	95	570	211	1398	0.000715	1.5583
100/2%	179	600	126	1523	0.000657	2.0743
100/2%	263	560	152	1548	0.000646	1.8810

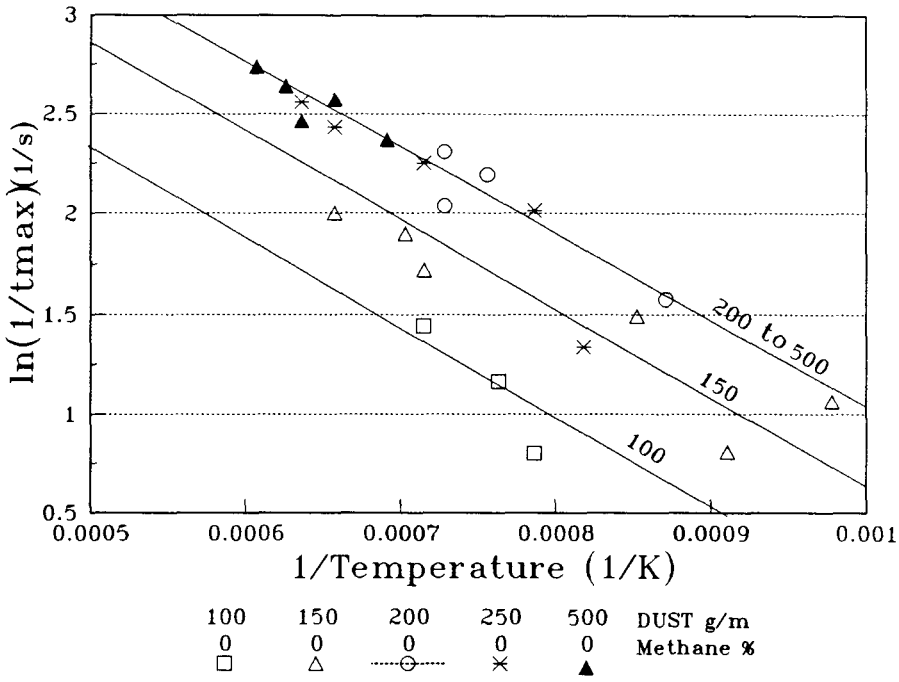

Fig.8.2. A plot of $\ln(1/t_{max})$ versus $1/T_r$ for different concentrations of Ermelo washed coal dust.

The curves of Figure 8.3 show the rapid increase in the rates of heat generation with increased combustion temperature. To ignite the 100 g/m^3 concentration, 213 J/l of chemical ignition energy is required. This results in sufficient energy transfer to allow the reaction to proceed at about 1300 K. The corresponding heat transfer rate at that temperature for this reaction is about 50 kJ/s, which means that it will take 320 ms to transfer 16 kJ to the system with the effect of raising the pressure to 400 kPa.

In the same way, activation and pre-exponential constants were obtained for hybrid mixtures of 100 g/m^3 dust and 1 % and 2 % methane. The activation constants are surprisingly higher at 40.513 kJ mol^{-1} with 1 % of methane present

and 47.564 kJ mol^{-1} for 2 % methane present. The corresponding pre-exponential factors are 106.80 s^{-1} and 296.29 s^{-1}. Using these constants, the curves in Figure 8.4 have been generated.

The same effect of higher energy release rates at higher concentrations for the same temperature can be seen in Figure 8.4 for hybrid mixtures. Ignition should therefore become easier with increased addition of methane.

8.3 A DISCUSSION OF HEAT LOSS CHARACTERISTICS OF EXPLOSIVE SYSTEMS

The rate of heat loss from the system determines the explosible limits of the mixture. One of the quasi heat release curves shown in Figure 8.3 is reproduced in Figure 8.5, but two hypothetical heat loss systems are also indicated with straight lines. In Figure 8.5 they are marked as the lower and upper heat loss lines.

The lower line represents a system which is more isolated, and heat can only escape at a controlled rate even at high temperatures. This situation is similar to volumetric ignition in a closed vessel. Even at high temperatures of combustion, the surface area through which an outflow of heat is possible stays constant and limited.

If a source of ignition is introduced that would result in a combustion temperature of less than 1000 K, as indicated by point X in the graph, heat loss is dominant and no heat is gained. With an ignition energy which achieves a combustion temperature above 1000 K, the heat inflow is suddenly far in excess of what is lost. No explosion is therefore possible below the crossover point, but above the crossover point heat loss is very small in comparison with heat inflow. For higher ignition energies, the heat release rate increases, and the total heat transfer occurs in a shorter and shorter time, as observed by shorter reaction times t_{max}.

The upper heat loss line in Figure 8.5 shows an explosion system with more severe heat loss characteristics. This situation is analogous to point source ignition.

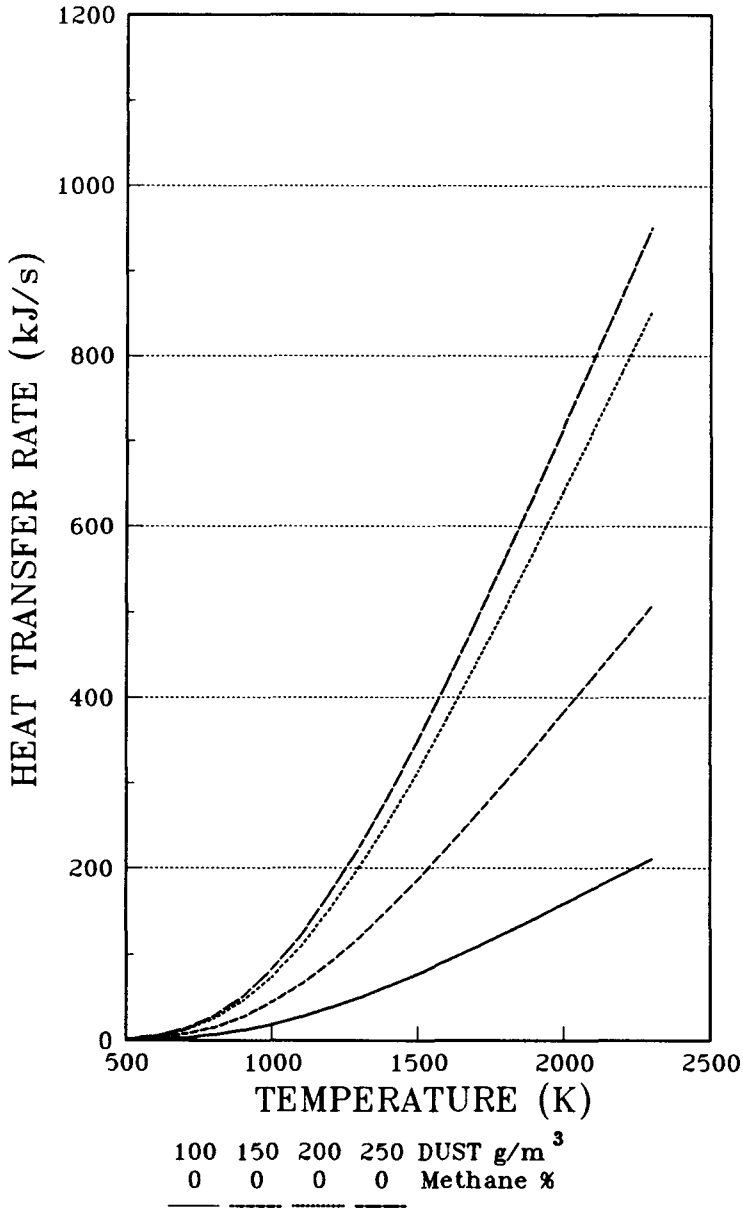

Fig.8.3. Quasi heat generation curves for Ermelo washed coal dust.

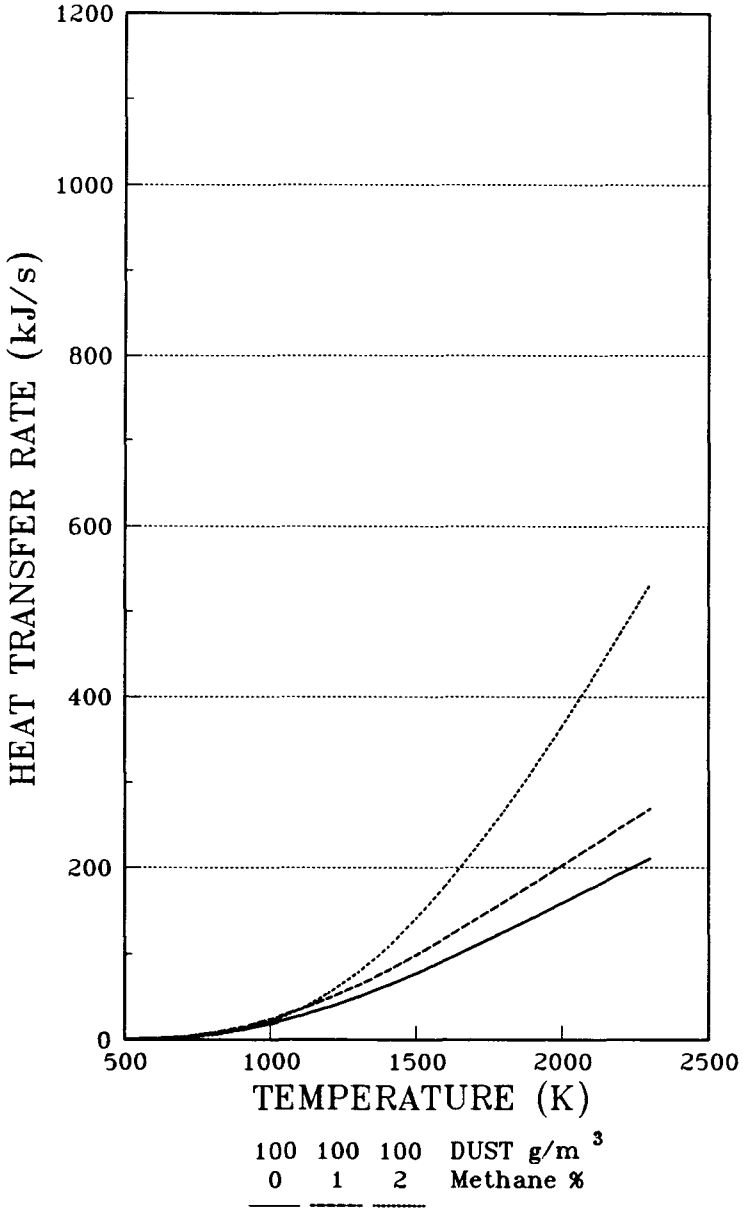

Fig 8.4. Heat generation curves for hybrid mixtures of methane and Ermelo washed coal dust.

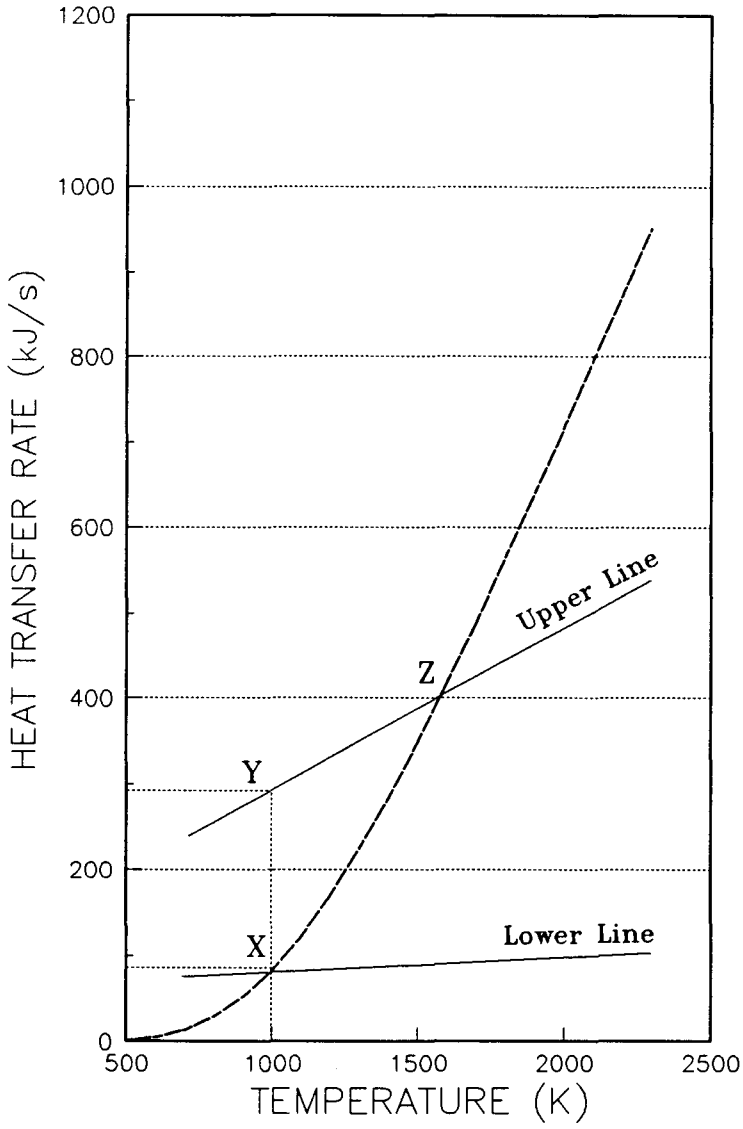

Fig.8.5. Behaviour of explosive systems with reference to the relation of the rate of heat release and the rate of heat loss.

As the combustion moves away from the source, a relatively thin combustion sphere develops, bordered on the outside by an area of equal size of unburnt mixture. Heat is immediately lost to the unburnt sphere which, on ignition, is again surrounded by unburnt mixture. The area through which heat is lost increases with combustion, and is not rate controlling.

It is clear from Figure 8.5 that at point Y no reaction is possible at ignition energies that can effect reaction temperatures of 1000 K. Higher concentrations with steeper heat release curves might be ignitable, or at higher ignition energies the minimum ignition point will be point Z.

If explosion characteristics of mixtures of similar ignition energy are compared, a similarity in maximum pressure, time to maximum pressure and ignition temperature is observed. For example, such values of mixtures around the 16 J/l and 200 J/l ignition contours for Ermelo washed hybrid mixtures are shown in Table VIII.II. Clearly the maximum pressures, or heat released, are of the same order. The time in which they are released is also of the same order, and finally the combustion temperatures effected by the source of ignition are similar. What is left unexplained by this simulation is the vast difference in the efficiency of the ignition source where a 16 J/l source results in a 1500 K combustion temperature, while a 200 J/l source only results in combustion temperatures of about 1200 K.

TABLE VIII.II Explosion characteristics of Ermelo coal dust hybrid mixtures of similar minimum ignition energy.

DUST CONC g/m^3	% CH_4	IGNITION ENERGY J/l	P_{max} kPa	t_{max} ms	T_r K
50	3.9	29	582	97	1473
75	3.9	16	632	129	1523
100	2.9	24	613	157	1523
150	2.0	16	655	196	1648
200	1.0	16	662	192	1523
250	0.0	20	630	134	-
25	2.9	229	360	468	1198
50	2.0	179	320	559	1273
75	1.0	213	354	435	1223
100	0.0	213	377	450	1273

8.4 CONCLUSION

It has been shown that heat loss from a system determines the lower explosive limits of the explosible mixture. Absolute volumetric ignition is unlikely to happen on a coal face, and the lower explosive limits determined with the chemical ignitor can be regarded as an unmistakable worst case. For volumetric ignition, however, ignition and initial combustion are similar in the 40 litre vessel to those on the working face. The larger volume of the working face will, however, modify the rate of flame dissemination and rates of heat build-up. It might happen that no pressure increase is experienced during a face ignition, but in such cases the fuel concentration should be within the explosible limits indicated by the spark ignitor in the 40 litre vessel.

CHAPTER IX

DUST CONCENTRATION AT THE CUTTING DRUM

An indication of the concentrations and size distributions of the dust clouds surrounding cutting drums on bord and pillar faces was required in order to evaluate the extent of the practical explosion risk. The instruments developed to obtain such information are described and illustrated. The sampling method only captured particles below 100 μm, *and only provides an indication of the more sensitive part of the total dust present. It was determined that very high concentrations can be present on the working face and therefore the lower explosive limit of methane alone cannot be regarded as a safe value.*

9.1 INTRODUCTION

Cybulski[1], as a result of experience gained over many years, has stated that, while explosibility is inversely related to particle size, all finely comminuted coal particles passing a 1 mm mesh sieve can be regarded as dangerous. However, most work related to dust counts at the working face has been aimed at obtaining the concentration of the respirable fraction and has excluded particle sizes above 10 μm. As was mentioned in Chapter II, one of the few references to total dust concentration in the vicinity of cutting drums is the work by Kachan, Kocherga and Kolchinskii[46], who report concentrations of 25,6 g/m^3 at a distance of 0.5 m from the drum in tests conducted in the Ukraine. Kachan et al only discuss concentrations measured, and little is known about the techniques or the particle size distributions of the samples collected.

In order to obtain data for typical South African conditions using continuous miners in bord and pillar sections, a cursory programme of gravimetric sampling was undertaken at five mines. The collieries requested that their names should be omitted, and the results are therefore coded as mines A to E. Collieries A and B are situated in the Eastern Transvaal coalfield, colliery C in the Highveld coalfield, colliery D in the Klipriver coalfield and colliery E in the South Rand coalfield. All samples

were taken around continuous miner cutting drums, but at one colliery in the Eastern Transvaal coalfield, a longwall shearer cutting drum was also sampled. All values were obtained as close to the coal face as possible, and are within 0.2 m from the engaged cutting picks. The objective of this research was to illustrate only what concentrations are possible, and the influence of geological and/or operational factors on dust production was not researched.

9.2 SAMPLING APPARATUS

The apparatus developed for this work consisted of open pots holding a large diameter filter, through which air is drawn by means of two personal sampling vacuum pumps operating in parallel. The filter was of large diameter, in order to obtain a sufficient amount of dust to determine the size distribution and, at the same time, to prevent the filter from clogging. The pots were machined from light but strong PVA and the walls of the pots were made thick to withstand the harsh environment expected around cutting drums.

Figure 9.1 shows the base of the pot, which is funnel shaped. The large end of the funnel is 55 mm in diameter, leading to a 5 mm outlet. The outlet end is connected to a plastic tube that leads to the vacuum pumps. At the open end of the funnel, a flat 7.5 mm shoulder is provided on which the 70 mm diameter filter rests. The filter placed in position is shown in Figure 9.2. An O-ring, 3 mm thick with a 55 mm inner diameter and 70 mm total diameter fits, on top of the filter. The latter is shown in Figure 9.3. A cylindrical section, shown in Figure 9.4, is threaded into the base section, holding the O-ring and filter in position. The O-ring prevents the filter from being damaged when the cylindrical part is fitted. Figure 9.5 shows a cover that can be put onto the open end of the pot to protect the filter during transportation. In Figure 9.6, two parallel connected MSA Flow-Lite flameproof vacuum pumps joined to the sampling pot, are shown.

The base of the pot is flattened at one end on the outside, noticeable on the bottom right corner of the pot in Figure 9.4. At this point the pot is bolted to a strong PVA

rod by means of a bolt and wingnut. The rod consists of four 1 m sections, threaded at the ends to reach a total length of 4 m when assembled. The MSA Flow-Lite pumps are carried on the waist belt of the observer and an adequate length of plastic tube connects the T-piece in the tube close to the pumps and the pot at the end of the stick. The arrangement is illustrated in Figure 9.7. Figure 9.8 shows the pot when opened in the laboratory after a sampling run, with two used filters in the foreground.

The instrument maintains a nominal flow velocity of 8 litres per minute, resulting in a flow velocity of 0.5612 cm/s through the filter paper. The sizes of particles entrained were evaluated by the Coal Mining Laboratory of the Chamber of Mines[117], and it was found that particles up to a 100 μm were entrained with 95 % efficiency, but that efficiency for larger particles was substantially reduced. Particles of up to 600 μm were captured.

9.3 THE SAMPLING PROCEDURE

Two filters per sampling pot were left open in the laboratory, exposed to ambient humidity, for at least 12 hours before they were weighed. One of the filters was then fitted to the sampling pot and the pot closed at the open end by the lid to protect the filter during transportation. The other filter was kept in the laboratory to serve as a weight control in case such changes occurred due to changing humidity. Four pots were manufactured, making four samples per visit possible. The vacuum pumps were calibrated and set to pump air at 4 litres per minute each, providing a total air velocity when sampling of 8 litres per minute.

Underground, the extension rod was assembled, and the pot connected to the far end of the rod. The pot was opened and connected to the vacuum pumps, which were carried on the waist belt of the person taking the sample. When the pumps were started, a stop watch was activated. The extension rod was then used to push the sampling pot face down through the spray screens of the continuous miner cutting drum to within 20 cm of where the cutting picks were breaking the coal.

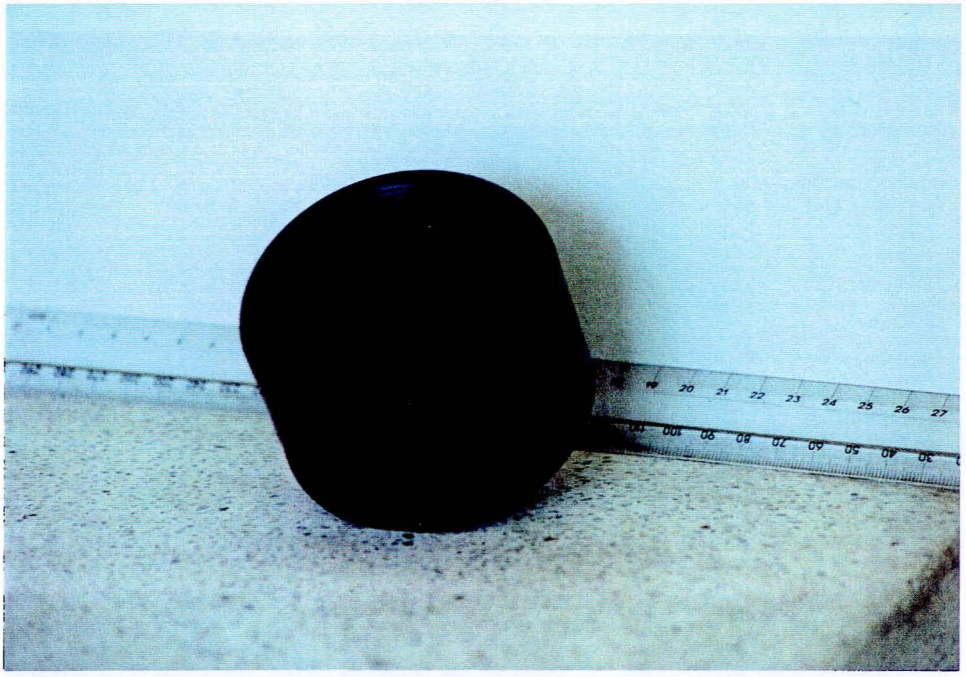

Fig.9.1. The base segment of the sampling pot, with a funnelled outlet which directs the air to the tube connecting the pots and the pumps.

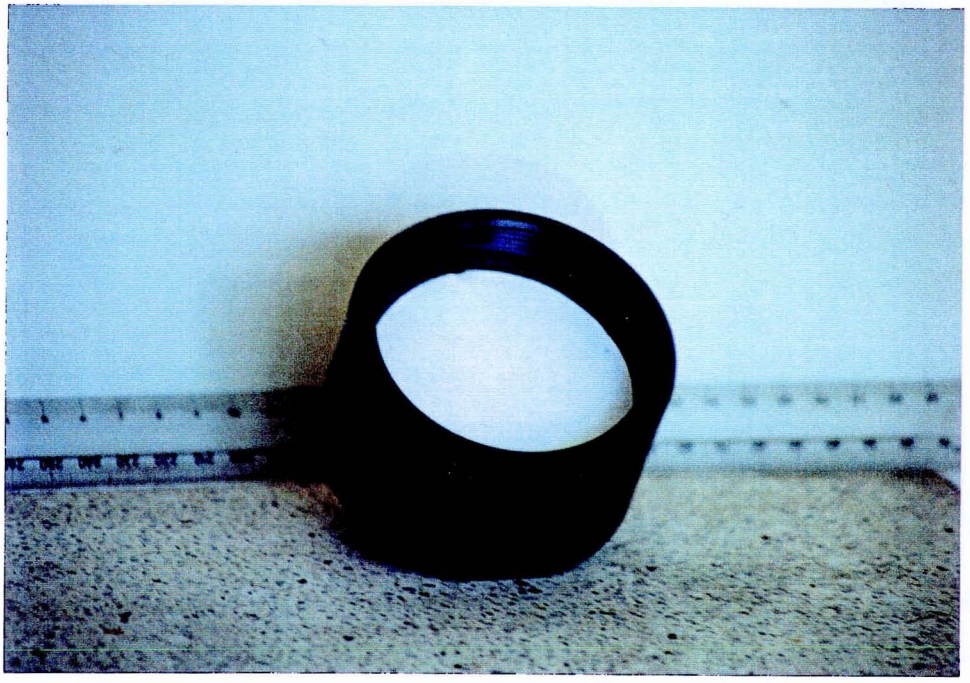

Fig.9.2. The filter laid into position in the base segment of the sampling pot.

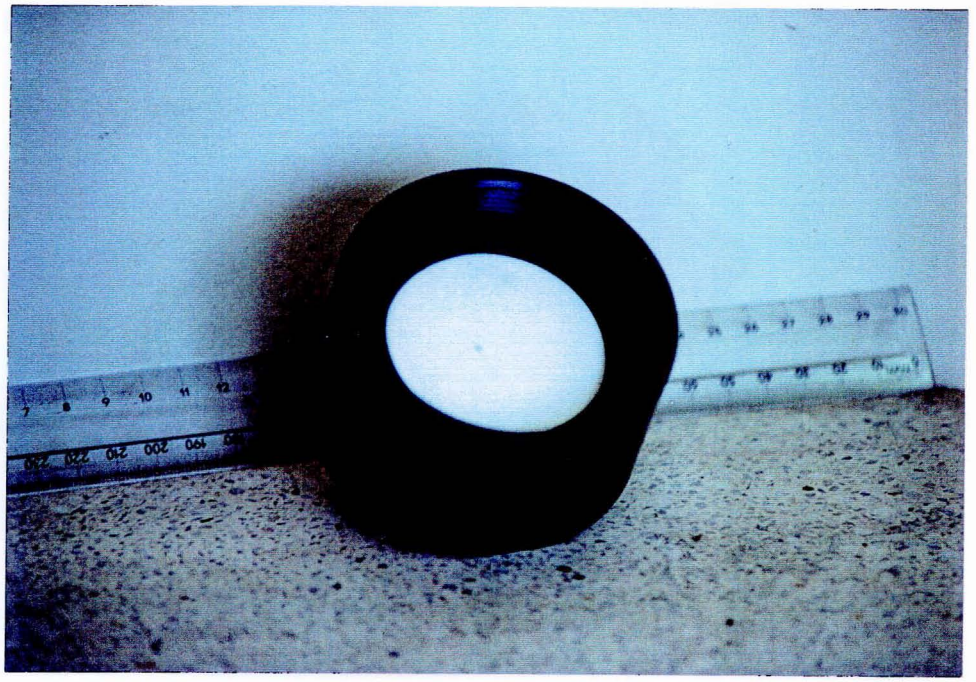

Fig.9.3. An O-ring fitted to hold the filter.

Fig.9.4. A cylindrical section threaded into the base segment, pressing the O-ring tight against the filter.

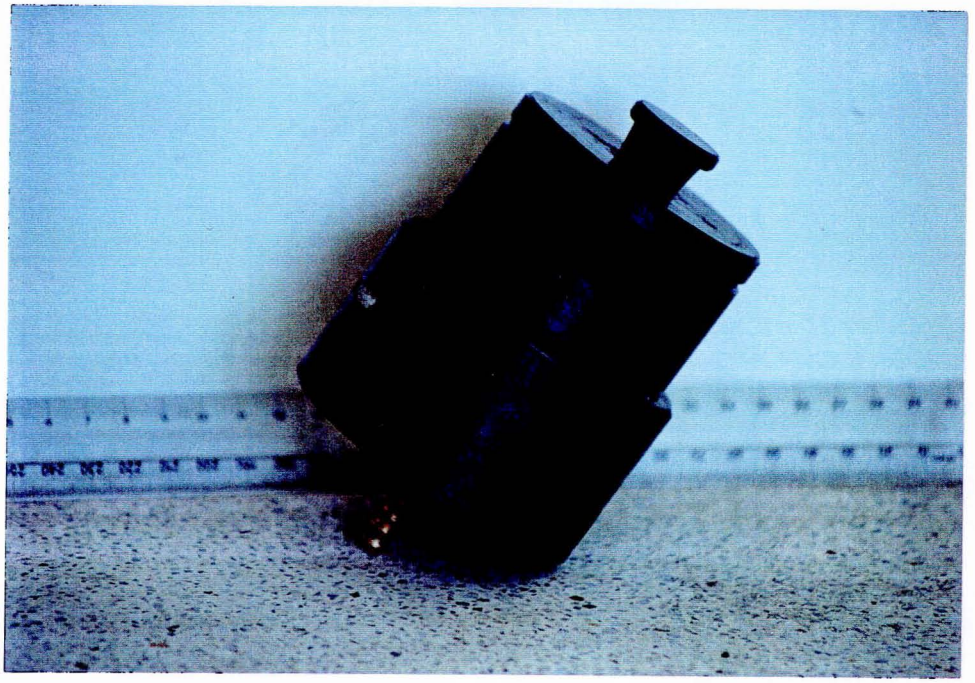

Fig.9.5. The assembled filter pot, with a lid fitted at the open end which protects the filter during transportation.

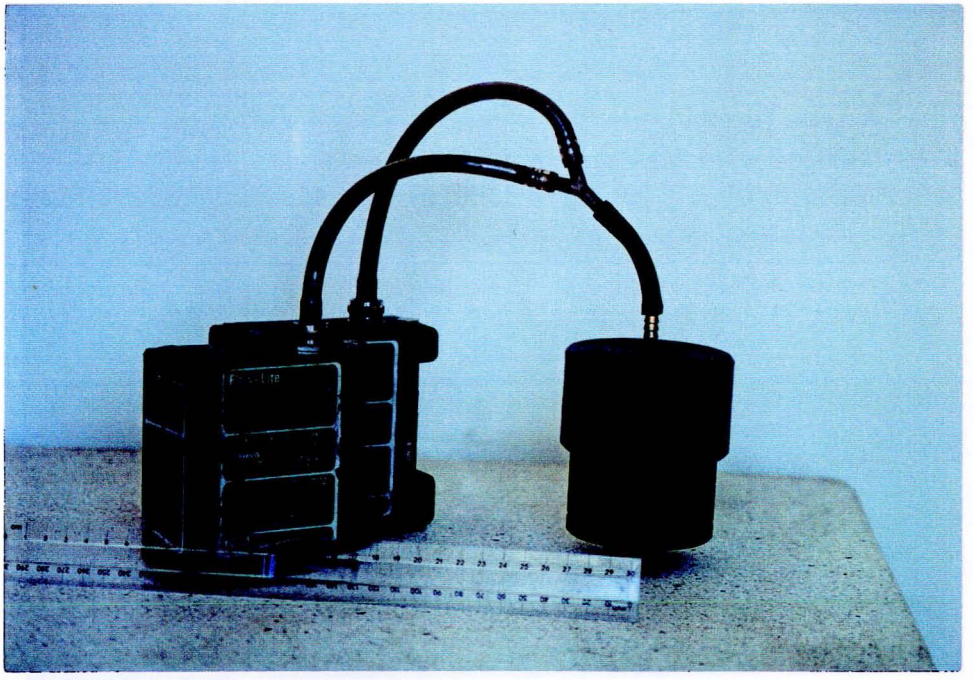

Fig.9.6. Two MSA Flow-Lite vacuum pumps connected in parallel to the sampling pot.

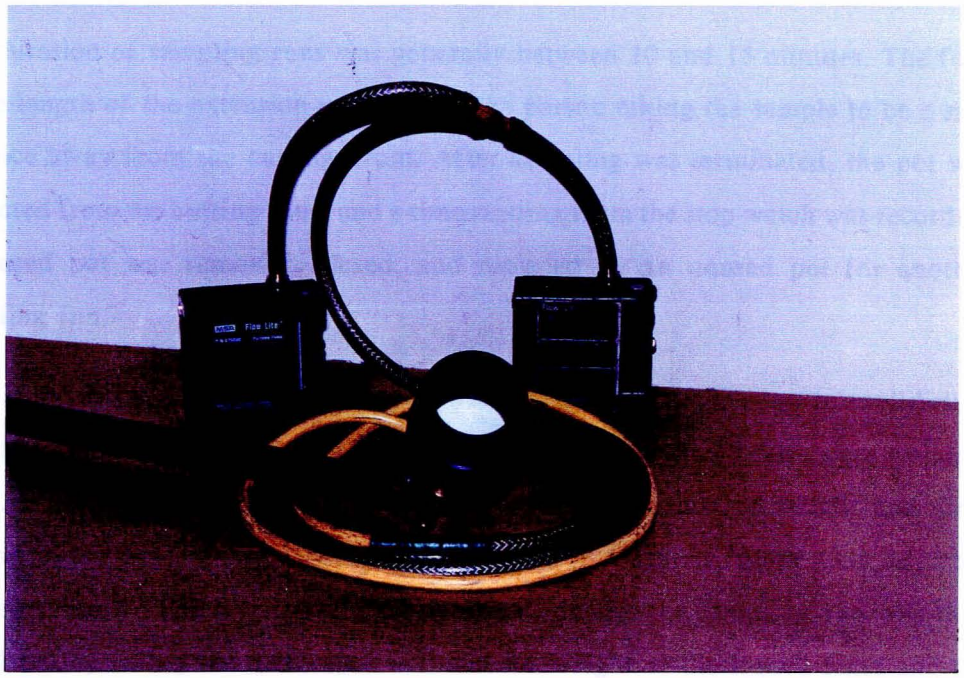

Fig.9.7. The sampling pot fitted to the extension rod with the plastic tube that joins the pumps and the pot.

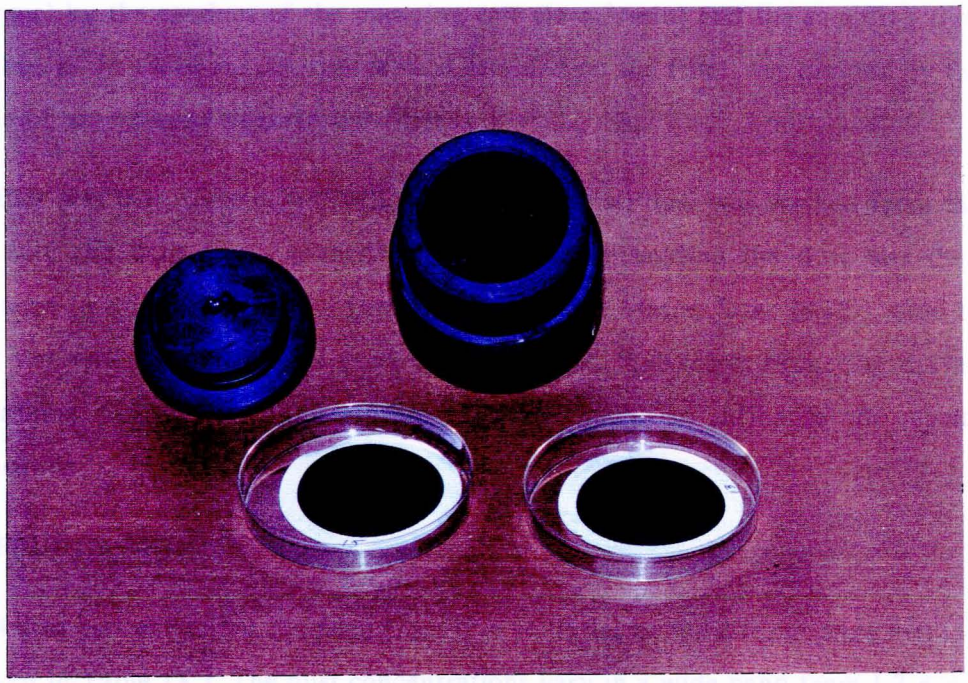

Fig.9.8. A used sampling pot opened in the laboratory, with two used filters in the foreground.

The duration of sampling runs was generally between 10 and 15 minutes. The four metre length of the extension rod allowed the person taking the sample to be a safe distance away from the cutting drum. After sampling was terminated, the pot was extracted from the cutting zone, and a time reading from the stop watch was recorded. The used pot was removed, closed, and replaced by an unused pot for another sampling run.

Back in the laboratory, the sampling pots were opened and left to come to equilibrium with the laboratory humidity. Both the used filters and control filters were weighed again. If a weight difference was noticed between the starting weight and final weight of the control filter, the original weight of the used filters were adjusted correspondingly. The amount of dust deposited during the sampling run was then calculated by taking the difference between the weight of the loaded filter and the adjusted weight of the same filter before use.

The dust cloud concentration was calculated by dividing the mass of dust sampled (in grams) by the product of the pumping rate (in m^3/min) and the sampling time (in minutes). In short, the amount of dust retained on the filter was divided by the volume of air pumped through the filter.

The filter was then soaked in distilled water, where all dust was washed from the filter with the help of an acoustic bath. The water holding the dust was then introduced to a laser diffraction instrument (Malvern Master Sizer MS20), used to obtain size analysis of particles contained in a fluid. The losses occurring during the washing process were not considered large enough to influence the results significantly.

9.4 RESULTS OBTAINED

The 14 dust concentrations obtained from five collieries by the pot sampling method are given in Table IX.I. The dust concentrations vary in a wide band from 1.7 g/m^3 to a 160 g/m^3. Figure 9.9 compares the cumulative size distributions of the samples, but for colliery B not enough dust was captured to allow this analysis to be completed.

Also indicated on the graph is the size distribution produced by the mill used for the main research programme. The mean particle size of the collieries tested varied between 20 μm and 50 μm. The milling to a 20 μm average for testing purposes can therefore be considered a worst case i.e. the finer dust will give the highest explosion risk, etc.

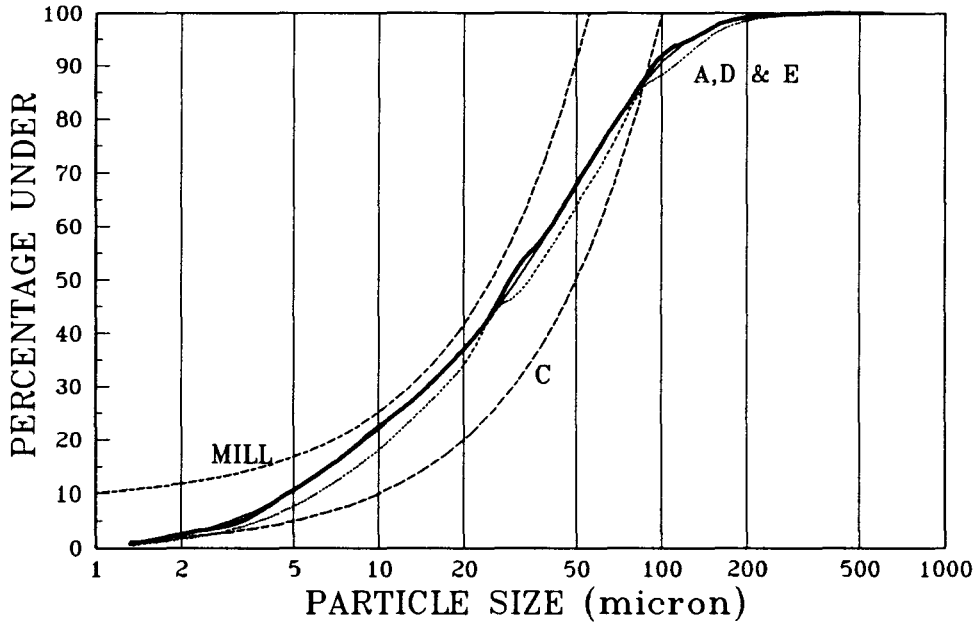

Fig.9.9. Cumulative distribution of dust around mechanized coal mining drums obtained by the pot sampling method.

TABLE IX.I Concentration of the size fraction below 100 μm for dust clouds around mechanized cutting drums in South African collieries[1&2].

MINE	SAMPLING TIME min	MASS CAPTURED g	CONCEN-TRATION g/m^3
A	10	3.2190	64.3800
	20	12.4000	124.0000
B	5	0.0519	2.0784
	5	0.0519	2.0792
	3	0.0518	3.4587
C	4	0.0276	1.7040
	4	0.7597	30.3900
D	4	0.0541	2.1664
	32	25.6000	160.0000
E	5	0.1064	4.2560
	5	0.1921	7.6840
	5	0.2246	8.9840
	5	1.1054	44.2160
	3	0.9230	61.5339

1 The pumping velocity for all tests was maintained at 5 l/min.

2 Mine A and D were sampled by COMRO[117].

9.5 CONCLUSIONS

The dust concentrations observed during these tests varied substantially. The highest observed concentration was 160 g/m^3, but values could possibly be higher. Also, small percentages of methane are normally simultaneously present in the air. Figure 9.10 is a reproduction of Figure 7.38 (page 187), showing the areas of explosibility and relative sensitivity compared to methane for Ermelo and Springfield coal dust. In Figure 9.10, however, a rectangle is shown on each diagram which indicates all possible combinations of methane and dust, below concentrations of 3 % for methane and 250 g/m^3 for coal dust. The concentrations are arbitrarily chosen and considered likely, but do not necessary contain all possible concentrations.

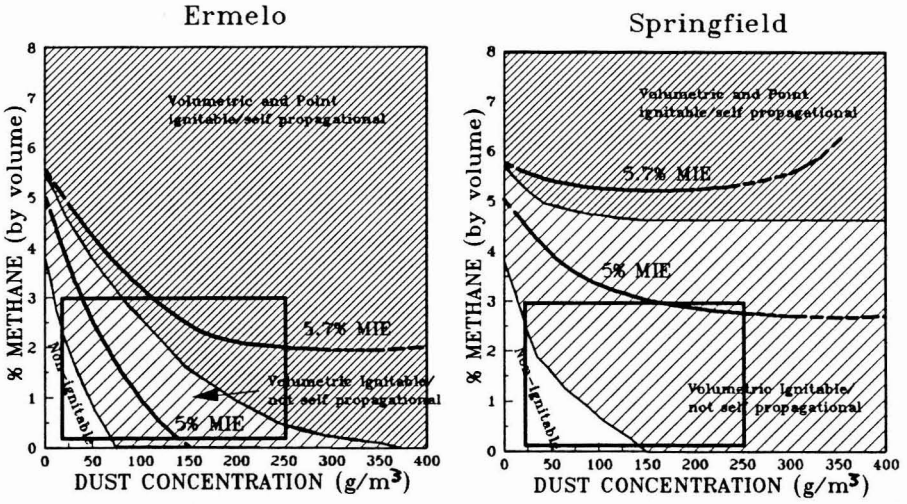

Fig.9.10. Sensitivity and explosion limits for Ermelo and Springfield hybrid mixtures. The rectangles indicate likely hybrid mixtures.

For the Ermelo hybrid rectangle, the top right corner indicates an extremely dangerous situation. The mixtures are ignitable from a point source, with a sensitivity to ignition comparable with a 5.7 % methane/air mixture. For the rest of the rectangle, most

combinations are volumetrically ignitable. The Springfield hybrid rectangle shows no combinations ignitable by point source. The latter situation therefore appears to be relatively safe.

It has been indicated that high dust concentrations with methane far below the lower explosive limits of methane can result in hybrid mixtures that are extremely sensitive to ignition. The presence of excessive levels of fully dispersed coal dust concentrations on the working face therefore increases the risk of an explosion taking place.

CHAPTER X

CONCLUSIONS AND RECOMMENDATIONS

The understanding of explosion safety at the working face, as approached in this thesis, is reviewed briefly. The conclusion is reached that total dust concentrations should be controlled within safe limits. A methodology to determine such safe levels is developed after which a few closing comments follow.

10.1 EXPLOSION SAFETY AT THE WORKING FACE

The sensitivity to ignition of hybrid mixtures of methane with coal dust in air which is likely to occur on the face has been investigated. When the three variables, namely, methane concentration, dust concentration and ignition energy were plotted on a three dimensional diagram, a volume has been delineated where the mixtures cannot be ignited with ease, while another was identified where mixtures could be ignited readily. Operational environments maintained within the former volume are desirable, while those inside the latter are most undesirable. The surface separating the two volumes has been termed the "ignition blanket", an area combining the minimum ignition energy of all possible combinations of methane and coal dust in air.

It was observed that volumetric ignition sources, which are spacially extended, resulted in a large explosible zone. Point source ignitors, which are spacially concentrated, were observed to reduce the dangerous zone. This zone is, however, considered to be very dangerous, since the mixtures are self propagational. This presents an unacceptable high risk on the working face, since the potential exists that the combustible mixture will propagate and burn workers in the vicinity. It was also observed that an increase in volatile content magnifies this risk due to an enlarged volume that is self propagational. Finally, it was observed that higher dust loadings in the air, which have been proved to exist around cutting drums, reduce the lower explosive limits of methane. Since methane concentration levels, rather

than total dust concentrations, are the variable normally measured and controlled in mines, this means that low concentrations of methane previously perceived as safe, might in fact be explosible.

To summarise, *the position of the ignition blanket in the space formed by methane concentration levels, dust concentration levels and ignition source intensities has been determined, and conditions under which coal mining can proceed in relative safety without the risk of explosions endangering life or property have been determined.*

10.2 CONCLUSION

The production of coal dust is inevitably linked to the excavation and handling of coal. At the same time, most coals inherently contain methane or other combustible gases. Legislation, however, stipulates a concentration level of 1.4 % methane in the air in which work takes place, according to regulation 10.25 of the Minerals Act of 1991[16]. Suspended coal dust loadings around excavation or other equipment is not considered in the Minerals Act, mainly because deposited dust outby the face area is generally considered as the only area where coal dust presents an explosion risk. Throughout the Act emphasis is put on the respirable fraction as the only part of suspended dust to be monitored and, if necessary, to be controlled.

This work proves that suspended dust present in high concentrations increases the explosion risk on the working face. One can therefore conclude that total dust concentration should be included in the variables that are to be considered when an explosion safe environment is contemplated.

The wide variation of dust loadings measured around continuous miner drums during this investigation, indicates that operational conditions exist where the dust loadings are well within safe limits. On the other hand, the same results also indicate the opposite, i.e. that operational environments also exist where dangerously high dust concentrations may well lead to an explosion should small quantities of methane be

present together with the necessary source of ignition. A better understanding of how dust is produced and effective suppression thereof can help to reduce the extent of this problem.

10.3 A SUGGESTED METHODOLOGY FOR DETERMINATION OF ACCEPTABLE DUST CONCENTRATION LEVELS

To limit concentration levels of explosible substances in the operational environment in coal mines is, in fact, an application of risk management. All activities incorporate a degree of risk, so a decision should be made as to what degree of risk is acceptable to all parties involved in the activity. The degree of risk can only be agreed upon if the risk can be quantified. An approach often pursued is to express risk in terms of the likelihood of the unwanted event happening. In instances where it is difficult or impossible to determine the probability of an undesirable event, as is the case with accidental mine explosions, a method can be followed where the input variables to the activity are over designed in order to reduce the chance of such an event occurring. The extent of over design, or the *safety factor*, is then agreed upon.

Since dust production is so intimately associated with the coal production process, the elimination of all dust to provide an infinitely large safety factor is not possible. Some realistic level should be chosen which allows the current high production tempos to be maintained and suppression to be effective but not complete. The presence of methane (without coal dust being present) can be used as an example. For point source ignition, the lower explosive limit of a methane/air mixture is 5.2 %, but 1.4 % is the maximum allowed by law. This results in a safety factor of 3.7 for the activity. It is, however, not considered impractical or unreasonably costly to improve ventilation around activities where such environments do exist, so that any methane present is diluted to an acceptable level.

When the only combustible component within the operational environment is dispersed dust, the same approach as for methane can be followed. If for example, the lower explosive limit of a dust for volumetric ignition is 75 g/m^3, limiting concentrations at about 20 g/m^3 will also result in a safety factor 3.7.

When, however, 1.4 % methane and 75 g/m^3 of coal dust are simultaneously present, the mixture is highly sensitive with a safety factor of below one. In determining an acceptable safety factor, the explosibility of the hybrid mixtures should therefore be considered. Le Chatelier's principle of additivity, although proved in this thesis to be inaccurate, can be of assistance in determining suitable dust concentration levels. If we assume Le Chatelier's principle holds true, as interpreted by Field[76] for hybrid mixtures (equation 3.39, page 81), then:

$$\frac{d}{N_d} + \frac{s}{N_s} = 1$$

where d and s are the concentrations of dust and methane below the lower explosive limits of each substance, and N_d and N_s the lower explosive limits of each individual substance.

Figure 10.1 shows s/N_s plotted against d/N_d for different values of s and d. A line connecting all possible concentrations of s and d connects the 1 value on the s/N_s axis and the 1 value on the d/N_d axis. Since this is the lower explosive limit for hybrid mixtures of s and d for the particular source of ignition, it is also a line representing a safety factor of one. If the concentrations of both s and d are halved proportionally, only half of the required combustible components to affect an explosion are present, and the safety factor should be two. Mixtures representing a safety factor of two therefore form another straight line below that of a safety factor of one. Lines for safety factors up to five are also indicated in Figure 10.1.

When a methane level of 1.4 % is allowed, a straight line parallel to the d/N_d axis shows the change in safety factor with increased dust concentrations present. Each

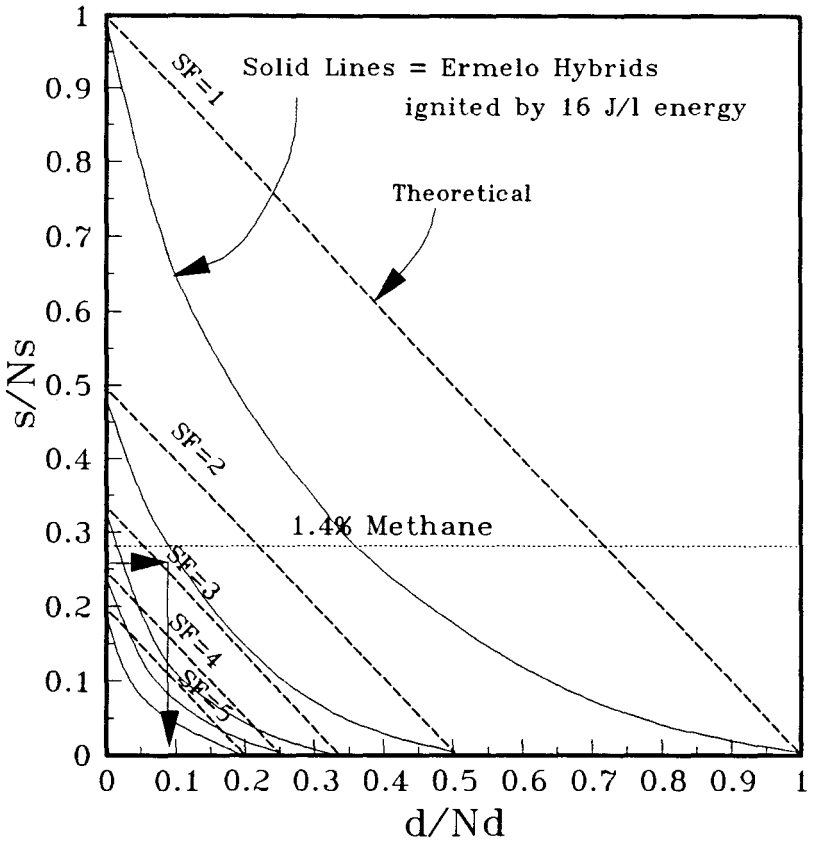

Fig.10.1. A safety factor diagram based on Le Chatelier's principle as interpreted by Field[76] for hybrid mixtures of gas and dust.

mine, or the mining industry as a whole, should decide what safety factor is acceptable and should then control dust levels to ensure that the safety factor holds. For example, for Ermelo coal dust, and with 1.4 % methane assumed to be present, a safety factor of two might be considered adequate. Dust levels should therefore be maintained to provide a d/N_d value of 0.1, as obtained from Figure 10.1 (indicated by arrows). Since N_d for Ermelo dust ignited by point source is 75 g/m^3, d should never be above 7.5 g/m^3 to maintain a safety factor of two. This concentration level will clearly differ for each mine, even if the safety factor is unchanged.

10.4 CLOSING REMARKS

This thesis has investigated the explosibility of coal face environments, and found that suspended coal dust might contribute to raising the risk of an explosion if present in high concentrations. The work reported in this thesis provides justification for research in the following areas:

Total dust generation: Although respirable dust generation and transmission are increasingly well understood, our current knowledge of the variables influencing total dust generation is inadequate.

Dust control: The effective removal, binding together and control of dust at the cutting drum can greatly enhance coal mine safety.

Rock and coal cutting technique: Rock breaking methods that can remove or reduce the chance of frictional smears that might cause ignitions will reduce the chance of ignitions occurring in dangerous environments.

Heat generation and heat loss: A more comprehensive understanding of heat generation and heat loss might help to bridge the difficulty of correlating explosive behaviour under optimum conditions, such as those created in explosion vessels or galleries with that prevailing in collieries.

Concern about the increased frequency of frictional ignitions in South Africa, and the high percentage of explosions originating in the face where mine workers are concentrated, inspired this study. Progress in reducing the number of explosions can be achieved by obtaining an improved understanding of all the processes involved, and an increased awareness of the explosion hazard. It is hoped that this thesis contributes to obtaining that better understanding and might assist mining engineers in creating and maintaining a safer working environment.

REFERENCES

1. Cybulski W. Coal Dust Explosions and Their Suppression. *Bureau of Mines, U.S. Department of the Interior and the National Science Foundation*, Washington D.C. TT 73-54001, 1975.

2. Basic A., Tanovic H., Micevic S., and Saracevic S. Explosiveness of wet coal dust- dilemmas and questions. *The 24th International Conference of Safety in Mines Research Institutes*, Donetsk, USSR, 23 to 28 September 1991.

3. *Mining Journal*, Vol 313 No 8038, ISSN 0026-5225, London, Sept 22 1989.

4. *Mining Journal*, Vol 314 No 8057, ISSN 0026-5225, London, Feb 2 1990.

5. *The Star*, Monday August 27 1990.

6. *The Citizen*, Thursday May 9 1991.

7. Ensiklopedie van die Wêreld, *Deel 7*, p414. C.F.Albertyn (Edms) Beperk, Stellenbosch, 1975.

8. Report of the Inspector of Mines, Kimberley and Inspector of Claims, Barkly West, Cape of Good Hope, *Department of Agriculture*. The Cape Times Limited, Government Printers, 1903.

9. Survey of the Coal fields, Natal. *Government Notice No 199*, 1881.

10. Vivian R.W. *Risk management and fatality frequencies*. Loss Control Survey, February 1987.

11. Whittaker J.D. *Evaluation of acceptable risk*. Journal of the Operational Research Society. Vol. 37 No. 6, pp541-547, 1986.

12. Bannister J.E. and Bawcutt P.A. *Practical Risk Management*. 1st Ed. London, Witherby and Co. Ltd. ISBN 0 900886 22 6, 1981.

13. *Reports of the Government Mining Engineer and Statistical Tables*, 1890 to 1990. Department of Mineral and Energy Affairs of RSA. Government printer, Pretoria.

14. Landman G.V.R. Coal mine explosions: the extent of the hazard in South Africa. *South African Mining World*. Vol. 9 No. 9, October 1990.

15. Regulations for the control and working of mines. *Natal Mines Act*, 1899.

16. Pretoruis J.J. (compiled by). *Minerals Act and Regulations*, Act 50 of 1991.

17. Till R. *Statistical Methods for the Earth Scientist, an Introduction*. pp 62-67. Exploration Department, British Petroleum Company, The Macmillan Press Ltd. 1982.

18. Sapko M.J., Grininger N.B. and Watson R.W. Review paper: prevention and suppression of coal mine explosions. *The 23rd International Conference for Safety in Mines Research Institutes*, Washington, D.C. September 1989.

19. Health and Safety Executive. *Annual Reports of the Safety in Mines Research Establishment, 1980 to 1985*, Her Majesty's Stationary Office, London.

20. Nagy J. The explosion hazard in mining. U.S. Department of Labour, Mine Safety and Health Administration. *Information Report IR 1119*, 1981.

21. Tideswell F.V. Mine explosions: the current hazard. *Trans. Inst. Mining Engineering*. Vol.114, London, 1954-55.

22. Ramsay H.T. Wass C.A.A. and Hartwell F.J. A summary account of the manner and the frequency of ignition of firedamp in British coal mines. *Journal of the Institution of Mining Engineers*, September 1965.

23. Health and safety commission annual report 1988/89. As reported in the *Journal of the Institution of Mining Engineers*, Vol.149 No.342. March 1990.

24. Courtney W.G. Frictional ignition with coal mining bits. U.S. Bureau of Mines, Department of the Interior, *Information Circular 9251*, 1990.

25. Swinburne U.P. Wybergh W. and Heslop W.T. Report of a committee appointed under government notice no. 358 of the 24th February 1911, to inquire into and report upon the most practical means to be adopted for the prevention of explosions of gas and dust in the collieries situated in the Province of Natal. *Union Gazette No.358*, 28 February 1911. The Government Printing and Stationary Office, 1912.

26. Flint J.D. *Mine Gas and Coal Dust Explosions and Methane Outbursts, their Causes and Prevention.* MSc thesis, University of the Witwatersrand, Johannesburg, 23 October 1990.

27. Wynn A.H.A. Applications of probability theory to the study of mining accidents. Safety in Mines Research and Testing Branch, *Research Report No 7*, July 1950.

28. Bartknecht W. *Explosions, Course, Prevention, Protection.* Springer-Verlag, Berlin Heidelberg New York, ISBN 3-540-09894-1, p77, 1981.

29. McQuaid J. From Buxton to Donetsk 1991: 60 years of international cooperation in mine safety research. *24th International Conference of Coal Mine Safety Research Institutes*, Donetsk, USSR, 1991.

30. Palmer K.N. *Dust Explosion and Fires.* Power Technology Series, Chapman and Hall, London, SBN 412 09430 4, 1973.

31. Helwig N. Investigation of the entrainment of different particle sizes in propagation of coal dust explosions (German). *Staub-Reinhalt.* Luft 26, Nr.2, February 1966.

32. Hertzberg M. A critique of the dust explosibility index: an alternative for estimating explosion probabilities. *Report of Investigations 9095*, US Department of the Interior, Bureau of Mines, 1987.

33. Edwards J.S. and Durucan S. The origins of methane. *Mining Science and Technology*, Vol 12, p193-204, Elsevier Science Publishers B.V., Amsterdam, 1991.

34. Jolliffe G.V. The emission of methane from rapidly advancing coalfaces. *The Mining Engineer*, February 1970.

35. Stripp G.P. *Methane Emission Characteristics of South African Coal Seam Strata.* PhD Thesis, University of the Witwatersrand, Johannesburg, 1989.

36. Kavonic M.F. Methane drainage at Majuba colliery. *Journal of the Mine Ventilation Society of South Africa*, Vol 43 No 11, November 1990.

37. Meets E.J. Personal communication. *South African Chamber of Mines Research Organization*, Coal division, December 1991.

38. Pickering A.J. Air flows and methane emissions on fully caved, mechanised coal faces in South Nottinghamshire. *The Mining Engineer*, November 1969.

39. Cecala A.B., Jankowski R.A. and Kissell F.N. Determining face methane-liberation patterns during longwall mining. U.S. Bureau of Mines, Department of the Interior, *Information Circular 9052*, 1985.

40. Meets E.J. The effects of airflow on methane and airborne dust in advanced bord and pillar headings. *The 23rd Conference of Safety in Mines Research Institutes*, Washington, September 1989.

41. Meyer C.F. The effect of the last through road velocities on the depth of air penetration into bord and pillar headings and an assessment of methods for improving air penetration. *The 24th International Conference of Mine Safety Research Institutes*, Donetsk, USSR, September 1990.

42. Joubert F.E. Methane survey in Indumeni Colliery. *Fuel Research Institute of South Africa*, Technical Memorandum No 44 of 1969.

43. Joubert F.E. Methane in South African collieries. *Fuel Research Institute of South Africa*, Technical Memorandum No 34 of 1965.

44. Reeh D. Recent investigations on the influence of particle size in coal dust explosions. *19th International Conference on Safety in Mines Research Institutes*, Katowice, Poland, 1981.

45. Zipf R.K. and Bieniawski Z.T. A fundamental study of respirable dust generation in coal. *Mining Science and Technology* 9(1989), Elsevier Science Publishers B.V., Amsterdam, 1989.

46. Kachan V.N., Kocherga N.G. and Kolchinskii A.I. Ignition of coal dust by frictional sparks during the operating of heading machines. *Safety in Mines Research Establishment* translation No 6519, June 1975.

47. Jankowski R.A. and Organiscak J.A. Dust sources and controls on the six U.S. longwall faces having the most difficulty complying with dust standards. U.S. Bureau of Mines, Department of the Interior, *Information Circular 8957*, 1983.

48. Barnard J.A. and Bradley J.N. *Flame and Combustion*, pp 1-56 and pp 148-160, Chapman and Hall, Second Edition, London, 1985.

49. Baker W.E., Cox P.A., Westine P.S., Kulesz J.J. and Strehlow R.A. *Explosion Hazards and Evaluation*, Fundamental Studies in Engineering 5, Elsevier, Amsterdam, 1983.

50. Petrucci R.H. *General Chemistry, Principles and Modern Applications*, Third Edition, Macmillan Publishing Co., Inc. New York, 1982.

51. Krazinski J.L., Buckius R.O. and Krier H. Coal dust flames: a review and development of a model for flame propagation, *Prog. Energy Combust. Sci.* Vol. 5, pp 31-70, U.K., 1979.

52. Sears F.W., Zemansky M.W. and Young H.D. *University Physics*. Fifth Edition, pp 299-300, Addison-Westley Publishing Company, 1978.

53. Gray P. and Lee P.R. (1967) Thermal Explosion Theory, pp 1-184, in Tipper C.F.H.(editor). *Oxidation and Combustion Reviews*, Volume 2, Elsevier Publishing Company, Amsterdam, 1967.

54. Thomas P.H. A comparison of some hot spot theories. *Combustion and Flame*, Vol 9, p369, December 1965.

55. Van Wylen G.J. and Sonntag R.E. *Fundamentals of Classical Thermodynamics*, 3 rd Edition, pp 464-512, John Wiley & Sons, New York, 1985.

56 Naylor C.A. and Wheeler R.V. The lag on ignition of firedamp. *Safety in Mines Research Board*, Paper No 9, London, 1925.

57. Bond J. *Sources of Ignition, Flammability Characteristics of Chemicals and Products*. Butterworth-Heinemann Ltd, 1991.

58. Conti R.S. and Hertzberg M. Thermal autoignition temperatures from the 1.2-l furnace and their use in evaluating the explosion potential of dusts, pp 45-59, in *Industrial Dust Explosions*, Symposium on Industrial Dust Explosions, Cashdollar K.L. and Hertzberg M. (Editors), ASTM, Philadelphia, 1986.

59. Stull D.A. Fundamentals of fire and explosion. *AIChE Monograph Series*, No. 10, Vol. 73, New York, 1977.

60. Moss K.N. *Gases, Dust and Heat in Mines*. pp 23-43, Charles Griffen and Company, Limited, London, 1927.

61. Wieman W. The influence of temperature on the explosion characteristics and the neutralisation of methane-air mixtures. Westfalische Berggewerkschaftskasse, *Bergbau-Versuchsstrecke*, Federal Republic of Germany.

62. Essenhigh R.H., Misra M.K. and Shaw D.W. Ignition of coal particles: a review. *Combustion and Flame*, Vol. 77, pp 3-30, 1989.

63. Howard J.B. and Essenhigh R.H. The mechanism of ignition of pulverised coal. *Combustion and Flame*, Vol. IX, pp 337-339, 1965.

64. Goldberg P.M. and Essenhigh R.H. Coal combustion in a jet-mix stirred reactor. *Proceedings of the 17th Combustion Symposium*, pp 145-153, 1979.

65. Hertzberg M., Cashdollar K.L. and Lazzara C.P. The limits of flammability of pulverised coals and other dusts. *Eighteenth Symposium (International) on Combustion*, pp 717-729, The Combustion Institute, 1981.

66. Knoetze T.P., Kessler I.I.M. and Mthombeni I.S. The explosibility of coal samples from underground collieries of the Anglo American Corporation. *Division of Energy Technology*, CSIR, ENER-C 91110, 1991.

67. Hertzberg M., Zlochower A. and Edwards J.C. Coal particle pyrolysis mechanisms and temperatures. *Bureau of Mines Report of Investigations 9169*, U.S. Department of the Interior, 1988.

68. Hartman I., Jacobson M. and Williams R.P. Laboratory explosibility study of American coals. *Bureau of Mines Report of Investigations 6344*, U.S. Department of the Interior, 1963.

69. Brooks P.J. and Essenhigh R.H. Variation of ignition temperatures of fuel particles in vitiated oxygen atmospheres: determination of reaction mechanism. *Twenty-first Symposium (International) on Combustion*, pp 293-302, The Combustion Institute, 1986.

70. Knoetze T.P. The volatile-based explosibility of South African coals. *Division of Energy Technology*, CSIR, ENER-I 91022, 1991.

71. Bradley D., Dixon-Lewis G. and El-Din Habik S. Lean flammability limits and laminar burning velocities of CH_4-air-graphite mixtures and fine coal dusts. *Combustion and Flame*, Vol. 77, pp 41-50, The Combustion Institute, 1989

72. Nagy J. And Portman W. Explosibility of coal dust in an atmosphere containing a low percentage of methane. *Bureau of Mines Report of Investigations 5815*, U.S. Department of the Interior, 1961.

73. Banhegyi M. and Egyedi J. Method for determining the explosive limits of a mixture of coal dust, methane and inert matter, Paper E5, *20th International Conference of Safety in Mines Research Institutes*, Sheffield, England, 1983.

74. Singer J.M., Cook E.B. and Grumer J. Equivalences and lower ignition limits of coal dust and methane mixtures. *Bureau of Mines Report of Investigations 6931*, U.S. Department of the Interior, 1967.

75. Napier D.H. and Roopchanc D.R. Ignition probability of hybrid mixtures. pp 310-323 in *Industrial Dust Explosions*, Symposium on Industrial Dust Explosions, Cashdollar K.L. and Hertzberg M. (Editors), ASTM, Philadelphia, 1986.

76. Field P. *Dust Explosions*, pp 89, Elsevier Scientific Publishing Company, 1967.

77. Ishihama W., Enomoto H. and Tadage H. Explosion characteristics of coal dust-methane-air mixtures. Paper B1, *18th International Conference of Mine Safety Research*, Washington, USA, 1975.

78. Reeh D. The influence of small concentrations of methane on the explosion characteristics of coal dust. *16th International Conference of Safety in Mines Research Institutes*, Washington, U.S.A., 1975.

79. Foniok R. Explosiveness and ignitability of hybrid dispersive mixtures and inertized mixtures of coal dust. *20th International Conference of Safety in Mines Research Institutes*, Sheffield, U.K., 1983.

80. Hey M.A. The explosion characteristics of methane/coal dust hybrid mixtures. *Health and Safety Executive*, Research and Laboratory Services Division, Explosion and Flame Laboratory, Buxton, U.K., 1985.

81. Lunn G.A., Quince B.W. and Brookes D.E. Explosions of methane/coal dust hybrid mixtures in the Buxton explosion gallery. *Health and Safety Executive*, Research and Laboratory Services Division, Buxton, U.K., 1986.

82. Marshall A. *Explosives, their Manufacture, Properties, Tests and History*. pp 25-39. J. and A. Churchill, London, 1915.

83. Krzystolik P.A. and Sliz J. Effectiveness of ignition sources of dust-air mixtures. *20th International Conference of Safety in Mines Research Institutes*, Sheffield, U.K. 1983.

84. Hertzberg M., Conti R.S. and Cashdollar K.L. Electrical ignition energies and thermal autoignition temperatures for evaluating explosion hazards of dusts. *Bureau of Mines Report of Investigations 8988*, U.S. Department of the Interior, 1985.

85. Urbanski T. *Chemistry and Technology of Explosives*. Vol. 3, pp 395-497, Pergamon Press Ltd., Oxford, 1967.

86. Grant R.L. and Mason C.M. The mechanism of ignition of firedamp by explosives. *Bureau of Mines Report of Investigations 5049*, U.S. Department of the Interior, 1954.

87. Fordham S. *High Explosives and Propellants*. pp 81-97, Pergamon Press Ltd., Oxford, 1966.

88. Sichel M., Baek S.W., Kauffman C.W., Maker B. and Nicholls J.A. The shock wave ignition of dusts. *AIAA Journal*, Vol. 23, No. 9, pp 1374-1380, 1984.

89. Crowther J.A. *Ions, Electrons and Ionizing Radiations*. Seventh Edition, pp 6-9 and 57-70, Edward Arnold & Co., London, U.K., 1945.

90. Cross J. and Farrer D. *Dust Explosions*. pp 15-42, Plenum Press, New York, 1982.

91. Ko Y., Anderson R.W. And Arpaci V.S. Spark ignition of propane-air mixtures near the minimum ignition energy: Part I. An experimental study. *Combustion and Flame*, The Combustion Institute, Vol. 83, pp 75-87, 1991.

92. Ko Y., Arpaci V.S. and Anderson R.W. Spark ignition of propane-air mixtures near the minimum ignition energy: Part II. A model development. *Combustion and Flame*, The Combustion Institute, Vol. 83, pp 88-105, 1991.

93. Powell F. Ignitions by machine picks: a review. *Health and Safety Executive*, Research and Laboratories Services Division, Buxton, U.K., 1990.

94. Wynn A.H.A. The ignition of firedamp by friction. *Safety in Mines Research Establishment*, Research Report No. 42, July 1952.

95. Courtney W.G. Preventing frictional ignitions. pp 48-58, *Coal Mining and Processing*, January 1981.

96. Titman H. and Wynn A.H.A. The ignition of explosive gas mixtures by friction. *Safety in Mines Research Establishment*, Research Report No. 95, July 1954.

97. Rae D. The ignition of gas by the impact of light alloys on oxide-coated surfaces. *Safety in Mines Research Establishment*, Research Report No. 177, November 1959.

98. Blickensderfer R., Kelly J.E., Deardorff D.K. and Copeland M.I. *Bureau of Mines Report of Investigations 7713*, U.S. Department of the Interior, 1972.

99. Lobejko A. The ignition of methane-air mixtures by frictional sparks. *Experimental Mine Barbara, Central Mining Institute* - 1977, Health and Safety Translation No. 8999, May 1980.

100. Bartknecht W. Ignition capabilities of hot surfaces and mechanically generated sparks in flammable gas and dust/air mixtures. *Plant/Operations Progress*, Vol. 7, No. 2, April 1988.

101. Coward H.F. and Ramsay H.T. Ignition of firedamp by means other than electricity and explosives: a review. *Safety in Mines Research Establishment*, Research Report No. 231, October 1965.

102. Blickensderfer R., Deardorff D.K. and Kelley J.E. Incendivity of some coal-cutter materials by impact-abrasion in air-methane. *Bureau of Mines Report of Investigations 7930*, U.S. Department of the Interior, 1974.

103. Rae D. The role of quartz in the ignition of methane by the friction of rocks. *Safety in Mines Research Establishment*, Research Report No. 223, August 1964.

104. Blickensderfer R. Methane ignition by frictional impact heating. *Combustion and Flame*, The Combustion Institute, Vol. 25, pp 143-152, 1975.

105. Larson D.A., Dellorfano V.W., Wingquist C.F. and Roepke W.W. Preliminary evaluation of bit impact ignitions of methane using a drum-type cutting head. *Bureau of Mines Report of Investigations 8755*, U.S. Department of the Interior, 1983.

106. Powell F. Design guidelines for picks. *Colliery Guardian*, July 1991.

107. Powell F. and Billinge K. The use of water in the prevention of ignitions caused by machine picks. *The Mining Engineer*, pp 81-85, August 1981.

108. Powell F. and Billinge K. The frictional ignition hazard associated with colliery rocks. *The Mining Engineer*, pp 527-533, July 1975.

109. Conti R.S., Cashdollar K.L., Hertzberg M. and Liebman I. Thermal and electrical ignitability of dust clouds. *Bureau of Mines Report of Investigations 8798*, U.S. Department of the Interior, 1983.

110. Joubert F.E. Dust explosions: a literature survey which includes small and large scale test facilities. *Fuel Research Institute of South Africa*, Report No. 9 of 1981, January 1981.

111. Helwig N. Die explosionseigenschaften von kohlenstaub verschiedener flöze. *Glückauf* Forschungshefte, December 1966.

112. Kessler I.I.M. Handleiding vir die gebruik van die 40 l ontploffingshouer. *Division of Energy Technology*, CSIR, ENER-U 91001, June 1991.

113. Hertzberg M., Conti R.S. And Cashdollar K.L. Spark ignition energies for dust-air mixtures: Temperature and concentration dependences. pp 1681-1690, *Twentieth Symposium (International) on Combustion*, The Combustion Institute, 1984.

114. Cobine J.D. *Gaseous Conductors*. pp 291-293/327-351, Dover, 1958.

115. Joubert F.E. The 40-litre explosion vessel: the state of the art and the future. *Fuel Research Institute of South Africa*, Report No. 11 of 1981, February 1981.

116. Knoetze T.P., Kessler I.I.M., Bryden D.J. and Van der Bank T. The relationship between the chemical properties of coals and their explosibilities. *CSIR Progress Report No. ESS8*, September 1990.

117. Sullivan P. Personal communication. *South African Chamber of Mines Research Organization*, Coal division, June 1992.

APPENDIX I
ANNUAL COAL MINE EXPLOSION STATISTICS FOR SOUTH AFRICA FOR THE PERIOD 1897-1991

A - Year.
B - Number of explosions during that year.
C - Number of separate accidents.
D - Run-of-mine production (tons).
E - Average number of persons at work underground.
F - Injuries due to explosions.
G - Fatalities due to explosions.
H - Total coal mine injuries.
I - Total coal mine fatalities.

A	B	C	D	E	F	G	H	I
1897	4	75	2039225	6900	0	0	29	30
1898	8	92	2532695	8768	13	2	33	35
1899	4	27	532816	4051	15	6	29	15
1900	0	35	439781	3799	0	0	25	9
1901	1	69	1787528	7686	14	31	56	51
1902	3	94	2689192	7328	3	0	73	38
1903	3	90	3795212	9965	4	4	74	43
1904	3	167	4175332	9809	4	1	129	48
1905	4	142	4570732	9364	6	2	115	48
1906	3	148	5146221	9763	4	21	113	72
1907	4	160	5499034	10675	5	3	132	51
1908	4	143	5903758	10711	11	78	112	123
1909	1	177	6400252	10784	1	0	160	62
1910	1	99	4658422	14352	2	0	67	39
1911	0	188	9931327	14235	0	0	151	37
1912	0	182	10059037	14120	0	0	145	43
1913	6	206	10732653	15213	9	3	162	76
1914	3	179	10220018	15076	3	2	142	52
1915	5	198	10053869	14366	13	10	171	54
1916	5	229	12281796	17661	8	3	184	60
1917	8	262	12817378	18527	13	7	215	68
1918	1	229	11975222	17454	2	0	188	52
1919	4	249	12443484	18387	7	2	212	60
1920	5	270	13691880	19985	6	3	212	83
1921	10	323	13658922	22345	15	12	278	65
1922	5	306	12031467	18833	6	23	234	67
1923	9	354	14678687	20506	11	18	301	94
1924	3	457	15564365	21582	6	2	397	85
1925	3	482	16114992	21846	0	5	419	86
1926	7	656	16820524	23031	7	129	593	219
1927	2	696	16331602	22035	3	0	637	86
1928	3	689	16397348	21505	4	1	633	105
1929	4	810	16944841	21070	5	0	748	78
1930	5	681	15721592	18875	8	41	637	118
1931	0	703	13847355	15321	0	0	665	57
1932	2	581	12611649	12799	2	0	545	50
1933	1	553	13796968	13635	1	0	521	49
1934	2	895	15543083	14874	11	7	853	67
1935	3	1070	17340916	17172	2	78	1024	141
1936	1	1073	18837730	18253	1	0	1027	79
1937	5	1035	19521623	18991	3	4	986	81
1938	0	1118	20511690	19922	0	0	1094	69
1939	0	1110	21524890	20505	0	0	1067	79
1940	0	1055	22536533	21919	0	0	1011	68
1941	3	1165	24115769	23526	2	16	1121	84
1942	1	1402	25186325	25469	0	15	1348	95

A	B	C	D	E	F	G	H	I
1943	2	1687	26332395	26250	5	78	1635	170
1944	5	2311	29311215	30393	19	58	2290	166
1945	4	3146	30703536	31621	37	15	3071	116
1946	0	3160	30317890	31122	0	0	3092	93
1947	2	3032	29922993	30645	1	2	2976	94
1948	1	2801	30607610	29716	1	0	2747	93
1949	7	3033	32946115	31485	7	0	3001	86
1950	0	2891	33916257	32403	0	0	2837	91
1951	4	2866	33660295	32692	23	30	2829	111
1952	2	3048	34702054	33623	0	0	3007	102
1953	1	3563	35628230	33244	6	5	3516	102
1954	2	3714	36839950	32953	5	1	3670	94
1955	2	3598	39675027	33493	6	1	3564	88
1956	4	3433	41118959	33728	8	14	3394	101
1957	2	3406	42288514	35413	5	8	3385	108
1958	0	3541	44979899	37899	0	0	3512	74
1959	0	3179	45263335	39019	0	0	3147	72
1960	2	2800	47090561	38634	0	0	2773	496
1961	3	2780	49347154	41598	0	8	2739	90
1962	4	2846	51769289	42060	22	16	2817	103
1963	1	2762	53929956	43302	0	1	2713	87
1964	2	2538	56614013	44666	2	0	2479	104
1965	4	2672	58887651	46979	6	0	2622	84
1966	3	2789	59725851	48835	0	0	2748	72
1967	4	2346	61039923	46479	0	3	2299	73
1968	7	2152	63892747	47186	1	4	2105	81
1969	1	1903	64566429	46271	0	0	1859	77
1970	3	1788	60682739	45607	4	0	1757	79
1971	1	1813	64656047	46824	0	28	1776	94
1972	2	1464	64897107	45763	8	0	1446	58
1973	1	1487	69147377	44407	8	0	1460	52
1974	2	1643	72103784	45015	13	1	1616	84
1975	2	1651	76221973	47887	0	0	1608	100
1976	3	1835	84118641	49718	1	1	1781	86
1977	6	2105	98103819	53210	6	0	2061	120
1978	2	1979	105178173	51337	1	0	1918	105
1979	7	1406	125825646	50902	0	0	1362	112
1980	6	1272	137893916	51030	0	0	1200	156
1981	15	1219	145831742	53857	20	15	1194	166
1982	6	951	172589539	52207	12	12	910	109
1983	7	826	173091561	47802	13	69	813	129
1884	7	840	191712427	50525	0	13	796	73
1985	7	802	206520615	52853	7	34	775	93
1986	0	714	212761329	52095	0	0	688	67
1987	1	582	210701518	48853	11	35	550	123
1988	2	438	224405852	46322	6	0	404	53
1989	6	387	222270000	45343	4	1	363	54
1990	9	479	219103124	49265	13	0	401	51
1991	6	468	227907097	39007	10	1	369	43

APPENDIX II
SOME DETAIL OF SOUTH AFRICAN COAL MINE EXPLOSIONS

COLLIERY	DATE	DAY	TIME	IN-JURED	KILL-ED
ELANDSLAAGTE COLLIERIES	1891		-	1	1
CAMPBELL COLLIERIES	17/02/98	THURSDAY	-	2	0
CAMPBELL COLLIERIES	08/03/98	TUESDAY	-	1	0
NATAL NAVIGATION COLLIERY	09/04/98	SATURDAY	-	2	1
CAMPBELL COLLIERIES	17/05/98	TUESDAY	-	2	0
CAMPBELL COLLIERIES	25/08/98	THURSDAY	-	2	0
ST GEORGE'S COLLIERY	28/08/98	SUNDAY	21h30	1	0
ST GEORGE'S COLLIERY	08/09/98	THURSDAY	17h15	2	0
CAMPBELL COLLIERIES	14/12/98	WEDNESDAY	15h30	0	0
ST GEORGE'S COLLIERY	17/01/99	TUESDAY	12h30	5	4
ELANDSLAAGTE COLLIERIES	03/02/99	FRIDAY	17h15	1	0
SOUTH AFRICAN COLLIERIES	21/04/99	FRIDAY	21h30	0	2
SOUTH AFRICAN COLLIERIES	26/05/99	FRIDAY	-	6	0
NATAL NAVIGATION COLLIERY	16/08/99	WEDNESDAY	6h30	3	0
NEW CAMPBELL COLLIERIES	22/05/01	WEDNESDAY	14h30	14	31
CROWN COLLIERY	04/10/02	SATURDAY	5h20	1	0
DUGMORE MINE/INGWE COMPANY	06/04/02	SUNDAY	-	1	0

GLENCOE COLLIERY	24/08/02	SUNDAY	21h30	1	0
ST GEORGE'S COLLIERY	06/02/03	FRIDAY	14h30	2	2
SOUTH AFRICAN COLLIERIES	16/05/03	SATURDAY	21h30	1	0
SOUTH AFRICAN COLLIERIES	20/11/03	FRIDAY	3h45	1	2
RAMSAY COLLIERY	16/05/04	MONDAY	4h43	3	0
RAMSAY COLLIERY	30/05/04	MONDAY	6h10	0	1
ELANDSLAAGTE COLLIERIES	01/10/04	SATURDAY	5h00	1	0
GLENCOE COLLIERY	05/04/05	WEDNESDAY	3h40	0	1
GLENCOE COLLIERY	05/04/05	WEDNESDAY	18h00	1	0
SOUTH AFRICAN COLLIERIES	11/07/05	TUESDAY	17h40	1	0
SOUTH AFRICAN COLLIERIES	28/09/05	THURSDAY	16h00	4	1
SOUTH RAND EXPLORATION CO. LTD.	06/01/06	SATURDAY	-	1	1
ELANDSLAAGTE COLLIERIES	26/04/06	THURSDAY	6h20	2	18
ELANDSLAAGTE COLLIERY	10/06/06	SUNDAY	19h30	4	1
RAMSAY COLLIERY	30/04/07	TUESDAY	15h00	1	0
RAMSAY COLLIERY	24/05/07	FRIDAY	22h45	3	1
GREAT EASTERN COLLIERIES LTD.	14/01/07	FRIDAY	-	0	1
GREAT EASTERN COLLIERIES LTD.	20/01/07	SUNDAY	-	1	1
GLENCOE COLLIERY	13/02/08	THURSDAY	9h00	5	50
GLENCOE COLLIERY	14/02/08	FRIDAY	8h15	4	27

NATAL CAMBRIAN COLLIERY	22/06/08	MONDAY	15h40	0	0
NATAL CAMBRIAN COLLIERY	28/06/08	SUNDAY	7h59	0	0
SOUTH AFRICAN COLLIERIES	24/09/09	FRIDAY	11h00	1	1
NATAL CAMBRIAN COLLIERY	1910		-	2	0
SOUTH AFRICAN COLLIERIES	02/02/14	MONDAY	6h00	0	1
CLYDESDALE COLLIERY	1915		-	0	8
HLOBANE COLLIERY	1915		-	0	1
HATTINGSPRUIT COLLIERY	13/11/15	SATURDAY	6h00	0	1
CLYDESDALE COLLIERY	1916		-	0	1
HLOBANE COLLIERY	1981		-	2	0
NORTHFIELD COLLIERY	1918		-	0	1
BRAKPAN STATE MINES	1919		-	0	3
DURBAN NAVIGATION COLLIERIES	1919		-	3	1
NORTHFIELD COLLIERY	1919		-	0	0
HLOBANE COLLIERY	1921		-	0	1
BANNOCKBURN COLLIERY	1921		-	0	0
BURNSIDE COLLIERY	1921		-	0	6
CORNELIA COLLIERY	1922		-	0	1
UTRECHT COLLIERY	02/06/22	FRIDAY	9h00	2	1

BURNSIDE COLLIERY	14/08/22	MONDAY	10h00	0	20
NATAL NAVIGATION COLLIERY	1922		-	0	0
HLOBANE COLLIERY	22/10/23	MONDAY	7h15	0	12
DURBAN NAVIGATION COLLIERIES	08/10/26	FRIDAY	18h15	0	125
BURNSIDE COLLIERY	17/05/26	MONDAY	16h00	2	1
NEW TENDEGA COLLIERY	23/01/28	MONDAY	10h00	10	1
TSHOBA COLLIERY	1928		-	0	0
BURNSIDE COLLIERY	13/05/30		-	0	0
BURNSIDE COLLIERY	20/05/30	TUESDAY	-	0	38
SCHOONGEZICHT COLLIERY	06/08/34	MONDAY	-	9	7
NEW MARSFIELD COLLIERIES	31/07/35	WEDNESDAY	12h00	0	78
UTRECHT COLLIERY	1937		-	4	0
UTRECHT COLLIERY	20/11/41	THURSDAY	7h00	0	15
NATAL NAVIGATION COLLIERY	26/05/43	WEDNESDAY	7h30	4	78
TSHOBA COLLIERY	11/08/44	FRIDAY	6h00	1	0
HLOBANE COLLIERY	12/09/44	TUESDAY	8h35	13	56
SOUTH AFRICAN COAL ESTATE	28/09/45	FRIDAY	-	34	14
TSHOBA COLLIERY	1945		-	0	0
CONSOLIDATED COLLIERIES	?/05/47		-	1	1

CAMBRIAN COLLIERY	1948		-	0	0
UTRECHT COLLIERY	1949		-	0	0
DURBAN NAVIGATION COLLIERIES	01/11/51	THURSDAY	8h30	2	9
CORNELIA COLLIERY	1951		-	0	16
NATAL NAVIGATION COLLIERY	1951		-	1	3
HLOBANE COLLIERY	06/03/52	THURSDAY	14h00	0	0
HLOBANE COLLIERY	01/04/52	TUESDAY	12h00	5	1
NATAL NAVIGATION COLLIERY	28/02/53	SATURDAY	9h15	0	6
NEWCASTLE-PLATBERG COLLIERY	06/12/54	MONDAY	9h15	3	1
CARNAVON ANTHRACITE	09/07/55	SATURDAY	8h00	3	1
SCHOONGEZICHT COLLIERY	1956		-	0	19
CAMBRIAN COLLIERY	22/07/56	SUNDAY	11h00	0	2
SPRINGFIELD COLLIERY	?/05/57		20h30	11	8
DURBAN NAVIGATION COLLIERIES	05/02/60	FRIDAY	17h35	0	0
SCHOONGEZICHT COLLIERY	02/12/60	FRIDAY	15h00	0	0
COALBROOK COLLIERY	01/05/61	MONDAY	-	0	8
ELANDSBERG ANTHRACITE	05/06/61	TUESDAY	8h15	0	0
NATAL COAL EXPLORATION	30/01/61	MONDAY	8h15	0	0

SPRINGFIELD COLLIERY	1962		-	0	0
INGAGANE COLLIERY	1962		-	0	0
NATAL NAVIGATION COLLIERY	02/06/62	SATURDAY	7h00	12	10
ENYATI COLLIERY	1962		-	0	1
HLOBANE COLLIERY	1965		-	0	0
INDUMENI COLLIERY	1965		-	0	0
DURBAN NAVIGATION COLLIERIES	06/09/65	MONDAY	8h00	0	0
NEWCASTLE-PLATBERG COLLIERY	03/11/65	WEDNESDAY	11h20	6	0
KILBARCHAN COLLIERY	19/03/66	SATURDAY	13h00	1	0
INDUMENI COLLIERY	29/03/66	TUESDAY	12h30	0	0
NATAL COAL EXPLORATION	29/10/66	SATURDAY	-	1	0
INDUMENI COLLIERY	01/10/67	SUNDAY	13h26	0	0
(COALBROOK) COLLIERY	1968		-	0	0
INDUMENI COLLIERY	09/04/67	SUNDAY	5h30	0	0
KILBARCHAN COLLIERY	14/11/67	TUESDAY	11h00	0	0
INDUMENI COLLIERY	15/12/67	FRIDAY	9h30	0	3
NATAL COAL	01/02/68	THURSDAY	9h15	0	0
KILBARCHAN COLLIERY	21/02/68	WEDNESDAY	15h00	0	0
INDUMENI COLLIERY	25/03/68	MONDAY	23h00	0	0

DURBAN NAVIGATION COLLIERIES	21/09/68	SATURDAY	8h30	0	0
ENYATI COLLIERY	29/10/68	TUESDAY	14h15	1	3
UTRECHT COLLIERY	12/11/68	TUESDAY	7h30	0	1
NATAL NAVIGATION COLLIERY	05/02/69	WEDNESDAY	15h40	0	0
DURBAN NAVIGATION COLLIERIES	21/05/70	THUSDAY	12h30	4	0
UNKNOWN	11/12/70	FRIDAY	-	0	0
H.C.J. COLLIERY	07/12/71	TUESDAY	8h10	13	28
NEWCASTLE-PLATBERG COLLIERY	15/02/72	TUESDAY	22h30	0	0
USUTU COLLIERY	28/08/72	MONDAY	17h00	6	0
USUTU COLLIERY	26/01/73	FRIDAY	1h00	0	0
DURBAN NAVIGATION COLLIERIES	1974		-	0	0
ALBION COLLIERY	03/01/74	THUSDAY	9h22	38	13
DURBAN NAVIGATION COLLIERIES	12/04/75	SATURDAY	4h30	0	0
DURBAN NAVIGATION COLLIERIES	23/12/76	THURSDAY	16h35	0	2
DURBAN NAVIGATION COLLIERIES	1977		-	0	0
DURBAN NAVIGATION COLLIERIES	1977		-	0	0
USUTU COLLIERY	15/12/76	WEDNESDAY	15h15	0	0

ERMELO MINE SERVICES	06/09/77	TUESDAY	8h30	0	0
USUTU COLLIERY	29/10/77	SATURDAY	-	0	0
COALBROOK COLLIERY	25/11/77	FRIDAY	21h15	0	0
NEWCASTLE-PLATBERG COLLIERY	17/10/78	TUESDAY	10h15	1	0
NEWCASTLE-PLATBERG COLLIERY	29/05/79	TUESDAY	-	1	0
BALGRAY COLLIERY	23/04/79	MONDAY	11h00	9	2
DURBAN NAVIGATION COLLIERIES	17/10/79	WEDNESDAY	-	0	0
BALGRAY COLLIERY	27/04/79	FRIDAY	13h20	17	2
DURBAN NAVIGATION COLLIERIES	09/01/80	WEDNESDAY	-	0	0
BALGRAY COLLIERY	04/07/80	FRIDAY	-	0	0
COALBROOK COLLIERY	12/02/80	TUESDAY	-	0	0
USUTU COLLIERY	15/02/80	FRIDAY	10h40	1	0
ERMELO MINE SERVICES	?/11/80		-	1	0
SPRINGFIELD COLLIERY	28/02/81	SATURDAY	7h20	7	2
ERMELO MINE SERVICES	21/03/81	SATURDAY	12h15	7	0
ERMELO MINE SERVICES	14/01/81	WEDNESDAY	11h15	2	0
ERMELO MINE SERVICES	25/04/81	SATURDAY	11h00	2	0
NEWCASTLE-PLATBERG COLLIERY	06/05/81	WEDNESDAY	12h00	0	10

BALGRAY COLLIERY	07/01/81	WEDNESDAY	-	0	0
DURBAN NAVIGATION COLLIERIES	06/04/81	MONDAY	-	0	0
BALGRAY COLLIERY	14/05/81	THURSDAY	14h15	0	0
NEWCASTLE-PLATBERG COLLIERY	22/05/81	FRIDAY	11h45	0	0
DURBAN NAVIGATION COLLIERIES	17/07/81	FRIDAY	12h45	0	0
BALGRAY COLLIERY	22/07/81	WEDNESDAY	18h15	0	0
ERMELO MINE SERVICES	23/12/81	WEDNESDAY	18h00	0	0
BOSJESSPRUIT COLLIERY	28/02/81	SATURDAY	1h15	0	0
DURBAN NAVIGATION COLLIERIES	08/04/82	THURSDAY	16h45	2	1
ERMELO MINE SERVICES	12/11/82	FRIDAY	10h00	11	11
BOSJESSPRUIT COLLIERY	09/03/82	TUESDAY	19h45	6	0
SPRINGFIELD COLLIERY	21/05/82	FRIDAY	9h00	1	0
SPRINGFIELD COLLIERY	04/11/83	FRIDAY	10h40	2	0
DELMAS COLLIERIES	21/11/83	MONDAY	18h50	0	0
HLOBANE COLLIERY	12/09/83	MONDAY	7h40	8	68
BOSJESSPRUIT COLLIERY	14/05/83	SATURDAY	18h00	4	0
ERMELO MINE SERVICES	06/11/83	SUNDAY	15h00	1	1
BRANDSPRUIT COLLIERY	29/04/83	FRIDAY	1h10	0	0
SPRINGFIELD COLLIERY	31/08/83	WEDNESDAY	-	1	0

ERMELO MINE SERVICES	25/02/84	SATURDAY	7h00	0	0
ERMELO MINE SERVICES	25/10/84	THURSDAY	21h15	0	6
BOSJESSPRUIT COLLIERIES	30/03/84	FRIDAY	23h30	0	0
TWISTDRAAI COLLIERY	04/05/84	FRIDAY	15h15	0	0
DURBAN NAVIGATION COLLIERIES	29/05/84	TUESDAY	11h00	0	0
DURBAN NAVIGATION COLLIERIES	31/05/84	THURSDAY	18h00	0	0
DURBAN NAVIGATION COLLIERIES	24/11/84	SATURDAY	9h55	0	0
SPRINGFIELD COLLIERY	21/06/85	FRIDAY	3h00	0	0
MIDDELBULT COLLIERY	12/08/85	MONDAY	12h00	7	34
BRANDTSPRUIT COLLIERY	24/06/85	MONDAY	20h15	0	0
USUTU COLLIERY	09/07/85	TUESDAY	11h15	0	0
BRANDSPRUIT COLLIERY	11/09/85	WEDNESDAY	5h15	0	0
BOSJESSPRUIT COLLIERY	22/10/85	TUESDAY	11h00	0	0
BRANDTSPRUIT COLLIERY	26/09/85	THURSDAY	11h45	0	0
SPRINGFIELD COLLIERY	07/07/85		-	0	0
ERMELO MINE SERVICES	09/04/87	THURSDAY	-	11	35
USUTU COLLIERY	11/02/88	THURSDAY	19h30	5	0
TWISTDRAAI COLLIERY	20/08/88	SATURDAY	12h30	1	0
PIET RETIEF COLLIERY	18/03/89	SATURDAY	6h00	4	1

DURBAN NAVIGATION COLLIERIES	21/01/89	SATURDAY	10h30	0	0
DELMAS COLLIERY	09/01/89	MONDAY	10h30	0	0
SPRINGFIELD COLLIERY	07/03/89	TUESDAY	8h30	0	0
ERMELO MINE SERVICES	25/06/90	MONDAY	2h30	10	0
ERMELO MINE SERVICES	06/07/89		11h30	0	0
MIDDELBULT COLLIERY	24/01/90	WEDNESDAY	1h30	3	0
ERMELO MINE SERVICES	27/02/90	THURSDAY	8h30	0	0
NEW DENMARK COLLIERY	17/02/90	SATURDAY	10h30	0	0
TWISTDRAAI COLLIERY	09/07/90	MONDAY	4h30	0	0
TWISTDRAAI COLLIERY	09/08/90	THURSDAY	2h30	0	0
MAJUBA COLLIERY	13/09/90	THURSDAY	23h30	0	0
MAJUBA COLLIERY	20/09/90	THURSDAY	12h30	0	0
DELMAS COLLIERY	29/07/90	SUNDAY	-	0	0
SIGMA COLLIERY	08/05/91	WEDNESDAY	3h30	1	0
DURBAN NAVIGATION COLLIERY	09/05/91	THURSDAY	10h30	0	0
TWISTDRAAI COLLIERY	12/12/91	THURSDAY	-	17	1

APPENDIX III
MEASUREMENTS AND CALCULATIONS OF POWER FOR DIFFERENT RESISTOR ARRANGEMENTS FOR THE SPARK IGNITOR

V_{in}- Voltage setting of variac
V_{act}- Voltage reading over the spark electrodes.
I_{act}- Current through spark
P_{int}- RMS instantaneous power
T_{act}- Actual cycle time at which spark existed
E_{cyc}- Energy per cycle
W_{avg}- Average spark power

---

50 kOhm 4 IN PARALLEL

Vin Volt	Vact Volt	Iact Amp	Pint Watt	Tact ms	Ecyc mJ/cyc	Wavg Watt
210	140	0.9756	96.58	19.2	1854	92.7
200	140	0.9512	94.17	19.2	1808	90.4
190	140	0.8780	86.92	19.2	1669	83.4
180	140	0.8293	82.09	19.2	1576	78.8
170	140	0.7805	77.26	19.2	1483	74.2
160	140	0.7317	72.44	19.2	1391	69.5
150	140	0.6829	67.61	19.2	1298	64.9
140	140	0.6341	62.78	19.2	1205	60.3
130	0	0.0000	0.00	20.0	0	0.0
120	0	0.0000	0.00	20.0	0	0.0
110	0	0.0000	0.00	20.0	0	0.0
100	0	0.0000	0.00	20.0	0	0.0

50 kOhm 3 IN PARALLEL

Vin Volt	Vact Volt	Iact Amp	Pint Watt	Tact ms	Ecyc mJ/cyc	Wavg Watt
210	140	0.7683	76.06	19.2	1460	73.0
200	140	0.7317	72.44	19.2	1391	69.5
190	140	0.6829	67.61	19.2	1298	64.9
180	140	0.6341	62.78	19.2	1205	60.3
170	140	0.5854	57.95	19.2	1113	55.6
160	140	0.5610	55.53	19.2	1066	53.3
150	140	0.5122	50.70	19.2	974	48.7
140	140	0.4878	48.29	19.2	927	46.4
130	140	0.4390	43.46	19.2	834	41.7
120	0	0.0000	0.00	20.0	0	0.0
110	0	0.0000	0.00	20.0	0	0.0
100	0	0.0000	0.00	20.0	0	0.0

50 kOhm 2 IN PARALLEL

Vin Volt	Vact Volt	Iact Amp	Pint Watt	Tact ms	Ecyc mJ/cyc	Wavg Watt
210	140	0.5610	55.53	19.2	1066	53.3
200	140	0.5366	53.12	19.2	1020	51.0
190	140	0.4878	48.29	18.8	908	45.4
180	145	0.4634	47.51	18.8	893	44.7
170	150	0.4390	46.57	18.8	875	43.8
160	150	0.4146	43.98	18.8	827	41.3
150	150	0.3902	41.39	18.8	778	38.9
140	160	0.3415	38.63	18.8	726	36.3
130	0	0.0000	0.00	20.0	0	0.0
120	0	0.0000	0.00	20.0	0	0.0
110	0	0.0000	0.00	20.0	0	0.0
100	0	0.0000	0.00	20.0	0	0.0

50 kOhm 1 IN SERIES

Vin Volt	Vact Volt	Iact Amp	Pint Watt	Tact ms	Ecyc mJ/cyc	Wavg Watt
210	160	0.2927	33.11	18.4	609	30.5
200	160	0.2683	30.35	18.4	559	27.9
190	160	0.2683	30.35	18.4	559	27.9
180	160	0.2561	28.97	18.4	533	26.7
170	160	0.2439	27.59	18.4	508	25.4
160	160	0.2195	24.83	18.4	457	22.8
150	160	0.2134	24.15	18.4	444	22.2
140	160	0.1951	22.08	18.4	406	20.3
130	0	0.0000	0.00	20.0	0	0.0
120	0	0.0000	0.00	20.0	0	0.0
110	0	0.0000	0.00	20.0	0	0.0
100	0	0.0000	0.00	20.0	0	0.0

50 kOhm 2 IN SERIES

Vin Volt	Vact Volt	Iact Amp	Pint Watt	Tact ms	Ecyc mJ/cyc	Wavg Watt
210	440	0.1463	45.53	18.4	838	41.9
200	440	0.1463	45.53	18.4	838	41.9
190	440	0.1341	41.74	18.4	768	38.4
180	440	0.1220	37.94	18.4	698	34.9
170	440	0.1159	36.05	18.4	663	33.2
160	460	0.1098	35.70	18.4	657	32.8
150	480	0.0976	33.11	18.4	609	30.5
140	480	0.0915	31.04	18.4	571	28.6
130	0	0.0000	0.00	20.0	0	0.0
120	0	0.0000	0.00	20.0	0	0.0
110	0	0.0000	0.00	20.0	0	0.0
100	0	0.0000	0.00	20.0	0	0.0

50 kOhm 3 IN SERIES

Vin Volt	Vact Volt	Iact Amp	Pint Watt	Tact ms	Ecyc mJ/cyc	Wavg Watt
210	600	0.0976	41.39	18.4	762	38.1
200	600	0.0915	38.80	18.4	714	35.7
190	600	0.0854	36.22	18.4	666	33.3
180	600	0.0756	32.08	18.4	590	29.5
170	605	0.0744	31.82	18.4	586	29.3
160	610	0.0732	31.56	18.4	581	29.0
150	640	0.0671	30.35	18.4	559	27.9
140	0	0.0610	0.00	18.4	0	0.0
130	0	0.0549	0.00	18.4	0	0.0
120	0	0.0000	0.00	20.0	0	0.0
110	0	0.0000	0.00	20.0	0	0.0
100	0	0.0000	0.00	20.0	0	0.0

500 kOhm 2 IN PARALLEL

Vin Volt	Vact Volt	Iact Amp	Pint Watt	Tact ms	Ecyc mJ/cyc	Wavg Watt
210	700	0.0537	26.56	16.0	425	21.2
200	700	0.0500	24.75	16.0	396	19.8
190	700	0.0463	22.94	16.0	367	18.4
180	720	0.0439	22.35	16.0	358	17.9
170	720	0.0415	21.11	16.0	338	16.9
160	730	0.0390	20.14	16.0	322	16.1
150	740	0.0341	17.87	16.0	286	14.3
140	750	0.0329	17.46	16.0	279	14.0
130	750	0.0305	16.17	16.0	259	12.9
120	760	0.0280	15.07	15.4	232	11.6
110	760	0.0244	13.11	14.0	184	9.2
100	0	0.0000	0.00	20.0	0	0.0

500 kOhm 1 IN SERIES

Vin Volt	Vact Volt	Iact Amp	Pint Watt	Tact ms	Ecyc mJ/cyc	Wavg Watt
210	750	0.0268	14.23	16.0	228	11.4
200	750	0.0256	13.58	16.0	217	10.9
190	750	0.0244	12.93	16.0	207	10.3
180	750	0.0220	11.64	16.0	186	9.3
170	750	0.0204	10.80	16.0	173	8.6
160	750	0.0198	10.48	16.0	168	8.4
150	800	0.0183	10.35	16.0	166	8.3
140	800	0.0159	8.97	16.0	143	7.2
130	850	0.0148	8.87	14.0	124	6.2
120	850	0.0146	8.80	14.0	123	6.2
110	900	0.0109	6.91	12.0	83	4.1
100	0	0.0000	0.00	20.0	0	0.0

500 kOhm 2 IN SERIES

Vin Volt	Vact Volt	Iact Amp	Pint Watt	Tact ms	Ecyc mJ/cyc	Wavg Watt
210	950	0.0134	9.01	16.0	144	7.2
200	950	0.0128	8.60	16.0	138	6.9
190	950	0.0116	7.78	16.0	125	6.2
180	950	0.0104	6.96	15.0	104	5.2
170	1000	0.0100	7.07	15.0	106	5.3
160	1000	0.0085	6.04	14.0	85	4.2
150	1050	0.0072	5.34	12.0	64	3.2
140	1050	0.0055	4.07	12.0	49	2.4
130	1250	0.0049	4.31	8.0	34	1.7
120	0	0.0000	0.00	20.0	0	0.0
110	0	0.0000	0.00	20.0	0	0.0
100	0	0.0000	0.00	20.0	0	0.0

APPENDIX IV

EXPERIMENTAL RESULTS OF TESTS DONE TO DETERMINE THE IGNITION PROPERTIES OF COAL MINE ATMOSPHERES

A computerised data acquisition system was used throughout the Experimental Programme. The edited data for Appendices IV and V is recorded on the enclosed diskette. To access this information the files should be read into Lotus 123, Version 2.1. The information was filed as follows:

A METHANE TESTS

A1 Methane/air mixtures (Chemical Ignition) - *APPEN4A1.WK1*

A2 Methane/air mixtures (Spark Ignition) - *APPEN4A2.WK1*

B ERMELO COAL DUST AND HYBRID MIXTURES

B1 Ermelo Washed (Chemical Ignition) - *APPEN4B1.WK1*

B2 Ermelo Washed (Spark Ignition) - *APPEN4B2.WK1*

B3 Ermelo Un-Washed (Chemical Ignition) - *APPEN4B3.WK1*

C SPRINGFIELD COAL DUST AND HYBRID MIXTURES

C1 Springfield Washed (Chemical Ignition) - *APPEN4C1.WK1*

C2 Springfield Washed (Spark Ignition) - *APPEN4C2.WK1*

C3 Springfield Un-Washed (Chemical Ignition) - *APPEN4C3.WK1*

APPENDIX V

TEMPERATURE MEASUREMENTS AND HEAT RELEASE CHARACTERISTICS OF ERMELO WASHED EXPERIMENTS

Again the numerical data contained in this Appendix can be accessed from the diskette. The data and file name is as follows:

ERMELO WASHED COAL TEMPERATURE MEASUREMENTS

Ermelo Washed (Chemical Ignition) - *APPEN5.WK1*